ANNÉE 2016

UNIVERSITÉ DE RENNES 1

UNIVERSITE BRETAGNE LOIRE

THÈSE / UNIVERSITÉ DE RENNES 1
sous le sceau de l'Université Bretagne Loire

pour le grade de

DOCTEUR DE L'UNIVERSITÉ DE RENNES 1

Mention : Biologie

Ecole doctorale Vie Agro Santé

présentée par

Bingning Xie

Préparée à l'unité de recherche Inserm U1085 IRSET
Institut de Recherche en Santé Environnement et Travail
UFR Sciences de la Vie et de l'Environnement

Long non-coding RNA-based mechanisms for the inhibition of cell growth and development by 5-fluorouracil

Thèse soutenue à Rennes
le 03/11/2016

devant le jury composé de :

Bernard JÉGOU
Directeur d'unité, Inserm U1085 IRSET / *Président*

Domenico LIBRI
Responsable d'équipe, Institut Jacob Monod / *Rapporteur*

Ned LAMB
Responsable d'équipe, Institut de Génétique Humaine / *Rapporteur*

Michael PRIMIG
Responsable d'équipe, Inserm U1085 IRSET / *Directeur de thèse*

Table of Content

Résumé

Les ARNs sont des molécules ayant des fonctions importantes dans divers processus cellulaires. Les ARNm codent pour les protéines, tandis qu'un grand nombre d'ARNs nommés longues ARNs non codants (ARNlnc) ne sont pas traduites en protéines. Les deux types d'ARNs existent en isoformes qui se distinguent par leurs régions non-traduites (UTRs) ou par leur contenu en exons qui est variable à cause de l'épissage alternatif.

Certains des ARNlnc jouent des rôles importants dans la croissance et différentiation cellulaire. Cependant, leurs fonctions dans la cytotoxicité de la chimiothérapie anti-cancéreuse médicamenteuse utilisant le 5-fluorouracile (5-FU) sont encore inconnues.

Pendant mes travaux j'ai trouvé que le traitement par le 5-FU cause l'accumulation des ARNlnc y compris certains qui sont à cheval et antisense à des ARNs. Ce phénomène est parfois, sous forme d'ARN double brin (ARNds) formé par une paire de transcrits chevauchant, corrélé négativement avec le niveau de la protéine codée par l'ARNm. Cette inhibition potentielle de la traduction des régulateurs du cycle cellulaire clés et les gènes essentiels en formant des l'ARNds peut éventuellement empêcher la progression du cycle cellulaire. Mes résultats suggèrent donc que les ARNlnc sont susceptibles de jouer un rôle important dans la cytotoxicité du 5-FU. Nos analyses prometteuses devraient inspirer des études approfondies des ARNlnc dans la cytotoxicité du 5-FU chez la levure et l'homme afin d''améliorer la chimiothérapie.

Le 5-FU est un médicament de chimiothérapie utilisé depuis de décennies au monde entier. Il tue les cellules cancéreuses en inhibant la thymidylate synthétase (impliquée dans la réplication d'ADN) et l'exoribonuclease Rrp6 (nécessaire pour la dégradation et modification d'ARNs). Cependant, l'efficacité de ce médicament est insuffisante, car un grand pourcentage des tumeurs résistent dès le début de la thérapie ou deviennent insensible au traitement. Le mécanisme derrière cette résistance n'est pas entièrement compris.

Rrp6 est une 3 '5' exoribonuclease, qui joue un rôle important dans la régulation et la modification de l'ARNr, l'ARNm et l'ARNlnc. J'ai trouvé que la surexpression de *RRP6*, l'homologue de la levure du gène EXOSC10 chez les mammifères, peut conduire à une résistance accrue au traitement par le 5-FU. Une mutation stabilisant la Rrp6 a également pour conséquence un taux de survie plus élevé lors du traitement 5-FU.

Je démontre ensuite que Rrp6 est un régulateur négatif qui cible des isoformes d'ARNm et lncRNAs méiotiques dans la mitose. Une étude précédente a trouvé que la protéine Rrp6 diminue au cours de la méiose mais la cause est inconnue. J'ai confirmé que l'ARNlnc *MUT1312* forme des ARNds avec *RRP6* qui sont négativement corrélés avec le niveau de la protéine Rrp6. Par ailleurs, la surexpression de *MUT1312* pendant la mitose et associé avec une diminution d'Rrp6. Ainsi, mon étude suggère que MUT1312 soit impliqué dans la régulation de Rrp6 pendant la différentiation cellulaire.

En outre, j'exploré la fonction de l'ARN double brin dans la méiose. Un des cas intéressant de l'ARN double brin dans la méiose est la paire *SWI4/MUT477*, où *MUT477* chevauche l'isoforme méiotique 5'UTR de *SWI4*. J'ai trouvé que MUT477 et *SWI4* 5'UTR forment un ARNds, et que ceci a une corrélation négative avec le niveau de la protéine. Ainsi, mes recherches indiquent la fonction importante de la méiose induite à long ARN non codantes en tant que forme d'ARN double brin

potentiellement réguler la traduction.

Un autre aspect de la fonction des ARNlnc est de réguler la transcription d'un l'ARNm en aval. J'ai trouvé que *SUT200* pourrait inhiber la transcription de *CDC6* durant la méiose par read-through. Un cas comparable est *MUT1465* et *CLN2*, en amont non codant l'ARN MUT1465 inhibent CLN2 par transcription lire arrêter le promoteur *CLN2*. J'ai fait un criblage *in silico* pour trouver des facteurs de transcription qui activent des MUTs durant la méiose. J'ai trouvé que la plupart des MUTs sont induites par Ndt80. MUT1465 est parmi eux : il pourrait être induite par Ndt80 ce qui inhiberait l'expression de *CLN2* après l'initiation de la méiose.

Ume6 interagit avec le site répresseur en amont 1 (URS1) et réprime la transcription à la fois par le recrutement de l'histone déacétylase conservé Rpd3 (à travers le co-répresseur Sin3) et le facteur chromatinien Isw2. Les cellules dépourvues Ume6 sont défectueux dans la croissance, la réponse au stress, et le développement de la méiose. J'ai trouvé que la répression de certains MUTs par le complexe Umew6/Rpd3 en mitose est différemment régulée entre JHY222 et SK1. MUT100 qui ne possède pas l'élément USR1 fixé par Ume6, et qui est donc une cible indirecte, est déréprimé dans JHY22 *ume6* mais pas dans SK1 *ume6*.

Pour la régulation de l'étude de isoforme méiose, j'ai participé à des recherches sur le mécanisme qui répriment l'isoforme méiotique du gène *BOI1* dans la mitose, et j'ai induction de la méiose de isoforme méiose. Les paralogues *BOI1* et *BOI2* sont importantes pour le cytosquelette d'actine et la croissance polaire. BOI1 code une isoforme de transcription méiotique avec une région non traduite en 5 prolongée prédit à altérer la traduction des protéines. Nous avons trouvé que le complexe histone déacétylase Rpd3/Sin3/Ume6, qui réprime les gènes méiotiques lors de la mitose, empêche également l'induction de l'isoforme longue de *BOI1* dans la mitose par liaison directe de liaison Ume6 à sa cible de URS1.

Orc1 est importante pour la réplication de l'ADN. Le gène code pour une isoforme de la transcription de la méiose (*mORC1*) avec une longue région non traduite en 5 '(5'UTR), qui inhibe la traduction des protéines. J'ai démontré que *mORC1* est une cible directe de l'activateur Ndt80 et que son motif de fixation (MSE) est nécessaire pour l'induction de l'isoforme *mORC1* et du gène méiotique *SMA2* transcrit de façon divergente. J'ai trouvé qu'une souche incapable d'induire *mORC1*, contient des niveaux anormalement élevés d'Orc1 pendant la gamétogenèse, ce qui corréle *mORC1* avec la baisse de la protéine Orc1. Étant donné que les gènes eucaryotes encodent fréquemment de multiples transcrits possédant 5'-UTR de longueur variable, les résultats sont vraisemblablement pertinents pour l'expression de gènes au cours du développement et des maladies chez les eucaryotes supérieurs.

En conclusion, mes études au cours du doctorat révèlent des nouvelles cibles et ainsi offrent des nouvelles perspectives de l'amélioration de la chimiothérapie par le 5-FU. Les mécanismes incluent (1) la formation d'un ARN double brin avec son ARNm anti-sens pour potentiellement inhiber la traduction de l'ARNm, et (2) inhibition en aval de l'ARNm par transcription read-through d'une ARNlnc. Mon travail a également révélé un mécanisme de régulation des ARNlnc et les isoformes d'ARN pendent la croissance et la différentiation cellulaire.

Abstract

The drug 5-fluorouracil (5-FU) was introduced as an effective agent in chemotherapy several decades ago. Although much work has focused on understanding its mechanism of action and the events that mediate resistance, some key issues remain unresolved. In my work I addressed the question if the deregulation of recently discovered long non-coding RNAs that depend upon the exoribonuclease Rrp6 (EXOSC10 in mammals) – an enzyme which is directly inhibited by 5-FU – may be involved in the drug's cytotoxicity. To this end, I studied the genome-wide effect of 5-FU treatment using RNA profiling in budding yeast, a major model organism for studying eukaryotic cell cycle progression. My major findings are that (i) some lncRNAs accumulate upon treatment including certain transcripts that can form double stranded RNAs with their overlapping sense mRNAs (and lncRNAs) and (ii) mRNAs and protein levels of the important Swi5 and Ace2 cell cycle regulators are decreased and their target gene mRNAs are down-regulated. In related work, I showed that (i) *RRP6* over-expression mediates elevated 5-FU resistance, which marks the protein out as a potential target for strategies to counter this critical phenomenon in cancer. Furthermore, I studied the transcriptional regulation of meiotic developmental stage specific lncRNAs, some of which are accumulating in cycling cells upon 5-FU treatment. Finally, I participated in work on the epigenetic control of mRNA isoforms that are repressed in mitosis, that can accumulate in 5-FU treated cells, and that are normally activated during various stages of meiotic cell differentiation. My work paves the way for further studies in mammalian cancer cells aiming at lncRNA accumulation upon 5-FU treatment and a possible correlation between EXOSC10 protein levels and 5-FU resistance in malignancies such as colon, breast and skin cancer.

Acknowledgements

First I would like to give my sincerest thanks to my PhD supervisor Michael Primig. I choose his lab is because the PhD project he offered was to study lncRNA, which matches my research interest very much. To study lncRNA is a very important step for me to understand my scientific question (like every established scientist has his or her own scientific question although I am not a scientist yet), which I put forward when I was a master student: how does transcription function in the three-dimensional space to regulate gene expression? My scientific question seems to be recognized by the transcription field: for example, a paper was published in Cell this August by one of the co-discoverers of lncRNA, John Rinn, who put forward the cat's cradle model about how lncRNA transcription shapes a genome's spatial organization to regulate gene expression. This not only confirms the scientific importance and interest of my scientific question, but also gives me confidence and courage to continue pursuing research to answer my question. This also confirms that my choice to study lncRNA during my PhD was right.

After we worked together, I found more and more scientific questions that we both were interested in, which really makes me happy and grateful. I learned the importance of antisense RNA and the naturally endogenous dsRNA in the cell, which is an exciting field. One of my main projects about regulation of *RRP6* by lncRNA is one exciting sample. I and my supervisor have a different view about the function of *MUT1312* in regulating *RRP6*, maybe we are both right, but I still think my idea about *MUT1312* playing a role in protecting *RRP6* during late meiosis and facilitating the fast translation of Rrp6 in the germinating cell could be right and inspire an exciting research direction in the early embryogenesis field. Coherently, the mouse project in his lab shows the importance of *Exosc10* in early embryo development. I think meiotic events are not merely for making meiosis different from mitosis to generate haploid genome, but the true role is to facilitate daughter cell survival. Since no report in the study of maternal RNAs field focuses on the role of lncRNA in masking maternal mRNA, this could be a new discovery, and a new exciting direction to understand meiotic lncRNAs. The second new direction which I am interested in in his lab, is the function of small peptides, which generated from meiotic UTRs or from putative lncRNA as indicated by the published ribosome footprint data, since this could be brand new perspective to understand lncRNAs from their peptide product. Thanks supervisor for giving me the opportunity to know these exciting fields. I feel it is a pity that I did not have a chance to study them, but they could be a potential choice for my future research direction.

It is really not easy to find one person who has same research interest. I am very grateful and very lucky that I had a supervisor who had similar research interests as I, and I thank and appreciate him a lot. It is really a pity that we could not accomplish more.

I thank my friends in American Ms. Ma WQ, for her kind help and advice, Dr. Wang B for his encouragement; my friend in Germany, Dr. Wei YY for her help and encouragement; my friend in China Dr. Wang S for his kind advice and generally sharing the experience, my sincerest thanks to Dr. He J for her kind and generals helps with solving all the experimental problems I encountered during this three years, I thank Dr. Wang W for his kind advice with western and antibody, thank Dr. Peng GX, Dr. Jiang F, Dr. Yang PC, for their kind help and advice with bioinformatics; Ms Han LL, Ms Chen YJ, Dr. Li X, Ms Liang J for their kind helps and support; my friend in France Dr. Zhang LL for her kind helps. Without the support and helps from all of you, I can't persist and pass

through these difficult three years.

I especially thank the new explanation from Ms. Ma WQ about the meaning of ancient Chinese motto from Mengzi, this gives me courage to regain self-confidence and regain my way of pursuing science. I have fallen down and failed, but life consists of pitch and high, I am confident that I will stand up again very soon, I will be back to science soon.

I thank the support from my family members, especially my mother.

I thank the President of the University 1 of Rennes David Alis, vice-president Jean-François Carpentier, IRSET director Bernard Jégou, deputy director Dominique Lagadic, general secretary Christelle Hays, and the director of VAS doctoral school Natalie Theret for their kind help. Thank you to Ned Lamb and Domenico Libri for serving as thesis evaluators in my jury.

I thank all the people who helped me in France inside and outside of the university.

Abbreviations

5’-m7G cap: 5’- 7-methylguanosine cap
5-FU: 5-fluorouracil
ADAR: adenosine deaminase acting on RNA enzyme
AMEN: Antagonist of Mitotic Exit Network
AP/AFE: Alternative promoter and first exon
APA/ ATE: Alternative poly A site and terminal exon
APC/C: Anaphase Promoting Complex/Cyclosome
aslncRNAs: antisense lncRNAs
ASOs: antisense oligonucleotides
CCAT1: Colon cancer associated transcript 1
ceRNA: competing endogenous RNA
CH2THF: 5,10-methylene tetrahydrofolate
circRNA: circular RNA
CRC: colorectal cancer cell
CUTs: Cryptic Unstable Transcripts
DPD: Dihydropyrimidine dehydrogenase
dsRNAs: double stranded RNAs
dTMP: Deoxythymidine Monophospate (nucleotide)
dTTP: Deoxythymidine Triphosphate
dUMP: 2'-Deoxyuridine 5'-Monophosphate
dUTP: Deoxyuridine Triphosphate
E. coli: *Escherichia coli*
EERs: editing-enriched regions
Exo10[44]: Cytoplasmic RNA exosome with core plus Rrp44
Exo11[44/6]: nuclear RNA exosome with core plus Rrp44 and Rrp6
Exo9: RNA exosome core contain 9 subunits
FdUMP: fluorodeoxyuridine monophosphate
H3K36me3: trimethylation of lysine 36 of histone H3
H3K4me3: trimethylation of lysine 4 of histone H3
Hnrnpk: heterogeneous nuclear ribonucleoprotein K
HRDC: helicase and RNase D C-terminal domain
IRES: internal ribosome entry site
ITS: internal transcribed spacers
lincRNA: long intergenic non-coding RNA
lncRNA: long non-coding RNA
MALAT1: metastasis associated lung adenocarcinoma transcript 1
MUTs: Meiotic Unannotated Transcripts
ncRNA: non-coding RNA
ndsRNAs: natural double strand RNAs
NEAT2: noncoding nuclear-enriched abundant transcript 2
NF90: nuclear factor 90
NLS: Nuclear Localization Signal
NMD: Nonsense mediated decay pathway

ORC: origin recognition complex
Pol II: RNA polymerase II
PTGS: post-transcriptional gene silence
Rnp4F: RNA-binding protein 4F
Rrp6: Ribosomal RNA Processing 6
RRS: Ribosome Release Score
sprcRNAs: short, polycistronic ribosome-associated coding RNAs
SUTs: Stable Unannotated Transcripts
Trp53cor1: Tumor protein p53 pathway corepressor 1
TS: Thymidylate synthase
UCA1: urothelial carcinoma associated 1
Uchl1: Ubiquitin carboxyl-terminal esterase L1
uORF: upstream Open Reading Frame
XUTs: Xrn1 deletion sensitive Unstable Transcripts
ZEB2: zinc-finger E-box binding homeobox 2

Introduction

1 . Chemotherapy

1.1 The aim of using chemotherapeutic drugs

Chemotherapy is a major form of cancer treatment. The aim of chemotherapy is curative or to prolong life or to palliate symptoms. Chemotherapeutic drugs are cytotoxic by interfering with cell division (mitosis) and damaging DNA, to damage or stress cells, which may lead to cell death by apoptosis.

1.1.1 Different types of chemotherapeutic drugs act via distinct mechanisms

(1) Alkylating agents

Alkylating agents can alkylate many molecules, like proteins, RNA and DNA. Alkylating agents can bind covalently to DNA via their alkyl group, which impairs DNA replication and repair, and can trigger apoptosis in cancer cells. Alkylating agents used for chemotherapy are mechlorethamine, cyclophosphamide, carmustine, mitozolomide, and thiotepa (Lind M.J., M.J. Medicine, 2008).

(2) Anti-microtubule agents

Anti-microtubule drugs are chemicals isolated from plants, which can inhibit cell division by interfering with microtubule function. Chemotherapeutic drugs in this class are for example paclitaxel, docetaxel, and podophyllotoxin (Rowinsky EK et al., Pharmacology & Therapeutics.1991; Yue QX, et al., Planta Medica.2010; Damayanthi Y et al., Current Medicinal Chemistry. 1998)

(3) Antimetabolites

Antimetabolites are molecules that target DNA and RNA synthesis to inhibit cancer cell growth. They have a similar structure as the nucleotides of DNA and RNA. The mechanism of action of this group of drugs is to block the enzymes required for DNA synthesis by being incorporated into DNA or RNA. In this way, the drug can prevent tumor growth by inhibiting DNA replication and blocking the cell cycle in S-phase. Antimetabolite drugs include cytarabine, gemcitabine, decitabine, and notably 5-Fluorouracil (5-FU), which is one of the most widely used anti-cancer drugs, especially in colon cancer treatment (Lind M.J., M.J. Medicine.2008; Parker WB. Chemical Reviews, 2009).

(4) Topoisomerase inhibitors

Topoisomerase inhibitors affect the activity of topoisomerase I and II. During DNA replication or RNA transcription, the DNA double helix unwinds, which results in supercoil formation in the wound part of DNA, thus the adjacent unopened DNA becomes tighter, and this stress is relieved by topoisomerase I and II. Both topoisomerases introduce single- or double-strand breaks into DNA, thereby reducing the tension in the DNA strand. Inhibitors of topoisomerase I and II will interfere with this process. Commonly used inhibitors for cancer therapy are irinotecan, topotecan, etoposide, and doxorubicin (Lodish H, et al.,2000; Goodsell DS. Stem Cells.2002; Nitiss JL. Nature Reviews. Cancer. 2009)

(5）Cytotoxic antibiotics

Cytotoxic antibiotics include different types of drugs with various mechanism of action. The common mechanism is to interrupt cell division. Major drugs in this group are mitomycin C and actinomycin (Antineoplastic Agents in Encyclopedia of Molecular Pharmacology.2008)

1.1.2 5-FU is widely used as a single or combined chemotherapeutic drug

5-FU is a widely used anti-metabolites type anti-cancer drug. In 1954, Abraham Cantarow and Karl Paschkis observed that radioactive uracil was absorbed more readily in liver tumors than in normal liver cells (Sneader W. Drug Discovery, 2005). Later, Heidelberger and Duschinsky found that 5-FU markedly inhibited tumors in mice. In 1957, Heidelberger et al. reported 5-FU as a promising anticancer drug (Chu E. Clinical Colorectal Cancer.2007; Heidelberger C. Nature.1957).

5-FU was first designed and synthesized as the analog of uracil and has since been widely used as first line of standard chemotherapy regimens for different cancers, like colon cancer (Longley D. B. Nat. Rev. Cancer.2003). However, a large percentage of patients who received 5-FU alone presented with tumor recurrence, which is caused by acquired drug resistance of exposed cancer cells. To solve this problem, strategies such as using combinations of chemotherapeutic drugs have been used in clinical chemotherapy. The commonly used combinations are 5-FU together with alkylating agents such as cisplatin. However, this treatment cannot permanently overcome the phenomenon of drug resistance. One key issue is that the mode of action of 5-FU is still not completely understood.

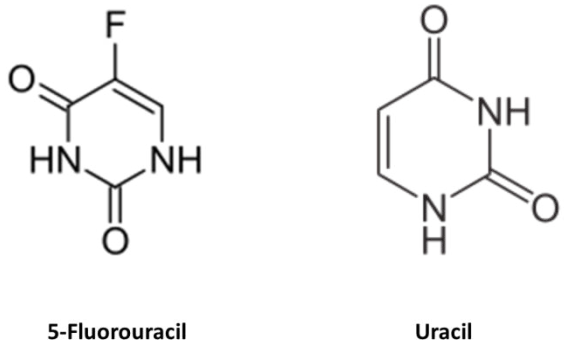

5-Fluorouracil Uracil

Figure 1. The structure of 5-Fluorouracil. Molecular structures of 5-FU and uracil are displayed. The image is from Valeriote et al., Pharmacol Ther. 1984.

1.2 Mechanism of 5-FU action

5-FU can inhibit cell growth via DNA based and RNA based mechanisms. 5-FU causes DNA damage by inhibiting Thymidylate Synthase (TS), and exerts RNA-based cytotoxicity by inhibiting Rrp6, which is a 3'-5' exoribonuclease conserved from yeast to human (Longley D. B. Nat. Rev. Cancer, 2003).

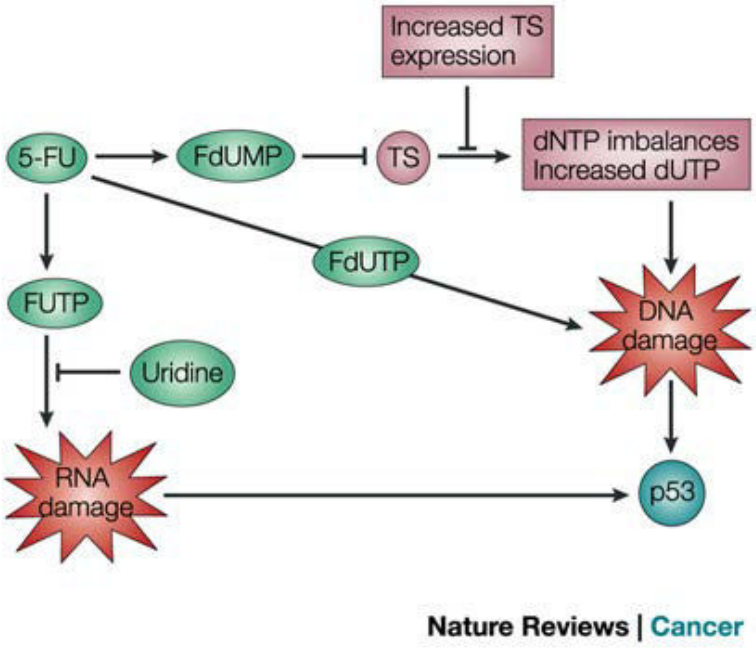

Figure 2. Activation of p53 by 5-fluorouracil. 5-Fluorouracil (5-FU) can activate p53 by more than one mechanism: incorporation of fluorouridine triphosphate (FUTP) into RNA, incorporation of fluorodeoxyuridine triphosphate (FdUTP) into DNA and inhibition of thymidylate synthase (TS) by fluorodeoxyuridine monophosphate (FdUMP) with resultant DNA damage. TS-directed cytotoxicity is abrogated by increased TS expression, whereas RNA directed cytotoxicity can be abrogated by increasing the intracellular levels of uridine. The image is from Longley DB., et al., Nature Reviews Cancer.2003

1.2.1 TS is the target of 5-FU

Since 5-FU is an analog of uracil, it can be metabolized into fluorodeoxyuridine monophosphate (FdUMP) to inhibit Thymidylate Synthase (TS). Inhibition of TS will result in inhibition of synthesis of Deoxyuridine Triphosphate (dUTP), since TS is the enzyme that converts 2'-Deoxyuridine 5'-Monophosphate (dUMP) to Deoxythymidine Monophospate (dTMP), which is the only source of *de novo* thymidylate synthesis. Its activity thus leads to a drop of Deoxythymidine Triphosphate (dTTP) concentration in the cell, and thereby affects the synthesis of DNA during DNA replication in S-phase. dFUTP can also incorporate into DNA through the replication process to therefore leads to DNA damage, which triggers the DNA repair process. (Longley D. B, et al. Nat. Rev. Cancer.2003).

Thymidylate synthase uses 5,10-methylene tetrahydrofolate (CH2THF) as the methyl donor. It catalyzes the conversion of dUMP to dTMP. The 5-FU metabolite FdUMP binds to the nucleotide-binding site and forms a stable ternary complex with TS and CH2THF, to block dUMP to get access to the nucleotide-binding site of TS and inhibit dTMP synthesis. This decreases the dTTP pool and elevates the level of dUTP in the cell, both of which will lead to DNA damage. (Longley D. B, et al. Nat. Rev. Cancer.2003).

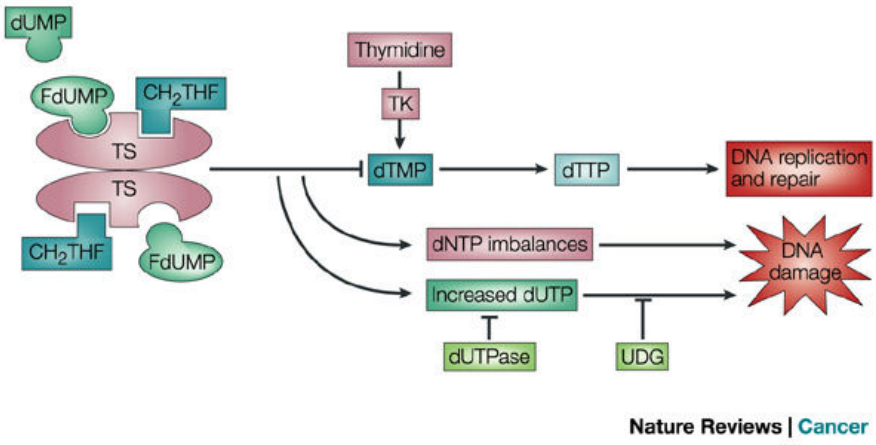

Figure 3. Mechanism of thymidylate synthase inhibition by 5-fluorouracil. Thymidylate synthase (TS) catalyzes the conversion of deoxyuridine monophosphate (dUMP) to deoxythymidine monophosphate (dTMP) with 5,10-methylene tetrahydrofolate (CH2THF) as the methyl donor. The 5-fluorouracil (5-FU) active metabolite fluorodeoxyuridine monophosphate (FdUMP) binds to the nucleotide-binding site of TS and forms a stable ternary complex with TS and CH2THF, blocking access of dUMP to the nucleotide-binding site and inhibiting dTMP synthesis. This results in deoxynucleotide (dNTP) pool imbalances and increased levels of deoxyuridine triphosphate (dUTP), both of which cause DNA damage. The extent of DNA damage caused by dUTP is dependent on the levels of the pyrophosphatase dUTPase and uracil-DNA glycosylase (UDG). dTMP can be salvaged from thymidine through the action of thymidine kinase (TK). Image from Longley D. B, et al. Nat. Rev. Cancer, 2003.

1.2.2 Rrp6 is a target of 5-FU

1.2.2.1 The RNA Exosome

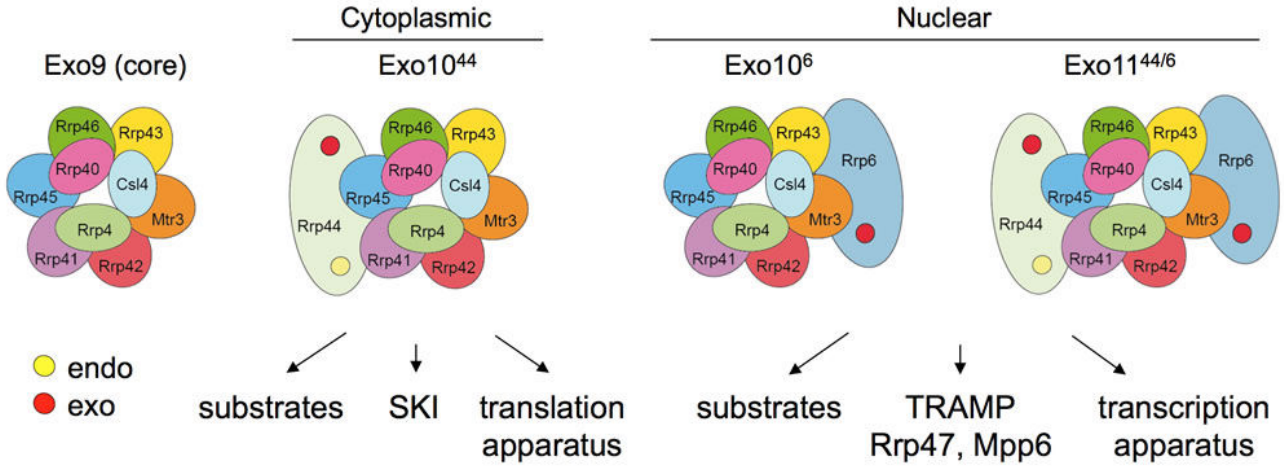

Figure 4. Component of exosome. Different forms of the exosome are given. Image from hhmi.org

The RNA exosome contains multiple subunits one of which is Rrp6, a 3'-5' exoribonuclease that can degrade and process RNA. The exosome in eukaryotic cells contains 9 core subunits (Exo9), and Rrp6 and Dis3 ribonucleases that are conserved among prokaryotic, archaea, and eukaryotic species (Januszyk K, Lima C, et al. 2014 Current Opinion in Structural Biology).

The eukaryotic exosome is present in the cell in two forms: (1) the cytoplasmic RNA exosome, comprising the exosome core (Exo9) and Dis3/Rrp44, and (2) the nuclear RNA exosome which is thought to contain Rrp6. Both of the forms interact with other co-factors to degrade or process particular target RNAs (Januszyk K, Lima C, et al. 2014 Current Opinion in Structural Biology; Butler J S and Mitchell P, RNA exosome, chapter 8, 2010).

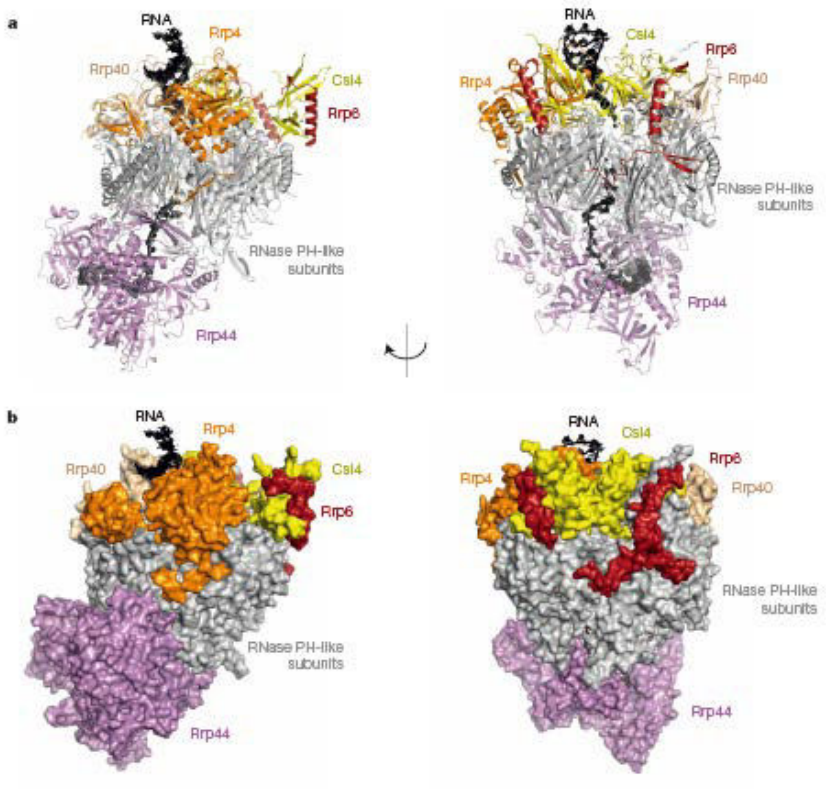

Figure 5. The crystal structure of a yeast exosome–RNA complex. a, b, The structure of S. cerevisiae Exo10–Rrp6C-term–RNA is shown as ribbon (a) and surface (b) representations in two orientations related by a ,90u rotation around a vertical axis. RNA is in black, together with the simulated annealing omit map (contoured at 2.5s). The exosome-binding region of Rrp6 wraps around Csl4 and contacts the RNase PH ring (right). The Rrp4 N-terminal tail reaches across the RNase PH-like barrel towards the N-terminal region of Rrp44 (left). RNA is enclosed in the complex (b).Image is from Makino DL, et al. Nature.2013

1.2.2.2 Rrp6

Rrp6 (ribosomal RNA processing) was first found in yeast by genetic selection for suppressors of a polyadenylation defect gene. The gene is the yeast homologue of human EXOSC10 (also called PM-Scl 100) and *E. coli* 3'-5' exoribonuclease RNase D (Briggs M, et al. The journal of biological chemistry, 1998).

Rrp6 contains a N-terminal domain, an Exo-domain, an HRDC domain (helicase and RNase D C-terminal), and a C-terminal Nuclear Localization Signal (NLS).

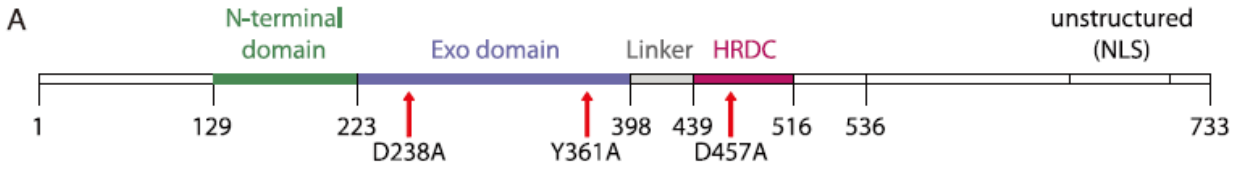

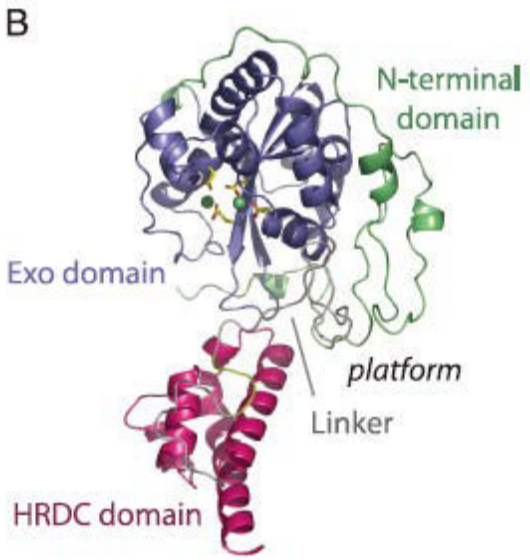

Figure 6. Structure of Rrp6. (A) Rrp6p sequence overview. Colored-coded segments are part of the current structure showing the N-terminal domain (green),exonuclease domain (blue), linker (gray), and HRDC domain (red). (B) Overview of the Rrp6p structure using the same color code as A. The ions and side chains in the active site are shown as balls and sticks. Image from Midtgaard SF., et al., PNAS. 2006.

Rrp6 is involved in processing of rRNA and the degradation of different categories of non-coding RNAs and mRNAs, including Cryptic Unstable Transcripts (CUTs). Eukaryotic ribosome 25S, 18S, and 5.8S rRNAs are transcribed as a single transcript with two internal transcribed spacers (ITS1 and ITS2), the long transcript undergo complex processing steps to remove the internal spacers then produce mature 25S, 18S, and 5.8S rRNA. ITS1 separate 18S rRNA from 5.8S rRNA, ITS2 separate 5.8S rRNA from 25S rRNA.

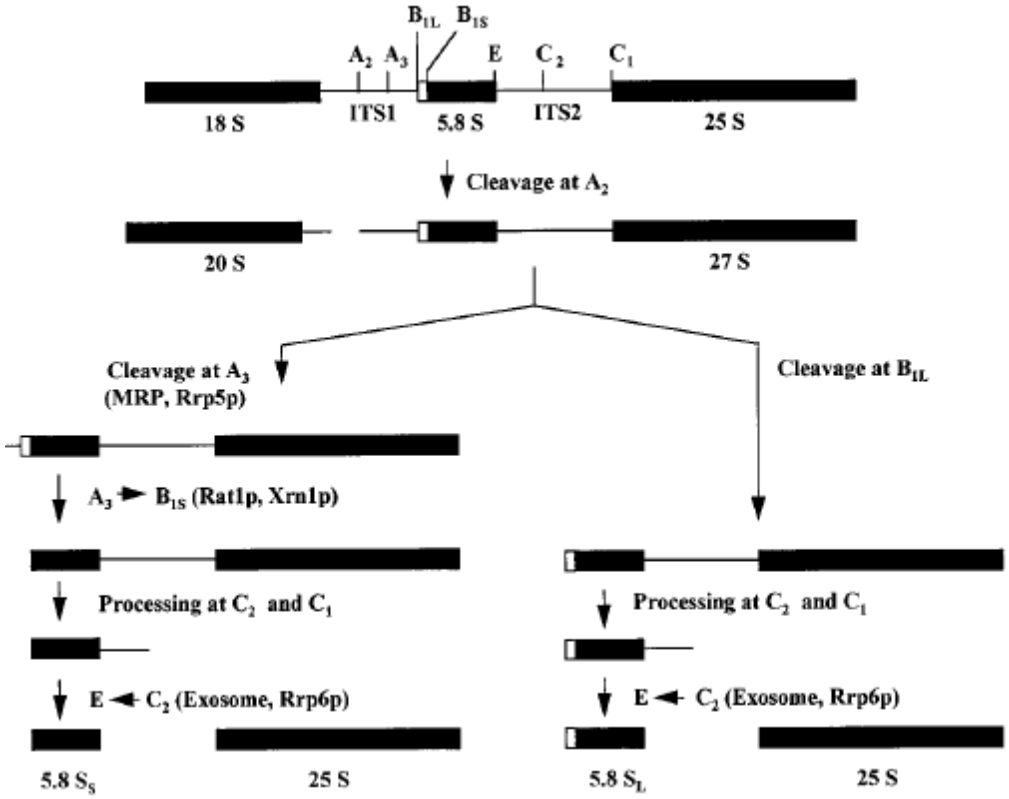

Figure 7. Diagram of the major processing events involved in removal of ITS1 and ITS2 from pre-rRNA. Image from Briggs MW., J, Biol. Chem, 1998.

As illustrated in Figure 7, the RNA exosome is responsible for the separation of 5.8S rRNA and 25S rRNA, cleavage and 3' end trimming of 5.8S rRNA. Particularly, Rrp6 is responsible for the removal of 30 nucleotides from the 3' end of 5.8S rRNA precursor. In an *rrp6* recessive mutant, a novel 5.8S rRNA processing intermediate accumulates, called 5.8S*, which has a normal 5' end, and an elongated 3' end because it retains 30 nucleotides of *ITS2*. Thus, Rrp6 is important for 5.8S rRNA 3'end formation (Michael W. Briggs, et al., JBC.1998).

Rrp6 also plays an important role in the maturation of snoRNAs. In *rrp6* deletion mutant, polycistronic snoRNAs with extended forms are accumulated and independently transcribed snoRNAs also accumulate (Midtgaard S, et al. PNAS.2006).

1.2.2.3 Rrp6 can target different RNAs as the core subunits and Rrp44

A genome wide study of the target of exosome core component and co-factors Rrp6 and Rrp44, as shown in Figure 8, revealed that core components have overlapping targets, while Rrp6 more specifically targets small, structured RNAs including tRNA, snoRNAs and snRNAs.

Rrp6 in budding yeast is thought to located in only in the nucleus, whereas the core components of the exosome are located in both nucleus and cytoplasm. Consistent with this, pre-mRNAs are more targeted by Rrp6 than by the core component and its associated exoribonuclease. In a CRAC-Seq experiment, which crosslinks RNA with RNA binding proteins *in vivo* then uses antibodies to pull down the crosslinked transcripts for RNA sequencing, the highest number of reads that mapped to introns were found associated with Rrp6. Since introns are removed in the nucleus, this result possibly shows that Rrp6 has major role in degradation of excised introns and pre-mRNA. The mRNAs preferentially bound by Rrp6 are enriched in a cluster of genes with introns, ribosomal protein genes, and genes that encode ribosome synthesis factors (Schneider C, et al., Mol Cell, 2012).

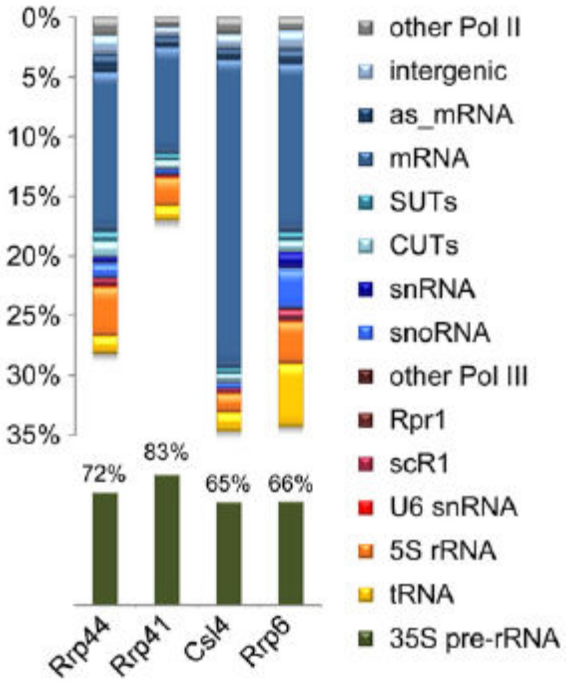

Figure 8. Targets of Exome. Image from Schneider C, et al., Mol Cell, 2012

1.3 Mechanism of resistance to 5-FU

The primary well known activity of 5-FU is to inhibit TS, thus causing a decreased level of dTMP. However, dTMP can also be synthesized by thymidine kinase (TK) through conversion of thymidine. Thus, it can alleviate the consequence of TS deficiency. This compensation pathway may represent a potential mechanism of resistance to 5-FU (Grem J.L. and Fischer. P.H Pharmacol. Ther 1989. Daniel B.L. et al. Nat Rev Cancer. 2003).

5-FU can be degraded by Dihydropyrimidine dehydrogenase (DPD) to DHFU, which cannot be absorbed by cells. Patients who are deficient in DPD display systemic toxicity in response to 5-FU. On the contrary, patients who express higher levels of DPD mRNA show resistance to 5-FU (Salonga D. et al., Clin Cancer Res. 2000. Daniel B.L. et al. Nat Rev Cancer. 2003).

Genome wide gene expression studies showed that in addition to the increase of TS mRNA in 5-FU resistant cells, multidrug resistant genes MDR3 and MDR4 also display expression patterns significantly correlated with 5-FU sensitivity (Zembutsu, H. et al. Cancer Res. 2002). The elevated level of both mRNA and protein of nuclear factor κB (NFκB) p65 and related anti-apoptotic c-Flip gene was detected in resistant cells. NFκB DNA-binding activity has also been found increased in 5-FU resistant cell lines, while other key genes involved in 5-FU activity, like thymidine kinase, were significantly down-regulated in 5-FU resistant cells (Wang W et al., Cancer Research 2004.).

In addition to mRNAs, some studies have shown that non-coding RNAs also have an important impact on 5-FU resistance. Lee et al., reported that snaR, a 117nt long non-coding RNA transcribed by RNA polymerase III and associated with nuclear factor 90(NF90), is downregulated in 5-FU resistant colon cancer cells. Down-regulation of snaR increases the viability of cells treated with 5-FU, which suggests that snaR negatively regulates 5-FU resistance (Lee et al. Mol Cells. 2014). Long non-coding RNA urothelial carcinoma associated 1(UCA1) has been found have the ability to promote tumor growth *in vivo* (Wang et al. Cancer Res 2006). Bian et al, reported that UCA1 can increase the resistance of colorectal cancer (CRC) cells to 5-FU by inhibiting apoptosis. UCA1 inhibits miR-204-5p by serving as a small RNA sponge. As a consequence, the target of miR-204-5p, CREB1, shows an elevated expression level (Bian Z, et al. Scientific reports 2016).

2. Protein coding and non-coding RNAs

RNAs have important roles in the cell. Francis Crick has put forward the concept of what is called the central dogma of molecular biology in 1970 (Crick F. Nature 1970). It stipulates that genetic information encoded by DNA is first transcribed into mRNAs, which are then translated into biologically active proteins.

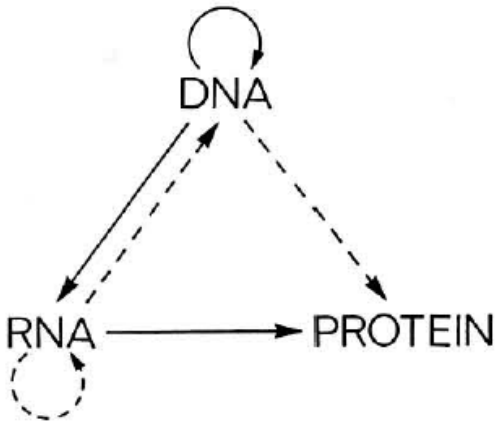

Fig. 3. A tentative classification for the present day. Solid arrows show general transfers; dotted arrows show special transfers. Again, the absent arrows are the undetected transfers specified by the central dogma.

Figure 9. The central dogma of molecular biology. Image from Crick F. Nature 1970

However, this initial perception about the role of RNA is incomplete, since many RNAs have been found which unlike mRNAs do not encode proteins, including tRNAs, rRNAs, and snRNA. Currently, more types of RNA molecules which do not appear to encode proteins have been found in the transcriptome, such as small non-coding RNAs like miRNAs, siRNAs and piRNAs by ultra-high throughput RNA-Sequencing. Small non-coding RNAs have important roles in regulating gene expression: miRNAs and siRNAs can inhibit translation by forming double-stranded RNA with their target RNA (post-transcriptional gene silencing; PTGS). They can also enhance gene expression by promoting translation, for example in insects where they promote egg-hatching synchrony by up-regulating their target genes (He J., et al. PNAS.2016) and in the ancient protozoan *Giardia lamblia*, where miRNA miR3 enhances translation when it is fully complementary with its target (Ashesh A. Saraiya, et al. PLoS One 2013). piRNAs also have important roles in negatively regulate gene expression in reproductive and nervous systems like brain (Siomi MC et al., Nat Rev Mol Cell Biol 2011; Rajan KS and Ramasamy S. Neurochem Int. 2014).

2.1 What are long-non-coding RNAs?

Recent advances in RNA profiling and computational analysis techniques have enabled a deep understanding of the transcriptome. Many loci have been found, which produce RNA transcripts >200 bases that appear to have little or no coding potential - they are called **long non-coding RNAs (lncRNAs)**.

In 2009, Guttman M, et al., reported the first comprehensive study of long non-coding RNAs in a genome. The authors used chromatin signatures to identify large non-coding RNAs in the mouse. Genes actively transcribed by RNA polymerase II (Pol II) have the histone marker H3K4me3 (trimethylation at lysine 4 of histone H3) in their promoters and H3K36me3 (trimethylation at lysine 36 of histone H3) in their transcribed regions; this distinctive structure is called "K4-K36" domain. They systematically discovered lincRNAs (Large intergenic non-coding RNAs) by identifying this K4-K36 domain structure outside of know protein coding gene loci and identified 1600 lincRNAs in four mouse cell types (Guttman M, et al. Nature. 2009).

Later studies found that lncRNAs are very much like mRNAs in several ways: the genomic loci of lncRNAs have similar features as mRNAs: lncRNAs are also transcribed by RNA polymerase II (PolII); they have a 5' cap, a 3' Poly(A) tail, and they can be spliced. However, there are distinct features that distinguish lncRNAs from mRNAs: first, the sequences of lncRNAs are not conserved among different species to the exception of lncRNAs in promoters in mice and human; second, lncRNAs typically show lower expression levels than mRNAs; third, lncRNAs are shorter than mRNAs; fourth, lncRNAs have fewer exons but they are longer than those in mRNAs (Quinn J and Chang Howard. Nature Reviews Genetics. 2016).

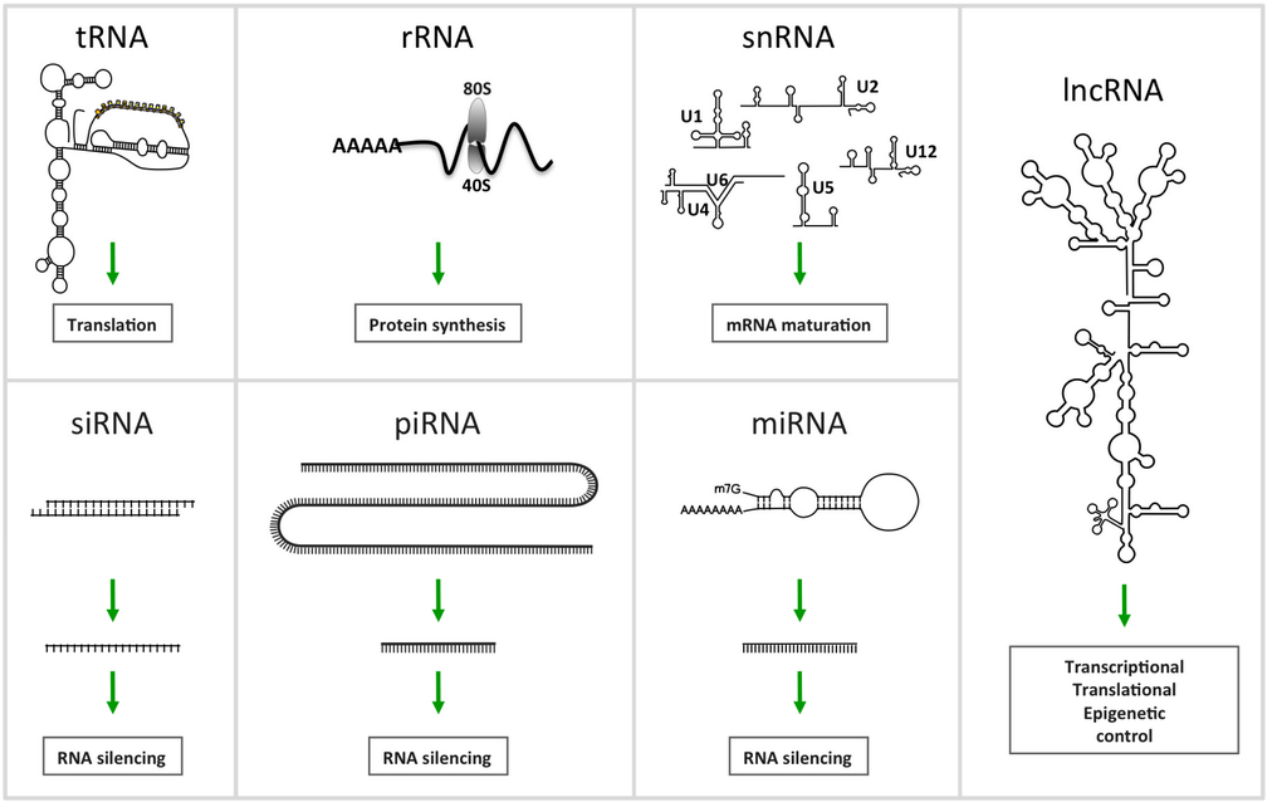

Figure 10. Categories of non-coding RNAs. Image from Morceau F, et al., Int. J. Mol. Sci. 2013

2.2 Function of long non-coding RNAs

How do lncRNAs function? Do some of them encode proteins? lncRNAs play important roles in connecting and mediating different component in the cells, protein complexes, genes, and chromosomes to reach appropriate place and function as activators and repressors of gene expression (Batista P. and Chang HY. Cell. 2013; Quinn J and Chang Howard. Nature Reviews Genetics. 2016).

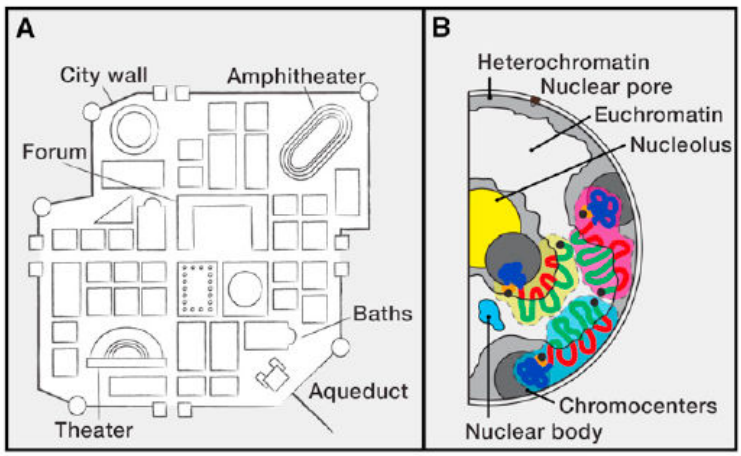

Figure 11. Comparison between a Roman City and the Cell Nucleus Reveals the Importance of Spatial Organization

(A) Depiction of the basic features of a Roman city. City walls delimit the city, with gates at the two main roads that intersect at the center of the city. The Forum was the business and political center of the city, and many buildings provided specific functions that were essential for city life. (B) Schematic representation of the typical nuclear organization during interphase. Each chromosome occupies a discrete territory. Euchromatin localizes to the interior

regions of the nucleus, and the densely compacted heterochromatin localizes near the nuclear envelope. Many specialized functions are executed in distinct regions in the nucleus, known as nuclear bodies. One example is the nucleolus, where ribosomes are assembled. Figure from Pedro J. Batista and Howard Y. Chang. Cell.2014.

LncRNA participate in nearly every steps of gene expression, from transcription to translation, from splicing to decay.

From a functional perspective lncRNAs can be divided into three categories: (1) lncRNA transcripts without any function, they are merely the result of transcription noise; (2) lncRNAs that function via their transcription; (3) lncRNAs that act in *cis* or in *trans* to regulate gene expression.
Unlike mRNAs which are translated into protein (isoforms), lncRNAs are thought do not encode proteins. However, the important question of the ability of lncRNAs to encode proteins is currently under debate. Ingolia N T, et al use mouse embryonic stem cells to do ribosome profiling and found that most of the lncRNAs are associated with ribosomes and have multiple small open reading frames (sORFs), and nearly half of the previously found candidate lncRNAs which are required for pluripotency are actually bound by active elongating ribosomes (Ingolia NT, et al., Science. 2009). The authors named those lncRNAs as short, polycistronic ribosome-associated coding RNAs (sprcRNAs). The author also identified thousands of true ncRNAs, which do not have ribosome associated with them, like the lncRNA NEAT1, which is important in RNA export. The phenomenon of ribosome binding to ncRNAs is not limited to mouse: Brar G, et al. used ribosome profiling to study the budding yeast meiotic program, and they also found that some ncRNAs in budding yeast are associated with ribosomes, for example MUT1465 (Brar GA, et al., Science.2012).

Contrary to the study above, the follow up study done by Guttman M, et al, re-analyzed the same dataset produced in Ingolia N T, et al's experiment, but they used a stringent metric, ribosome release score to distinguish between productive ribosome (translating ribosome) and non-productive ribosome (scanning ribosome). The metric is based on the known principle of translation that translating ribosome will release and disassemble from mRNA when they encounter a true stop codon. The metric successfully distinguished between classical ncRNAs (like snoRNAs, RNase P RNA) and protein coding mRNAs. The authors used this metric and found that both classical ncRNAs and lncRNAs show the same ribosome occupancy as the scanning ribosomes on the 5'-UTR region. The Ribosome Release Score (RRS) shows that unlike protein coding mRNAs, the lncRNAs are the same as 3'UTR, 5'UTR, and classical ncRNAs which rarely have the known signature of translational termination. Consequently, the study reaches the opposite conclusion as

the original ribosome profiling study (Guttman M et al., Cell. 2013).

Proteomic approaches have also been used to detect the translation ability of lncRNAs. By using sensitive mass spectrometry, the researchers also failed to detect translation protein products of 92% GENCODE lncRNAs. Other mass spectrometry studies found poly-peptide products of classical lncRNAs, such as H19, but protein products are not identified in common lncRNAs. Taken together, these results support that idea that lncRNAs normally do not encode a translation product. (Banfai, B. et al. Genome Res. 2012; Gascoigne, D. K. et al. Bioinformatics. 2012)

2.2.1 Long non-coding RNAs can regulate gene expression at the transcriptional level

Long noncoding RNA regulate mRNA transcription mainly via transcription interference, whereby transcription of antisense long noncoding RNA inhibits the transcription of the overlapping sense mRNA. Another type is promoter interference where the lncRNAs is transcribed over a protein-coding gene's regulatory region. Transcription interference is a cis-regulatory event, in which the transcription itself but not the RNA molecule has a biological function.

2.2.2 Long non-coding RNAs regulate gene expression at post-transcriptional level

lncRNAs can regulate mRNA expression at various post-transcriptional processing steps, including post-transcriptional splicing and editing, translation, mRNA stability, and miRNA expression.

In mammalian cells, lncRNs can influence the splicing patterns of mRNAs directly, possibly by masking the splice site and preventing spliceosome recognition and recruitment. For example, antisense long non-coding RNAs can regulate the splicing patterns of *MYC*, and *ZEB2* (zinc-finger E-box binding homeobox 2). For *MYC*, antisense lncRNA forms an RNA duplex with MYC mRNA to inhibit its splicing. In the case of *ZEB2*, the antisense lncRNA suppresses the splicing of an internal ribosome entry site (IRES)-containing intron, which is needed for translation initiation. Via this mechanism the translation of *ZEB2* mRNA is enhanced by antisense lncRNA (Beltran, M. et al. Genes Dev. 2008; Hastings, M. L., Nucleic Acids Res.1997; Krystal, G. W., Mol. Cell. Biol.1990; Munroe, S. H. J. Biol. Chem.1991).

lncRNAs can also affect splicing in indirect ways, like in the case of *MALAT1* (metastasis associated lung adenocarcinoma transcript 1) also known as NEAT2 (noncoding nuclear-enriched

abundant transcript 2), which is a long non-coding RNA with multiple regulatory functions including splicing, nuclear organization, epigenetic modulation, and pathological processes such as cancer. (WU Y., et al., Current Pharmaceutical Design 2015; Yoshimoto R, et al., Biochemica et Biophysica Acta. 2016). *MALAT1* influences splicing by interacting with splicing activator Ser/Arg proteins, thus altering the distribution and the level of phosphorylated Ser/Arg protein. Thus, it indirectly changes the mRNA splicing patterns that *MALAT1* targeted.

Antisense lncRNAs also have the potential to influence mRNA editing. In *Drosophila* Rnp4F (RNA-binding protein 4F) forms a double strand region with the 3'UTR of antisense mRNA to allow ADAR enzyme (adenosine deaminase acting on RNA) to do RNA editing to convert adenosine to inosine. lncRNA could also have the potential to regulate mRNA editing in a similar way (Peters N T., et al. RNA. 2003).

In addition to influence mRNA splicing and editing, antisense lncRNAs have also been reported to regulate translation in various kinds of organisms. The mouse *Uchl1* (Ubiquitin carboxyl-terminal esterase L1) locus contains an antisense lncRNA, which is located divergently with *Uchl1*, i.e. head to head overlap 73 nucleotides with the 5'UTR of *Uchl1*. The antisense lncRNA AS *Uchl1* has a role in enhancing the translation of *Uchl1* by overlapping with the 5'UTR: this role is mediated via a SINEB2 motif in the antisense lncRNA transcript that activates polysome translation (Carrieri, C. et al., Nature. 2012). As opposed to activating translation, yeast antisense lncRNA of *KCS1* was reported to inhibit translation by promoting the production of a truncated Kcs1 protein (Nishizawa et al., PLoS Biol. 2008).

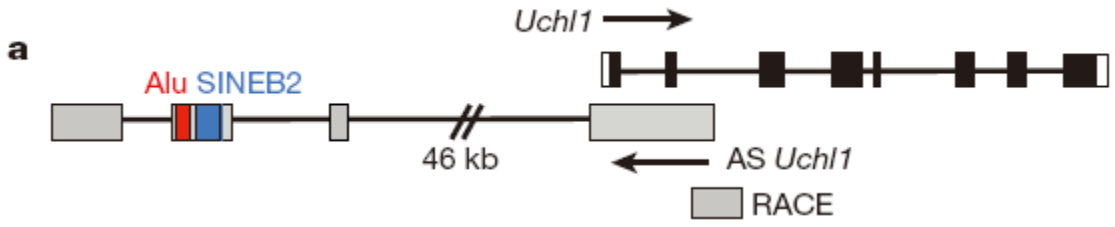

Figure 12. Uchl1/antisense (AS) Uchl1 genomic organization. Uchl1 exons are in black; 3′ and 5′ UTRs are in white; antisense Uchl1 exons are grey; repetitive elements are in red (Alu) and blue (SINEB2). Introns are indicated as lines. Image from Nishizawa et al., PLoS Biol. 2008

Apart from influencing translation by direct base-pairing with sense mRNAs, lncRNAs also have indirect roles in regulating translation by serving as a sort of molecular sponge to sequester negative

regulators of translation such as miRNAs. This kind of lncRNA is called competing endogenous RNA (ceRNA). Like the lncRNA linc-MD1 which is a muscle-specific long non-coding RNA that controls muscle differentiation by serving as a competing endogenous RNA. Linc-MD1 can bind to miR133 and miR135 to relieve their suppressor activity on MAML1 and MEF2C, which are important transcription factors for muscle-specific gene expression (Cesana, M. et al., Cell.2011). Furthermore, another kind of important and possibly conserved regulatory lncRNA, circular RNA (circRNA) was found have roles in sequestration of miRNAs and indirect activation of target gene translation (Hansen, T. B. et al. Nature.2013, Memczak, S. et al., Nature.2013). In addition to sequester miRNAs, lncRNA *rncs-1* in *Caenorhabditis elegans* was reported to bind *Dicer* through the double strand helix in its sequence, however, unlike mRNA-miRNA pairs, *rncs-1* has an inhibitory secondary structure flanking its double strand helix, and therefore it cannot be cleaved by Dicer. Thereby, *rncs-1* indirectly elevates target mRNA levels (Hellwig, S. & Bass, B. L. PNAS. 2008).

2.3 Regulation of long non-coding RNAs

lncRNAs expression is often spatially and temporally regulated, which is consistent with the idea that lncRNA have important functions in cells, including gene expression, such as gene-dosage compensation, epigenetic regulation, cell cycle control, imprinting, nuclear and cytoplasmic trafficking, transcription, translation, splicing, and cell differentiation (Wapinski O, Chang HY Trends in cell biology, 2011).

2.4 lncRNA and cancer

As the body of knowledge about lncRNAs grows, more evidence shows the link of dysregulation of lncRNAs and human diseases: the involvement of lncRNA in human disease is more common than previously thought (Wapinski O and Chang HY, Trends in cell Biology 2011).

Schmitt A and Chang HY reported that inhibition of two lncRNAs that bind to and regulate the function of the androgen receptor can block the growth of prostate-cancer cells, which are resistant to hormone therapy owing to a mutation in the androgen receptor (Schmitt A and Chang HY. Nature. 2013).

A growing number of studies reveal the involvement of lncRNAs in cancer. Since lncRNAs are regulated by transcription factors, they are tightly controlled in fundamental cellular processes. lncRNAs participate in both tumor suppress pathway and oncogene activation pathway. Tumor protein p53 pathway corepressor 1 lincRNA-p21 (Trp53cor1) interacts with heterogeneous nuclear

ribonucleoprotein K(Hnrnpk) protein to exert p53-dependent transcriptional repression, and thus leads to apoptosis (Huarte M., Cell. 2011). In addition to their roles in tumor suppressor pathways, numerous lncRNAs been found to function in proto-oncogene regulation. For instance, lncRNAs were reported to regulate MYC, PCAT1, MYCLo-1, MYCLo-2, PRNCR1 and CCAT1. Colon cancer associated transcript 1(CCAT1) was reported to promote long-range chromatin looping to regulate MYC transcription (Xiang J F., et al Cell Res. 2014; Calin G A, et al. Cancer Cell 2007).

Table 1 Examples of lncRNAs with tumor-suppressor or oncogenic function (see Supplementary Table 1)

Symbol[a]	Accession no.[b]	Cancer phenotype	Cancer association	Mechanism	Ref.
GAS5	Ensembl ID: ENSG00000234741	Induces cell arrest and sensitizes cells to apoptosis. Alters cell metabolism	Downregulated in breast cancer	Outcompetes DNA binding to the glucocorticoid receptor (GR)	102,103
LINC-PINT (MKLN1-AS1)	GEO profile: FLJ43663	Inhibits cell proliferation and promotes apoptosis	Downregulated in colorectal cancer	Interacts with PRC2 to silence gene targets	38,65
MEG3	Ensembl ID: ENSG00000214548	Inhibits cell proliferation	Downregulated in multiple tumor types	Downregulates MDM2 and promotes p53 accumulation. Also controls expression of gene loci through recruitment of PRC2	82,128
NBAT1 (CASC14)	GEO profile: LOC729177	Inhibits cell proliferation and invasion, and impairs differentiation of neuronal precursors	High expression predicts a good clinical outcome of neuroblastomas. CpG methylation and a high-risk neuroblastoma-associated SNP contribute to low expression	Promotes the silencing of *REST* by PRC2	32
PR-lncRNA-1	Ensembl ID: ENST00000562178.1	Inhibits cell proliferation, and promotes apoptosis	Downregulated in colorectal cancer	Enhances p53 transcriptional activation	40
PTENP1		Inhibits cell proliferation, migration, invasion and tumor growth	Locus selectively lost in sporadic colon cancer, prostate cancer and melanoma	Decoy for microRNAs that target *PTEN*	111,114
CDKN2B-AS1 (ANRIL, p15AS)	Ensembl ID: ENSG00000240498	Promotes cell proliferation	Cancer-associated SNPs and high expression linked to bad prognosis in prostate and gastric cancer	Epigenetic silencing of the locus by interaction with CBX7 and PRC2	7–11
BCAR4	Ensembl ID: ENSG00000262117	Promotes proliferation and migration	Expression correlates with advanced breast cancer, metastasis and anti-estrogen resistance	Activates the hedgehog/GLI2 transcriptional program, by binding to and activating the transcription factors SNIP1 and PNUTS	106,107
HOTAIR	Ensembl ID: ENSG00000228630	Promotes metastasis	Overexpressed in liver, metastatic breast, lung and pancreatic tumors	Acts as scaffold for the chromatin repressors PRC2 and LSD1. Silences *HOXD* and other gene loci	6,76,97
MALAT1 (NEAT2)	Ensembl ID: ENSG00000251562	Promotes cell proliferation and metastasis	Overexpressed in lung adenocarcinoma, breast, pancreatic, colon, prostate and hepatocellular carcinomas. SNP linked to hepatocellular carcinoma	Related to alternative splicing and active transcription. Conserved tRNA-like sequence at the 3′ end cleaved off and processed to generate a short tRNA-like ncRNA (mascRNA)	20–25,129
PCAT1	Ensembl ID: ENST00000561978.1	Promotes cell proliferation	Upregulated in prostate cancer. Contains disease-associated SNPs	Interacts with PRC2 and silences genes *in trans*. Also post-transcriptionally activates c-MYC, and inhibits *BRCA2*	89–91
SCHLAP1 (PCAT11)	NCBI Reference Sequence: NR_104321.1	Promotes invasion and metastasis	Upregulated in prostate cancer	Interacts with SWIF/SNIF complex and antagonizes its regulatory functions genome-wide	101

[a]Official symbols are given; symbols in parentheses are alternate symbols. [b]Ensembl Genome Browser, Gene Expression Omnibus (GEO), or other accession IDs.

Table 1. Examples of lncRNA with tumor suppressor or oncogenic functions. From (Huarte M. Nature Medicine.2015)

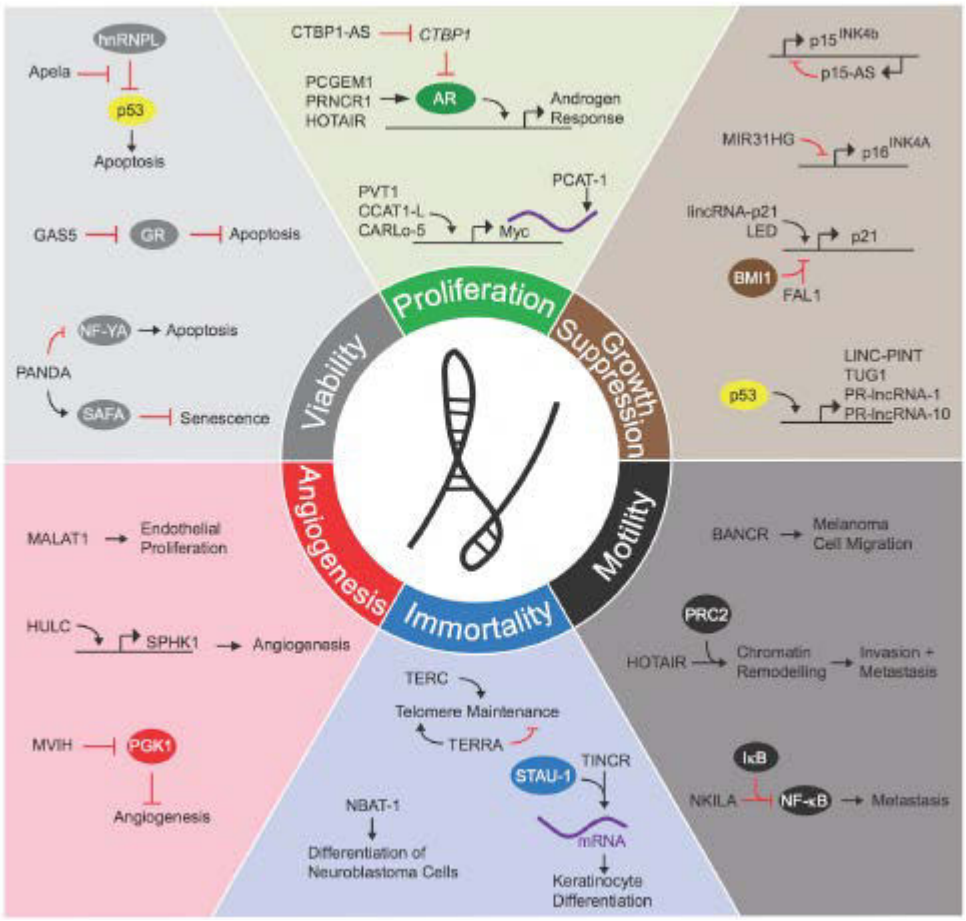

Figure 13. lncRNAs function in various cellular processes. Image from Schmitt AM and Chang H. Cell. 2016.

2.4.3 lncRNAs as novel therapeutic targets in cancer

lncRNAs have become the new targets of cancer therapy. Research about lncRNA-targeting therapeutics now focuses on multiple ways to modulate lncRNAs in order to inhibit cancer. The strategies are depletion of lncRNAs, altering lncRNA splicing to excise functional exon in the target mRNA and steric blocking oligonucleotides to disrupt the interaction between lncRNA and its binding partner (Kole et al., 2012). For the depletion of lncRNAs, certain studies used RNAi to down regulate lncRNA, while others employed antisense oligonucleotides(ASOs), which form RNA/DNA hybrids with target mRNAs that trigger cleavage of hybrids by RNaseH, thereby substantially depleting the target mRNA levels (Ideue et al., 2009). For example, in a mouse model where *Malat1* promotes the growth and metastasis of MMTV-PyMT breast cancer, ASO targeting of Malat1 was shown to increase cell adhesion, promote cystic differentiation and decrease the migration. This shows the efficiency of ASO in vivo (Arun et al. 2016).

2.5 lncRNA in budding yeast

2.5.1 The life cycle of budding yeast *Saccharomyces cerevisiae*

The budding yeast *S. cerevisiae* is a single cellular organism. It exists in both haploid and diploid forms that undergo cell proliferation, whereby a mother cell produces a genetically identical daughter cell via budding. Diploid cells can reduce their ploidy via meiosis to produce haploid spores that can germinate and either grow or mate to produce a diploid cell (Herskowitz I. Microbiological Reviews 1988)

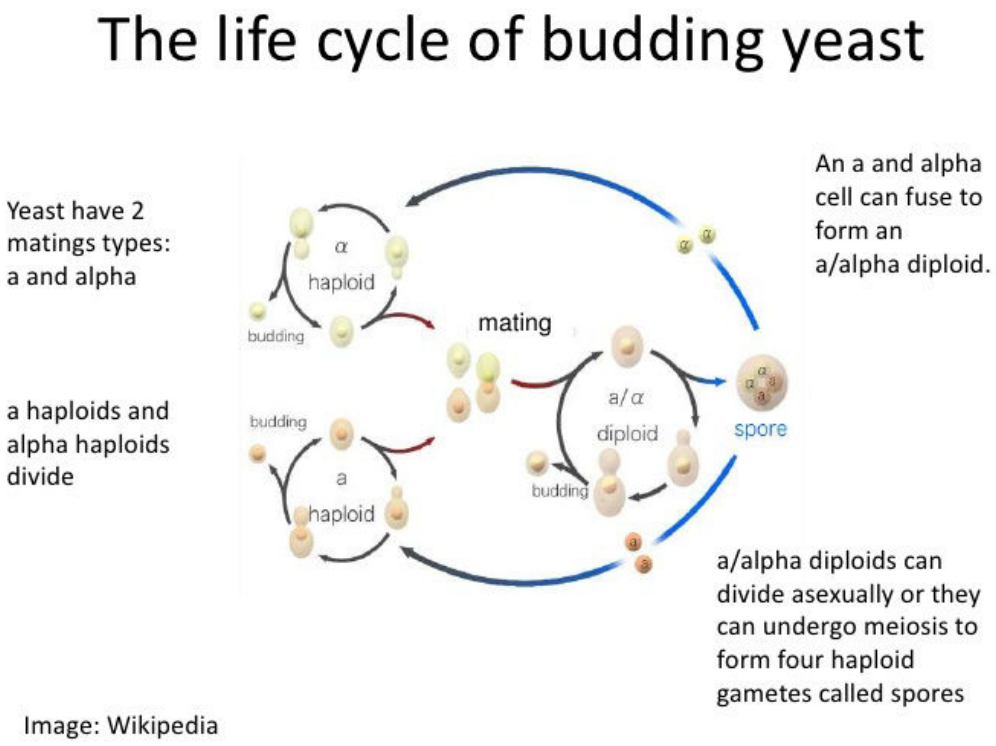

Figure 14. The life cycle of budding yeast. Image from Wikipedia.

The mitotic cell cycle in budding yeast like in other organisms contains five phases. Cells divide their chromosomes during M phase. In G1 phase cells do most of the transcription and translation to prepare for the division. In S phase DNA is replicated. In G2 phase cells undergo metabolic changes to finish preparation of mitosis and cytokinesis. In M phase the chromosomes are separated. G0 phase is entered only when nutrient are limited.

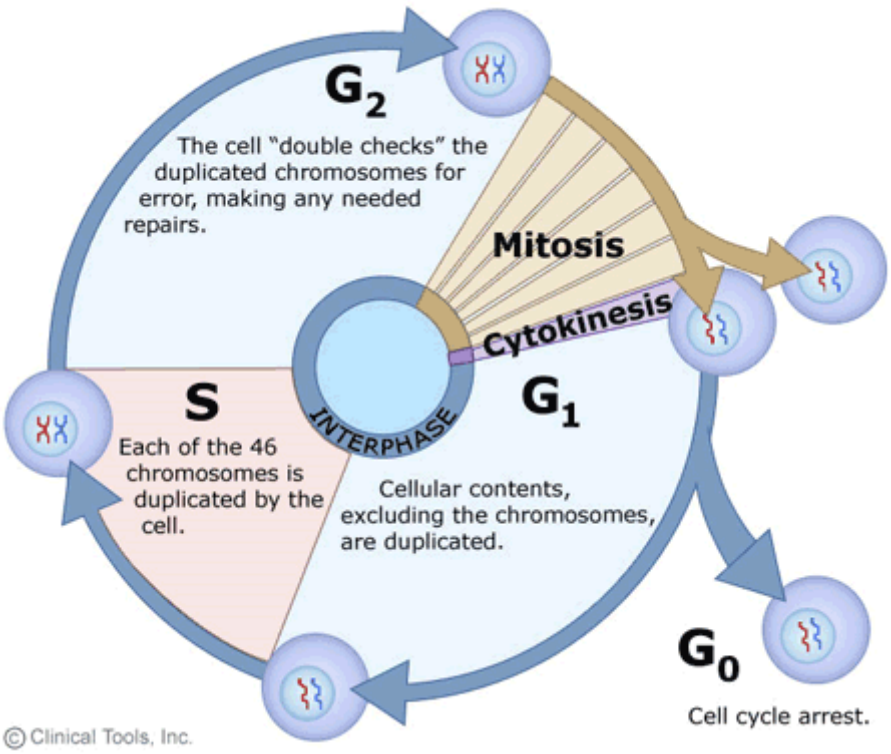

Figure 15. The mitotic cell cycle. Image from youngbloodbiology.wikispace.com

M phase in budding yeast is similar in other higher eukaryotic organisms: it contains prophase, prometaphase, metaphase, anaphase, and telophase. One exception is that the nuclear membrane does not break down when cell enter prophase (Balasubramaniam M, et al. Current Biology. 2004).

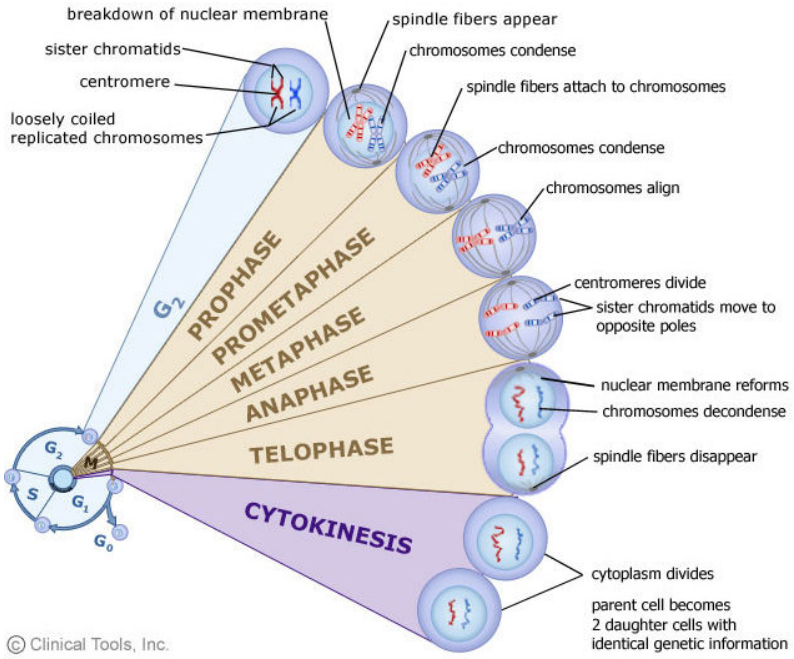

Figure 16. The meiotic cell cycle. Image from youngbloodbiology.wikispace.com

The second aspect of budding yeast life cycle is meiosis, which is a series of well-regulated and ordered transcriptional cascades. Yeast cells first sense the environmental cues that can trigger meiosis, then they progress from Meiosis I to Meiosis II (Clancy MJ. Curr Biol. 1998, Vershon AK and Pierce M. Curr Opin Cell Biol .2000). Budding yeast meiosis is followed by gametogenesis where four spores are formed and encapsulated in an ascus (Simchen G, et al. Experimental Cell Research 1972).

2.5.2 ncRNAs in budding yeast

The existence of ncRNA was reported in eukaryotic organisms from yeast to human. In budding yeast, the categories of ncRNAs are (1) small structural ncRNAs which are also commonly found in higher eukaryotes, like tRNAs, rRNAs, snRNAs; and (2) long non-coding RNAs, namely SUTs (Stable Unannotated Transcripts), CUTs (Cryptic Unstable Transcripts), MUTs (Meiotic Unannotated Transcripts), and XUTs (Xrn1 sensitive Unstable Transcripts). Because budding yeast lacks the RNAi machinery, there are no small regulatory RNAs, like miRNAs and siRNAs in budding yeast.

2.5.1 Cryptic Unstable Transcripts (CUTs)

Wyers et al. reported that some transcripts, which are undetectable in wild type (WT) cells, accumulate in an *rrp6* mutant, while there are little changes in the expression of most protein coding genes (mRNAs). Those abnormally accumulated transcripts in the *rrp6* mutant normally are targeted by the exosome and rapidly degraded in WT cells, therefore those transcripts are named Cryptic Unstable Transcripts (CUTs). CUTs are transcribed by RNAPII (RNA polymerase II), like mRNAs, they also have 5'- 7-methylguanosine cap (5'-m7G cap), and a 3' polyadenylated tail. (Wyers, F. et al., Cell, 2015)

2.5.2 Stable Unannotated Transcripts (SUTs)

A genome-wide study found in wild type budding yeast cells that a new type of non-coding transcripts is expressed at low levels in exponentially growing cells, and they do not have any features that have been annotated before. This new class of non-coding transcripts were named as stable unannotated transcripts (SUTs). SUTs amount to approximately 12% of all the transcripts in normal budding yeast cells. These studies provide further evidence for pervasive transcription of the budding yeast genome. (David, L.et al. PNAS.2006; Neil, H., et al. Nature. 2009 ; Xu, Z., et al., Nature. 2009)

2.5.3 Meiotic Unannotated Transcripts (MUTs)

During meiosis, Rrp6 protein becomes unstable when cell changes from vegetative growth medium (fermentation, YPD medium) to pre-sporulation medium (respiration, YPA medium). The protein level is further going down when cells are transferred to sporulation medium, and then Rrp6 remains undetectable when cells enter meiotic M-phase and spore/ascus formation. At the same time, a new class of ncRNAs accumulated in the cell, which was named Meiotic Unannotated Transcripts (MUT). Some MUTs are found to be transcribed antisense to ORFs, indicating the possible role of this meiotic ncRNAs in regulating sense genes expression during meiosis (Lardenois A. et al., PNAS. 2011).

2.5.4 Xrn1-sensitive Unstable Transcripts (XUTs)

Xrn1 is a cytoplasmic exonuclease, which degrades RNA in 5' to 3' direction (Mullen, T. E. et al., Genes & Development. 2008). van Dijk E.L. et al., used strand-specific RNA-Seq to identify genome-wide ncRNA targets of Xrn1 in *xrn1* mutant budding yeast, and named them Xrn1-sensitive Unstable Transcripts (XUTs). XUTs are transcribed by RNA polymerase II and they also have a polyadenylated tail. 66% of XUTs are antisense to open reading frames. XUTs are normally longer than SUTs, and ribosome profiling study shows that XUTs are translated by ribosome thus renders them to Nonsense mediated decay pathway (NMD) (van Dijk, E.L., Nature. 2011).

2.5.5 Antisense RNA in budding yeast

lncRNAs in budding yeast can be divided into (1) intergenic lncRNAs, which are located between ORFs; (2) bidirectional promoter driven lncRNAs that are simultaneously transcribed with mRNAs, although in divergent directions; (3) antisense lncRNAs (aslncRNAs), which are on the opposite strand and totally or partially overlap with sense mRNAs. Budding yeast have a very condensed genome, most of lncRNAs are on the opposite strand of mRNAs. In budding yeast, two antisense lncRNAs have been reported have important role in regulation their sense mRNAs: *GAL10* and *PHO84* are repressed by their overlapping antisense RNAs in response to stress (Houseley, J., et al., Mol Cell. 2008, Camblong, J. et al. Genes Dev. 2009, Camblong, J. et al. Cell. 2007, Castelnuovo, M. et al. Nat. Struct. Mol. Biol.2013). In addition to repress sense gene expression, antisense lncRNAs also has been found to positively regulate its sense gene expression: *CDC28* is associated with a stress induced antisense lncRNA, which totally overlaps CDC28, and recruits transcription activation factors to the promoter of *CDC28* through spatially looping. This process connects the promoter of antisense lncRNA to the promoter of *CDC28* (Nadal-Ribelles, M. et al., Mol Cell. 2014). In addition to regulate gene expression at the transcriptional level, antisense lncRNAs can also regulate translation: *KCS1* is associated with an antisense lncRNA that regulates Kcs1

translation to produce a truncated protein through an unknown mechanism, possibly through sense and antisense RNA base-pairing (Nishizawa et al., PLoS Biol. 2008).

Antisense lncRNAs have also been found in other species, for example, Xist and HOTAIR in mammalian cells, which indicate that antisense lncRNAs have important functions among evolutionary divergent species. However, the roles of most antisense RNAs are currently unknown.

Eric A Alcid and Toshio Tsukiyama used budding yeast *Saccharomyces cerevisiae* and *Naumovozyma castellii* as models to understand the role of antisense lncRNAs by exploring the evolutionary dynamics of ASlncRNA. They found that due to loss of RNAi machinery the repertoire of antisense lncRNAs was pervasively expanded in budding yeast, they have relatively higher expression, greater length, increased overlapping with sense mRNAs compare to the species which retain RNAi machinery. They further show that RNAi has an inhibitory effect on antisense transcriptomes, as antisense lncRNAs expression levels decrease in budding yeast cells that express reconstituted RNAi machinery, as compared to wild type cells. Furthermore, it is deleterious to globally increase the level of antisense RNAs in budding yeast with a reconstituted RNAi machinery. Increased level of antisense RNA is also toxic to *N. castellii* that has a RNAi machinery, since sense and antisense RNAs can form double stranded RNAs that is targeted by RNAi machinery to inhibit the sense genes function as well: this was demonstrated by the finding that the temperature sensitive growth deficiency of a *N. castellii rrp6* mutant was partially rescued in a *drc1 rrp6* double mutant, which the Drc1 can degrade ASlncRNA-mRNA duplex (Eric A Alcid, and Toshio Tsukiyama. Nat Struct Mol Biol. 2016).

Antisense lncRNAs in budding yeast are often associated with meiotic genes (Yassour M, et al. Genome Biol.2010). A genome wide study of nucleosome states in meiosis, reported that histone markers for active promoter are often found in the 3' end of meiotic genes, which may reveal the promoters of antisense ncRNAs (Zhang L, et al., Genome Res. 2011). Association of antisense ncRNAs with meiotic genes are thought to be a mechanism for inhibiting meiotic gene expression during vegetative growth (Chen H M and Neiman A, M. Current Opinion in Microbiology. 2011).

2.5.6 Double strand RNA in budding yeast

When sense and antisense RNAs are transcribed in the same genomic loci with different direction, the RNA molecules can form double stranded RNAs (dsRNAs) *in vivo* that were shown to have a biological effect on gene expression (Sinturel et al., Cell Rep 2015; Wery et al., Mol Cell 2016)

Studies of prokaryotic organisms such as *E. coli*, and microbial populations showed that they contain naturally double strand RNA formed by sense and antisense RNAs (Decker C and Parker R. Cell Report. 2014, Lybecker M, et al., PNAS.2014). A genome-wide dsRNAome analysis in *Caenorhabditis elegans* discovered dsRNAs by identifying RNA editing sites, i.e. target site for RNA editing enzyme Adenosine Deaminaases that act on RNA (ADAR). 664 editing-enriched regions (EERs) containing RNAs were found. Most of them are mRNAs, which represent about 1.7% of the total mRNAs in *C. elegans*, and a subset of EERs are non-coding RNAs. EERs plays important roles in cellar signaling, since many EERs are developmentally regulated and respond to starvation and infection with bacteria and fungi (Whipple J, et al. RNA.2015).

Portal M, et al., reported the existence of natural double strand RNAs (ndsRNAs) in human cells. The authors reported hundreds of putative ndsRNAs which are potentially involved in major biological processes in human cells. Some of these ndsRNAs are located in nucleus and interact with nuclear proteins. One of the nuclear ndsRNAs - nds-2a - shows differential localization during the cell cycle and can interact with RCC1 and the mitotic RANGAP1-SUMO1-RANBP2 complex component RAN. Nds-2a has important functions in mitosis as changing its expression will result in mitotic defects, such as post-mitotic abnormalities, mitotic catastrophe and cell death (Portal M, et al., Nature structural and molecular biology. 2014).

Recently, three papers appeared in press about human and budding yeast RNA-RNA interactions (Lu Z P, et al., Cell.2016; Sharma E, et al., Molecular Cell. 2016; Aw J G. Cell.2016). RNA interactome work found that RNA interaction structure is very important for the post-transcriptional regulation of gene expression. The interaction between two RNA molecules often occurs at the same structure. As 5'UTR, coding sequence, and 3'UTR tend to interact with other molecules with the base located in the same domain. Intramolecular interaction sites predominantly occur near the start and stop codon. Consistent with a circulation model for translation, efficiently translated mRNAs tend to have long interaction connections at their 5' and 3' ends. As opposed to that, poorly translated mRNAs tend to have short interactions near the 5'end. Moreover, mRNAs which have interaction in their 5'end show increased decay rates, while interaction that occur in the 3'end of the transcript block the exosome and thus protect the mRNA from degradation (Aw J G. Cell.2016).

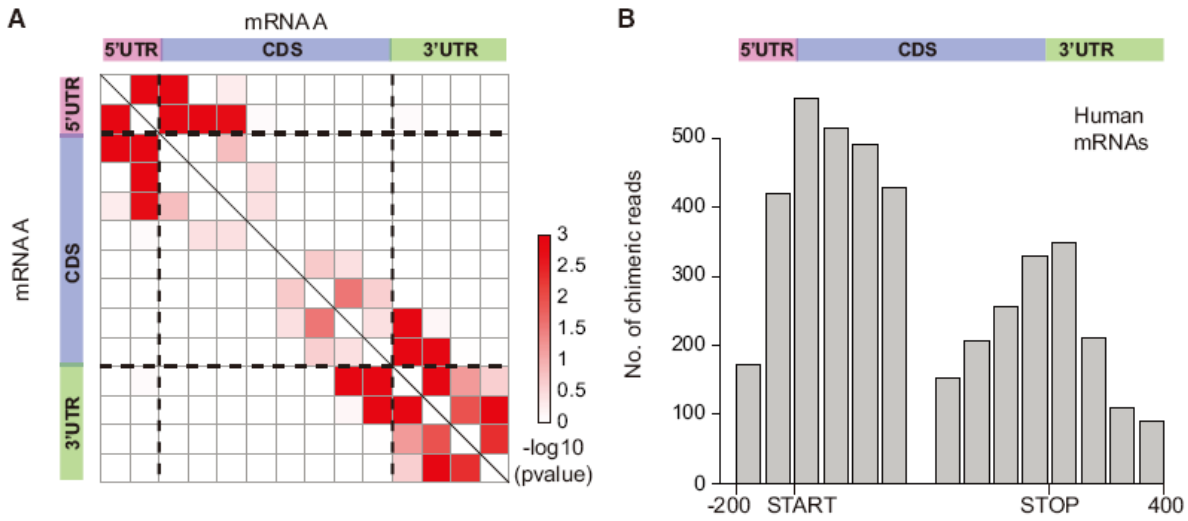

Figure 17. (A) Two-dimensional heatmap showing enrichment of intramolecular mRNA interactions based on the location of chimera ends. We aligned transcripts according to their translation start and stop sites and plotted interactions from the last 200 bases of the 50 UTR, the first and last 400 bases of the coding region, and the first 400 bases of the 30 UTR. Enrichment was calculated as –log10(p value) based on random sampling across the transcript with 100 bp windows. The black dotted lines demarcate boundaries between the 50 UTR, CDS, and 30 UTR.
(B) Metagene analysis of the frequency of intramolecular interactions along human mRNAs, by aligning mRNAs along their translation start and stop. We plotted interactions that are present in the last 200 bases of the 50 UTR, the first and last 400 bases of the coding region, and the first 400 bases of the 30 UTR. Image from Aw J G., et al., Cell.2016.

RNA intermolecular interactions tend to occur at both ends of mRNA as well, however, the interaction patterns are different from intramolecular interactions, that usually occur when the 5' end of one mRNA interacts with the distal domain of another mRNA. Intermolecular interactions require physical proximity as they have a propensity to occur in between the mRNAs in the same cellular compartment. Dynamic RNA interaction changes in different cell states show that interaction score is correlated with translation: the interaction score shifts from high interaction in ESCs to low interactions in RA cells that display decreased translation efficiency. This indicates that RNA conformation changes are a potentially important mechanism to regulate translation under different conditions (Aw J G., et al. Cell.2016).

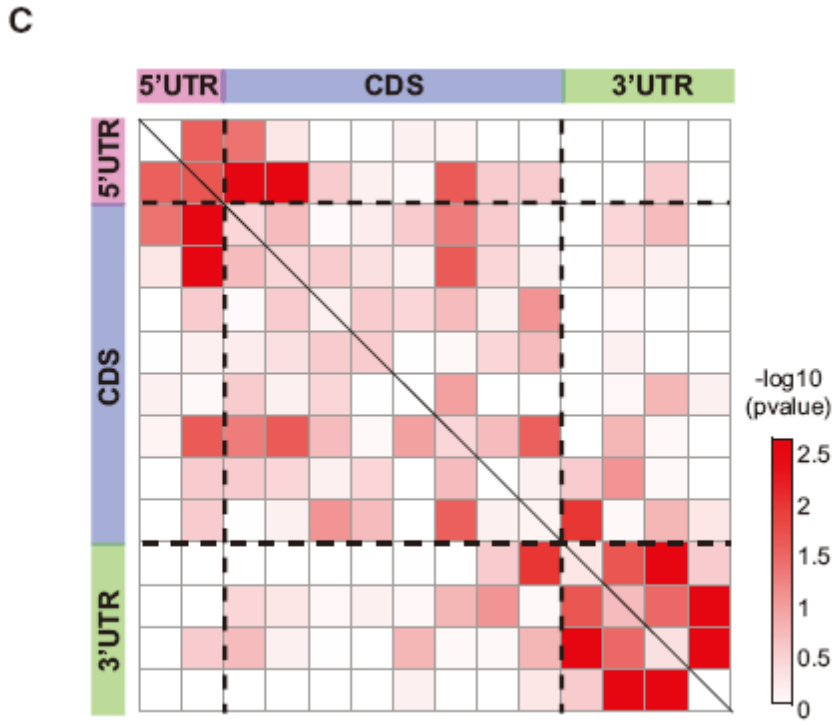

Figure 18. Two-dimensional heatmap showing enrichment of intermolecular interactions based on the location of chimera ends across mRNA pairs. We aligned transcripts according to their translation start and stop sites and plotted interactions from the last 200 bases of the 50 UTR, first and last 400 bases of the coding region, and first 400 bases of the 30 UTR. Enrichment was calculated as –log10 (p value) based on random sampling across the transcript with 100 bp windows. Black dotted lines demarcate the boundaries between 50 UTR, CDS, and 30 UTR. Image from Aw J G., et al. Cell.2016

Studies about double strand RNAs in budding yeast shows that overlapping mRNA and mRNA which are on opposite strand can form double strand RNAs. Convergent mRNAs pairs overlapping on the 3' region have an impact on translation and mRNA stability, and lead to no-go decay if the overlapping region covers stop codon of one mRNA. While the other one mRNA will stay intact if overlapping region does not cover the stop codon (Sinturel F, et al., Cell report. 2015). ncRNA formed double strand RNA also have important function in budding yeast, as XUTs form double strand RNA that increase their stability, because the RNA duplex protects them from non-sense mediated decay (NMD): XUTS accumulate in *mtr4* and *dbp2* mutants since the dissociation of double stranded regions by Mtr4 and Dbp2 helicase has been impaired, which causes XUTs to become inappropriate target for the NMD pathway (Wery M, et al., Mol Cell.2016). However, the roles of double strand RNAs in meiosis are still unknown.

3. mRNA isoforms

3.1 5'-UTRs are flexible

Kim Guisbert K, et al used tilling arrays to detect genome wide transcript architecture alterations during meiosis, and reported that during meiosis extensive changes occurred to coding transcriptomes, including 5' ends, 3' ends, and splice sites in gene body region (Kim Guisbert K, et al., RNA 2012).

Transcript 5' UTR changes, including both extension and regression, were detected during meiosis and sporulation. Both extension and regression were also found in 3' UTRs, but 3' UTR shortening is more common than extension during meiosis (Kim Guisbert K, et al., RNA 2012).

The regulatory mechanism governing flexible 5' UTRs are unknown. The mechanism driving the changes of 3'UTRs could be different choices of the 3' cleavage site or a down-stream post transcriptional processing step (Kim Guisbert K, et al., RNA 2012).

3.2 Function of different mRNA isoforms with flexible 5'UTRs

5'UTR transcript architecture changes include both extension and shortening. Several shortened 5' ends of transcripts were found to delete parts of the coding region, which changes the protein product encoded by this sequence (Kim Guisbert K, et al., RNA 2012). Extension of 5'UTR, however, typically does not affect the protein coding region of a transcript. It is possible that extended 5'UTRs contain upstream open reading frames (uORFs). According to a genome wide cDNA analysis of budding yeast transcriptomes, 2415 5'-UTR been found to contain at least one uORF (Miura F, et al., PNAS, 2006).

The 5'UTR region of the transcript is critical to translation because it is bound by ribosome that scan for cis-acting elements like the Kozak sequence, which plays a major role in the initiation of the translation process (De Angioletti M, et al., Br J Haematol. 2004). Other DNA sequence elements are upstream open reading frames (uORFs) and upstream AUGs and termination codons (uAUGs). They can have a great impact on the regulation of translation. The consequence of translating an upstream ORF is illustrated as the following figure (Morris D and Geballe A. Molecular and cellular biology 2000):

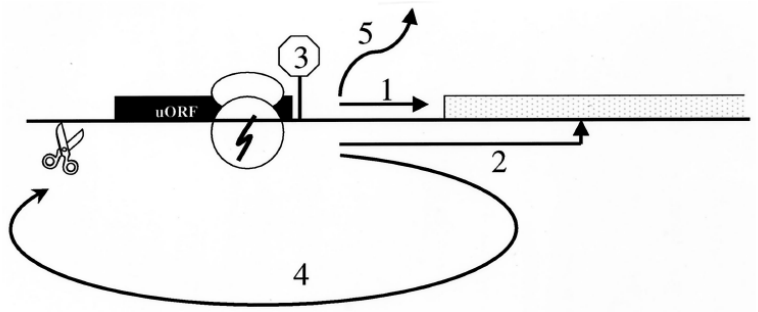

Figure 19. Alternative fates available to a ribosome after translating a uORF

(1) The presence of uORF doesn't affect gene expression. As illustrated in the option 1 and 2 in the figure that ribosome remain bind to mRNA after scanning the uORF region and continue scanning and reinitiate translation downstream in the AUG of ORF region.

(2) Ribosome stalled that uORF region and block the additional ribosome bind to the mRNA. The structure of the peptide may mediate the stalling of ribosome in either the elongation or termination phase of the uORF translation (option 3 in the figure).

(3) Translation of uORF may influence the stability of the mRNA, uORF bearing mRNA may trigger the nonsense-mediated decay pathway (option 4 in the figure).

(4) Ribosome may dissociate from mRNA after translation (option 5 in the figure)

Image from Morris D and Geballe A. Molecular and cellular biology 2000

Different types of start codons in the uORF appear to have different effects on translation, since AUG in uORF typically inhibits translation, while non-AUG codons seem to enhance translation.

Finally, architectural changes of 3'ends in transcripts have a great impact on their stability, processing and regulation (Barrett L W, et al., Cellular and Molecular Life Sciences.2012).

Results

1. Genome-wide RNA profiling of the transcriptional response to 5-FU treatment

Long non-coding RNA mediate 5-FU cytotoxicity by forming double stranded RNA potentially inhibiting translation of key cell cycle regulators

Bingning Xie[1], Emmanuelle Becker[1], Igor Stuparevic[1,3], Maxime Wery[2], Marc Descrimes[2], Antonin Morillon[2], and Michael Primig[1,*]

[1]Inserm UMR 1085 IRSET, Université de Rennes 1, 35042 Rennes, France

[2]Institut Curie, PSL Research University, CNRS UMR 3244, Université Pierre et Marie Curie, 75248 Paris, France

[3]Present address: Faculty of Food Technology and Biotechnology, University of Zagreb, 10000 Zagreb, Croatia

[*]Corresponding author: michael.primig@inserm.fr

Key words: 5-FU, lncRNA, mitosis, *rrp6*, double stranded RNA, budding yeast

Abstract

5-Fluorouracil is a widely used anti-cancer drug. The mechanisms underlying its cytotoxicity range from DNA based pathways to inhibiting thymidylate synthase and RNA based disruption by targeting Rrp6, which is a 3'-5' exoribonuclease required for processing and degrading rRNA and long non-coding RNAs. However, the mechanism of how 5-FU acts through long non-coding RNAs to exert its toxicity is still unknown. Here, we show that long non-coding RNAs accumulate in 5-FU treated cells and that some can form double stranded RNAs with their overlapping sense mRNAs. The formation of double stranded RNA is negatively correlated with protein levels. Potential translation inhibition of key cell cycle regulators and essential genes by forming double stranded RNA impedes cell cycle progression in the treated cells. Thus, our results demonstrate how long non-coding RNAs are likely to function in mediating 5-FU cytotoxicity, potentially inhibiting the translation of key cell cycle regulators and essential genes by forming double stranded RNA with its sense mRNA to suppress the progress of cell cycle. We anticipate our study to be a starting point for more sophisticated roles of long non-coding RNA in mediating 5-FU cytotoxicity in both budding yeast and higher eukaryotes like human. Furthermore, long non-coding RNA could be new

targets for improvement of 5-FU based chemotherapy.

Introduction

5-FU is a chemotherapy drug that has been widely used to treat various cancers. It was originally designed as the homologue of uracil to inhibit thymidylate synthase to disrupt DNA associated processes like DNA replication and repair (Longley DB, et al., Nat Rev Cancer.2003 ; Scartozzi M, et al., Pharmacogenomics. 2011). A growing number of evidence from budding yeast and mammals shows Rrp6 to be a target of 5-FU, thereby mediating RNA based cytotoxicity by disrupting RNA processing (Fang F, et al., Mol Cell Biol. 2004; Kammler S, et al., Mol Cancer Res.2008 ; Silverstein RA,, et al. Mol Cancer Res. 2011). Rrp6 is a 3'-5' exoribonuclease, a homologue of mammalian EXOSC10 gene, which processes 5.8S rRNA 3'ends, and targets and degrades various kinds of RNAs, for example, snoRNA, tRNA, lncRNA and pre-mRNA (Xu Z, et al. Nature.2009 ; Schneider C, et al., Mol Cell. 2012; Gudipati RK., et al., Mol Cell. 2012). Over several decades since the invention of 5-FU, research is still focused on searching for ways to improve the efficiency of 5-FU, such as combining 5-FU with other drugs to enhance its toxicity, as many patients show resistance to it (Scartozzi M, et al., Pharmacogenomics. 2011). Therefore, the mechanisms underlying 5-FU toxicity need to be further understood and novel therapeutic targets need to be discovered.

Long noncoding RNA (lncRNA) is defined as being longer than 200nt and having little potential to encode a protein. lncRNAs have been found to play important functions in various cellular processes, for example regulating gene expression and transcript splicing, regulating translation, mediating cell-cell signaling, organization of protein complex, and shaping nuclear architecture (Geisler S and Coller J. Nature reviews Molecular Cell Bio. 2013; Mele M, Rinn J. Mol Cell. 2016). As the body of knowledge about lncRNAs grows, more evidence shows the link of dysregulations of lncRNAs to human diseases, especially the involvement of lncRNA in cancer is more pervasive than previously thought (Wapinski O and Chang HY, Trends in cell biology 2011.) lncRNAs participate in both tumor suppression pathways and oncogene activation pathways. Tumor protein p53 pathway corepressor 1 lincRNA-p21 (Trp53cor1) interacts with heterogeneous nuclear ribonucleoprotein K (Hnrnpk) protein to exert p53-dependent transcriptional repression, which leads to apoptosis (Huarte, Cell. 2010). Colon cancer associated transcript 1(CCAT1) was reported to promote long-range chromatin looping to regulate proto-oncogene MYC transcription (Xiang J F., et al Cell Res. 2014; Calin G A, et al. Cancer Cell 2007). This indicate that lncRNA could be a potential target for cancer treatment. lncRNA also been found implicated in 5-FU therapy, as

lncRNA UCA1 enhances 5-FU resistance in colorectal cancer by suppressing miR-204-5P (Bian ZH, et al. Scientific Report 2016), and snR is down-regulated in a 5-FU resistance colon cancer cell line, which leads to decreased cell death upon treatment with 5-FU (Lee H, et al. Molecules and Cells.2014).

Budding yeast is a perfect model to study RNA based 5-FU cytotoxicity since it lacks thymidine kinase (TK), also contains diverse long non-coding RNAs, such as SUTs, MUTs, CUTs, and XUTs. (Hoskins J and Butler J.S. Yeast 2007; Grem J.L. and Fischer. P.H Pharmacol. Ther 1989; Daniel B.L. et al. Nat Rev Cancer. 2003; Xu Z, et al. Nature.2009; Wyers F., et al., Cell.2005; Mullen, T. E. et al., Genes & Development. 2008; Lardenois A. et al., PNAS. 2011). Most lncRNAs in budding yeast are on the antisense strand of mRNAs; this is one of the consequences of its dense genome. Sense and antisense transcripts tend to form double strand RNAs to regulate gene expression. For example, convergent mRNAs pairs overlapping on the 3'region have an impact on translation and mRNA stability by leading to no-go decay, if the overlapping region covers the stop codon of the mRNA (Sinturel F, et al., Cell report. 2015). ncRNA formed double stranded RNAs also have important function in budding yeast, as XUTs form double stranded RNAs that increase their stability, since the RNA duplex protects it from non-sense mediated decay (NMD). XUTs accumulate in *mtr4* and *dbp2* mutants since the dissociation of double strand regions by Mtr4 and Dbp2 helicase is impaired, which leads to XUTs become inappropriate targets for the NMD pathway (Wery M, et al., Mol Cell.2016). However, the role of double strand RNAs in mediating 5-FU toxicity is still unknown.

Here, we carried out RNA- profiling to explore the transcriptomes of mRNA and lncRNAs in 5-FU treated diploid yeast and an *rrp6* mutant. Our study finds accumulated double stranded RNA formation, which shows negative correlation with protein levels, down-regulates key cell cycle regulators and essential genes and thereby may lead to impaired cell cycle progress. Our work provides a new mechanism of lncRNA based 5-FU cytotoxicity by forming double stranded RNA, suggesting that antisense lncRNA overlapping with mRNA could be a potential therapeutic target for the enhancement of 5-FU efficiency and improving the clinical outcome.

Materials and methods

Yeast strains and growth media. Strains used in this study are JHY222 wild-type and *rrp6* mutant as published (Lardenois et al., PNAS 2011). Growth media were prepared according to standard

protocols of yeast YPD media (with glucose), YPGal media (with Galactose).

Growth assay. A growth assay was performed with YPD medium or YPD medium containing 20□g/ml of 5-FU. Yeast cells were grown in YPD medium overnight, then diluted into $2x10^6$ cells/ml with fresh YPD medium and further diluted ranging from 10-fild to 10^4-fold before incubation at 30ºC. Pictures were taken using the GelDoc XRS system (Bio-Rad. USA) at 48h.

Diploid yeast cell synchronization. Diploid budding yeast cells were synchronized by using a starvation method. Briefly, yeast cells were cultured in YPD medium for 19 hours until they reached stationary phase, and then released into a new cell cycle by transferring them into fresh YPD medium at a final concentration of $2x10^6$ cells/ml. Samples were collected every 20 minutes. 40min and 100min samples corresponding to G1 and S phase were used for RNA-sequencing.

Mitosis dynamics analysis. Flow cytometry was used to monitor mitotic cell cycle progression as described in Lardenois et al.,2011. Briefly, 10^7 re-suspended cells were fixed with 70% ethanol, sonicate with Branson Sonifier 250 for 10s at 20% power.

RNA-Seq and bioinformatics analysis.

RNA sequencing was performed with 40min (G1 phase) and 100min (S phase) synchronized diploid budding yeast samples and an Illumina HiSeq 2000 system (Illumina, USA).

For the selection of differentially expressed mRNA and lncRNAs, normalized values were used to select transcripts showing a 2-fold change. Cluster and heatmap displays of those differentially expression transcripts were produced with R.

GO term analysis of differential mRNAs and mRNAs overlapping with differentially expressed antisense ncRNAs was performed with the GO terms tool provided by the Saccharomyces Genome Database (SGD; yeastgenome.org).

RT-PCR assay. RNA was extracted by Hot phenol method, followed by DNase I treatment with TURBO DNA-free Kit (Ambion, USA). RT-PCR reactions were carried out using 2 μg of RNA reverse transcribed with Reverse Transcriptase (High Capacity cDNA Reverse Transcription kit; Life Technologies, USA) and amplified using Taq Polymerase (Qiagen, France) at 60ºC for 28 cycles. RT-PCR products were separated on 2% agarose gels and photographed using the Gel-doc

XRS image system (Bio-Rad, USA) Primers used for RT-PCR were designed with Primer3 (simgene.com/Primer3; Table 1).

	Forward primer	Reverse primer
ACE2	TGCCCATGCGGAAAGAGATT	TCGCAGCTGTTCCTCCATTT
SWI5	CGCTGGGACCACTTTCTGAT	TCGCGCAACTCTTGTTGTTG
CUT508	GGCATTGGATTCTAGGGCCA	TCCTCTCTACTTGCCCGGAT
AMN1	AAGGAGAAGAAGCAAGGGGC	GCAAACCCCACAGTTTCCAC
MTR3	GCTAGCCTTAGCTGATGCCG	GCAACGATCAAGGCATTCCA
MNL1	GCAGGAAGTGAAGGAGCTGT	TGCCATATTCTGGGCGAGAC
CDC4	TGGCGAATCCACTCCTGAAC	AAGCAGTGGGTGATAACGGC
SUT2107	CTGCAATGACACCCCACAAA	CCTCGTGCTTGTATGACTGC
CUT377	ATGGAACATCTCGCCAACGA	ACAGATCCCTACAGGCCCTT
YNG1	TCGAGGGAAAGAAAAGAGAGCA	TTGCCCTTGGGAGCTTGTTT
SUT597	TGTCTACTCGTCGCACTTGG	GTAGCCTCTTCGTCTGGTGG
YGL195C	CTGGAAAATGGAGGACGGCT	CAGAACACTGCGCTGCACTA
CDC6	TGTGCTGGAAATACGGGTGA	TGATTGAAACCAGCCCACAA
CUT158	AGGACACCAAACATCGCTCA	TTTGCTTTGCGAATCGTCGT
CUT575	ATATTCCTGATGGTTCTTGGCCC	ACGGGAGGTTGAGCGTAGA
ACT1	CTGCCGGTATTGACCAAACT	AGATGGACCACTTTCGTCGT

Table 1. Primers used for RT-PCR assays.

Western blot assay. Protein extract was prepared with YPD, YPA, and full meiotic time course sample, by using method described in (Vitaly V. Kushnirov, Yeast, 2000). 20μg protein extract was used for electrophoresis with SDS-PAGE gel (BIO-Rad, USA). Proteins were transferred to ImmobilonPSQ membranes (Millipore, France) with an electro-blotter (TE77X; Hoefer, USA) set at 50mA for 2.5h. The membrane was blocked by incubation in 5% milk powder at room temperature for 1h, then incubate with anti-Rrp6, anti-Swi5 and anti-Ace2 antibodies overnight at 4°C. Incubate with secondary antibody anti-rabbit at 1:10000 at room temperature for 1h. Use Pgk1 as internal control, the primary antibody was at 1:10000 at room temperature for 1 h, then use anti-mouse secondary antibody at 1:10000 at room temperature for 1h. Protein band signals were detected by ECL-Plus Chemiluminescence kit (GE Healthcare, USA) with ChemiDoc XRS system (Bio-Rad. USA). Signal were quantified by using ImageQuant TL 7.0 software package (GE Healthcare,

USA).

J2-RIP assay. J2-RIP assay was performed as the method used in the paper about RRP6 in preparation. Briefly, 35µg RNA was incubated with magnetic beads and J2 antibody, then RNA was eluted and reverse transcribed with 2µg RNA by using High Capacity cDNA Reverse Transcription kit (Life Technologies, USA) and amplified using Taq Polymerase (Qiagen, France) at 60ºC for 28 cycles.

Results

Diploid yeast synchronization, 5-FU concentration determination and RNA-Seq sampling

Many yeast genes are cell cycle regulated. In order to study the role of lncRNA in the cytotoxicity of 5-FU treatment, we therefore decided to examine G1 and S cell cycle phases individually. This avoids that transcripts, which fluctuate during the cell cycle are diluted out in total RNA samples from unsynchronized cells. We use starvation to synchronize cells in G0. Unlike the synchronization method that uses drugs to block cell cycle progression or temperature sensitive alleles to arrest the cell cycle in one particular phase, this method will not influence 5-FU's effect. We synchronize diploid budding yeast cells by culturing them in rich medium (YPD) until they entered G0 phase, and then releasing cells into a new cell cycle by transferring them into fresh YPD medium +/- 5-FU at a final concentration of $2x10^6$ cells/ml (Figure 1).

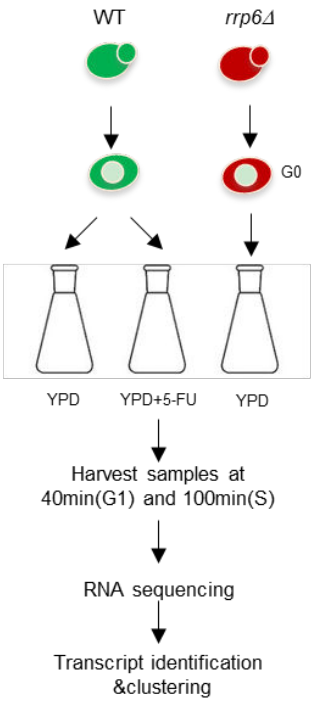

Figure 1. Experimental design and sample collection. A schematic figure shows yeast synchronization and sampling method. Mitotic growth yeast culture in liquid YPD medium until reach G0 phase, then release cell cycle by transferring into fresh YPD medium with or without 5-FU, then collect sample every 20 minutes.

In order to explore 5-FU's RNA based cytotoxicity, which is likely based on inhibitions of Rrp6, we assumed that the optimal concentration of 5-FU to be used should have a similar growth phenotype as the *rrp6* mutant. Based on this, we diluted 5-FU ranging from 2.5µg/ml to 20µg/ml, and performed a drop assay with yeast at original concentration of $2x10^6$ cells/ml with serial dilution ranging to 10^4X and found that 20µg/ml 5-FU best mimics the growth deficient phenotype of *rrp6* mutant (Figure 2A).

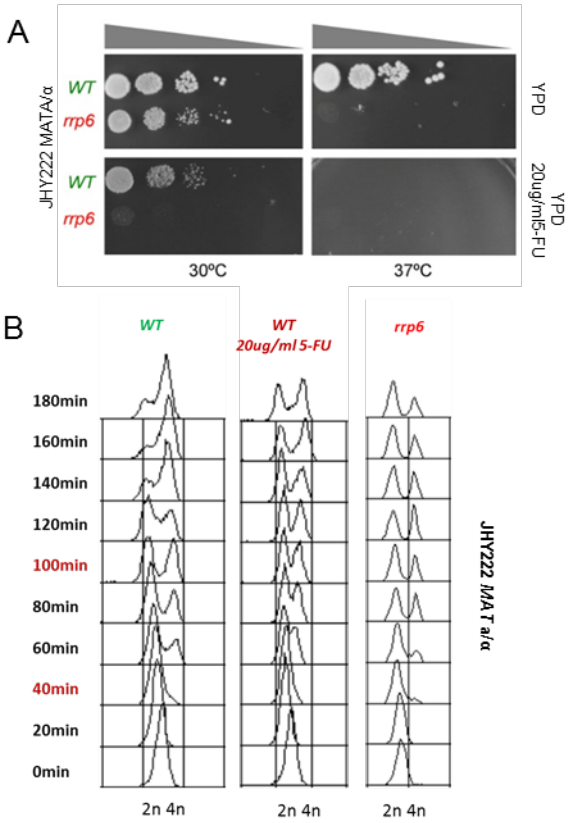

Figure 2. Growth assay and DNA replication dynamics of 5-FU treated vs. *rrp6* mutant cell. (A) Drop assay of yeast growth. Serial diluted wild type (WT) and *rrp6* mutant cells (*rrp6*) grown on YPD medium with or without 5-FU at the temperature shown below. (B) Mitotic DNA replication dynamics. DNA replication dynamics of wild type cells with (WT 20μg/ml 5-FU) or without 5-FU (WT) and *rrp6* mutant are monitored by FACS every 20 min. Samples used for RNA-Seq experiment are indicated in red.

We used a starvation method to synchronize diploid budding yeast wild type and *rrp6* mutant cells, and treated WT cells with 20μg/ml 5-FU. We monitored the cell cycle progression by FACS, and found that the 5-FU treated cells have the similar DNA replication dynamics as *rrp6* mutant, as the cells tend to accumulate in G1 phase and DNA replication is delayed (Figure 2B). We took 40 min sample as G1, since cells are mostly in G1 phase and 40min is the time point that cells recovered from stress and re-initiate their cell cycle. 100 min was taken as S phase sample for RNA sequencing because at this time point a large portion of cells are S phase.

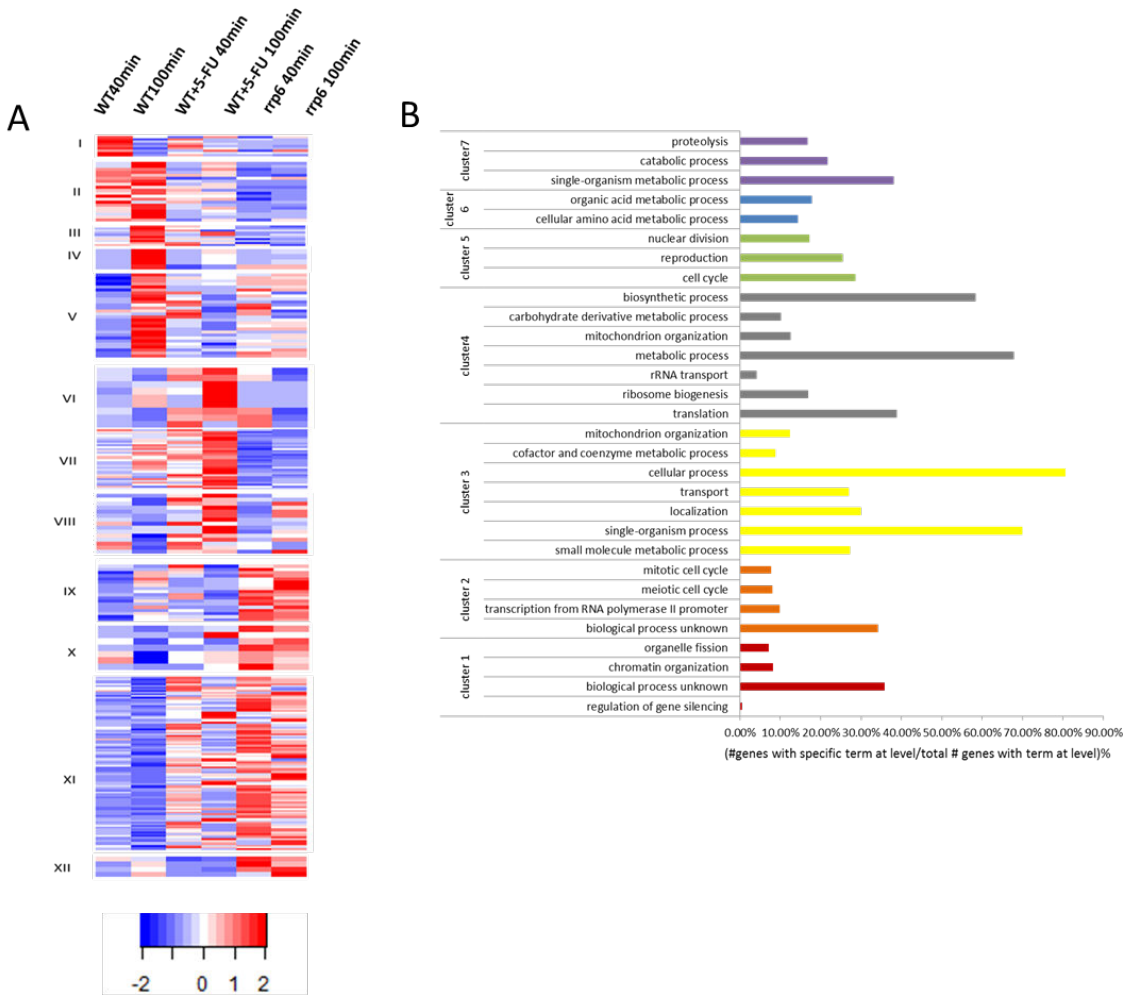

Figure 3. Differentially expressed mRNAs landscape. (A) Selection of mRNA transcripts showing differential signals was shown in the heatmap. Scale bar representing the expression level is shown below. (B) Gene ontology analysis of the differentially expressed genes in WT, 5-FU treated cells (WT+5-FU), and *rrp6* mutant cells. For each functional category is shown the percentage of genes differentially expressed.

RNA sequencing data analysis

Transcriptome sequencing indicates that mRNAs respond to 5-FU treatment, whereby most of them decrease. For example, ribosome and translation related genes show downregulation as previously reported (5-FU inhibits Rrp6, and can also directly target ribosome RNA processing).

By comparing 5-FU treated cells and *rrp6* mutant cells, we found genes involved in translation, ATP and nucleoside metabolism to show the same pattern in treated cells and in *rrp6* cells. This may stem from inhibition of Rrp6 by 5-FU. Only the *rrp6* mutant shows up-regulation of gene that function in gene silencing, amino acid biosynthesis and metabolism, and down-regulation of genes that function in steroid biosynthesis, proteasome and catabolism.

5-FU treated cells' transcriptomes respond to drug treatment in the following ways: (1) genes involved in translation are down-regulated, genes involved in amino acid catabolism and proteasome are up-regulated, while genes involved in amino acid synthesis are not changed compared to wild type (WT). This indicates that protein levels are inhibited by 5-FU through translation and through protein degradation by up-regulation of the proteasome pathway, but not because protein synthesis per se is inhibited, since the amino acid biosynthesis process is not affected. (2) Genes involved in nucleoside synthesis and cell division are down-regulated. Some *SIC1* cluster genes are important for cell division and cytokinesis, which is consistent with the phenotype of 5-FU treated cells, since daughter cell and mother cell are deficient in cell separation. In conclusion, cells respond to 5-FU treatment in three ways: first, by decreasing down protein levels; second, by inhibiting nucleoside metabolism; and third, via inhibition of cell division. In this way, 5-FU inhibits the cell cycle G1/S transition by perturbing cell division, and it inhibits growth by negatively affecting protein synthesis and nucleoside metabolism.

The *rrp6* transcriptome is very different from WT. Up-regulation of amino acid related genes may indicate the way the *rrp6* mutant responds to nutrient depletion. At 40 min in *rrp6*, metabolism and cell cycle related genes are down-regulated, which indicates that the *rrp6* mutant has a lower total metabolic rate in nutrient-depleted G0 phase. Some genes that function in meiosis and silencing are upregulated. This may be a response to nutrient depletion. During nutrient depletion, amino acid biosynthesis processes are up regulated, which reflects the rrp6 mutant's need for amino acids.

The SIC1 cluster contains genes that are affected most by 5-FU treatment

Among mRNAs that respond to 5-FU treatment, we found genes in the so-called *SIC1* cluster (Zhu G et al., Nature.2000) to be down-regulated by 5-FU treatment. The phenotype of 5-FU treated cells also shows the expected phenotype in SIC1 cluster gene mutant (Figure 4A). Genes in the *SIC1* cluster are strikingly down regulated in 5-FU treated 100min sample while the *rrp6* mutant shows a similar pattern but a weaker decrease in the 100min sample (Figure 4B). *AMN1* belongs to the *SIC* cluster, and has an important role in negatively regulating mitotic exit, as it is the key regulator in the AMEN pathway (Wang Y, et al. Cell.2003). We confirmed the expression of *AMN1* by RT-PCR and that the induction of *AMN1* in S phase is suppressed in 5-FU treated samples and the *rrp6* mutant (Figure 4C and D).

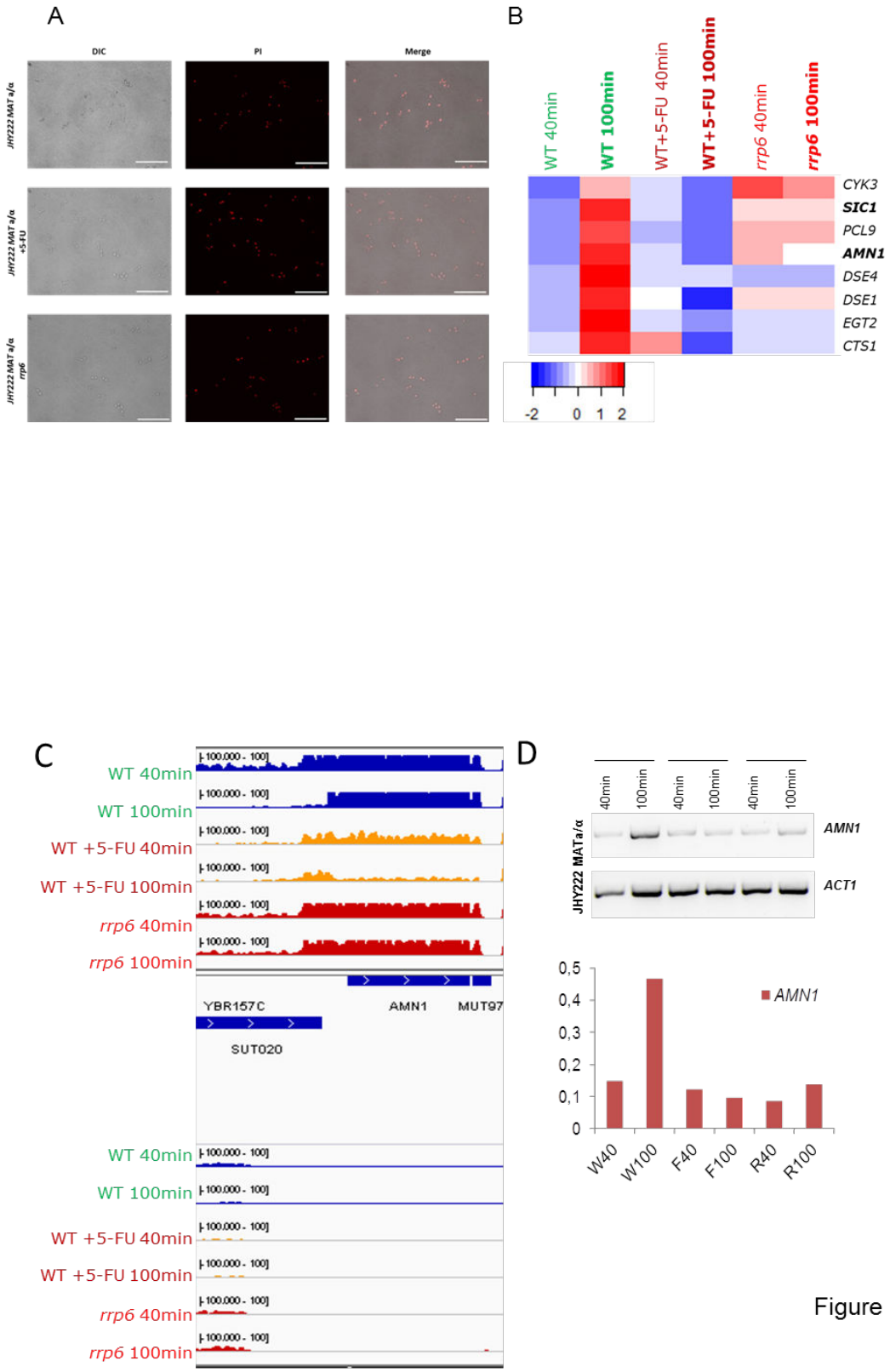

Figure

Figure 4. Expression of *SIC1* cluster genes. (A) Phenotype of 5-FU treated cell. A fluorescent photo shows the phenotype of 5-FU treated cell. (B) Expression pattern of *SIC1* cluster genes. A heatmap shows expression patterns of genes in SIC1 cluster. A color scale indicates expression levels. (C) A histogram shows expression of *AMN1* using RNA-Seq data. (D) RT-PCR validation result of *AMN1* gene and quantification. *ACT1* is the internal control.

SWI5 and ACE2, transcription factors acting upstream of the SIC1 cluster show the same inhibited pattern as the SIC1 cluster

We next asked why *SIC1* cluster genes were down-regulated upon 5-FU treatment. We first searched transcription factors upstream of the *SIC1* cluster genes and found that Swi5 and Ace2 regulate them and that *AMN1* is a direct target of these activators to trigger the AMEN pathway. We confirmed that *SWI5* and *ACE2* mRNAs also shown the same repressed pattern as SIC1 cluster genes (Figure 5 and 6). We checked the protein level of Swi5 and found that (i) it shows the same pattern as its mRNA, that (ii) it is down-regulated in the 5-FU treated 100min sample and that (iii) expression weakly drops in *rrp6* mutant cells. This indicates that the decrease of *SWI5* mRNA results in the drop of Swi5 protein in the 5-FU treated cells (Figure 5C, quantified in 5D).

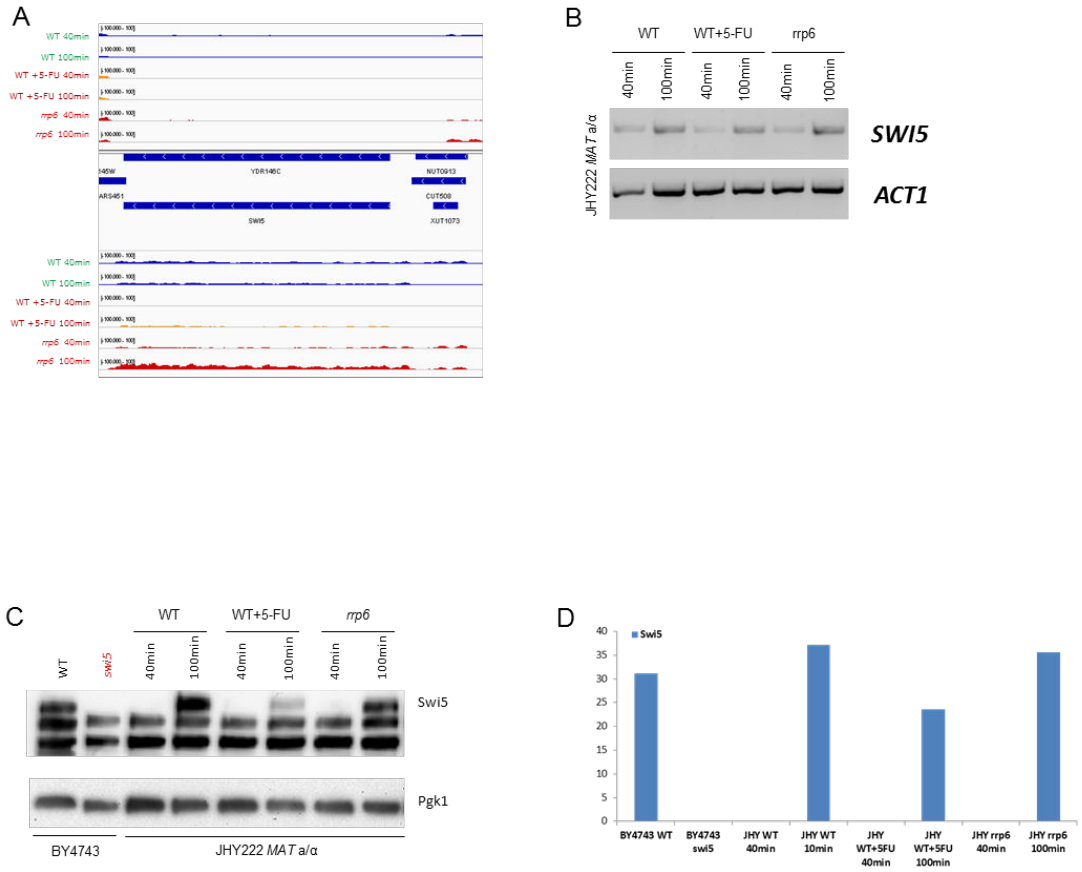

Figure 5. Expression pattern of *SWI5* gene. (A) Heatmap shows expression pattern of *SWI5* gene using RNA-Seq data. (B) RT-PCR validation result of *SWI5* gene. *ACT1* is internal control. (C) Western blot analysis for the expression of Swi5 protein in wild type cell (WT), 5-FU treated cells (WT+5-FU), and *rrp6* mutant cells (rrp6) with 40min, 100min and 160min samples. Pgk1 in the panel below is used as internal control. The strain background is indicated at the bottom.

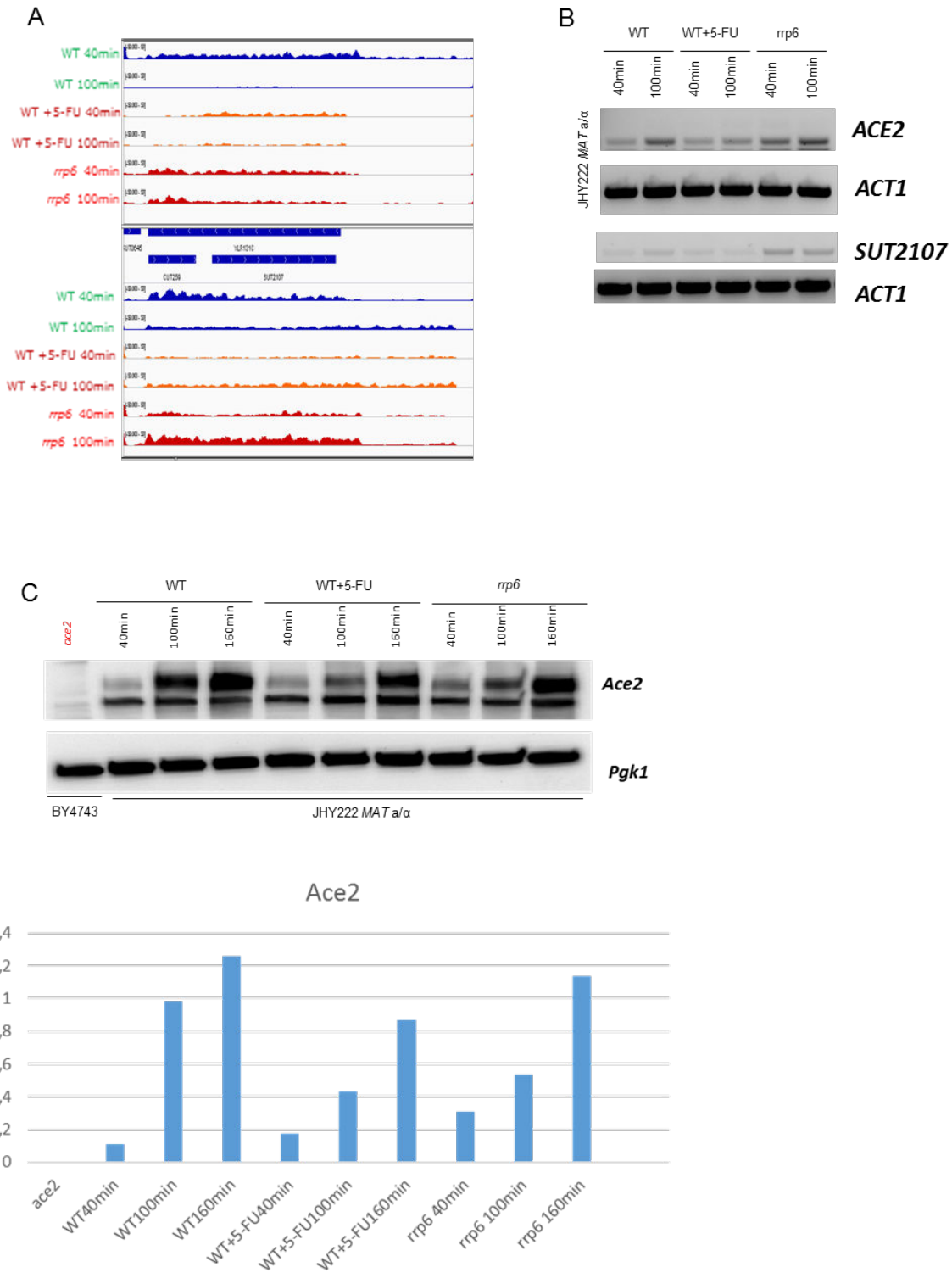

Figure 6. Expression pattern of *ACE2* gene. (A) A histogram shows the expression pattern of *ACE2*. (B) RT-PCR validation of *ACE2* gene. *ACT1* is the loading control. (C) Western blot analysis for the expression of Ace2 protein in wild type cell (WT), 5-FU treated cells (WT+5-FU), and *rrp6* mutant cells (rrp6) with 40min, 100min and 160min samples. Pgk1 in the panel below is used as internal control. Strain background is indicated on the bottom. Quantification result is shown below.

Like in the case of *SWI5*, we confirmed that *ACE2* mRNA is also down regulated in 5-FU treated cells, however it is not that obvious as for *SWI5*. And the Ace2 protein is also decreased in the treated cell, that is to say it has the same pattern as Swi5 (Figure 6). However, the mRNA level of decrease cannot fully explain the dramatic drop of protein levels in the treated cells. Together, this result shows that both mRNA and protein of the key transcription factor regulating *SIC1* cluster genes have been inhibited by 5-FU.

From the RNA-Seq result we conclude that lncRNAs respond to 5-FU weakly, and most of lncRNAs are up-regulated. Among the differentially expressed ncRNAs which have clear 5'- and 3' -ends, 16 ncRNAs are on the antisense strain of protein coding genes and have the same expression pattern as their overlapping sense mRNAs. 53 ncRNAs are on the antisense strain of protein coding gene and have the opposite expression pattern as the protein coding genes. 2 ncRNAs upstream of protein coding genes show the opposite pattern as protein coding genes, 28 ncRNAs show bidirectional expression patterns. In the cases of 53 ncRNAs that are on the opposite strand, their expression is not correlated with sense protein coding genes; among them 43 ncRNA/mRNA pairs show a dsRNA signal. ncRNAs regulate genes in cell division and cell wall biosynthesis, cell cycle, DNA replication and damage, ribosome, exosome and RNA degradation, transcription and termination, NAD metabolic, and RAS pathways have differential expression.

SUTs and CUTs constitute most of the differentially expressed lncRNAs upon 5-FU treatment, maybe this is due to their large numbers within the lncRNA population. Note that most of the lncRNAs that respond to 5-FU treatment are antisense lncRNAs, which comprise nearly 50% of differential lncRNAs. I analyzed the function of mRNAs on the sense strand of those antisense lncRNAs, trying to infer a possible function for the lncRNAs. I found that they are different from the functions of the mRNAs that respond to 5-FU treatment. Most mRNAs associated with differential lncRNAs do not have a known function. Those that do are involved in anatomical structure formation, morphogenesis, spore wall biogenesis and assembly, meiotic cell cycle process, and reproductive process. This indicate that cells use different ways to regulate genes and lncRNAs that respond to 5-FU treatment.

Differentially expressed antisense lncRNA regulate their sense mRNAs by forming double strained RNA

We next explored the potential function of differentially expressed lncRNAs by picking up the antisense ones that overlapped with mRNAs encoding proteins that have important cellular

functions (Figure 7). This group includes essential genes.

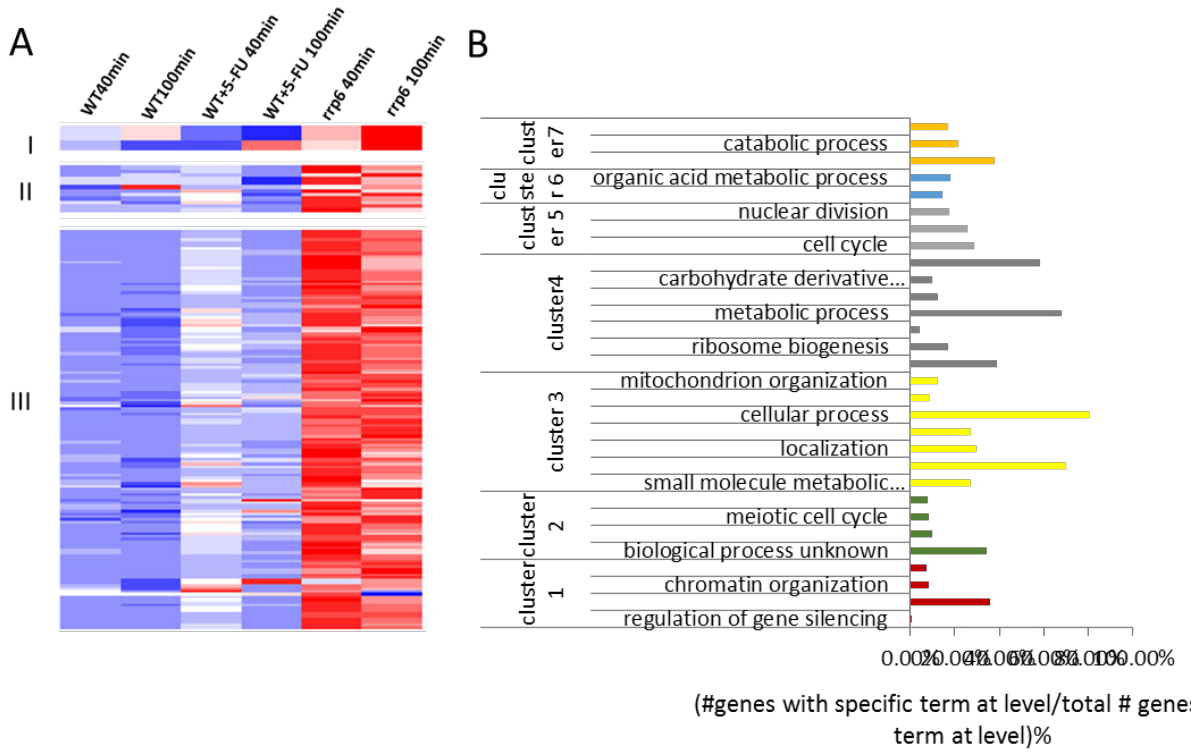

Figure 7. ncRNA response to 5-FU treatment. (A) Differentially expressed ncRNAs are grouped into 3 clusters according to their expression patterns. (B) GO terms of BP ontology of mRNAs antisense to differential ncRNAs. Different clusters are color coded. Cluster names and GO terms are given to the left.

We selected *CUT377/YNG1, SUT597/MNL1. YJL195C/CDC6, CUT158/MTR3, CUT575/CDC4*, which are all confirmed to form double stranded RNAs (Figures 8 and 9).

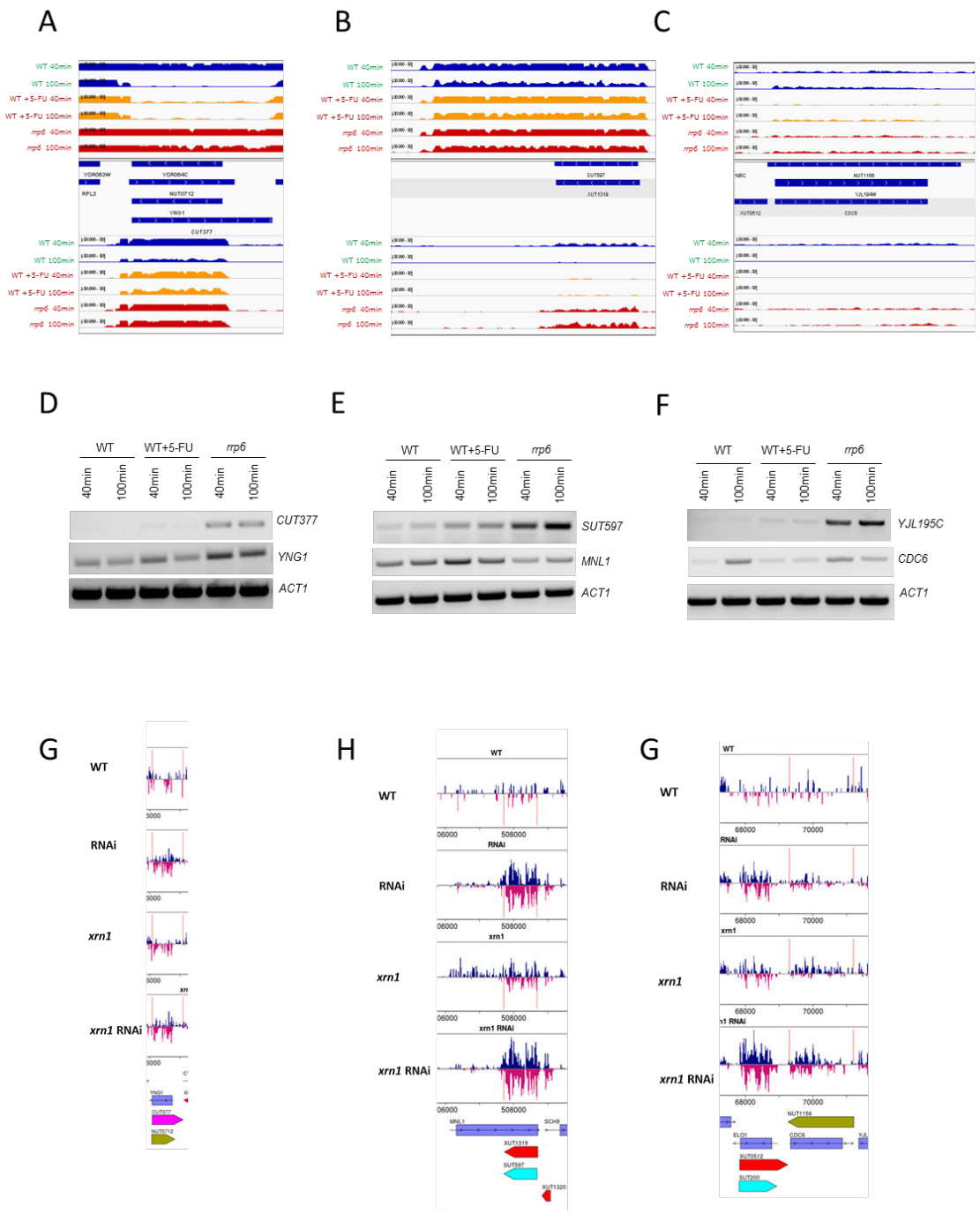

Figure 8. Expression pattern of differentially expressed essential genes and their antisense lncRNAs. (A) A histogram shows the expression pattern of essential genes and their antisense lncRNAs, *YNG1/CUT377,* *MNL1/SUT597*, and *CDC6/YJL195C*. Protein coding genes are shown in blue box, different types of ncRNAs are shown in different colors, MUTs in yellow, XUTs in red, SUTs in light blue. (B) RT-PCR validation results of those essential genes. *ACT1* was used as a loading control. (C) Haploid double stranded RNA (dsRNA) sequencing result of those essential genes. Peaks represent dsRNA signals detected in the locus from Wery M et al. Mol Cell. 2016..

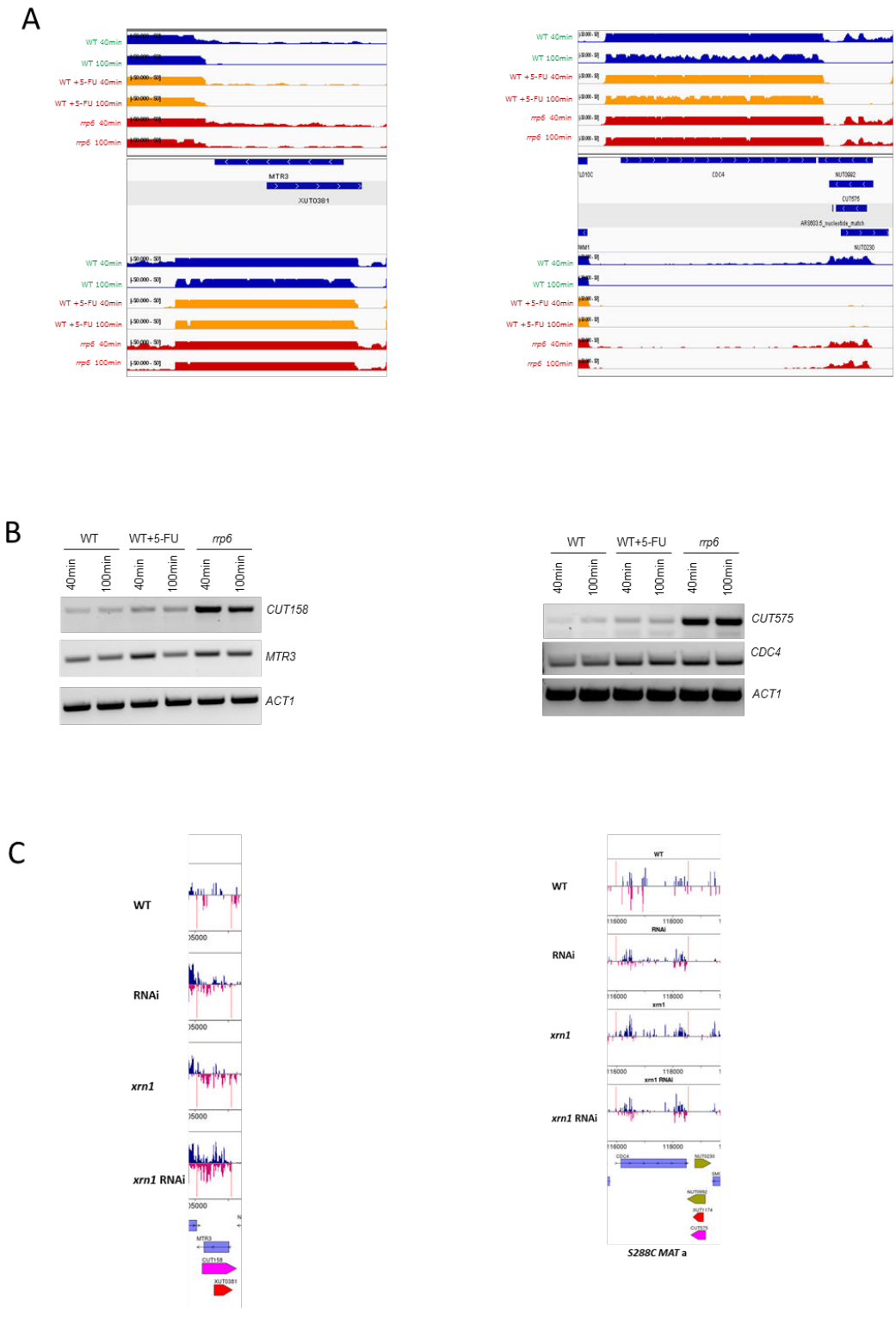

Figure 9. Expression pattern of differentially expressed essential genes and their antisense lncRNAs. (A) Heatmap shows the expression pattern of essential genes and their antisense lncRNAs, *MTR3/CUT158*, *CDC4/CUT575*, from RNA-Seq result. Protein coding genes are shown in blue box, different types of ncRNAs are shown in different colors, MUTs in yellow, XUTs in red, SUTs in light blue. Color scale is shown in the bottom. (B) RT-PCR validation results of those essential genes. ACT1 used as internal control. (C) Haploid double strand RNA (dsRNA) sequencing result of those essential genes. Peak represent dsRNA signals detected in the locus.

We explored the formation of double stranded RNA in the *CDC4* locus, by using an antibody that specifically recognizes the double helix region in RNA molecules. As shown in Figure 10A, we find a weak dsRNA signal in the 5-FU treated 100 min sample, while the signal in the *rrp6* mutant is very strong. We further validated Cdc4 protein level in order to see the function of double strand RNA formed by sense mRNA and antisense lncRNA (Figure 10B). As shown in figure, the protein level of Cdc4 has dropped dramatically in 5-FU treated cells and *rrp6* mutant, consistent with the double strand RNA formation in those two cells. Ace2 shows potential post-transcription regulation by ds RNA since *ACE2* mRNA formed ds RNA in 5-FU treated cells. We checked Ace2 protein expression and found that Ace2 protein drops in 5-FU treated cells and the *rrp6* mutant. This shows the negative correlation of dsRNA formation and Cdc4 protein levels.

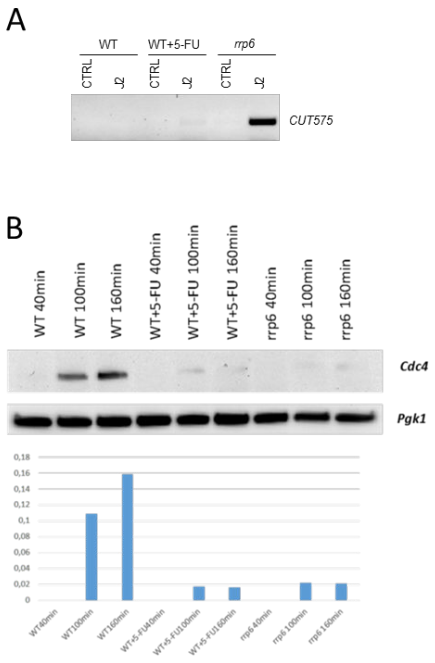

Figure 10. Expression pattern of Cdc4 protein. (A)Double stranded RNA validation result of CDC4 locus. Using double stranded RNA specific J2 antibody detect the formation of dsRNA(J2), samples without treatment of J2 antibody are used as control. (B) Western blot analysis for the expression of Cdc4 protein in wild type cell (WT), 5-FU treated cells (WT+5-FU), and *rrp6* mutant cells (*rrp6*) with 40min, 100min and 160min samples. Pgk1 in the panel below is used as internal control Quantification result is shown below.

We next assayed dsRNA formation at the *ACE2* locus, and found dsRNA in 5-FU treated cells; as expected the signal is elevated in *rrp6* mutant cells (Figure 11). The formation of dsRNA is negatively correlated with the protein level of Ace2, which indicates that dsRNA formation in the 5-FU treated cell may inhibit the translation of *ACE2* mRNA. By decreasing the protein level of Ace2, 5-FU may be able to down-regulate the downstream SIC1 cluster genes. Taken together, we found that 5-FU treated cells have abnormally accumulated lncRNAs which can form dsRNA with their antisense mRNAs to potentially inhibit important cell cycle regulators like *ACE2*, thus inhibiting their target SIC1 cluster genes, which could impair cell division.

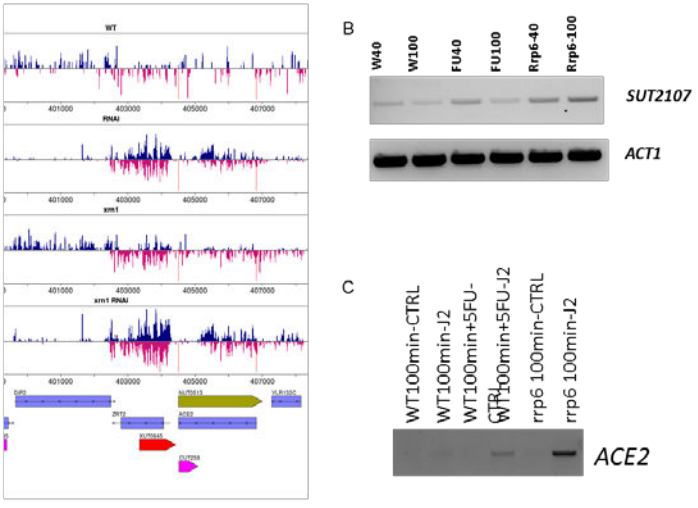

Figure 11. Expression pattern of dsRNA in ACE2 locus. (A) double stranded RNA (dsRNA) sequencing result for *ACE2*. Peaks represent dsRNA signals detected at the locus. (B) RT-PCR validation results for *SUT2107*. *ACT1* was used as a control. (C) J2 validation result of dsRNA formation at *ACE2* locus. J2 pull-down of 100min sample used as input for RT-PCR. A sample without J2 antibody was used as a control.

Discussion

Recent studies have revealed important roles of lncRNAs in mediating 5-FU's resistance in cancer cell lines. However, the role of lncRNA in 5-FU's cytotoxicity is still unknown. In this study, we have shown that lncRNA accumulates in cells treated with 5-FU, and elevated antisense lncRNA form double stranded RNA with its sense mRNA, to potentially inhibit the translation of key cell cycle regulators and essential genes, thereby mediating in part 5-FU cytotoxicity.

Mitotic time course ncRNA expression upon 5-FU treatment and rrp6 mutant

We found lncRNAs to be weakly induced in the treated cells, compared with *rrp6* mutant. This is an effect that one can expect because the drug inhibits Rrp6 but does not totally abolish its activity like the case of the *rrp6* mutant. I am trying understand the functions of those differently expressed ncRNAs by analyze the function of mRNAs associated with them, since 49% of differently expressed ncRNAs have mRNA associated on the opposite strand. Most of the lncRNAs that respond to 5-FU treatment are associated with antisense mRNAs that involve different functions as those mRNAs that differentially expressed in 5-FU treated cells. This indicates that the cells use different pathways to respond to 5-FU, to regulate genes in processes like cell division, by adjusting the levels of essential proteins via antisense lncRNAs that may exert post transcriptional regulation activities. Thus, cells respond to 5-FU via both transcriptional and post-transcriptional mechanisms.

Double strand RNA formation has potential role to inhibit translation

We found a negative correlation between mRNA/lncRNA formed dsRNA and protein level, this may indicate that dsRNA formation can inhibit translation. As reported before in Sinturel F, et al., converted mRNA pairs overlap with each other and can form double stranded RNA. This influences the translation of mRNAs and its stability, as the mRNA with a stop codon in the overlapping region is targeted by the NO-GO decay pathway, because ribosomes are blocked by the RNA duplex (Sinturel F, et al., Cell Rep.2015). Thus, it is possible that the lncRNA accumulated in 5-FU treated cells inhibits mRNA translation post-transcriptionally by forming double stranded RNA with its sense mRNA. More work should be done to check this possibility directly with knock down of the lncRNA or overexpression of lncRNA in normal cells under normal condition.

lncRNA regulation of AMEN pathway lead to cell cycle impair in 5-FU treated cells

Our RNA-Seq transcriptome profiling results show that *SIC1* cluster genes respond to 5-FU. They are involved in mitotic exit and cell division. Swi5 and Ace2 are transcription factors that regulate *SIC1* cluster genes expression. Ace2 protein levels decrease when cells are treated with 5-FU or

lack Rrp6. Note that *ACE2* mRNA and its antisense lncRNA form double stranded RNAs. Thus, abnormally accumulated lncRNAs in 5-FU treated cells may lead to inhibition of the key cell cycle transcription factor Ace2, resulting in defect in cell division. Chromosome segregation is another possible aspect of 5-FU toxicity, and could be due to the suppression of Ace2. Ace2 in fission yeast was reported to have a role associated with cohesion. Ace2 recruits Condensin to the centromere and mediates the association of Ace2 target genes locus to centromere and compaction of local chromosomal compaction during mitosis. Loss of Ace2 may result in abnormal conformation of chromatin since Ace2 target genes are no longer associated with centromere, while centromeres still continue to segregate, thus leading to the chromosome segregation defects (Kim KD, et al. Nature Genetics.2016).

References

Longley D. B.; Harkin D. P.; Johnston P. G. (May 2003). "5-fluorouracil: mechanisms of action and clinical strategies". Nat. Rev. Cancer. 3 (5): 330–8. doi:10.1038/nrc1074. PMID 12724731.

Scartozzi M, Maccaroni E, Giampieri R, Pistelli M, Bittoni A, Del Prete M, Berardi R, Cascinu S. 5-Fluorouracil pharmacogenomics: still rocking after all these years? Pharmacogenomics. 2011 Feb;12(2):251-65. doi: 10.2217/pgs.10.167.

Fang F, Hoskins J, Butler JS. 5-fluorouracil enhances exosome-dependent accumulation of polyadenylated rRNAs. Mol Cell Biol. 2004 Dec;24(24):10766-76.

Kammler S, Lykke-Andersen S, Jensen TH. The RNA exosome component hRrp6 is a target for 5-fluorouracil in human cells. Mol Cancer Res. 2008 Jun;6(6):990-5. doi: 10.1158/1541-7786.MCR-07-2217.

Silverstein RA1, González de Valdivia E, Visa N. The incorporation of 5-fluorouracil into RNA affects the ribonucleolytic activity of the exosome subunit Rrp6. Mol Cancer Res. 2011 Mar;9(3):332-40. doi: 10.1158/1541-7786.MCR-10-0084. Epub 2011 Feb 2.

Xu Z, Wei W, Gagneur J, Perocchi F, Clauder-Münster S, Camblong J, Guffanti E, Stutz F, Huber W, Steinmetz LM. Bidirectional promoters generate pervasive transcription in yeast. Nature. 2009 Feb 19;457(7232):1033-7. doi: 10.1038/nature07728. Epub 2009 Jan 25.

Schneider C, Kudla G, Wlotzka W, Tuck A, Tollervey D. Transcriptome-wide analysis of exosome targets. Mol Cell. 2012 Nov 9;48(3):422-33. doi: 10.1016/j.molcel.2012.08.013. Epub 2012 Sep 20

Gudipati RK1, Xu Z, Lebreton A, Séraphin B, Steinmetz LM, Jacquier A, Libri D. Extensive degradation of RNA precursors by the exosome in wild-type cells. Mol Cell. 2012 Nov 9;48(3):409-21. doi: 10.1016/j.molcel.2012.08.018. Epub 2012 Sep 20.

Geisler S1, Coller J. RNA in unexpected places: long non-coding RNA functions in diverse cellular contexts. Nat Rev Mol Cell Biol. 2013 Nov;14(11):699-712. doi: 10.1038/nrm3679. Epub 2013 Oct 9.

Melé M, Rinn JL. "Cat's Cradling" the 3D Genome by the Act of LncRNA Transcription. Mol Cell. 2016 Jun 2;62(5):657-64. doi: 10.1016/j.molcel.2016.05.011.

Wapinski O1, Chang HY. Long noncoding RNAs and human disease. Trends Cell Biol. 2011 Jun;21(6):354-61. doi: 10.1016/j.tcb.2011.04.001. Epub 2011 May 6.

Xiang JF, Yin QF, Chen T, Zhang Y, Zhang XO, Wu Z, Zhang S, Wang HB, Ge J, Lu X, Yang L, Chen LL. Human colorectal cancer-specific CCAT1-L lncRNA regulates long-range chromatin interactions at the MYC locus. Cell Res. 2014 May;24(5):513-31. doi: 10.1038/cr.2014.35. Epub 2014 Mar 25.

Huarte M., Guttman M., Feldser D., Garber M., Koziol M.J., Kenzelmann-Broz D., Khalil A.M., Zuk O., Amit I., Rabani M., et al. A large intergenic noncoding RNA induced by p53 mediates global gene repression in the p53 response. Cell. 2010;142:409–419. doi: 10.1016/j.cell.2010.06.040.

Calin GA1, Liu CG, Ferracin M, Hyslop T, Spizzo R, Sevignani C, Fabbri M, Cimmino A, Lee EJ, Wojcik SE, Shimizu M, Tili E, Rossi S, Taccioli C, Pichiorri F, Liu X, Zupo S, Herlea V, Gramantieri L, Lanza G, Alder H, Rassenti L, Volinia S, Schmittgen TD, Kipps TJ, Negrini M, Croce CM. Ultraconserved regions encoding ncRNAs are altered in human leukemias and carcinomas. Cancer Cell. 2007 Sep;12(3):215-29.

Bian Z, Jin L, Zhang J, Yin Y, Quan C, Hu Y, Feng Y, Liu H, Fei B, Mao Y, Zhou L, Qi X, Huang S,

Hua D, Xing C, Huang Z. LncRNA-UCA1 enhances cell proliferation and 5-fluorouracil resistance in colorectal cancer by inhibiting miR-204-5p. Sci Rep. 2016 Apr 5;6:23892. doi: 10.1038/srep23892.

Lee H, Kim C, Ku JL, et al (2014). A long non-coding RNA snaR contributes to 5-fluorouracil resistance in human colon cancer cells. Mol Cells, 37, 540-6.

Grem JL, Fischer PH (1989) Enhancement of 5-fluorouracil's anticancer activity by dipyridamole. Pharmacol Ther 40:349–371.

Daniel, B.L., Paul, D.H., Patrick, G.J. 5-Fluorouracil: mechanisms of action and clinical strategies. Nat. Rev. Cancer. 2003;3:330–338.

Xu, Z., Wei, W., Gagneur, J., Perocchi, F., Clauder-Munster, S., Camblong, J., Guffanti, E., Stutz, F., Huber, W. and Steinmetz, L.M. (2009) Bidirectional promoters generate pervasive transcription in yeast. Nature 457, 1033–1037

Wyers, F., Rougemaille, M., Badis, G., Rousselle, J.C., Dufour, M.E., Boulay, J., Regnault, B., Devaux, F., Namane, A., Seraphin, B. et al. (2005) Cryptic pol II transcripts are degraded by a nuclear quality control pathway involving a new poly(A) polymerase. Cell 121, 725–737
Mullen, T. E.; Marzluff, W. F. (1 January 2008). "Degradation of histone mRNA requires oligouridylation followed by decapping and simultaneous degradation of the mRNA both 5' to 3' and 3' to 5'". Genes & Development. 22 (1): 50–65. doi:10.1101/gad.1622708.

Lardenois A1, Liu Y, Walther T, Chalmel F, Evrard B, Granovskaia M, Chu A, Davis RW, Steinmetz LM, Primig M. Execution of the meiotic noncoding RNA expression program and the onset of gametogenesis in yeast require the conserved exosome subunit Rrp6. Proc Natl Acad Sci U S A. 2011 Jan 18;108(3):1058-63. doi: 10.1073/pnas.1016459108. Epub 2010 Dec 13.

Sinturel F., Navickas A., Wery M., Descrimes M., Morillon A., Torchet C., Benard L. Cytoplasmic control of sense-antisense mRNA pairs. Cell Rep. 2015;12:1853–1864.

Wery M, Descrimes M, Vogt N, Dallongeville AS, Gautheret D, Morillon A. Nonsense-Mediated Decay Restricts LncRNA Levels in Yeast Unless Blocked by Double-Stranded RNA Structure. Mol

Cell. 2016 Feb 4;61(3):379-92. doi: 10.1016/j.molcel.2015.12.020. Epub 2016 Jan 21.

Kim KD, Tanizawa H, Iwasaki O, Noma KI. Transcription factors mediate condensin recruitment and global chromosomal organization in fission yeast. Nat Genet. 2016 Aug 22. doi: 10.1038/ng.3647

2. RRP6 overexpression enhances 5-FU resistance

Introduction

Rrp6 is the target of 5-FU to exert its RNA based cytotoxicity. Rrp6 deletion was shown to render yeast cells hypersensitive to 5-FU treatment, interestingly, deletion of one allele of *RRP6* results in a more severe growth defect than homozygote deletion (Fang F. et al., Mol Cell Biol.2004). The study indicates that *RRP6* is an important gene for 5-FU resistance. Thus, elevated *RRP6* expression could lead to cell being more resistant to 5-FU treatment. To test this hypothesis, we carried out a study with a yeast strain overexpressing *RRP6*.

Materials and methods

Yeast strains and growth media. Strains used in this study are JHY222, SK1, MPY721 (TEF1-*RRP6*), and MPY576 (GAL-*RRP6*). Growth media were prepared according to standard protocols of yeast YPD (glucose), and YPGal (galactose).

Growth curve measurement. Overnight cultured yeast cells were diluted to $2x10^6$ cells/ml with fresh YPD medium, and then cultured in the shaker incubator at 30°C. We measured the cell concentration every hour by counting the cells with cell count chamber or by measuring the OD600 with an Eppendorf BioPhotometer (Eppendorf, Germany).

Growth drop assay. Drop assay was performed with YPD medium or YPD medium containing various concentrations of 5-FU, or YPA medium and YPA medium with various concentration of 5-FU. Yeast cells grown in YPD medium overnight, then diluted into $2x10^6$ cells/ml with fresh YPD medium. Then we serially diluted cells ranging from 10 fold to 10^4 fold and plated them. We incubated the plate at 30ºC, and recorded growth by taking pictures with the GelDoc XRS system (Bio-Rad. USA) at 24h and 48h.

Mitosis dynamics analysis. Flow cytometry was used to record mitotic cell cycle progression as

described in Lardenois et al.,2011. Briefly, 10^7 cells were re-suspended, fixed with 70% ethanol, and sonicated with a Branson Sonifier 250 for 10s at 20% power.

Results and discussion

To explore the effect of elevated Rrp6 levels on 5-FU treatment in budding yeast, I measured the growth rate of both a TEF promoter driven *RRP6* overexpression strain (TEF-*RRP6* O/E strain) and a GAL promoter driven *RRP6* overexpression strain (GAL-*RRP6* O/E strain). Furthermore, I used the TEF-*RRP6* overexpression strain to do a drop assay to measure its growth rate. As shown by growth curve and plate growth assay, overexpression of Rrp6 will result in elevated resistance to 5-FU (20□g/ml), since the growth rate and cell viability are both increased in liquid culture measured by growth curve (10 hour) and in solid culture measured by drop assay (48 hours) (Figure 1AB)

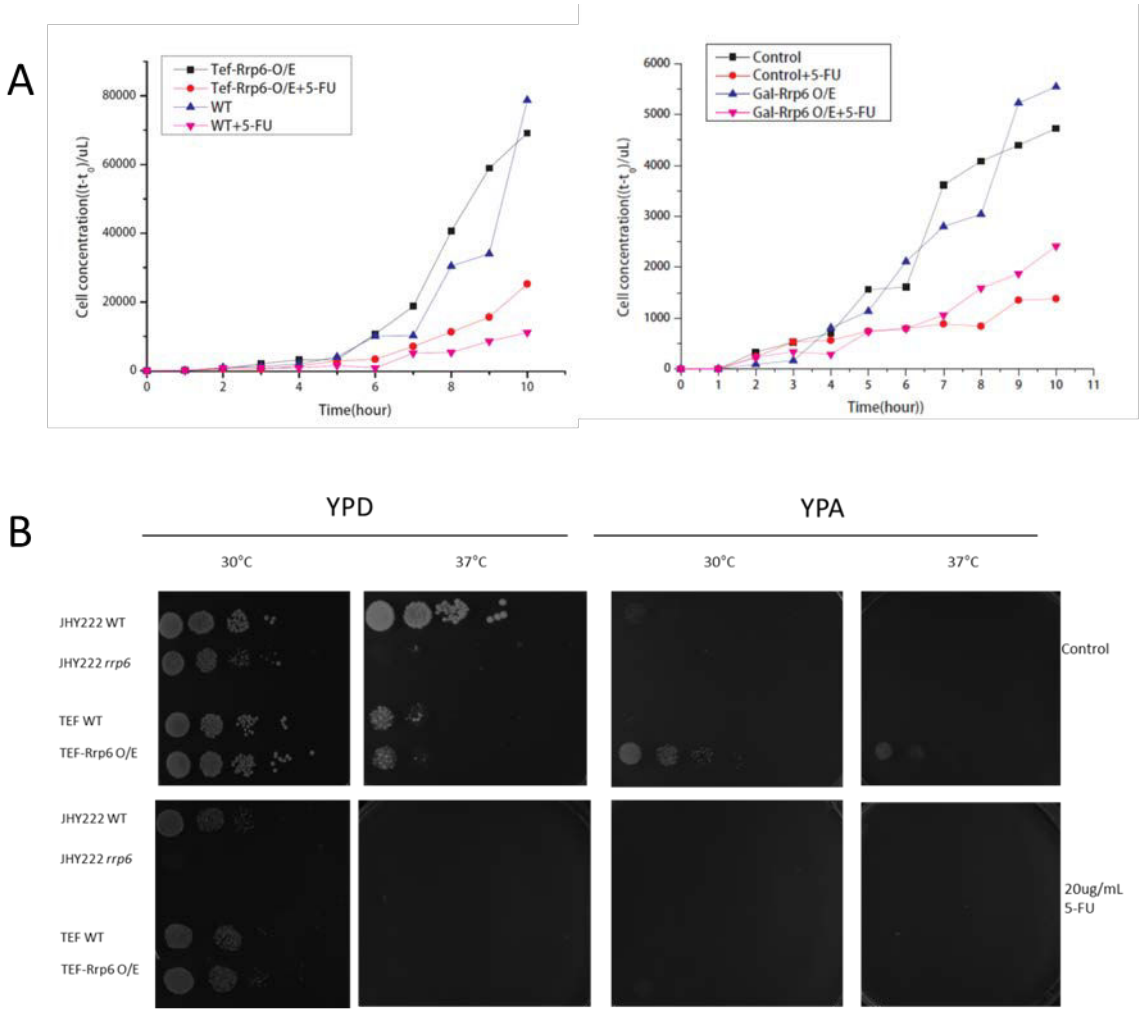

Figure 1. Growth assay of WT vs. Rrp6 overexpression strain. (A) Drop assay of WT and Rrp6 overexpression strain (B) Growth curve of WT and Rrp6 overexpression strain treated with 5-FU.

It was also shown that the resistance to 5-FU is 5-FU dosage dependent, as upon increased 5-FU concentration the resistance will diminish in the *RRP6* overexpression strain, and eventually there is no difference when the concentration of 5-FU reaches a very high level at 2000μg/ml (Figure 2)

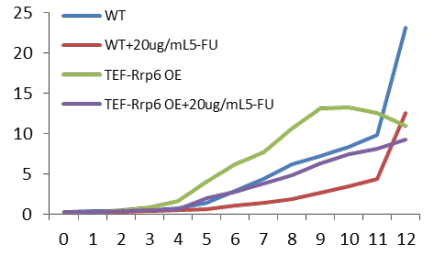

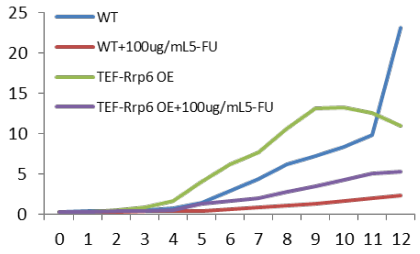

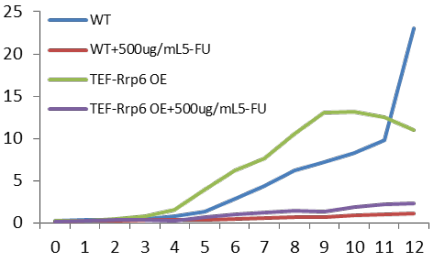

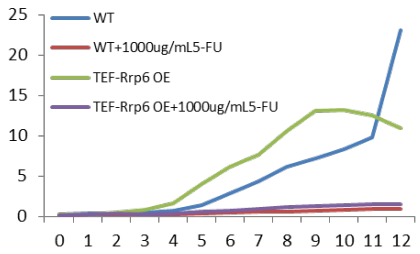

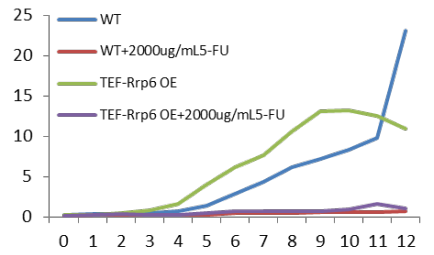

Figure 2. Growth curve of WT and Rrp6 overexpression strain treated with different concentration of 5-FU. WT cells and TEF-*RRP6* overexpressing cells were treated with 5-FU concentration ranging from 20μg/ml to 2000μg/ml, and growth were recorded for 12 hours.

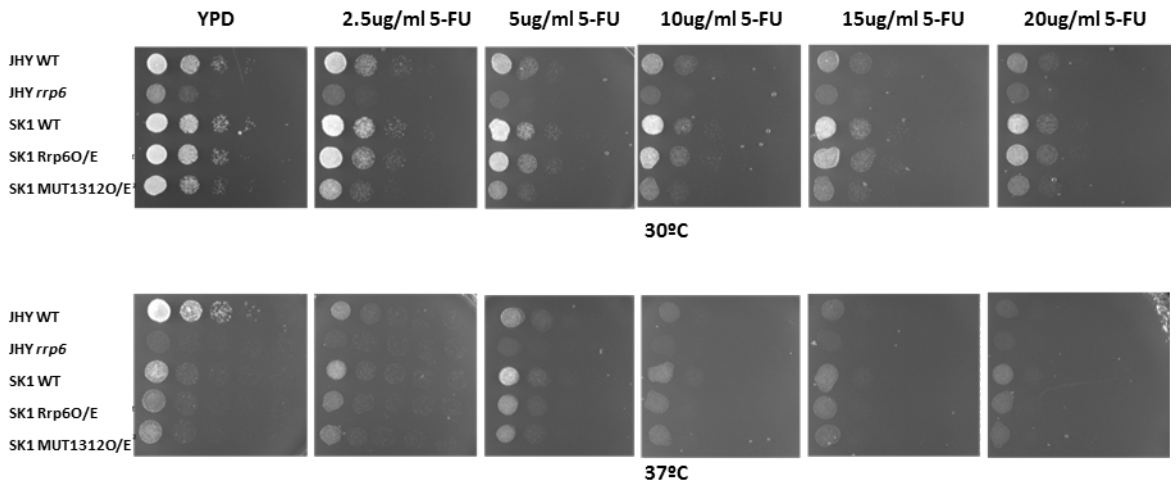

Figure 3 Drop assay of WT and *MUT1312* overexpression strain. SK1 WT, *rrp6,* TEF-*RRP6* overexpression strain, TEF-*MUT1312* overexpression strain were treated with various concentration of 5-FU ranging from 2.5μg/ml to

20μg/ml, then incubated at 30ºC and 37ºC for 48h.

It is known that an *rrp6* mutant is hypersensitive to 5-FU treatment; a heterozygous mutation of *rrp6* results in greater sensitivity to 5-FU treatment than homozygous *rrp6* mutant (Fang F. et al., Mol Cell Biol. 2004). The Rrp6 protein level decreases about 50% in cells cultured in pro-sporulation medium where cells undergo respiration (YPA) (Lardenois A., et al., PNAS. 2011). Therefore, I used the WT JHY222 strain cultured in YPA medium with 5-FU treatment to test if it becomes hypersensitive to 5-FU treatment. As shown in Figure 1, yeast cells cultured on YPA become more sensitive to 5-FU than YPD. Note that the *RRP6* locus is associated with an antisense lncRNA called *MUT1312* that overlaps with its 3' region. When *MUT1312* is induced Rrp6 protein levels decrease, therefore it could be that *MUT1312* inhibits the translation of *RRP6* mRNA. If this is true then cells with elevated *MUT1312* should be more sensitive to 5-FU treatment due to the lower concentration of Rrp6 protein. To test this idea, I used the *MUT1312* overexpression strain for 5-FU treatment and found indeed that it is more sensitive to 5-FU treatment (Figure 3).

From the experiments above, I show that Rrp6 protein level determines a cell's response to 5-FU treatment, and elevated Rrp6 could lead to resistance to 5-FU. This result is potentially important, since the mammalian homologue of Rrp6 (EXOSC10) shows an elevated expression level in several cancer cell lines, including colon cancer, which may help the tumor resist 5-FU chemotherapy (M. Primig; personal communication). Therefore, our study provides a new perspective to improving 5-FU chemotherapy by targeting Rrp6.

3. Meiotic lncRNA control in mitosis by RRP6

Introduction

Meiotic Unannotated Transcripts, are induced during early and middle meiosis, which coincides with the time point when Rrp6 protein gradually disappears (Lardenois A., et al., PNAS. 2011). Whether all MUTs are direct Rrp6 targets of if some are predominantly transcriptionally regulated is unclear.

Materials and methods

Yeast strains and growth media. Strains used in this study are JHY222 wild-type and *rrp6* mutant (Lardenois et al., PNAS 2011). Growth media were prepared according to standard protocols of yeast growth (YPD, glucose and YPA acetate), and sporulation (SPII) media.

RT-PCR assay. RNA was extracted by Hot phenol method, followed by DNase I treatment with TURBO DNA-free Kit (Ambion, USA). RT-PCR reactions were carried out using 2 μg of RNA reverse transcribed with Reverse Transcriptase (High Capacity cDNA Reverse Transcription kit; Life Technologies, USA), for poly(A) detect use the same kit but use Oligo dT (T15 or T25) as primer. cDNA was amplified using Taq Polymerase (Qiagen, France) at 60ºC for 26 cycles. RT-PCR products were separated on 2% agarose gels and photographed using an ImageQuant 350 digital Imaging 381 System at the default settings (General Electric, USA) Primers used for RT-PCR were designed with Primer3 (simgene.com/Primer3; Table 1).

Results and Discussion

Tiling array data obtained with WT versus *rrp6* mutants indicate that a large number of MUTs fail to accumulate in *rrp6* cells that are cultured in sporulation medium (A. Lardenois et al., unpublished).

lncRNAs become more stable in *rrp6* mutant

According to unpublished WT vs. *rrp6* tilling array data, certain MUTs fail to be detected in samples from *rrp6* mutant cells cultured in sporulation medium (*MUT1465, MUT1290, MUT523*, and *MUT100*), while others accumulate (*MUT81, MUT338*). To verify this puzzling result, I did RT-PCR to test the lncRNA expression in WT strain and *rrp6* strain with mitotic samples (YPD samples and YPA samples) and meiotic time course samples (SPII 2h to SPII10h). As expected, MUTs are upregulated in *rrp6* mutant (Figure 2). The RT-PCR results confirm that some MUTs are targets of Rrp6, and therefore MUTs accumulate when Rrp6 is absent. Panels A and B, C indicate that for some lncRNAs tiling array and RT-PCR data correspond to each other, while for other they do not.

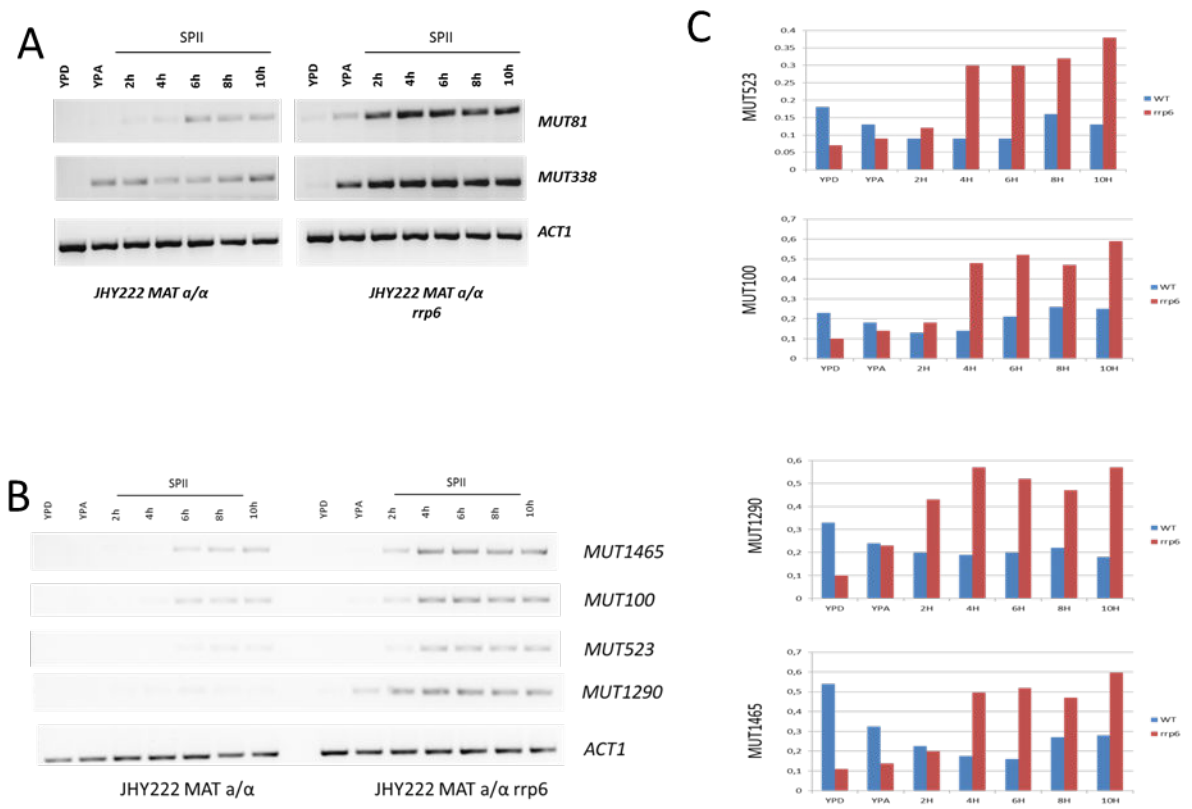

Figure 2. Expression patterns of MUTs in WT vs. *rrp6*. RT-PCR result shown the expression patterns of selected MUTs during meiosis (A and B) and quantification (C). *ACT1* was used as a loading control.

rrp6 mutant cells accumulate polyA ncRNAs

This led to the question why RT-PCR and tilling arrays yield contradictory results for certain lncRNAs. The possible explanations are (1) RT-PCR and tilling array based RNA profiling are different methods and therefore can lead to different results, and (2) the tiling array data are not reproducible by RT-PCR for all lncRNA in an *rrp6* mutant background.

To test the first possibility, we thought there might be some different steps during two protocol which lead to the distinct result. After carefully examine the protocols, we thought it could be either strand specific transcription or polyadenylated RNA enrichment step in tilling array lead to lost some RNAs. However, according to the strand specific RNA-Seq result in WT vs. *rrp6* that strand specific transcription cannot lead to lose of RNA. To verify if decreased polyadenylation in *rrp6* mutant cells lead to the difference, I used oligo d(T) as primer for reverse transcription since Oligo d(T) primer can only reverse transcribe RNA molecules with polyadenylated tail. As the result shown in Figure 3A demonstrates for *MUT1465*, its poly adenylation is increased in the *rrp6* mutant. Thus it is not the two-step enrichment for polyadenylated transcripts in the tiling array protocol (which may have depleted the library of lncRNAs that were not polyadenylated in the *rrp6*

mutant) that led to the different result in RT-PCR (where no enrichment step is done) and tiling arrays. It is currently unclear what causes this discrepancy. It is possible that the tiling array data algorithm for detecting transcripts in WT cells may not suitable for the *rrp6* mutant, since it shows a broad genome-wide pattern of altered transcript architecture, notably it shows elongated read-through transcripts, which do not have normal boundaries for the transcripts.

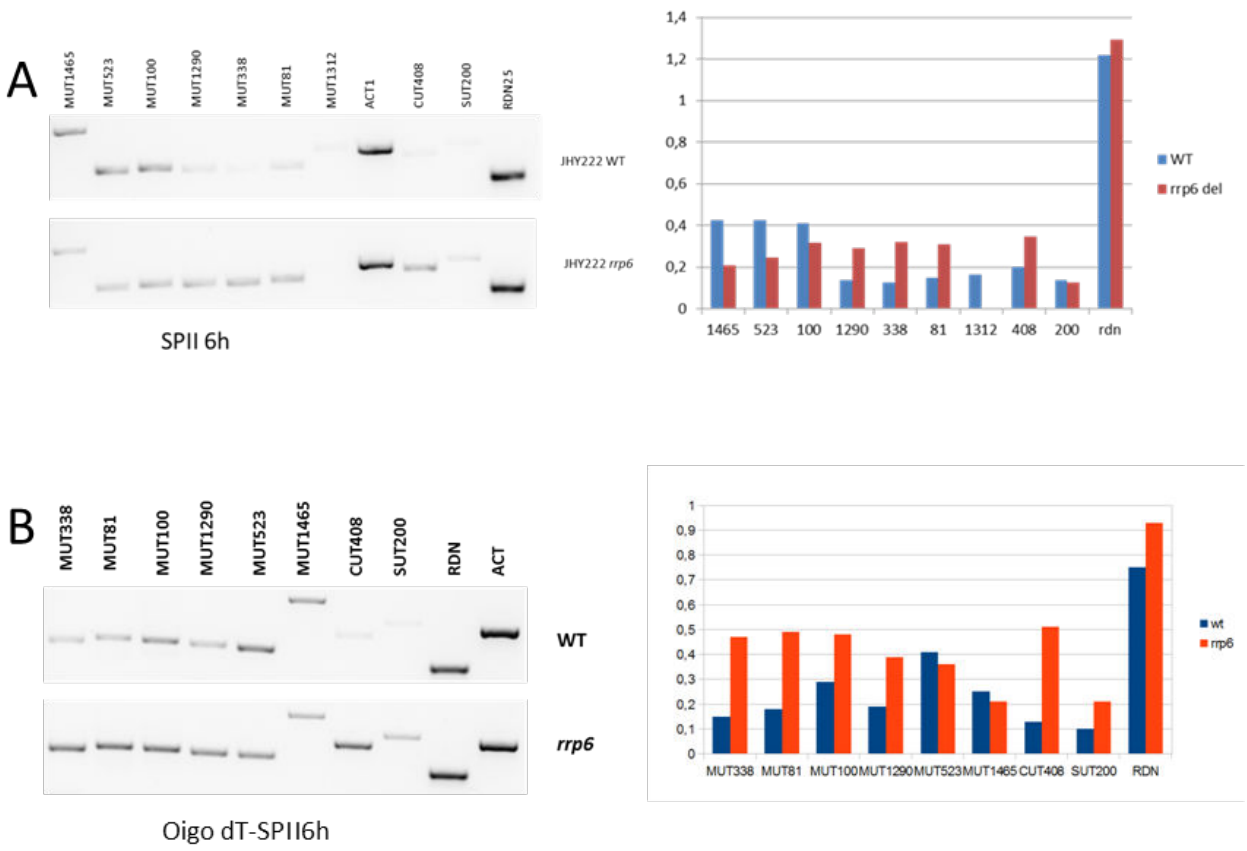

Figure 3. Polyadenylated patterns of MUTs during meiosis in WT vs. *rrp6* cells. (A) MUT expression patterns in WT vs. *rrp6* during meiosis. (B) Polyadenylated MUT expression patterns in WT vs. *rrp6* during meiosis.

4. Meiotic transcript isoform control in mitosis by RRP6

Previous study in budding yeast shows that mRNAs have isoform changes during meiosis with extended 5'-UTR or 3'-UTR (Lardenois A., et al., Nucleic Acids Research. 2015). In the WT vs. *rrp6* tilling array data, the meiotic isoforms of some mRNAs show delayed induction in *rrp6* mutant. This could be expected since *rrp6* mutant shows delayed sporulation phenotype therefore the meiotic induced RNA isoforms could respond by showing delayed induction pattern. However, there is also the possibility that they are directly dependent on Rrp6. Thus I performed experiments to know more about a possible role of Rrp6 in regulating those meiotically induced 5' extended mRNA isoforms.

Results and discussion

Meiotic isoforms accumulate in *rrp6* mutant cells

According to unpublished WT vs. *rrp6* tilling array data, some mRNAs have 5' end extended isoform been induced in meiosis, and the expression level of those meiotic extensions have decreased in *rrp6* strain, for example *MCM5*. To validate this, I use RT-PCR to verify the isoform expression in WT strain and *rrp6* strain with mitotic samples (YPD samples and YPA samples) and meiotic time course samples (SPII 2h to SPII10h samples). However, contrary to what was found by tilling arrays, the RT-PCR results shows that in the *rrp6* mutant, the extended 5'UTR is very moderately up-regulated (Figure 1 AB).

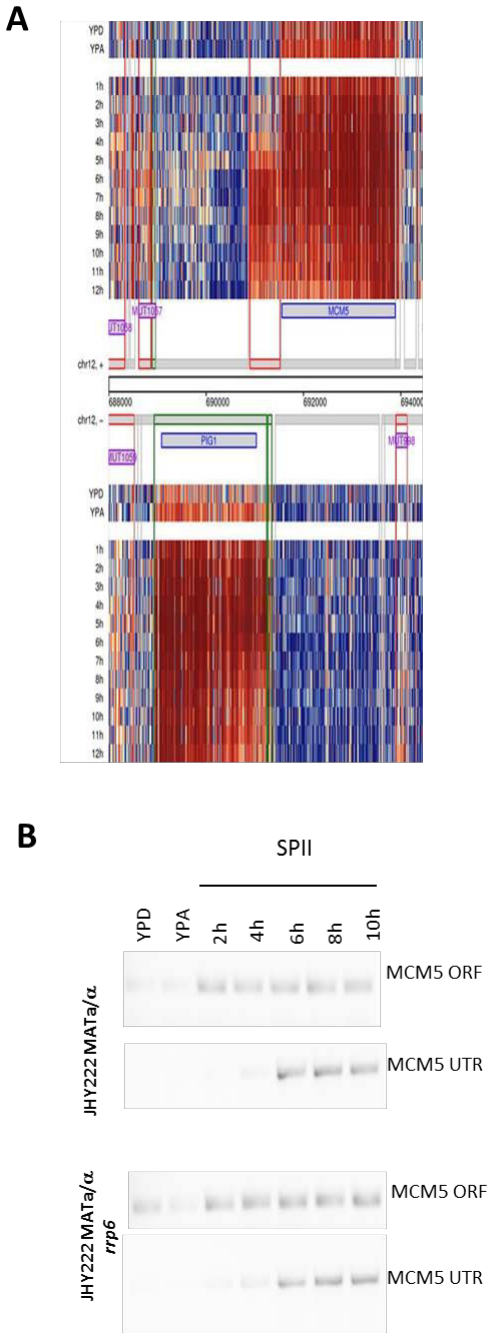

Figure 1. Expression pattern of *MCM5*. (A) A heatmap shows the expression pattern of MCM5, in the meiotic tilling array of WT cell. (B) RT-PCR validation of *MCM5*. Expression pattern of ORF and meiotic UTR of MCM5 in mitotic YPD and YPA sample and meiotic time course samples of WT and *rrp6* mutant strains were checked by RT-PCR.

This is consistent with the result in WT cells that meiotic isoforms are induced when Rrp6 protein levels progressively decrease during meiosis and spore formation. Together, those results indicate that certain meiotic mRNA isoforms may be a target of Rrp6 once they are transcribed in mitosis. Some meiotically induced 5'UTR extended mRNA isoforms may be cell cycle regulated during mitosis, which attenuates the signal in asynchronous WT cells, while the *rrp6* mutant shows cell cycle progression deficiency during mitosis (see Figure 2A in the results section),. So, *rrp6* mutant cells tend to accumulate in G1 phase and therefore cell cycle regulated mRNA isoforms can be detected in vegetatively growing *rrp6* cells. This has been confirmed by validation result of meiotic mRNA isoforms in the 5-FU project. Therefore, certain meiotic isoforms are not strictly meiosis specific, but are cell cycle regulated during mitosis and may thus be undetectable in asynchronous YPD samples. This

suggests that YPD samples are not an optimal control for a meiotic time course study of highly cell cycle regulated mRNA isoforms since asynchronous mitotic cells are compared with semi-synchronous cells in meiosis. It is also possible that the Ume6 and perhaps even Sum1 repressors become unstable in *rrp6* mutants, which could lead to partial de-repression of meiotic isoforms during vegetative growth.

5. 5-FU treatment induces MUTs and meiotic isoforms in vegetatively growing cells.

Since 5-FU inhibits Rrp6, which targets certain MUTs, I sought to investigate if MUTs accumulate upon 5-FU treatment. Therefore I choose some MUTs to do validations, and found that some MUTs appear indeed to be mitotically cell cycle regulated, as shown in WT 40min (G1 phase) and WT 100min (S phase) samples with fluctuated expression. Thus I found that some MUTs may not be strictly meiosis specific, but cell cycle regulated in mitosis. Therefore, the signal was attenuated in mitotic samples from unsynchronized cells. The phenomenon of cell cycle fluctuation of lncRNAs is not surprising, because it was reported before in the case of SUTs (Granovskaia et al., Genome Biol 2010).

In addition to MUTs, I was also interested to know if mRNA have isoform changes upon 5-FU treatment, since many papers reported that alternative splicing occurs upon drug treatment and that this phenomenon has important role in mediating drug toxicity (Rehman SU et al., Wiley Interdiscip Rev RNA. 2015 Garcia-Blanco MA, et al., Nature Biotechnology.2004).

I validated selected genes which are shown in SGV (sgv.genouest.org) to have meiotic induced 5'UTR extension: *UTP6*, *MCM5*. I found that 5'-extended isoforms are detectable in synchronized untreated cells, and they accumulate in 5-FU treated cells. This indicates that 5-FU treatment can alter of the architecture of transcript isoforms in a cell. This also suggests that some meiotically induced extended isoforms is not strictly meiosis-specific but cell cycle regulated in mitosis. These questions notwithstanding, our findings may have interesting implications about how protein may be regulated by 5'-extended isoforms not only during meiosis but also during mitosis.

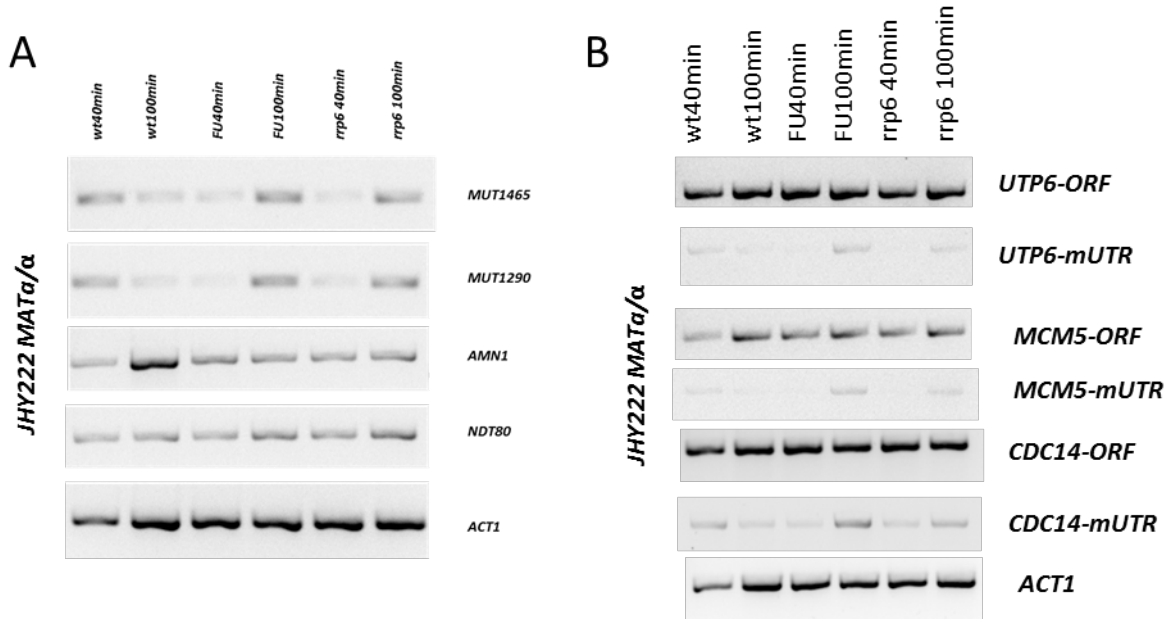

Figure 1. Expression pattern of MUTs and mRNA isoforms in 5-FU treated cells. (A) Expression pattern of MUTs in WT, 5-FU treated cells and rrp6 mutant. (B) Expression pattern of mRNA meiotic isoforms in WT, 5-FU treated cells and *rrp6* mutant.

All isoforms show altered patterns in 5-FU treated cell and *rrp6* mutant as compared to WT cells. The isoforms are normally induced at 40min which is the G1 phase in WT cells, then down regulated when cells entering S phase. However, in the treated cells and mutant cells, the extended isoform shows up at 100 min when cell entering S phase. This may due to the cell cycle progression problem in the treated cells and mutant cells.

Especially *CDC14* has the most obvious and highest expression. Cdc14 is a protein important for cell cycle progression by promoting mitotic exit (Marston A., et al. Developmental Cell.2003; Stegmeier F.et al., Annu. Rev.Genet.2004). Misregulation of *CDC14* in treated cells, as shown by the mRNA level indicating that *CDC14* is upregulated, thus may lead to the continuous activation of the mitotic exit network.

Taken together, previous I found that AMEN pathway, which inhibit mitotic exit network pathway, has been down regulated in 5-FU treated cells, as the two transcription factor *SWI5/ACE2* which activate AMEN pathway shown declined pattern in treated cells. Here I found MEN pathway been continuous activated in treated cells by the induction of meiotic isoform of *CDC14*. Thus, mitotic exit has been aberrantly activated both by inhibit its inhibitor and activate its activators. This, is together with *SWI5/ACE2* decline that down-regulates the AMEN pathway (which inhibits mitotic

exit), may deregulate cell cycle progression in drug treated cells and, to a certain extent, the *rrp6* mutant.

6. The regulation of RRP6 during growth and development

Introduction

Rrp6 is 3' to 5' exoribonuclease which participates in processing or degrade various RNAs including mRNA, rRNA and ncRNAs. Previous study from Lardenois et al., shows that Rrp6 is gradually diminished in early meiosis and disappeared in middle late meiosis, which is the opposite patterns of meiotic ncRNAs. An ncRNA antisense to *RRP6*, *MUT1312*, also shows the inversed expression pattern as *RRP6*. The authors proposed two mechanisms to explain the decrease of Rrp6 protein during meiosis: (1) *MUT1312* inhibits translation of Rrp6; (2) Rrp6 protein is degraded by a protease called Anaphase Promoting Complex/Cyclosome (APC), which only exerts partial activity during respiratory growth, but full function during sporulation (Lardenois A, et al., PNAS.2011).

The APC/C complex is an E3 ligase with multiple subunits that targets mitotic cyclins and proteins that inhibit anaphase, which need to be degraded by proteasome to trigger chromatid separation and mitosis exit. APC/C consists of 13 core submits and two cell cycle dependent activator subunits, Cdc20 and Cdh1, which stage specifically associate with the APC/C during the cell cycle. Cdc20 is required to activate APC/C complex at early mitosis, whereas Cdh1 activates APC/C complex in late mitosis during the G1-S transition (Peters J M, et al. Nat.Rev.Mol.Cell Biol.2006). The association of Cdc20 and Cdh1 to the APC/C core complex requires the different phosphorylation status of APC/C core complex, as Cdc20-APC/C interaction requires the phosphorylation of several core subunits of APC/C by mitotic kinases, such as Cdk1 and Plk1. While phosphorylation of Cdh1 by Cdk 1 or Cdk2 during S-phase, G2-phase, and early mitosis inhibits the association of Cdh1with APC/C core complex, Therefore, the status of APC/C (inactive in S phase, activated by Cdc20 in early-mid-mitosis, and activated by Cdh1 during late mitosis to G1/S phase transition) is mainly determined by Cdk activity. (Manchado E et al., Biochem. Soc. Trans. (2010)). Conversely, the APC/C complex could also regulate Cdk activity, as during G2/M-phase it can degrade A-type cyclins or B-type cyclins during the metaphase–anaphase transition. Thus, the protein level and activity of major cell cycle regulators are regulated by the reciprocal control between Cdks and APC/C, which is essential for the proper transition between replication and mitosis (Thornton B R. et al, Genes Dev 2006, Peters J M Nat Rev Mol Cell Biol. 2006, Manchado E et al., Biochem. Soc. Trans. (2010). The way Cdc20 and Cdh1recognize their substrate is mediated by C-terminal WD40

domain, which specifically bind to the element D-box, KEN-box, A-box, or O-box on the target proteins.

As it has important roles in mitosis, the APC/C complex has also been found to have important functions to degrade key regulators of meiosis. In budding yeast a third activator of APC/C is used specifically in meiosis, Ama1. Ama1 is essential for exit from meiosis II (Cooper KF, et al. Proc Natl Acad Sci USA.2000; McDonald C M, et al., Genetics. 2005 Diamond A E., et al Mol Biol Cell 2009; Tan G S, et al., Mol Biol Cell. 2011). The APC/C complex is required for the entry into meiosis, as it plays important role in degrading Ume6 which is a transcription repressor that needs to be degraded during mitotic and meiotic transition. APC/C^{Cdc20} is also required for Meiotic I division and meiotic II division. A *cdc20* mutant arrests at prophase I and a heterozygous destructible mutant of Pds1, which is a target of APC/C^{Cdc20} also arrests at prophase I (Tan G S., et al. Mol Biol Cell. 2011; Salah S M., et al. Chromosoma. 2000, Shonn MA, et al. Science 2000. Oelschlaegel T. Cell. 2005; Cooper K F, et al., Genetics.2009).

To test these hypotheses, we searched Rrp6 protein sequence and found conserved destruction box motif therefore we constructed strain with mutation of destruction box of Rrp6 and we further explored the possible mechanism of *MUT1312* in controlling of *RRP6*.

Materials and methods

Yeast strains and growth media. Strains used in this study are JHY222 and SK1 wild-type and *rrp6* (Lardenois et al., PNAS 2011), MPY646 and MPY648 (*rrp6* db mutant), MPY665 (*MUT1312* CIS-ON), and MPY721 (TEF1-*RRP6* OE). Growth media were prepared according to standard protocols of yeast YPD media (with glucose), YPA media (with acetate), SPII and SPIII media.

Growth drop assay. Drop assay was performed with YPD medium. Yeast cells were grown in YPD medium overnight, then diluted to $2x10^6$ cells/ml with fresh YPD medium. Then further serial dilution ranging from 10-fold to 10^4-fold was done before plating the cell suspensions. Culture the plate at 30ºC, and record the growth by taking photo with GelDoc XRS system (Bio-Rad. USA) at 24h and 48h.

RT-PCR assay. RNA was extracted by Hot phenol method, followed by DNase I treatment with TURBO DNA-free Kit (Ambion, USA). RT-PCR reactions were carried out using 2 μg of RNA

reverse transcribed with Reverse Transcriptase (High Capacity cDNA Reverse Transcription kit; Life Technologies, USA) and amplified using Taq Polymerase (Qiagen, France) at 60ºC for 26 cycles. RT-PCR products were separated on 2% agarose gels and photographed using an ImageQuant 350 digital Imaging 381 System at the default settings (General Electric, USA) Primers used for RT-PCR were designed with Primer3 (simgene.com/Primer3; Table 1).

Table 1. Primer sequences.

RRP6-5'	CCCACCAAAAGAGTCGAAAA	CGAATCATCCCAGGATTTTG
RRP6-3'	CGCACCTAATCACTCGCCT	AGCTGCCCTTGGTCCATTAC
MUT1312	AGAGAAAATGGTGTGCATGG	CGGAAAAAGATGCTGTGGAT
GAP1	TTGTTGCCGCCTCCAAAAAG	CCCCAGTAGGAACCCCAAAC
SWI6	TGAGACCCGTGGATTTTGGG	GCTCTTTCGACTCCGCTTCT
ACT1	CTGCCGGTATTGACCAAACT	AGATGGACCACTTTCGTCGT

Western blot assay. Protein extract was prepared with YPD, YPA, and full meiotic time course sample, by using method described in Vitaly V. Kushnirov's paper (Vitaly V. Kushnirov, Yeast. 2000). 20μg protein extract was used for electrophoresis with SDS-PAGE gel (BIO-Rad, USA), then protein was transferred to ImmobilonPSQ membranes (Millipore, France) with electro-blotter (TE77X; Hoefer, USA) with 50mA for 2.5h. Membrane was block by incubate in 5% milk powder at room temperature for 1h, then incubate with anti-Rrp6 antibody at 1:3000 overnight at 4°C. Incubate with secondary antibody anti-rabbit at 1:10000 at room temperature for 1h. Use Pgk1 as internal control, the primary antibody was at 1:10000 at room temperature for 1 h, then use anti-mouse secondary antibody at 1:10000 at room temperature for 1h., Protein band signals were detected by ECL-Plus Chemiluminescence kit (GE Healthcare, USA) with ChemiDoc XRS system (Bio-Rad. USA). Signal were quantified by using ImageQuant TL 7.0 software package (GE Healthcare, USA).

RNaseONE protection assay. RNaseONE (Promega, USA) digestion of RNA was carried out with serial dilution of RNaseONE. RNA purified with phenol/chloroform then reverse transcribed with 2μg RNA by using High Capacity cDNA Reverse Transcription kit (Life Technologies, USA) and amplified using Taq Polymerase (Qiagen, France) at 60ºC for 28 cycles.

J2-RIP assay. Use 35μg RNA incubated with magnet beads and J2 antibody, then RNA was eluted and reverse transcribed with 2μg RNA by using High Capacity cDNA Reverse Transcription kit

(Life Technologies, USA) and amplified using Taq Polymerase (Qiagen, France) at 60ºC for 28 cycles.

Spore formation efficiency test. 5 colonies of yeast from both the WT strain and MUT1312 overexpression strain were grown on YPD plate for two days, then replicated onto SPIII plate, and asci were counted after 24h and 48h.

Results and discussion

Previous research shows that Rrp6 protein become unstable in acetate medium (YPA) and further diminish in sporulation medium (Lardenois A., et al., PNAS. 2011). In order to know why Rrp6 become unstable and what mechanism behind this, we carried out a study and found that Rrp6 has a conserved APC/C complex destruction box (E. Becker, personal communication) which could be targeted by APC/C complex to trigger degradation by the proteasome. Since APC/C become unstable during middle late meiosis, the authors put forward hypothesis that Rrp6 stability is controlled by APC/C complex during onset of meiosis, or the antisense *MUT1312* could decrease the Rrp6 protein level via an interference independent mechanism, for example by forming dsRNA that inhibits mRNA translation.

As result, I first tested the hypothesis if Rrp6 protein is targeted by the APC/C complex. To this end, we constructed a strain bearing mutant allele deleting the destruction box, and grew the cells on YPD plate at 30ºC and 37ºC to test their growth properties. The destruction box mutant db*rrp6* does not show the temperature sensitive phenotype known for *rrp6* cells, when switched to the non-permissive temperature (Figure 1).

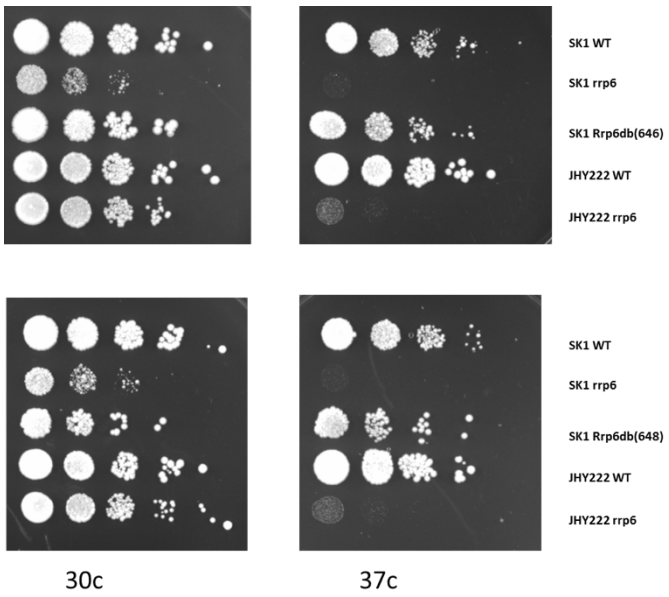

Figure 1. Drop assay of yeast growth on YPD plate. WT, *rrp6,* and two different strains of Rrp6 destruction box mutant (dbRrp6 646 and dbRrp6 648) was grown on the YPD plate at 30 and 37 for 48 hours.

In addition, I tested the hypothesis that antisense non-coding RNA controls the translation of Rrp6. I first used a strain that overexpresses *MUT1312* driven by a TEF-promoter to test its sporulation dynamics and efficiency. It was reported that a *rrp6* mutant has deficiency in meiotic DNA replication and poor spore formation (Lardenois A, et al., PNAS.2011). If antisense lncRNA *MUT1312* indeed inhibits the translation of *RRP6* mRNA, then the protein level of Rrp6 should drop in the strain that overexpresses *MUT1312*, and thus lead to similar sporulation phenotype as in the *rrp6* mutant. Indeed, I found that the *MUT1312* overexpression strain shows relatively slow meiotic DNA replication dynamics (Figure 2A) and lower sporulation efficiency (Figure 2B). I further checked the mRNA level of *RRP6* in *MUT1312* overexpression strain in mitosis: *RRP6* mRNA seems to be moderately decreased. This may be due to the TEF1 promoter being very strong, which could lead transcription interference. I verified the growth phenotype of *MUT1312* overexpression strain, and found a growth deficiency like in *rrp6* mutant cells when switched to the non-permissive temperature.

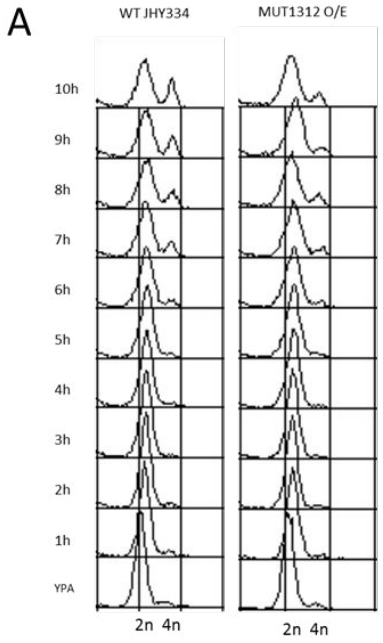

B **Table1. Sporulation efficiency(percentage of spores count on SPIII plate)**

		24h	48h
WT	colony1	48,5	72,5
	colony4	62,5	90,5
	colony6	70	62,5
	colony8	79	94
	colony9	79,5	96
MUT1312	colony3	44,5	84,5
	colony5	9,5	45
	colony6	1,5	49,5
	colony7	2,5	74
	colony10	49	73,5

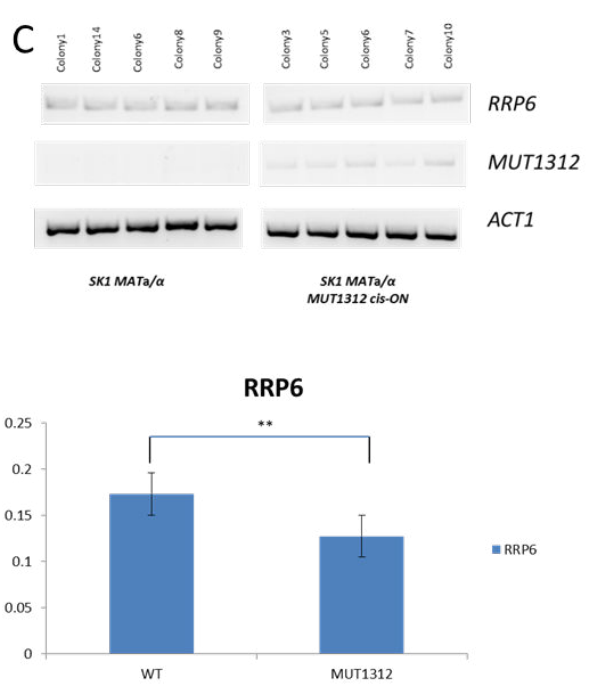

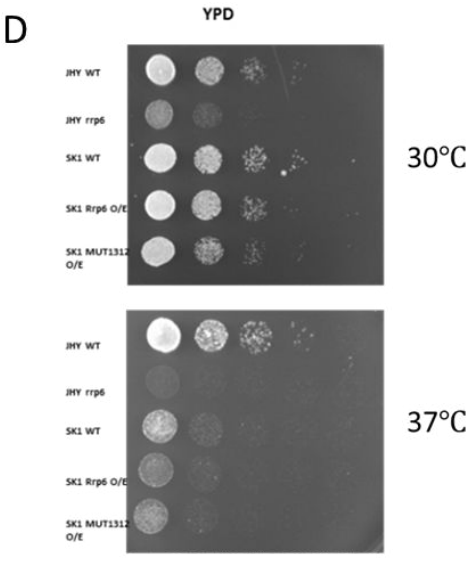

Figure 2. Sporulation efficiency and gene expression in *MUT1312* overexpression strain. (A) Meiotic DNA replication dynamics of WT and *MUT1312* overexpression strain as measured by FACS. (B) Ascus count shows sporulation efficiency of WT and *MUT1312* overexpression strain on SPIII plate. (C) Expression pattern of *MUT1312* and *RRP6* in WT and *MUT1312* overexpression strain. Quantification of RT-PCR result, is shown below. (D) Drop growth assay. JHY222 back ground WT and *rrp6* mutant, SK1 background WT, TEF-*RRP6* overexpression strain, and *MUT1312* overexpression strain on YPD medium at 30℃ and 37℃.

To test the idea that *RRP6* and *MUT1312* form double stranded RNA during meiosis, we used a strain that ectopically expresses Dicer and Argonaut proteins, which can cut endogenous dsRNA *in vivo*. dsRNAs were revealed by isolating RNA and carrying out small RNA-sequencing. The resulting reads were then mapped back onto the genome (manuscript in preparation). The data indicate that *RRP6* and *MUT1312* form dsRNA in both YPD and SPII 8h samples (Figure 3A). I confirmed this by using two different methods: (1) RNaseONE which cuts single stranded RNA and leaves the double stranded region intact. I used primers to check the single stranded region of *RRP6* (RRP6-5') and *MUT1312* (MUT1312), and the double stranded region (RRP6-3'): as shown in Figure 3B, only the double stranded region (RRP6-3') yields a band. (2) I carried out a J2-RIP experiment which employs an antibody that recognizes dsRNA. It precipitates RNA molecules with double stranded regions but unlike the case of RNaseONE, the J2 antibody is binding but not cut RNA, and thus leaves the RNA with the double stranded region intact. Both *RRP6* mRNA and *MUT1312* are detected in the J2 antibody pull-down sample, and the 3' end of *RRP6* seems to have higher expression level than its single stranded 5' end region (Figure 3B). This is likely due to the overlap with MUT132, which results in both *RRP6* and *MUT1312* being amplified by PCR. Taken together, both enzymatic digestion and double stranded RNA antibody precipitation confirm RNA-Seq data suggesting that *RRP6* and *MUT1312* form dsRNA during meiosis.

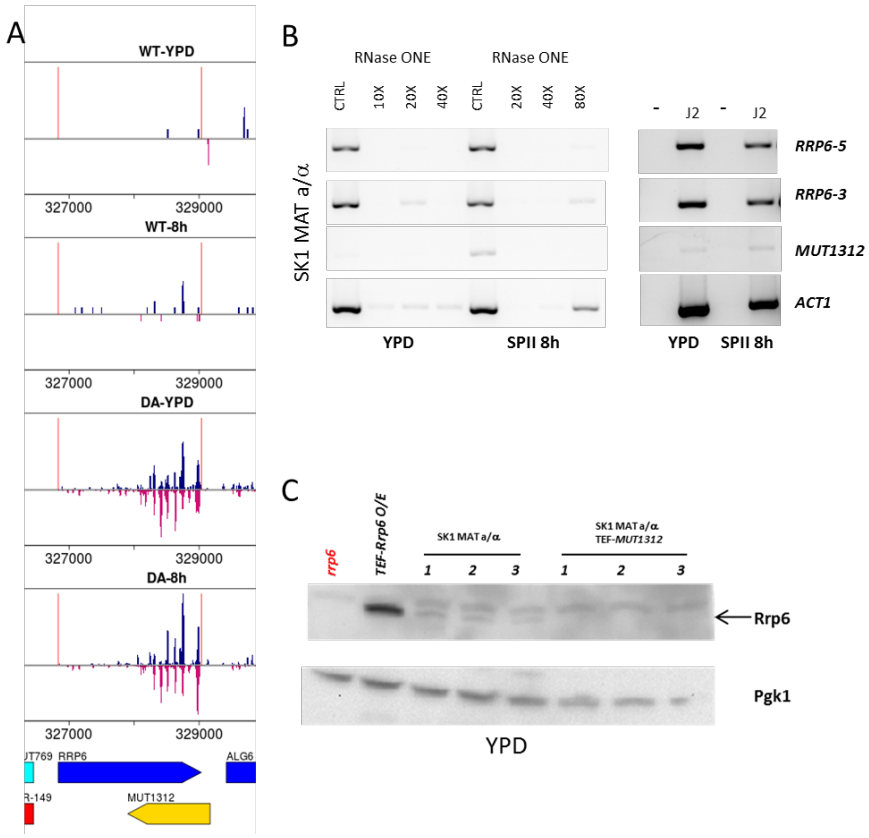

Figure 3. Double strand formation and protein expression level of Rrp6 in MUT1312 overexpression strain. (A) A diagram shows the expression level of double stranded RNA signals in *MUT1312/RRP6* locus. (B) Double stranded RNA validation by RNase ONE and J2-RIP experiment. The PCR assay uses primers to check the single strand region of *RRP6* (RRP6-5') and *MUT1312* (MUT1312), and double stranded region (RRP6-3'). (C) Western blot shows the expression level of Rrp6 in *MUT1312* overexpression strain.

To further test the idea that dsRNA inhibits translation of Rrp6, I used a strain that overexpresses *MUT1312* and tested Rrp6 protein during growth in rich YPD medium. Rrp6 protein does show a significant decrease in the *MUT1312* overexpression strain. Due to the low detection efficiency, Rrp6 bands in WT have low signal and there's no Rrp6 protein signal above the detection threshold in MUT1312 overexpression strain (Figure 3C). This associates *MUT1312* over-expression with undetectable levels of Rrp6 protein.

Via 5-FU transcriptome sequencing, I found that *RRP6* may be cell cycle regulated and it shows the opposite expression pattern of its antisense lncRNA *MUT1312* (Figure 4A, B). This indicates that *MUT1312* may regulate cell cycle fluctuation of *RRP6* probably through transcription interference and translation inhibition.

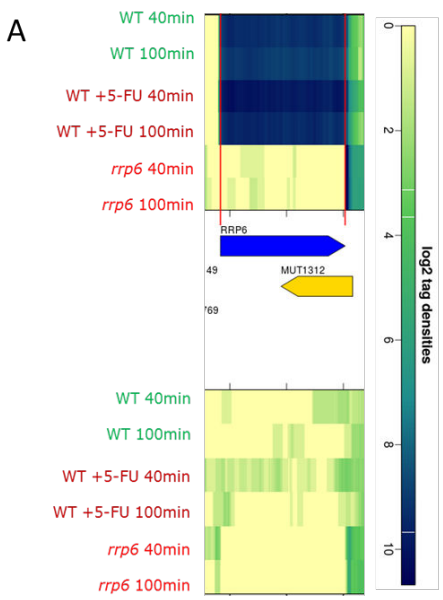

Figure 4. Cell cycle fluctuating expression pattern of *RRP6* during mitosis. (A) a heatmap shows the expression pattern of RRP6 during mitosis time course, 40min represents G1 phase, 100 min represents S phase. Color code scale bar is shown on the right. (B) RT-PCR validation result of *RRP6* and *MUT1312*.

To further provide direct evidence that dsRNA formed by *RRP6* and *MUT1312* can inhibit *RRP6*, more experiments should be done to knock out *MUT1312*. Possible ways are (1) to insert a shorter gene like KanMX into the single stranded region of *MUT1312* in the same direction, thus the stop codon of KanMX should lead to transcription termination of *MUT1312*. (2) to use CRISPR-dCas9 (the dead allele of Cas9) to inhibit *MUT1312* transcription.

Our laboratory found that the mouse ortholog of *RRP6* – *Exosc10* - is essential for early embryo development, since a knock out strain shows an embryonic lethal phenotype (Jamin and Petit, et al., in preparation). From RNA interactome studies it is known that RNA interaction on its 3' part will make it more stable, since the interaction masks the target sequences needed by the exosome for degradation. We note that human EXOSC10 gene is also associated with an overlapping antisense

ncRNA the 3'end. Based on this, I think the function of MUT1312 is to maintain the stability of *RRP6* mRNA late in gametogenesis, as an analogous mechanism of storage of maternal mRNAs in higher eukaryotes before the transcriptional activation of the zygote's genome. Thus the mRNA of *RRP6/EXOSC10* can be passed on to daughter cells that can use it to translate Rrp6 protein quickly before the transcriptional activation of the zygote's genome.

Currently, the role of long non-coding RNAs in regulate maternal RNAs is still unknown. *MUT1312* in budding yeast could be a good model to explore the mechanisms controlling maternal RNAs via lncRNAs.

7. Mechanisms of SWI4 5'-UTR extended isoform control during mitosis and meiosis

Analysis of *SWI4* isoform expression and dsRNA formation with overlapping antisense MUT

Abstract

Swi4 is a component of the SBF complex which has important role in regulating G1/S phase gene expression. Swi4 binds Swi6 to activate important G1/S regulator like *CLN1* and *CLN2* during mitosis to ensure the normal progression of cell cycle. How *SWI4* is regulated in meiosis is still unknown. Here we show that *SWI4* has a 5'-UTR extension during meiosis and that *MUT477*, which is expressed on the opposite strand of *SWI4* shows the same induction pattern as the extended isoform. Furthermore, we found that the *MUT477* region that overlaps with the extended 5'UTR region of *SWI4* forms a double stranded RNA, that negatively correlates with Swi4 protein levels. Our results suggest a possible mechanism of inhibiting mitotic regulator expression in meiosis by forming doubles stranded RNA at its 5'UTR region to inhibit translation. Our study provides a new mechanism for the regulation of gene expression in meiosis that involves double stranded RNA, which also been found in mammalian cells. Therefore, our research is relevant for higher eukaryotes, and could be the starting point for further study of the function of double stranded RNA using budding yeast as a model organism.

Introduction

SWI4 is a gene encoding a DNA binding protein, which is a component of SBF complex. *SWI4* gene was first found in 1984 through a screen of factors that regulate budding yeast mating type switching gene—*HO* endonuclease gene. 5 *SWI* genes, *SWI1* to SWI5, were found to be required for the cell cycle regulated expression of HO gene as mutant of those 5 does not express *HO*. In addition to regulate *HO* gene, all *SWI* genes been found have other functions, for example, double mutant of *SWI4* and one of other *SWI* genes result in an inviable phenotype (Stern M, et al., J. Mol. Biol. 1984). Swi4 regulates *HO* gene expression by forming the SBF complex with Swi6 and that binds SCB (SWI4 and SWI6 dependent cell cycle box) CACGAAAA sequence within the promoter of *HO* gene. Matches to SCB motifs were found in the promoter of other G1 cyclin genes, and SBF was be found essential for the expression of *CLN1*, *CLN2* and *CLN3* (Harris M, et al., PloS ONE. 2013, Stern M, et al., J. Mol. Biol. 1984). G1 cyclins have important roles together with *CDC28* to activate checkpoint START which is the time point that cell committed to entry into the mitotic cycles. Thus *SWI4/SWI6* deficiency will lead to a defect in cell division and eventually to cell death.

SWI4 is also cell cycle regulated and expressed in G1 phase. The periodic fluctuation of *SWI4* is regulated by the G1 transcription factor SBF and MBF (Swi6/Mbp1), as the promoter of *SWI4* contains binding site for Swi4 itself and Mbp1 (Leem Sun, et al., Nucleic Acids Research. 1998).

Although both SBF and MBF have important function in mitosis, only MBF act to induce some MCB regulated genes in meiosis, whereas SBF is inactivated in meiosis, since *SWI6* changes its partner to Mbp1 in meiosis. However, *SWI4* mRNA is expressed during meiotic time course and shows peak expression in middle meiosis, which is different from *SWI6*. *swi6 mutant cells display* both reduced recombination frequency and spore viability, while *swi4 cells* only show lower spore viability, which may indicate that *SWI4* has important function in sporulation process but not recombination (Leem Sun, et al., Nucleic Acids Research. 1998). However, the mechanism governing *SWI4* isoform expression during meiosis is unknown.

Here, we carried out research to investigate the regulation of *SWI4* during meiosis. Using combined RNA-Seq results and molecular assays, we found that the *SWI4* meiotic 5'UTR extension overlaps with antisense *MUT477*, which forms dsRNA, and potentially lead to the down regulation of Swi4 protein, since the formation of double stranded RNA is negatively correlated with Swi4 protein levels during meiosis and spore formation.

Materials and methods

Yeast strains and growth media. Strains used in this study are SK1, MPY702 (SK1 *ume6*), JHY222, MPY542 (JHY222 *ume6*) and MPY816 (Swi4myc). Growth media were prepared according to standard protocols of yeast YPD (glucose), YPA (acetate), and SPII media.

RT-PCR assay. RNA was extracted by Hot phenol method, followed by DNase I treatment with TURBO DNA-free Kit (Ambion, USA). RT-PCR reactions were carried out using 2μg of RNA reverse transcribed with Reverse Transcriptase (High Capacity cDNA Reverse Transcription kit; Life Technologies, USA) and amplified using Taq Polymerase (Qiagen, France) at 60ºC for 26 cycles. RT-PCR products were separated on 2% agarose gels and photographed using an ImageQuant 350 digital Imaging 381 System at the default settings (General Electric, USA) Primers used for RT-PCR were designed with Primer3 (simgene.com/Primer3; Table 1).

Table 1. Primers for RT-PCR assay

Gene	**Forward Primer**	**Reverse Primer**
SWI4	GGGCTACAGCTATGGCGAAT	ACGCAGGCGATTCGTTATCT
mSWI4	TACAATTACCTTCGGCGGCT	GCGTGATGTTCTGGTGATTGG
MUT477	ACGACCTAAGATCCGCAGTC	TGTGTACGGTGGCGGAAAA
ACT1	CTCGTGCTGTCTTCCCATCT	AGATGGACCACTTTCGTCGT

Construction of a Swi4-tagged strain. Tagging of Swi4 protein with *myc* tag was done according to the method reported in Yanke C, et al. 2004, which use a PCR base one-step tagging method. Primers used in amplification of the PCR-module were listed in the table below. Recombination colonies screened by selective medium were confirmed by colony PCR.

Western blot assay. Protein extract was prepared with YPD, YPA, and full meiotic time course sample, by using a method described in (Vitaly V. Kushnirov, Yeast. 2000). 20□g protein extract was separated via electrophoresis with SDS-PAGE gel (BIO-Rad, USA), and then proteins were transferred to ImmobilonPSQ membranes (Millipore, France) with an electro-blotter (TE77X; Hoefer, USA) set at 50mA for 2.5h. The membrane was blocked by incubation in 5% milk powder at room temperature for 1h, before incubation with anti-myc antibody at 1:1000 ((Life Technologies, USA) overnight at 4°C. Protein was detected with ECL-Plus Chemiluminescence kit (GE Healthcare, USA) and the ChemiDoc XRS system (Bio-Rad. USA). Signals were quantified by using ImageQuant TL 7.0 software package (GE Healthcare, USA).

J2-RIP assay. J2-RIP assay was performed by incubating 35μg RNA with magnet beads and J2 antibody. Then RNA was eluted and reverse transcribed with 2μg RNA using the High Capacity cDNA Reverse Transcription kit (Life Technologies, USA) and amplified with Taq Polymerase (Qiagen, France) at 60℃ for 28 cycles.

Results

SWI4 mRNA expression pattern during meiosis

From the tilling array study of the transcriptomes of budding yeast cell in fermentation, respiration and sporulation it is known that *SWI4* mRNA is constitutively expressed during mitosis and meiosis. Consistent with the previous study by Leem S, et al., *SWI4* mRNA accumulates in middle meiosis. However, unlike unsynchronized diploid cells grown in fermentation (YPD) and respiration (YPA) and synchronized haploid cells in mitotic time course which only express the shorter isoform of *SWI4*, we observe a 5'UTR extended transcript in early meiosis. The *SWI4* 5'UTR extended region partially overlaps with an antisense noncoding RNA (*MUT477*). *MUT477* is also induced in early meiosis and has peak expression in middle meiosis, the same pattern as *SWI4* 5'UTR extension (Figure 1).

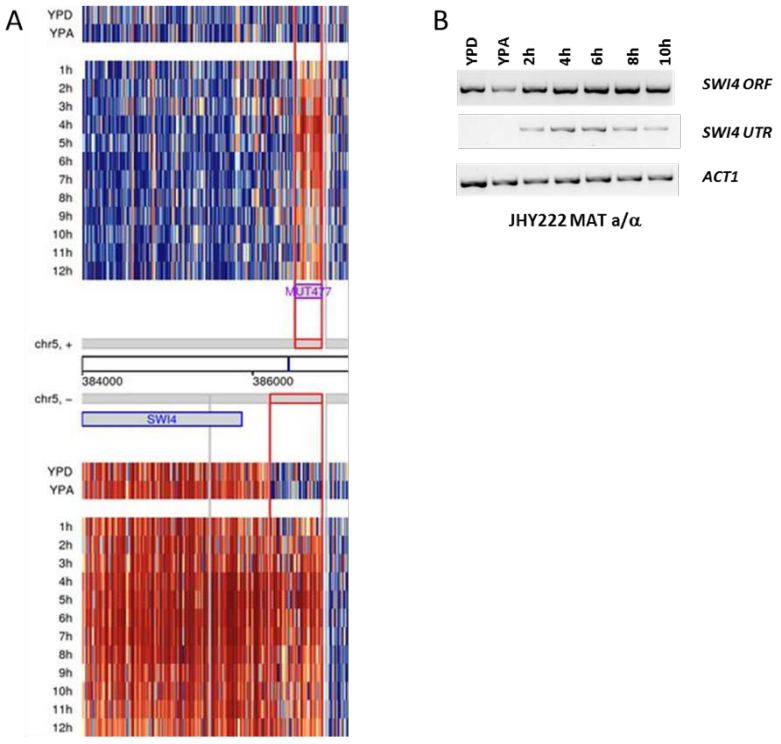

Figure 1. *SWI4* mRNA expression pattern during meiosis. (A) a heatmap shows the expression pattern of *SWI4*. (B) RT-PCR validation result of *SWI4*. *ACT1* was used as internal control.

Three questions arose from these observations: first, are the *SWI4* meiotic long isoform and *MUT477* controlled by the same factor via a bi-directional promoter? Second, if yes, which transcription factor governs their expression? Third, does *MUT477* influence Swi4 by inhibiting the translation of *SWI4* mRNA via dsRNA formation?

A URS1 element controls the expression of *SWI4* meiotic isoform

We first analyzed the *SWI4* locus on the genome, we found that there is a URS1 element located at the upstream of *MUT477* and inside of *SWI4* meiotic 5'UTR region (Figure 2A). This motif is the target of Ume6, the DNA binding subunit of the histone deacetylase Rpd3.

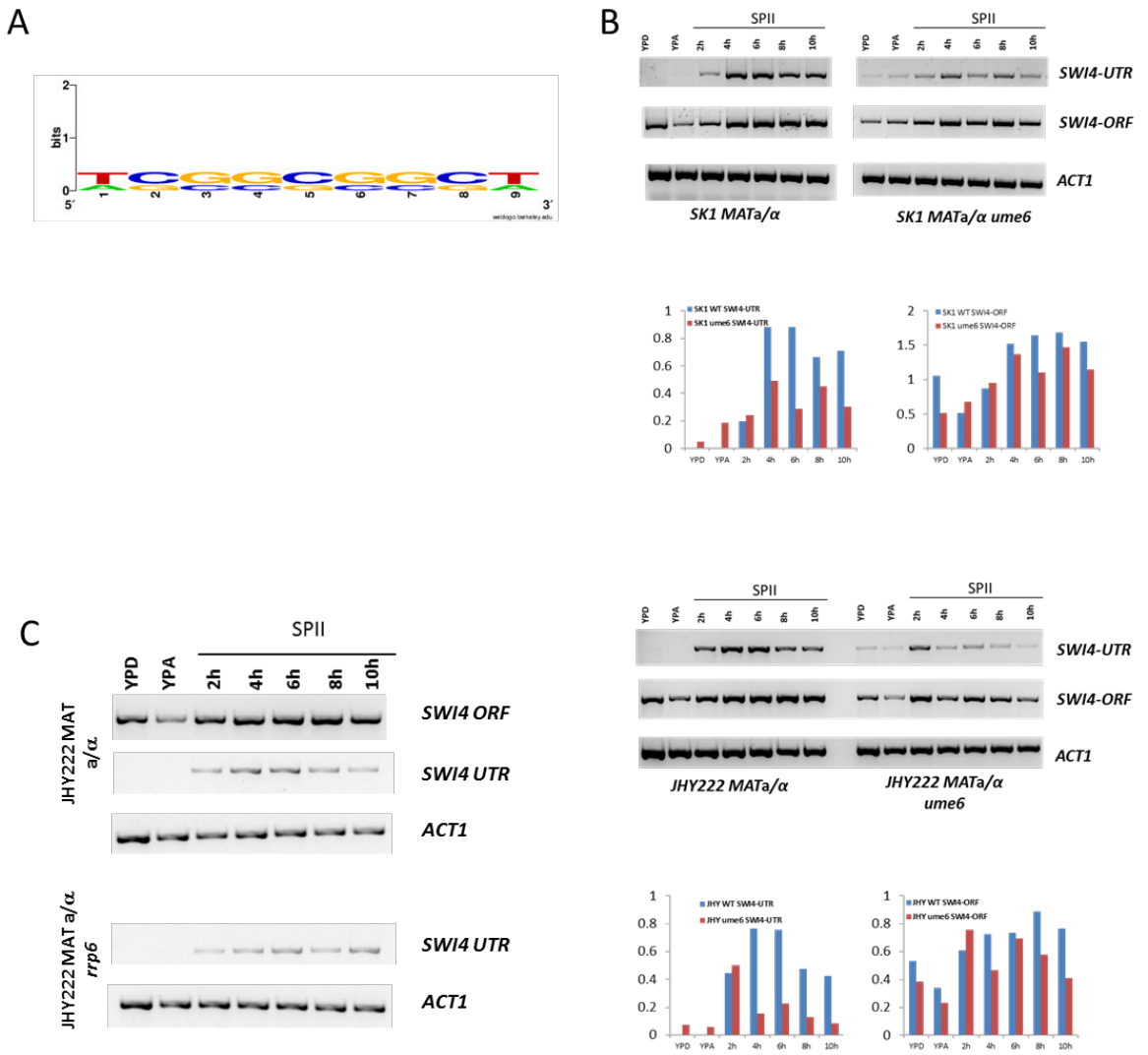

Figure 2. URS1 element controls the expression of *SWI4* meiotic isoform. (A) Motif pattern of URS1 in the promoter of *MUT477*. (B) RT-PCR validation result of *SWI4*, CUT477 gene in JHY222 and SK1 WT vs *ume6* mutant. *ACT1* as internal control. (C) RT-PCR validation of *SWI4* meiotic UTR expression during meiosis in the WT vs. *rrp6* mutant. *ACT1* is the internal control.

We next used *ume6* mutants in both JHY222 and SK1 strain. As shown in Figure 2B, *ume6* gene deletion does not alter the expression of the mitotic *SWI4* isoform in both JHY222 and SK1 strains cultured in fermentation (YPD), respiration (YPA) and sporulation medium (SPII), while the meiotic 5'-extended isoform of *SWI4* accumulates in mitotically growing cells (YPD and YPA sample) in both strains. Our result shows that the repression of *SWI4*'s meiotic isoform in mitosis requires Ume6.

The *SWI4* meiotic isoform shows decreased expression in *rrp6* mutant cells

Previous report shows that the meiotic isoform is not only induced by starvation alone, since diploid *MAT***a**/a cells cultured in sporulation medium do not express the meiotic isoform. And the meiotic non coding RNA regulator Rrp6 may also have impact on meiotic isoform expression pattern, since the meiotic isoform is not induced in normal level in the *rrp6* mutant cell due to the deficient sporulation process. *SWI4* meiotic isoform expression in the *rrp6* mutant also does not reach the normal level as in WT cells (Figure 2C). However, the expression pattern tends to be the same, as the meiotic isoform also tend to be have peak expression in middle meiosis. This cannot explain by the impaired sporulation process in *rrp6* cells, since the slow downed sporulation process will result in the delayed shown up of meiotic isoform. Therefore, it could be that Rrp6 somehow affect the expression level of the meiotic *SWI4* isoform.

Potential function of *SWI4's* meiotic 5'extended UTR to inhibit Swi4 protein during meiosis

The function of extended 5'UTR isoforms is normally either to affect the translation of the mRNA since the 5' extended region can contain upstream open reading frames (uORFs) that sequester and stop the ribosome and thus inhibit the translation of the ORF downstream. Or it can affect the stability of the mRNA as the small open reading frame in the extended 5'UTR region may trigger the NMD pathway, which leads to the degradation of mRNA. To address this question, we analyzed the extended 5'UTR of *SWI4* mRNA in meiosis, and found that there are two small open reading frames upstream of *SWI4* open reading frame, which encode peptides of 11 and 8 amino acids. (Figure 3A). It could be that those small open reading frames inhibit the translation of *SWI4* mRNA thus down-regulating the protein level of Swi4 during middle and late meiosis.

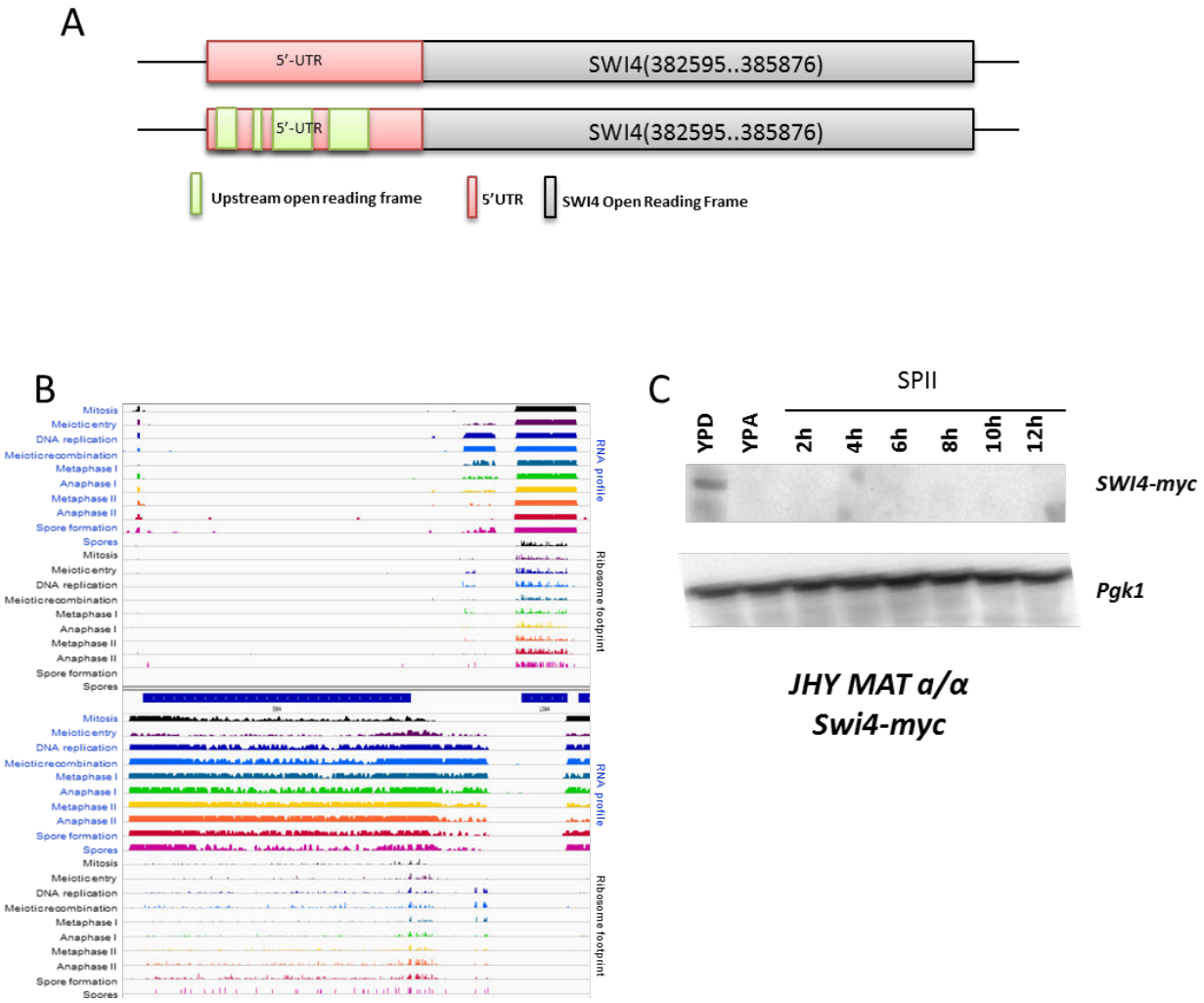

Figure 3. *SWI4* meiotic isoform 5'UTR open reading frame prediction and Swi4 protein expression pattern. (A) A schematic diagram shows the open reading frame in the 5'UTR region of *SWI4*. (B) Ribosome footprint result of Swi4 locus mRNA and protein expression pattern (Brar G., et al., Science. 2012). (C) Western blot analysis of Swi4 protein expression. Samples in mitosis (YPD and YPA) and meiotic time course (SPII2h to SPII12h) were analyzed. Pgk1 was used as an internal control.

Swi4 protein levels decrease as cells enter meiosis

We next sought to explore if Swi4 protein is down-regulated during meiosis. We first checked the published ribosome footprint data by Brar G., et al., 2011, who studied the translation of RNAs during the entire meiotic process. As shown by the ribosome footprint data, *SWI4* mRNA translation is going down during meiosis (Figure 3B). To complement and validate this information, we constructed a strain with myc-tagged Swi4 and tested the protein level of Swi4 during meiosis by Western blot. We confirmed that Swi4 protein levels decrease in meiosis (Figure 3C). As the Swi4 protein is unstable, the signal was not that strong in mitosis and we observe bands in the lower molecular weight which could be breakdown products of Swi4. The signal is even weaker during

meiosis as Swi4 protein become more unstable, therefore, the bands during meiosis are below the threshold level of detection. This result shows that Swi4 protein is down regulated in meiosis in our strain background.

Antisense *MUT477* overlaps with the extended meiotic 5'-UTR of *SWI4*

When we examined the genome locus of *SWI4*, we found that *MUT477* overlaps with the extended 5'UTR region of *SWI4* mRNA, and it has a similar expression pattern during meiosis. It also seems to be controlled by Ume6 which suppress it during mitosis (Figure 1A). When the meiotic extended mRNA and *MUT477* are induced, the open reading frame region of *SWI4* tends to be down regulated in both the SK1 and JHY222 background yeast during mitosis and meiosis time course sample in *ume6* mutant. What is the role of *MUT477*? Previous work shows that dsRNA can inhibit translation (Sinturel F. Cell Report. 2015). Therefore, it could be that MUT477 and the 5' extended region of *SWI4* form dsRNA that may contribute to the inhibition of *SWI4* mRNA translation.

To test this hypothesis, we first checked our unpublished small RNA sequencing data (obtained with a yeast strain that contains ectopically expressed Dicer and Argonaut, which digest dsRNA *in vivo*). We found that *SWI4* shows a small dsRNA signal at the region overlapping with *MUT477* in meiosis (SPII8h sample) in the DA strain, while there's no signal in the mitosis YPD sample, and nearly no signal in the control WT strain's YPD and SPII8h sample. Furthermore, we confirmed the existence of dsRNA of *SIW4* and MUT477 by a dsRNA-RIP experiment in WT with an antibody that specifically binds dsRNA of at least 40 bp. The result shows a clear dsRNA signal in the WT strain (Figure 4B). This indicates that the dsRNA is formed *in vivo* by *SWI4*'s extended 5'UTR region and MUT477. It is possible that this structure inhibits the translation of *SWI4* mRNA during meiosis.

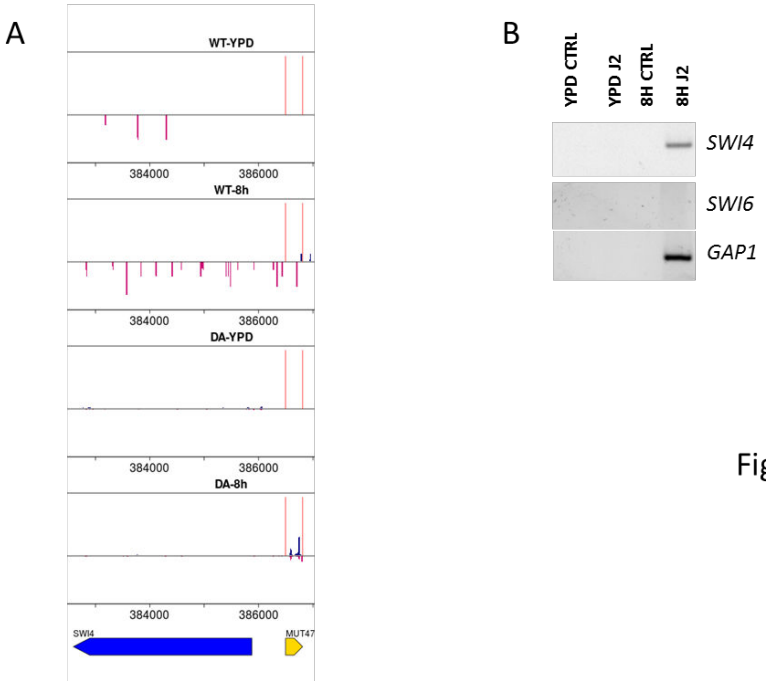

Fig

Figure 4. Swi4 protein expression pattern. (A) A histogram shows the dsRNA-Seq signal in the *SWI4* region. (B) RT-PCR validation result of J2-RIP *SWI4* signal. *SWI6* and *GAP1* were used as negative and positive controls, respectively.

Discussion

In this study we found *SWI4* mRNA has a 5'-UTR extension which overlaps with its antisense non coding RNA *MUT477*. The formation of dsRNA is negatively correlated with meiotic protein levels of Swi4. However, different from the case of *RRP6/MUT1312*, *MUT477* overlaps with the meiotic extended 5'UTR of *SWI4* rather than overlapping at 3'end. 5'UTR is important for translation of mRNA since it allows ribosome to search and bind to the mRNA. A dsRNA formed in the 5'UTR region could block the entry of ribosome onto mRNA and thus inhibit translation.

The overlapping region between *SWI4* and *MUT477* also covers uORFs in the extended region of SWI4 5'UTR that can inhibit translation, sequester ribosomes, or lead to NMD of the mRNAs when ribosomes reach the stop codon in the small ORF. Therefore, it could be that uORFs in the extended 5'UTR region of *SWI4* mediate the down regulation of Swi4 protein in meiosis. Further studies should be carried to distinguish if the inhibition is come from the uORF or dsRNA.

The result from our research, together with studies in mammalian cells and budding yeast shows that dsRNAs naturally occurring in the cell have important function in regulating gene expression by influence of mRNA stability and inhibition of translation. Our study points to a novel function for meiotic induced non-coding RNAs in regulating genes during meiosis.

References

Stern M, Jensen R, Herskowitz I. Five SWI genes are required for expression of the HO gene in yeast. J Mol Biol. 1984 Oct 5;178(4):853-68.

Harris MR1, Lee D, Farmer S, Lowndes NF, de Bruin RA. Binding specificity of the G1/S transcriptional regulators in budding yeast. PLoS One. 2013 Apr 4;8(4):e61059. doi: 10.1371/journal.pone.0061059. Print 2013.

Leem SH, Chung CN, Sunwoo Y, Araki H. Meiotic role of SWI6 in Saccharomyces cerevisiae. Nucleic Acids Res. 1998 Jul 1;26(13):3154-8.

8. lncRNA based regulation of transcription (SUT200/CDC6)

Introduction

CDC6 is a gene encoding protein important for DNA replication initiation in budding yeast. *CDC6* mRNA is cell cycle regulated: it is transcribed in late mitosis/telophase and peaks in G1 phase, then disappears at bud initiation (S phase), and reappears at the telophase of the second mitotic cycle (Zweerschke W., et al., The journal of biological chemistry. 1994). In cells with long G1 phase, there has a second wave of *CDC6* transcription which occurred in late G1 phase. This second burst of *CDC6* transcription is important for the normal progress of S phase, as small G1 phase cell which lacks *CDC6* transcription in late G1 phase move forward very slowly during S phase. c*dc6* mutant lacks both waves of *CDC6* transcription and can undergo mitosis without replicating their chromosomes, which leads to chromosomes fractionation in the daughter cells. Transcriptional regulation of these two waves of *CDC6* is achieved partially by Swi5 for the telophase and by MBF for the late G1 phase *CDC6* transcription (Piatti S., et al., Embo J. 1995).

As the fluctuation of mRNA, Cdc6 protein is also unstable and periodically fluctuates during the cell cycle. Cdc6 protein is synthesized at late mitosis and in late G1 phase of cells with prolonged G1 phase (Piatti S., et al., Embo J. 1995).

According to a tilling array study of budding yeast meiotic transcriptomes, *CDC6* is transcribed in mitosis and early meiosis, then transcription decreased from middle meiosis. The mechanism of meiotic down-regulation of *CDC6* is unknown. During middle meiosis a novel lncRNA is transcribed over the upstream promoter region of *CDC6*, but whether this lncRNA plays function to inhibit *CDC6* transcription is unknown.

Transcription is not only regulated by transcription factors, since some lncRNAs can also have great impact on gene expression. As in budding yeast, two long non-coding RNA been reported to have function to inhibit meiotic genes, meiosis inducer IME1, in mitosis by promoter interference, which the long non-coding RNA *IRT1* is located at the promoter of *IME1*. Transcription of *IRT1* inactivate *IME1* promoter by recruit histone methyltransferase Set2 and histone deacetylase Set3 to establish repressive chromatin status (van Werven F, et al., Cell. 2012).

Materials and methods

Yeast strains and growth media. Strains used in this study are JHY222 wild-type and *rrp6* (Lardenois et al., PNAS 2011), MPY689 (SUT200 CIS-OFF), MPY687 (SUT200 CIS-ON),

MPY685 (SUT200 TRANS-ON). Media were prepared according to standard protocols for yeast growth (YPD, YPA), and sporulation (SPII).

RT-PCR assay. RNA was extracted by Hot phenol method, followed by DNase I treatment with TURBO DNA-free Kit (Ambion, USA). RT-PCR reactions were carried out using 2 μg of RNA reverse transcribed with Reverse Transcriptase (High Capacity cDNA Reverse Transcription kit; Life Technologies, USA) and amplified using Taq Polymerase (Qiagen, France) at 60ºC for 26 cycles. RT-PCR products were separated on 2% agarose gels and photographed using an ImageQuant 350 digital Imaging 381 System at the default settings (General Electric, USA). Primers used for RT-PCR were designed with Primer3 (simgene.com/Primer3; Table 1).

Table 1. Primers for RT-PCR assay

Gene	Forward Primer	Reverse Primer
SUT200	5'-TTTCTGGCTTCCTTTCTTTCC-3'	5'-TTTCTGCCAGCCAACTCAAT-3'
CDC6	5′-CGAATCCGAACTTGCAGAAT-3′	5′-CCCGTATTTCCAGCACACTT-3′
MUT1465	5′-GGGCCAACAGTTGTTTCAGT-3′	5′-CATCGCGAAATTTGTCTCAA-3′
CLN2	5'-TTTGTTCGAGCTGTCTGTGG-3'	5'-GTATACGTGCCCTTGGGTTG-3'
ACT1	5'-CTCGTGCTGTCTTCCCATCT-3'	5'-AGATGGACCACTTTCGTCGT-3'

Results and discussion

According to tilling array results the lncRNA *SUT200* is transcribed upstream of *CDC6* and strongly induced during middle meiosis at the time when *CDC6* mRNA declines. I validated *CDC6* and *SUT200* expression by RT-PCR and found the same expression pattern as tilling array and the expression of *CDC6* and *SUT200* seems to be enhanced in *rrp6* mutant (Figure 1A and B).

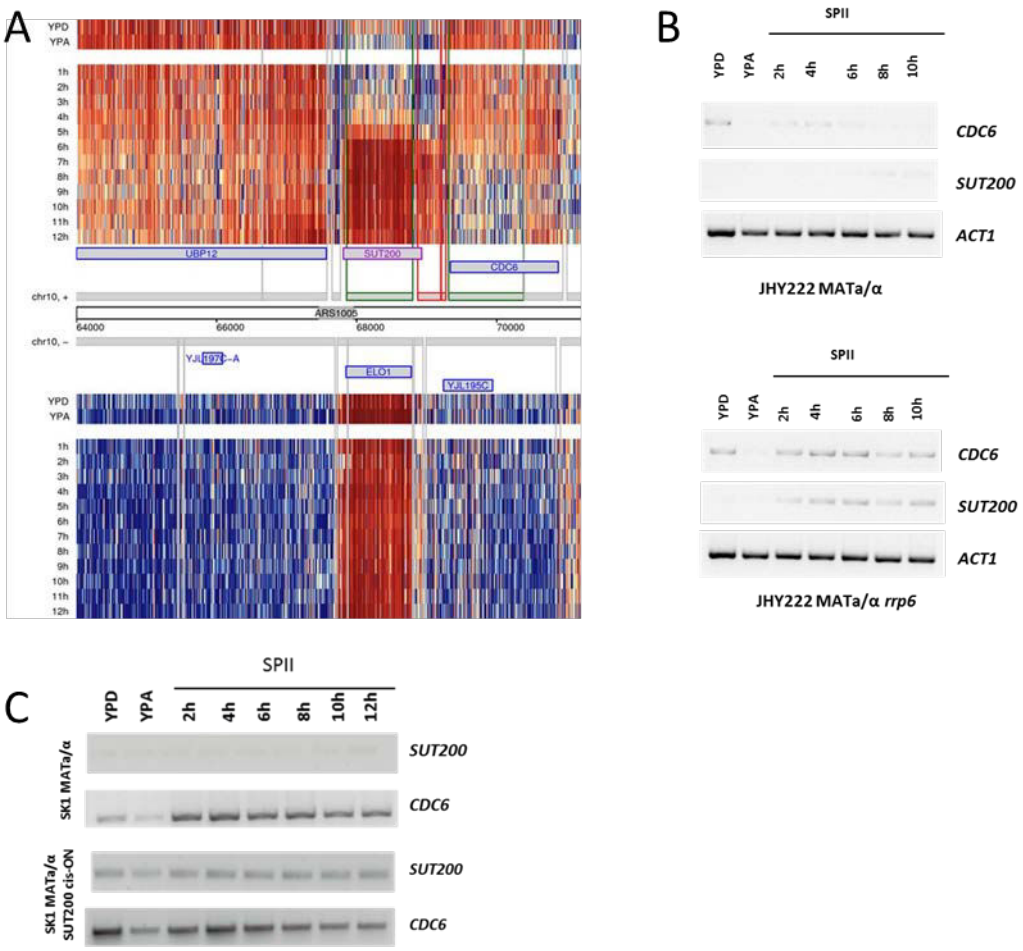

Figure 1. *CDC6* expression pattern. (A) A heatmap shows the tilling array data about *CDC6* expression during meiosis. (B) RT-PCR validation result of *CDC6* and *SUT200* during meiosis sample in WT strain and *rrp6* mutant strain. (C) RT-PCR validation result of *CDC6* and *SUT200* during meiosis sample in WT strain and TEF-SUT200-cis-ON strain.

To test whether *SUT200* plays a role in the repression of the *CDC6* promoter, we inserted a transcription terminator downstream of *SUT200* transcription initiation site. *SUT200* knock out yeast show slightly faster sporulation than WT (Figure 2). However, when checked with RT-PCR, *SUT200* RNA still can be detected. This may due to an unconventional transcription mechanism of lncRNAs, which may not be controlled by exactly the same initiation site and termination site as RNA polymerase II transcribed mRNA. For the cis-ON strain, although *SUT200* is expressed during mitosis, *CDC6* also seems to be enhanced, as shown in Figure 1C. This may be the consequence of strong *TEF1* promoter activity, which result in transcriptional read-through from the *SUT200* promoter to *CDC6*.

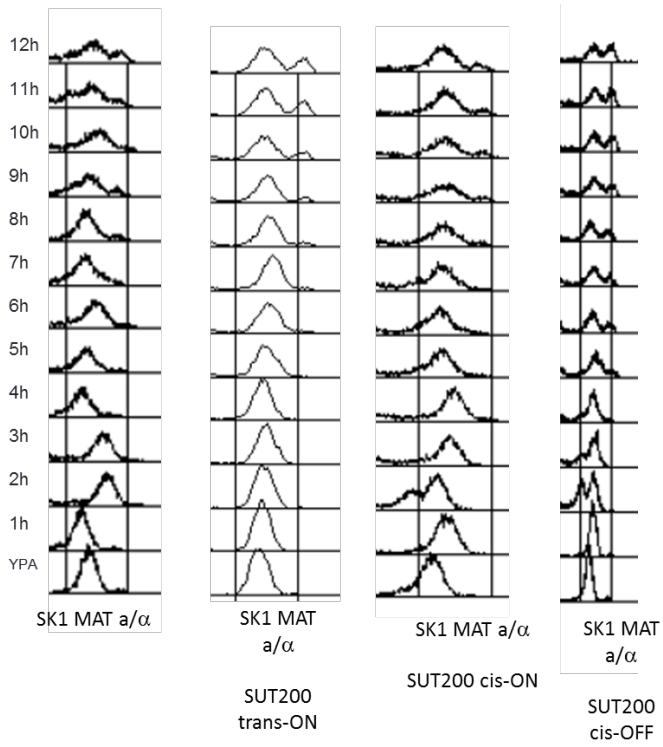

Figure 2. DNA replication dynamics in *SUT200* overexpression cis-ON, trans-ON, and cis-OFF strain. FACS data are shown for the strain give at the bottom, time points are indicated to the left.

By carefully examining the tilling array data, I found that *SUT200* has 3'end extension at SPII 6 h and 7h, which seems to have no gap with *CDC6* mRNA signal. *SUT200* seems to show transcription read-through into the *CDC6* locus. This may mean that the repression of *CDC6* transcription during middle and late meiosis is due to transcriptional read through from *SUT200*. To test this idea, I use the primer pair with forward primer located in *SUT200* locus and reverse primer located in *CDC6* locus. I found a long transcript, which appears to be transcribed from *SUT200* read-through to *CDC6* (Figure 3).

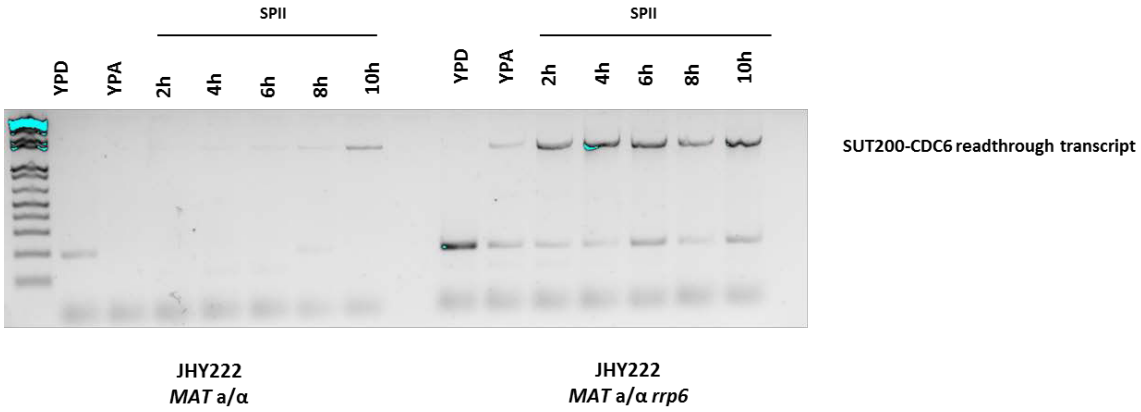

Figure 3. RT-PCR validation result of *CDC6-SUT200* transcription read-through transcript. A primer pair was used whereby the forward primer was located in SUT200 and reverse primer located in *CDC6*. RT-PCR validation was carried in the mitotic samples (YPD and YPA) and meiotic time course samples (SPII2h to SPII10h).

In conclusion, our results suggest that *SUT200* does not repress *CDC6* transcription in middle late meiosis by promoter interference. Rather, *SUT200* displays read-through into the *CDC6* locus. This indicates that the *CDC6* promoter is somehow repressed and read-through may contribute to the

weak signals that were detected in middle meiosis by tilling arrays.

9. The transcriptional regulation of meiotic lncRNAs: Ndt80 activates MUT1465

Abstract

Meiotic Unannotated Transcripts (MUTs) are lncRNAs which accumulate in meiosis. Previous research showed that some MUTs are degraded by Rrp6 during vegetative growth and early meiosis, thus limiting their presence to meiosis. However, the mechanism that actively induce MUTs in meiosis is still enigmatic. Here, we carried out genome wide transcription factor site analysis of MUT promoter regions. We found middle sporulation elements (MSEs), bound by Ndt80. Furthermore, target MUTs fail to be up-regulated in an *ndt80* mutant strain. This indicates that Ndt80 is a transcription factor that actives MUT expression in middle meiosis. Our study is the first to show the induction and the potential function of MUTs in meiosis.

Introduction

MUTs are meiotic unannotated transcripts, which have been shown to be induced when Rrp6 is diminished (Lardenois A., et al., PNAS.2011). Rrp6 is a catalytic subunit of the exosome, which degrade nascent RNA which are unstable or transcription noise, like promoter associated RNA transcripts. MUTs have been shown to expressed in the mitosis sample in *rrp6* mutant, since there's no more Rrp6 in the cell. This explains the mechanism that suppresses MUTs and limits their expression to meiosis. However, if and how MUTs are transcriptionally induced in differentiating cells is unknown.

Current research found long non coding RNAs in various organisms from budding yeast to higher eukaryotes. Studies in human found that the induction of long non coding RNAs are different from those of mRNAs, although they both been transcribed by RNA Polymerase II, the promoter of long non coding RNAs are different from protein coding mRNAs' promoters, and the transcription factors that bind and regulate the long non coding RNAs are also different (Alam T., et al. PLoS ONE.2014). However, transcription factors regulating of lncRNAs in budding yeast is still unknown.

Here we carried out study to analyze genome widely transcription factors that bind to the promoter

of MUTs. We found that Ndt80 induces MUTs that possess an MSE element in their promoters in middle meiosis. We also found that Ndt80 induces *MUT1465* via a bi-directional promoter.

Material and methods

Yeast strains and growth media. Strains used in this study are JHY222 wild-type and *rrp6* and MPY553 (JHY222 *ndt80*), MPY672 (TEF1-MUT1465 CIS-ON) and MPY674 (CYC1t-MUT1465 CIS-OFF). Media were prepared according to standard protocols for yeast growth (YPD, YPA), and sporulation (SPII).

RT-PCR assay. RNA was extracted by Hot phenol method, followed by DNase I treatment with TURBO DNA-free Kit (Ambion, USA). RT-PCR reactions were carried out using 2 μg of RNA reverse transcribed with Reverse Transcriptase (High Capacity cDNA Reverse Transcription kit; Life Technologies, USA) and amplified using Taq Polymerase (Qiagen, France) at 60ºC for 28 cycles. RT-PCR products were separated on 2% agarose gels and photographed using an ImageQuant 350 digital Imaging 381System at the default settings (General Electric, USA). Primers used for RT-PCR were designed with Primer3 (simgene.com/Primer3; Table 1).

Table 1. Primers for RT-PCR assay

MUT1465	GGGCCAACAGTTGTTTCAGT	CATCGCGAAATTTGTCTCAA
MUT1290	AGCTGGTACTGCCCGTACAT	ACAGGGAACTCCAGCGTATG
MUT100	GCCAAATATTTCCACTCAATCA	CCAACAAGAACAGCGCTACA
MUT523	TCCTTCTATGGACTGCGACA	TCTCGTTATTATTGGTTCGTTCAA
NDT80	AAGCACCCAGTTTGTTCTGG	ACCTTTCATGGGGAGAATCC
CLN2	TTTGTTCGAGCTGTCTGTGG	GTATACGTGCCCTTGGGTTG
BBP1	AGGTATGCCCAAGACGACAC	CGGAGCAGGACTTCGTAAAG
ACT1	CTGCCGGTATTGACCAAACT	AGATGGACCACTTTCGTCGT

MUTs clustering analysis. MUTs expression were analyzed by clustering according to their expression pattern. Data were obtained from Lardenois A, et al. 2011. A heatmap representing each cluster was produced by R.

Transcription factor binding site analysis. MUTs coordinates were obtained from A. Morillon's laboratory. Transcription factor binding site in the promoter of MUTs were analyzed by Galaxy and MEME suite. Briefly, retrieve sequence that located at 300 bp upstream of MUT transcription start

site as promoter and input dataset for analyze transcription factor binding site. Then a transcription factor binding motif search was carried out using MEME.

Chromatin interaction analysis. Data of Chromatin region that interact with *CLN2* region in budding yeast were obtained from Wu Y J, et al., 2009.

Results

Temporal induction pattern of MUTs during meiosis

MUTs were found by Lardenois et al, 2011. They are a group of lncRNAs that accumulate during meiosis. Here, we use the data from the initial study, to analyze the expression pattern of MUTs during meiotic time course in more detail. Figure 1A shows that MUTs have distinct expression pattern as they can be induced in early, middle and late meiosis, and most of them show a middle meiotic pattern. This suggest that MUTs expression is tightly controlled during meiosis and spore formation. Therefore, we are interested in exploring the mechanism that governs MUTs temporal expression pattern during meiosis.

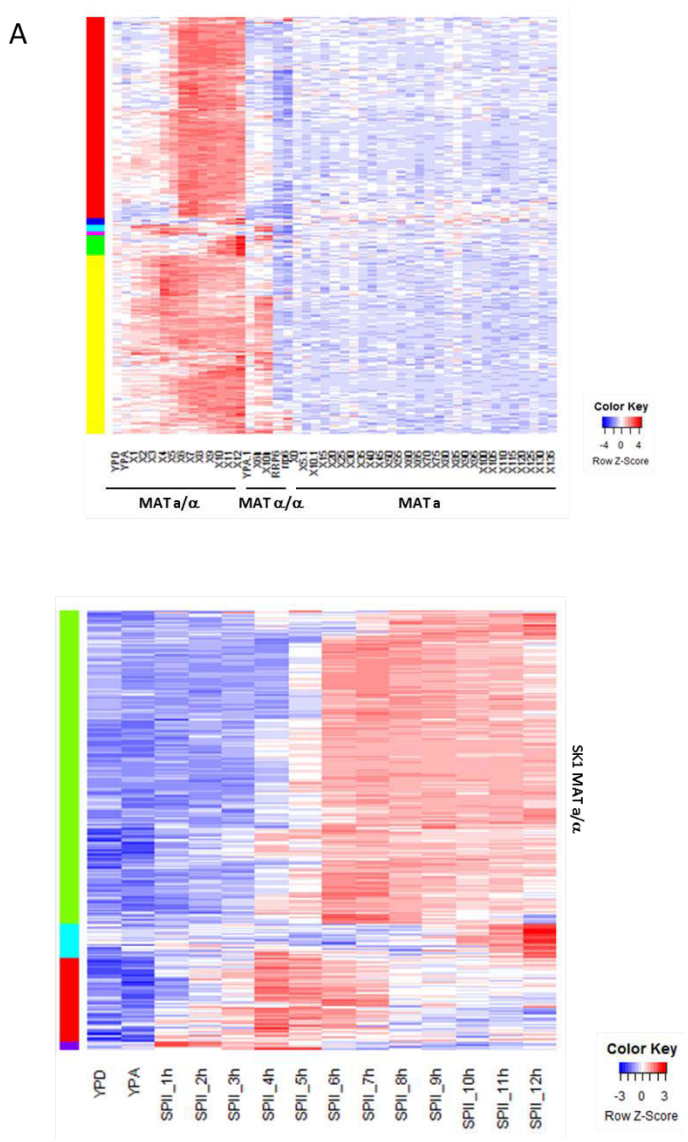

Figure 1. MUTs expression pattern and transcription factor motif search. (A) A heatmap shows the expression pattern of MUTs during meiosis. MUTs expression is shown in a color scale is shown on the right bottom. (B) A heatmap shows the expression pattern of MUTs induced only in *MAT***a**/α sporulation sample but not in *MAT*α/α meiosis-deficient starvation control samples.

Landscape of genome-wide transcription factor binding site on MUTs promoter

In order to know the temporal expression pattern control mechanism for MUTs, we first performed a genome-wide analysis of the MUT upstream regions searching for the binding sites for the known

transcription factors in budding yeast. We analyzed MUTs by searching the sequence at 350 bp upstream of its transcription start site, since Pelechano V., et al., reported that yeast promoters are on average 309bp long (Pelechano V., Yeast, 2006). We found among the target sites of 732 known transcription factor in budding yeast 43 motifs bound by 32 transcription factors. Among them, the Ndt80 binding site MSE was found in middle meiotic MUTs.

Ndt80 is the transcription factor that responsible for the induction of most MUTs in meiosis

Most of the MUTs are induced in middle meiosis and genome wide transcription factor analysis suggests that Ndt80 is a key factor that induces the expression of MUTs during middle meiosis.

Previous study by Lardenois A et al., reported that Rrp6 suppresses the MUTs expression in mitosis, therefore a lot of MUTs been induced upon loss of Rrp6 in middle meiosis. This helps explain how MUTs may be repressed until middle meiosis, but the mechanism that activates MUTs is unknown. Here from our genome wide transcription factor analysis, we found Ndt80 is the transcription factor responsible for the activation of MUTs in middle meiosis.

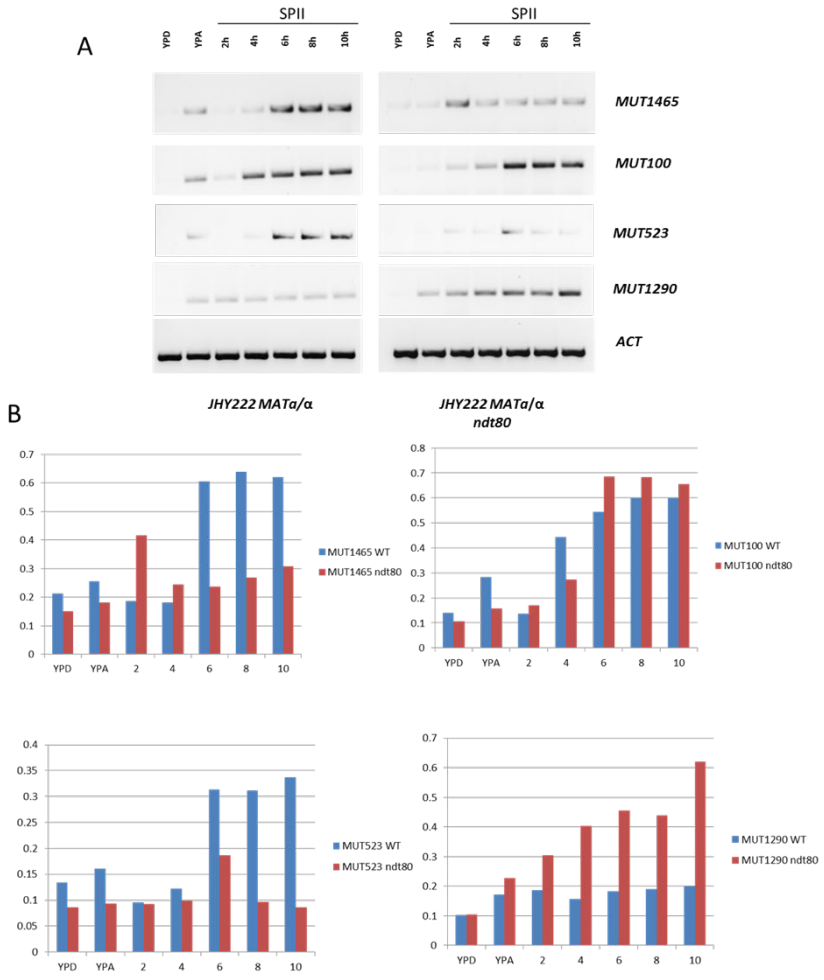

Figure 2. Ndt80 dependent induction of MUTs in middle meiosis. (A) RT-PCR validation result. (B) Signal quantification. *ACT1* is an internal control.

We confirmed that *MUT1465* and *MUT523*, which possess MSE elements in their promoter regions, fail to be induced in the *ndt80* mutant, while MUTs for which upstream regions do not contain MSE

element (*MUT100* and *MUT1290*) were not affected in the *ndt80* mutant.

MUT1465 is a Ndt80-dependent MUTs induced via a bi-directional promoter during middle meiosis

Among *Ndt80* regulated lncRNAs *MUT1465* is particular interesting, because it seems to be bidirectionally induced during middle meiosis. *MUT1465* is located at chromosome 16 between *CLN2* and *BBP1*, the latter of which is further induced during middle meiosis at the same time as *MUT1465* is upregulated. The genome wide transcription factor binding site result predicts that Ndt80 is involved in this pattern via the MSE motif between *MUT1465* and *BBP1* (Figure 3).

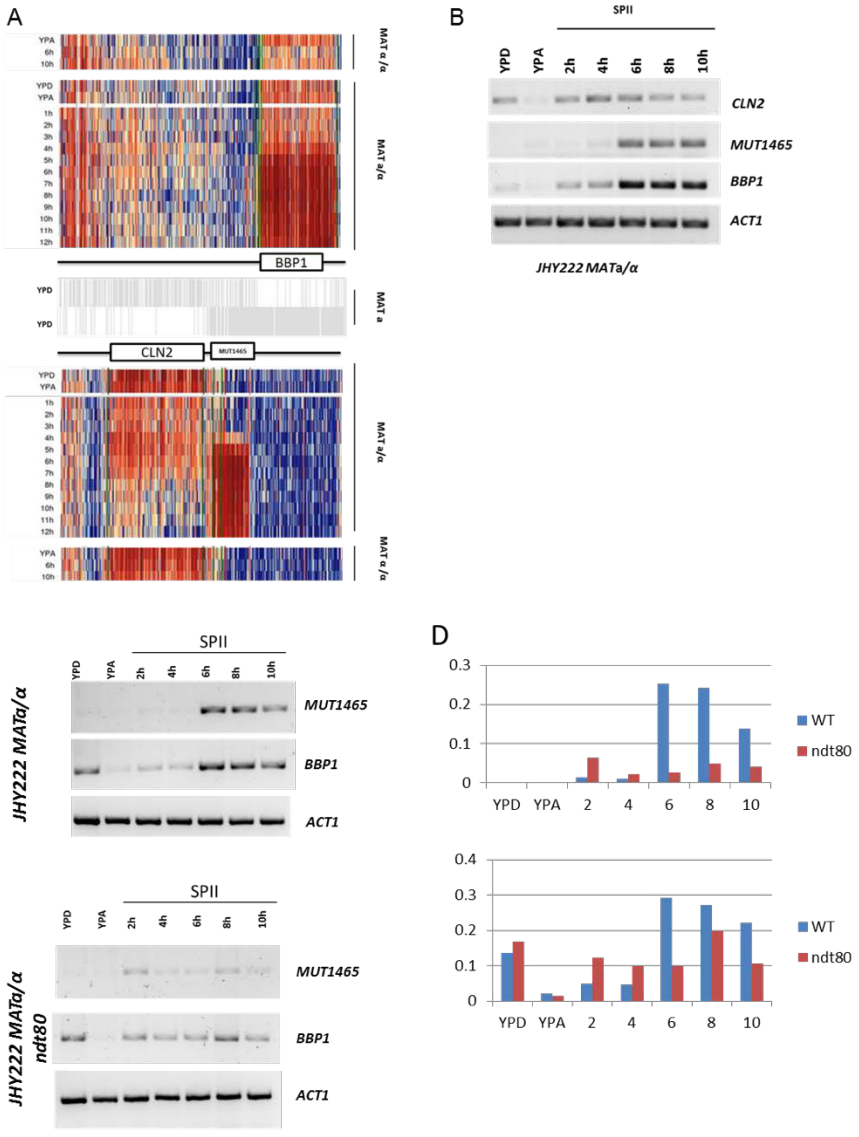

Figure 3. Bidirectional expression of *MUT1465* and *BBP1*. (A)a heatmap shows the expression pattern of *MUT1465* and *BBP1*. (B) RT-PCR validation of *MUT1465*, *CLN2*, and *BBP1* result in wild type yeast and quantification. *ACT1* as internal control. (C) RT-PCR result of *MUT1465*, *BBP1* in WT vs. *ndt80* mutant. (D) Quantification result of RT-PCR shown in C.

We next sought to explore if Ndt80 control the expression of *MUT1465*. We use RT-PCR and found that the induction of *MUT1465* is impaired in *ndt80* mutant (Figure 3C). The same pattern was observed for *MUT523*, which is a positive control since it contains a known MSE element, whereas the lncRNAs *MUT100* and *MUT1290* that lack MSE elements in their promoters are not affected in *ndt80* mutant.

When we verified the expression of *BBP1* in the *ndt80* mutant, we confirmed the tilling array result by RT-PCR by showing that the expression of *BBP1* increases in middle meiosis in WT strain, while no up-regulation occurs in the *ndt80* mutant (Figure 3C). Together, this indicates that *Ndt80* controls the bi-directional expression of *MUT1465* and *BBP1*.

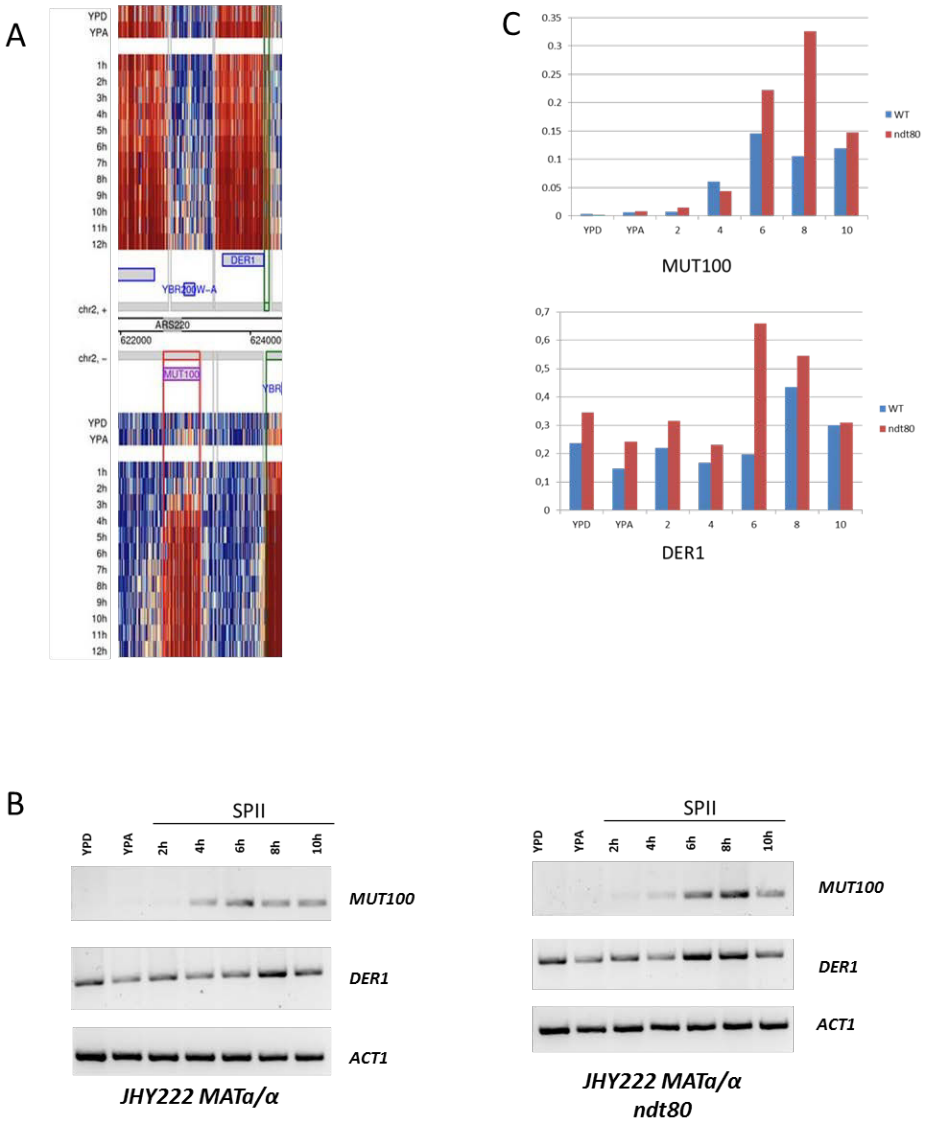

This kind of bidirectional control of a mRNA gene and a non-coding RNA gene by *Ndt80* seems not to be limited to *BBP1/MUT1465*. We checked the positive control ncRNA *MUT523* and found that it also under bidirectional control by *Ndt80* together with *PES4*. As expected, the negative controls *MUT100* and *MUT1290* do not appear to be under bi-directional control by Ndt80 (Figure 4 and 5).

Figure 4. Bidirectional expression of *MUT100* and *DER1*. RT-PCR validation result and quantification. *ACT1* was used as an internal control.

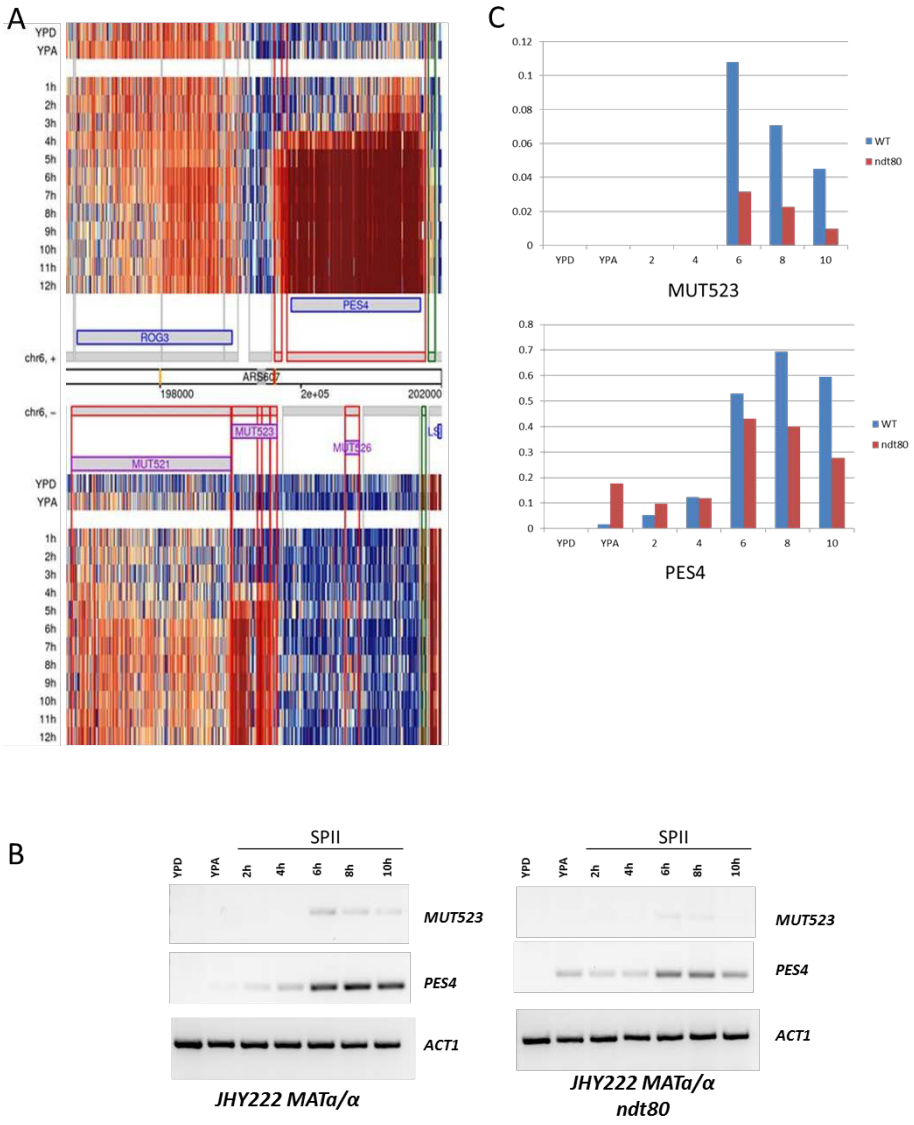

Figure 5. Bidirectional expression of *MUT523* and *PES4*. RT-PCR validation result and quantification. *ACT1* was used as internal control.

When we assayed the expression of *BBP1/MUT1465* in the *rrp6* mutant strain, we found that both *MUT1465* and *BBP1* are up-regulated in mitosis YPD sample. (Figure 6A).

Since *MUT1465* is induced and *BBP1* is further up-regulated in middle meiosis by Ndt80, we speculate that the accumulation of these transcripts in mitosis could be mediated by Ndt80. Therefore, we checked the expression of *NDT80* in the *rrp6* mutant and indeed found that *NDT80* mRNA accumulates somewhat in mitosis (Figure 6C). The abnormally high level of *NDT80* in the YPD sample of the *rrp6* mutant, is consistent with the idea that *NDT80* controls the bi-directional induction of *BBP1* and *MUT1465*.

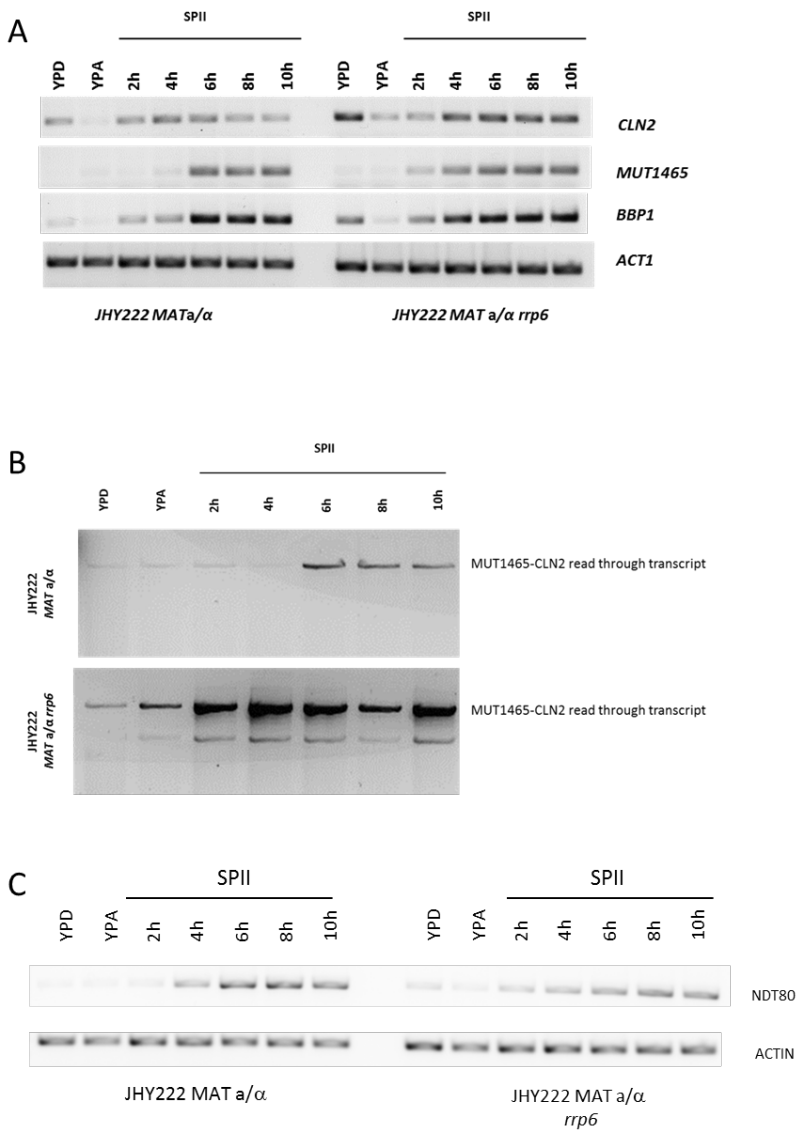

Figure 6. *MUT1465* expression and transcription read-through, and *NDT80* expression in WT vs. *rrp6* mutant. RT-PCR validation result and quantification. *ACT1* is the loading control.

MUT1465 induction may have an important function in repressing CLN2 expression during meiosis

We next sought to ask what is the function of this bi-directional induced ncRNA during meiosis, is it just the bi-directional by-product without any function or it can act as a meiotic regulator? We found that the gene downstream of *MUT1465*, *CLN2* (a G1 cyclin for which the function is restricted to G1 phase and which is not needed in middle meiosis where DNA replication occurs) was down-regulated during middle meiosis when *MUT1465* is induced. Therefore, it could be that *MUT1465* inhibits the expression of *CLN2* by promoter interference.

To test this hypothesis, we first constructed a strain with *MUT1465* driven by a *TEF1* promoter, (MUT1465 cis-ON). We checked the expression of *CLN2* in this strain, and found that *MUT1465* was strongly induced in mitotic YPD samples and meiotic time course SPII samples (Figure 7). Moreover, the expression of *CLN2* was also increased in middle meiosis, instead of being down-regulated. This may be caused by the strong *TEF1* promoter, which may lead to transcription read through to the *CLN2* locus. We verified this idea by using a primer pair where the forward primer was located in the *MUT1465* region and the reverse primer was located in the *CLN2* region: as expected, we found a read-through transcript from *MUT1465* to *CLN2* (Figure 6B). As in the *rrp6* mutant the read-through transcript is induced in mitosis YPD and YPA sample and have higher expression level in sporulation sample than WT strain. Therefore, it would be interesting to know if

Ndt80 is responsible for the induction of read-through transcript in the mitosis samples of *rrp6* mutant. Indeed, we found that *NDT80* accumulates to low levels in mitotic *rrp6* cells. This may mean that *NDT80* is responsible for the induction of *MUT1465-CLN2* read-through transcripts that repress *CLN2* expression (Figure 6C).

.

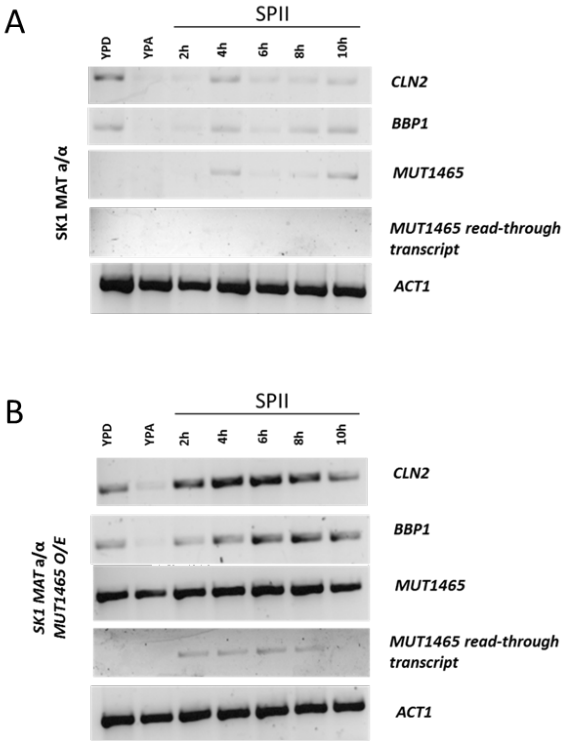

Figure 7. Expression pattern of *MUT1465* in *MUT1465* overexpression strain. RT-PCR validation result and quantification. *ACT1* was used as internal control.

Since during middle meiosis, the *CLN2* signal tends to be very low at the time when *MUT1465* is induced, it could be that this signal in the *CLN2* locus is due to read-through transcription from *MUT1465*. We confirmed by RT-PCR that the read-through transcript is strongly induced in middle meiosis at the same time when *CLN2* is down-regulated and *MUT1465* is induced. A previous study reported that Rrp6 degradation during middle meiosis results in the stabilize of MUTs, and there are also studies in the literature showing that Rrp6 can act to inhibit read-through, as in the case of snRNA (Fox M et al., PLoS Genet. 2015). Therefore, the read-through should be also enhanced in *rrp6* mutant. We confirmed by RT-PCR that read-through is slightly induced in mitotic YPD sample in *rrp6* mutant, while it was strongly induced in early meiosis. This may explain why *CLN2* expression signals are up-regulated in the *rrp6* mutant during the meiotic time course.

We further constructed a strain with a transcription terminator inserted downstream of the putative *MUT1465* transcription start site in order to prevent its expression (*MUT1465* cis-OFF). However, we tested by RT-PCR and found that *MUT1465* is still expressed. This is not surprising, since a lncRNA knock out is very difficult not only in budding yeast but also in other higher eukaryotes as lncRNAs cannot easily be inactivated by insertion of transcription terminator or frame shift mutations (Quinn J and Change H Y. Nature Reviews Genetics. 2016)

If *MUT1465* really acts as read-through to inhibit the expression of *CLN2* during meiosis, then the transcription of *MUT1465* but not the transcript itself is important. We tested this hypothesis by

constructing a strain where TEF1-*MUT1465* is inserted into the HO locus while leaving the *MUT1465* locus intact (*MUT1465* trans-ON). We found that *MUT1465* increases in *MUT1465* trans-ON, while the expression pattern of *CLN2* remains the same as in the WT strain. And the read-through transcript also has the same expression pattern as in WT strain. This confirms that *MUT1465* appears to act in cis through read-through to inhibit the transcription of *CLN2* during middle and late meiosis.

MUT1465 is bidirectionally regulated with *BBP1*. The expression of *BBP1* in *MUT1465* cis-ON also shows slightly elevated expression, but not in *MUT1465* trans-ON. This may be the result of intrinsic bi-directional characteristics of the TEF promoter. Taken together, these results suggest that Ndt80 induces the bi-directional expression of *MUT1465* and *BBP1* during middle and late meiosis, and this may inactivate *CLN2* by transcriptional read-through and activate *BBP1* at the same time.

Discussion

BBP1 is essential for mitosis and therefore shows basic transcription during cell division. *BBP1* and *MUT1465* seem to use a bi-directional promoter. How does this regulatory region shift from a uni-directional to a bi-directional pattern? It could be that the promoter is bi-directional also in mitosis, and it can transcribe towards upstream direction to transcribe *MUT1465*, but the nascent *MUT1465* transcript is degraded quickly by Rrp6. However, this seems not to be the case, since *MUT1465* is only slightly increased in the mitotic YPD sample of *rrp6* mutant. The spatial organization of chromatin was found to play an important role in regulating gene expression. We searched the *CLN2* locus interaction with published 4C (Circularized Chromosome Conformation Capture) data in mitosis of budding yeast, and found that the promoter region of *CLN2* interacts with its 3'end, thus forming a loop. This connection may facilitate RNA polymerase II binding to the *CLN2* promoter faster after it has finished the first round of transcription. This connection may also limit the accessibility of RNA PolII to the promoter of *BBP1*, since the loop may block spatial access. In meiosis the chromatin conformation may change and thus the loop may be broken and the *BBP1* promoter may fully exposed so that RNA Pol II can transcribe through it, and the transcription of *MUT1465* also occurs. It could be that the chromatin conformation change facilitates Ndt80 binding to the *BBP1* promoter or on the contrary Ndt80 may function as a chromatin conformation modifier whose expression and binding to *BBP1* promoter in middle meiosis lead to the conformation change, and thus facilitates the transcription of *MUT1465*.

MUTs have been shown to be regulated by Rrp6, which is a 3' to 5' exoribonuclease to degrade MUTs in vegetable growth and onset of meiosis (Lardenois A., et al., PNAS, 2011). However, little is known about how those non-coding RNA been induced during meiosis. Here, we show that Ndt80 is the main transcription factor that activates MSE-dependent MUT expression during middle meiosis. We propose that this activation can result in regulatory lncRNA interfering with mRNA transcription.

Ndt80 is a transcription factor, which is active in middle meiosis. It can induce genes with MSE elements in their promoters. Thus, Ndt80 is important for the activation of middle meiosis induced genes and the boost of other genes necessary for middle and late meiosis. Ndt80 target genes by binding at the MSE motif. Through genome wide promoter analysis for the transcription factor binding site on the promoter of MUTs, we found MSE elements are among MUTS which induced in middle meiosis. MSE elements located in the intergenic region between two transcript locus can induce those transcripts bidirectionally. Thus, Ndt80 can up-regulate two genes via the same promoter. We analyzed *MUT1465* and *BBP1* that are activated by Ndt80 because *BBP1* is a gene important for spindle formation in mitosis and – by inference – in meiosis. We propose that *MUT1465* has role in inhibiting downstream gene *CLN2*, which is not needed in meiosis. Thus, Ndt80 not only activates a gene important for meiosis, but also indirectly represses a gene that is not by transcriptional read-through. *MUT1465* locus seems interact with the *CLN2* 3'end in mitosis, which enables fast re-cycling and re-use of the RNA Pol II and cofactors to allow normal expression of *CLN2* during mitosis. This kind of looping is common in budding yeast to facilitate gene expression. During meiosis the chromatin spatial organization may change to release the attachment, thus allowing the further induction of *BBP1* and the repression of *CLN2*. Additional work may prove the spatial structure theory.

References

Pelechano V, García-Martínez J, Pérez-Ortín JE. A genomic study of the inter-ORF distances in Saccharomyces cerevisiae. Yeast. 2006 Jul 15;23(9):689-99.

Alam T, Medvedeva YA, Jia H, Brown JB, Lipovich L, Bajic VB. Promoter analysis reveals globally differential regulation of human long non-coding RNA and protein-coding genes. PLoS One. 2014 Oct 2;9(10):e109443. doi: 10.1371/journal.pone.0109443. eCollection 2014.

Cross FR, Hoek M, McKinney JD, Tinkelenberg AH. Role of Swi4 in cell cycle regulation of CLN2

expression. Mol Cell Biol. 1994 Jul;14(7):4779-87.

Fox MJ, Gao H, Smith-Kinnaman WR, Liu Y, Mosley AL. The exosome component Rrp6 is required for RNA polymerase II termination at specific targets of the Nrd1-Nab3 pathway. PLoS Genet. 2015 Feb 13;11(2):e1004999. doi: 10.1371/journal.pgen.1004999. eCollection 2015.

10. Different control of lncRNA by Ume6 in JHY222 and SK1 strains

Introduction

Ume6 is the DNA binding subunit of the Rpd3L histone deacetylase complex. It binds the DNA target sequence AGCCGCCGA (also called URS1 element). URS1 is repressor site, which has been found in various promoters that respond to stress and meiotic induction. Ume6 recruits conserved histone deacetylase Rpd3 and chromatin remolding protein Isw2 to the URS1 site to remodel chromatin and suppress transcription by DNA looping (Yukawa M, et al. Biosci Biotechnol Biochem.2009; Gailus-Durner V, et al. Mol Cell Biol.1997).

JHY222 background yeast is homogeneous to S288C yeast genome, while SK1 strain is crossed between the West African lineage and the European lineage (Liti G., et al., Nature. 2009). SK1 genome sequence is phylogenetic distant from JHY222 (S288C) genome (Liti G., et al., Nature. 2009). While both SK1 and JHY222 strains can efficiently form asci, SK1 strain shows faster and more synchronous sporulation. The genome wide comparisons of transcriptomes of SK1 strain and W303 during sporulation time course shown that SK1 genome has 39 gene deletions and 2025 SNPs distinct to S288C, and the sporulation transcriptomes analysis shown that the two strains have similar core meiotic transcriptomes, yet there are also a large set of genes been differently regulated in those two strains. Among them classical early meiotic genes shown the most distinct expression pattern among two strains, as those early meiotic genes are more efficiently expressed in SK1 strain. Early meiotic genes are unstable and have relatively low abundance. Therefore, the transcriptome differences between two strains may reflect the more efficient and highly synchrony of SK1 cells, which make the transient and low abundance genes more visible (Primig M, et al., Nature Genetics. 2000)

Materials and methods

Yeast strains and growth media. Strains used in this study are SK1 and JHY222 (Lardenois et al., PNAS 2011), MPY542 (JHY222 *ume6*) and MPY702 (SK1 *ume6*). Media were prepared according

to standard protocols for growth (YPD, YPA) and sporulation (SPII).

RT-PCR assay. RNA was extracted by Hot phenol method, followed by DNase I treatment with TURBO DNA-free Kit (Ambion, USA). RT-PCR reactions were carried out using 2 μg of RNA reverse transcribed with Reverse Transcriptase (High Capacity cDNA Reverse Transcription kit; Life Technologies, USA) and amplified using Taq Polymerase (Qiagen, France) at 60ºC for 28 cycles. RT-PCR products were separated on 2% agarose gels and photographed using an ImageQuant 350 digital Imaging 381System at the default settings (General Electric, USA). Primers used for RT-PCR were designed with Primer3 (simgene.com/Primer3; Table 1).

Table 1. Primers for RT-PCR assay

Gene	Forward Primer	Reverse Primer
MUT100	5′-GCCAAATATTTCCACTCAATCA-3′	5′-CCAACAAGAACAGCGCTACA-3′
MUT1290	5′-AGCTGGTACTGCCCGTACAT-3′	5′-ACAGGGAACTCCAGCGTATG-3′
MUT1465	5′-GGGCCAACAGTTGTTTCAGT-3′	5′-CATCGCGAAATTTGTCTCAA-3′
MUT523	5′-TCCTTCTATGGACTGCGACA-3′	5′-TCTCGTTATTATTGGTTCGTTCAA-3′
ACT1	5’-CTCGTGCTGTCTTCCCATCT-3’	5’-AGATGGACCACTTTCGTCGT-3’

Results and discussion

MUT1290 has a known URS1 element. *MUT100* does not have URS1 in its promoter, *MUT100* overlaps with ARS220. *MUT100*, *MUT1290* are de-repressed in JHY222 *ume6* while only *MUT1290* shows show de-repression in SK1 *ume6* mutant (Figure 1).

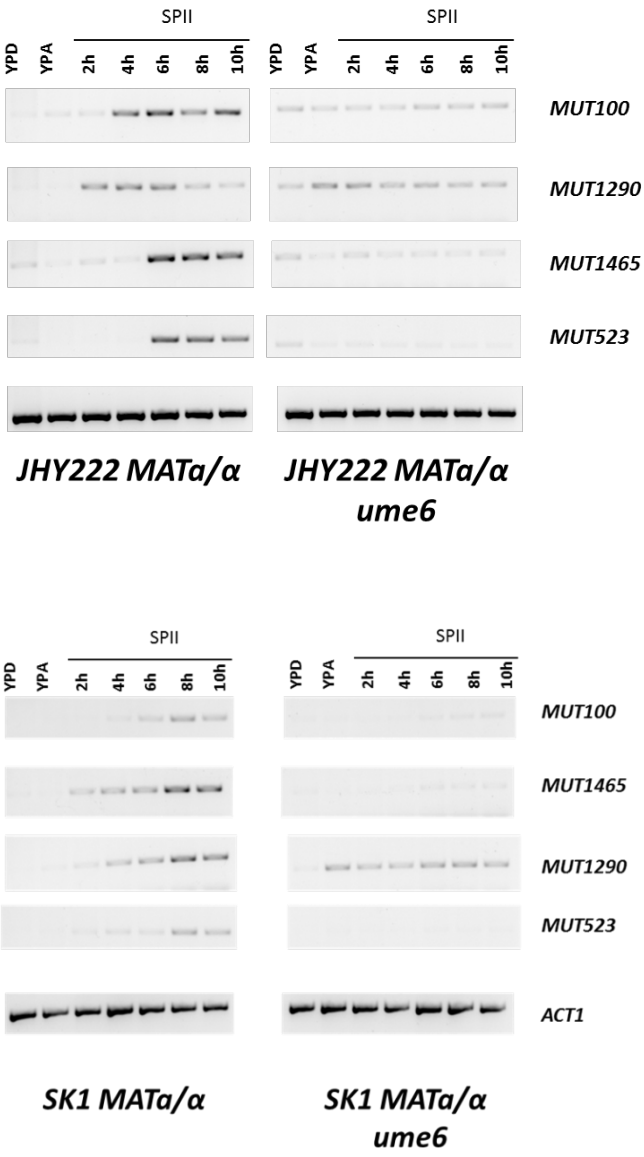

Figure 1. RT-PCR assay of MUTs in wild-type versus *ume6* mutant strains. Strain backgrounds are given at the bottom, MUT numbers to the left and samples from growing (YPD, YPA) and sporulating cells (SPII) are shown at the top.

Ume6 is known to be a repressor of numerous protein coding genes involved in starvation and (mostly) early meiosis. In its absence, direct target mRNAs accumulate but other transcripts are indirectly affected. We provide initial evidence that Ume6 is also directly and indirectly involved in the transcriptional control of certain MUTs.

UME6: Lardenois et al., Mol Genet Genomics 2015

Global alterations of the transcriptional landscape during yeast growth and development in the absence of Ume6-dependent chromatin modification

Aurélie Lardenois, Emmanuelle Becker, Thomas Walther, Michael J. Law, Bingning Xie, Philippe Demougin, Randy Strich & Michael Primig

Molecular Genetics and Genomics

ISSN 1617-4615
Volume 290
Number 5

Mol Genet Genomics (2015)
290:2031-2046
DOI 10.1007/s00438-015-1051-5

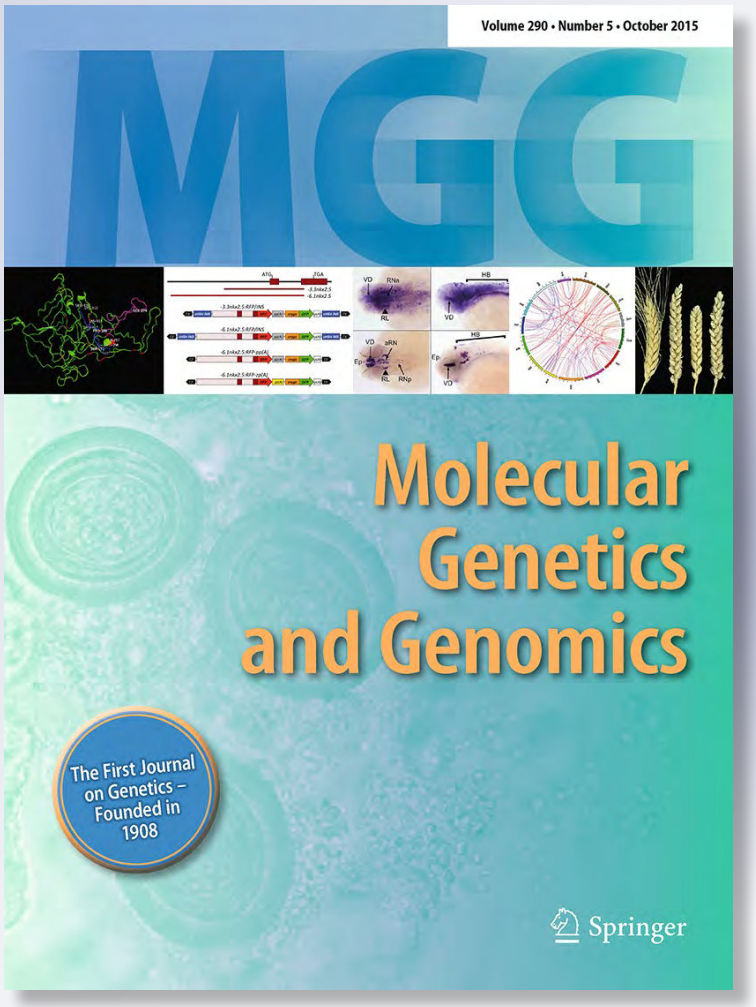

Springer

Your article is protected by copyright and all rights are held exclusively by Springer-Verlag Berlin Heidelberg. This e-offprint is for personal use only and shall not be self-archived in electronic repositories. If you wish to self-archive your article, please use the accepted manuscript version for posting on your own website. You may further deposit the accepted manuscript version in any repository, provided it is only made publicly available 12 months after official publication or later and provided acknowledgement is given to the original source of publication and a link is inserted to the published article on Springer's website. The link must be accompanied by the following text: "The final publication is available at link.springer.com".

Author's personal copy

Mol Genet Genomics (2015) 290:2031–2046
DOI 10.1007/s00438-015-1051-5

ORIGINAL PAPER

Global alterations of the transcriptional landscape during yeast growth and development in the absence of Ume6-dependent chromatin modification

Aurélie Lardenois[1,4] · Emmanuelle Becker[1] · Thomas Walther[2,5] · Michael J. Law[3] · Bingning Xie[1] · Philippe Demougin[2] · Randy Strich[3] · Michael Primig[1]

Received: 24 February 2015 / Accepted: 17 April 2015 / Published online: 10 May 2015
© Springer-Verlag Berlin Heidelberg 2015

Abstract Chromatin modification enzymes are important regulators of gene expression and some are evolutionarily conserved from yeast to human. *Saccharomyces cerevisiae* is a major model organism for genome-wide studies that aim at the identification of target genes under the control of conserved epigenetic regulators. Ume6 interacts with the upstream repressor site 1 (URS1) and represses transcription by recruiting both the conserved histone deacetylase Rpd3 (through the co-repressor Sin3) and the chromatin-remodeling factor Isw2. Cells lacking Ume6 are defective in growth, stress response, and meiotic development. RNA profiling studies and in vivo protein-DNA binding assays identified mRNAs or transcript isoforms that are directly repressed by Ume6 in mitosis. However, a comprehensive understanding of the transcriptional alterations, which underlie the complex *ume6Δ* mutant phenotype during fermentation, respiration, or sporulation, is lacking. We report the protein-coding transcriptome of a diploid *MAT***a**/α wild-type and *ume6*/*ume6* mutant strains cultured in rich media with glucose or acetate as a carbon source, or sporulation-inducing medium. We distinguished direct from indirect effects on mRNA levels by combining GeneChip data with URS1 motif predictions and published high-throughput in vivo Ume6-DNA binding data. To gain insight into the molecular interactions between successive waves of Ume6-dependent meiotic genes, we integrated expression data with information on protein networks. Our work identifies novel Ume6 repressed genes during growth and development and reveals a strong effect of the carbon source on the derepression pattern of transcripts in growing and developmentally arrested *ume6*/*ume6* mutant cells. Since yeast is a useful model organism for chromatin-mediated effects on gene expression, our results provide a rich source for further genetic and molecular biological work on the regulation of cell growth and cell differentiation in eukaryotes.

Keywords Ume6 · Rpd3 · Sin3 · Isw2 · Transcriptome · Interactome

Communicated by A. Aguilera.

A. Lardenois, E. Becker, T. Walther contribued equally to this work.

Electronic supplementary material The online version of this article (doi:10.1007/s00438-015-1051-5) contains supplementary material, which is available to authorized users.

✉ Michael Primig
michael.primig@inserm.fr

[1] Inserm U1085-IRSET, University of Rennes 1, 35042 Rennes, France

[2] Biozentrum, University of Basel, 4056 Basel, Switzerland

[3] School of Osteopathic Medicine, Rowan University, Stratford, NJ 08084, USA

[4] Present Address: INRA, UMR 703, ONIRIS, 44307 Nantes, France

[5] Present Address: INSA, UMR CNRS 5504 and INRA 792, 31077 Toulouse, France

Introduction

Chromatin modification enzymes are part of multi-subunit regulatory complexes, which control gene expression in eukaryotic cells. Identifying their target promoters at the genome-wide level helps understand their roles and contributes to future work that aims at a system-level understanding of processes that govern cell growth and development. The budding yeast *Saccharomyces cerevisiae* is a very useful model organism for genetic and genomic

Author's personal copy

studies that aim at a better understanding of transcriptional regulatory mechanisms, which involve conserved proteins.

UME6 (*U*nscheduled *M*eiotic *E*xpression 6) was initially identified in a screen for haploid mutants that express meiosis-specific genes during vegetative growth in *S. cerevisiae* (Strich et al. 1989). The gene is conserved among fungi where it plays important roles in establishing cellular identity in *K. lactis* and controlling filamentous growth in the human pathogen *C. albicans* (Carlisle et al. 2009; Zeidler et al. 2009; Carlisle and Kadosh 2010; O'Connor et al. 2010; Banerjee et al. 2013; Childers et al. 2014). Mutant budding yeast cells lacking *UME6* show a pleiotropic phenotype including defective mitotic growth, abnormal vacuolar fragmentation, broadly impaired stress response, and failure to enter meiotic M-phase (Strich et al. 1994; Hillenmeyer et al. 2008; Yoshikawa et al. 2011; Michaillat and Mayer 2013). In addition to genes required for metabolic functions and meiosis, Ume6 also represses *ATG8*, which is important for autophagy, a conserved process that recycles cellular components (Tsukada and Ohsumi 1993; Kratzer and Schuller 1997; Messenguy et al. 2000; Bartholomew et al. 2012). Recently, we reported a new role for Ume6 in preventing the expression of early meiosis-specific transcript isoforms with an extended 5′-untranslated region (UTR) during rapid mitotic growth (Lardenois et al. 2015).

In budding yeast, Ume6 is regulated at the post-transcriptional level at three stages. First, the Spt-Ada-Gcn5-acetyltransferase (SAGA) complex acetylates Ume6 when cells switch from fermenting glucose to respiring acetate conditions, and thereby diminishes its DNA binding activity. A second acetylation event stimulates protein degradation by the anaphase promoting complex/cyclosome (APC/C) ubiquitin ligase and Inducer of Meiosis 1 (Ime1) during the onset of meiotic development. Ume6 levels remain below the limits of detection during the meiotic divisions before it accumulates again at late stages of sporulation to ultimately exert a function during spore germination (Mallory et al. 2007, 2012; Strich et al. 2011; Law et al. 2014).

Ume6 is a C6 zinc cluster protein, which directly binds the upstream repressor site 1 (URS1) motif (5′-TAGCCGCCGA-3′) present in single or multiple copies within target promoters (Park et al. 1992; Anderson et al. 1995), for review, see (Mitchell 1994; Kassir et al. 2003). Initially, URS1 sites were identified using sequence homology searches within the 5′-upstream regions of potential target genes (Williams et al. 2002). When several genomes of related yeasts were sequenced, discovering regulatory DNA elements such as URS1 was facilitated because transcription factor binding sites located within intergenic regions were conserved (Cliften et al. 2003; Kellis et al. 2003). Moreover, genome-wide protein-DNA binding assays identified direct targets for most regulatory proteins, including Ume6, in yeast (Kurdistani et al. 2002; Harbison et al. 2004). A current method to analyze promoter regions employs position weight matrices (PWMs), which are established by aligning experimentally verified binding sites of transcription factors (TFs), and log-transforming the number of observations of each nucleotide within their target motifs (Orenstein et al. 2012). PWMs are available for nearly all yeast TFs via the TRANSFAC database (Wingender 2008; Spivak and Stormo 2012).

Ume6-dependent transcriptional repression is mediated by recruitment of the conserved histone deacetylase Rpd3 through the co-repressor Sin3 and the chromatin-remodeling factor Isw2 (Anderson et al. 1995; Kadosh and Struhl 1997; Rundlett et al. 1998; Goldmark et al. 2000). In addition, biochemical studies and high-throughput assays have shown that Ume6 interacts with many proteins both physically and genetically (for more details, see www.ebi.ac.uk/intact/) (Baryshnikova et al. 2010; Ngounou Wetie et al. 2014; Orchard et al. 2014). The yeast interactome includes physical interactions established via yeast two-hybrid assays (direct binding) and co-immunoprecipitation (direct and indirect binding in a complex) and genetic interactions determined by screening double mutants for growth phenotypes. Integrating expression profiling data with protein network information provides insight into the dynamic nature of protein interactions during normal growth or cell differentiation pathways (Prinz et al. 2004; de Lichtenberg et al. 2005).

In this study, we compared the protein-coding transcriptome in triplicate samples from a wild-type diploid strain to a *ume6* mutant strain cultured in rich fermentation or respiration conditions (YPD or YPA, respectively), or in sporulation medium, which lacks both glucose and nitrogen (SPII). In addition to asynchronously growing diploid cells, we used published data from synchronized *MAT***a** cells progressing through the mitotic cell cycle to determine which Ume6-dependent mRNAs induced during sporulation are undetectable in both haploid and diploid cells cultured in YPD (Orlando et al. 2008). We further differentiated between direct and indirect effects by combining GeneChip data with URS1 motif predictions and published high-throughput in vivo Ume6-DNA binding data (Harbison et al. 2004). For a better understanding of the physical and genetic interactions between successive waves of meiotic genes, we integrated expression data with information on protein networks. Using this integrative approach, we identify new Ume6-dependent genes, and demonstrate that the nutritional status of the cells affects the derepression of most Ume6 target genes. These expression data, which are available for further analyses at the EBI's ArrayExpress (Rustici et al. 2013), and for viewing in the GermOnline database (www.germonline.org) (Lardenois et al. 2010),

Author's personal copy

represent a rich source for further investigation of epigenetic control mechanisms governing yeast cell growth and differentiation.

Materials and methods

Yeast strains

We employed a diploid SK1 *MAT***a**/α wild-type strain and a diploid SK1 *MAT***a**/α *ume6*/*ume6* mutant strain as published (Williams et al. 2002).

Media and culture conditions

For RNA profiling experiments, three independent samples of wild-type versus mutant strains were cultured in rich media with glucose (YPD) or acetate (YPA) or sporulation medium (SPII at 4, 8, and 10 h) under standard conditions as published (Primig et al. 2000).

Total RNA isolation and cRNA target synthesis

5 μg of total RNA was subjected to double-stranded cDNA synthesis using the One-Cycle cDNA synthesis kit (Affymetrix, Santa Clara, USA). The cDNA was purified with the Sample Cleanup Module (Affymetrix) and used to synthesize cRNA in the presence of a biotin-conjugated ribonucleotide analog with the IVT labeling kit (Affymetrix). Approximately 45 μg of labeled cRNA from each reaction was purified and the average size of the cRNA molecules was assessed with a BioAnalyzer and RNA Nano 6000 Chips (Agilent, Santa Clara, USA). cRNA targets were incubated at 94 °C for 35 min in fragmentation buffer and the resulting fragments of 50–150 nucleotides were again monitored using the BioAnalyzer. Synthesis reactions were carried out using a T1 Thermocycler (Biometra, Göttingen, Germany). 80 μl hybridization cocktail containing fragmented biotin-labeled target cRNA at a final concentration of 0.05 μg/μl was loaded into Yeast Genome 2.0 GeneChips (Affymetrix) and incubated at 45 °C in a hybridization oven 640 (Affymetrix) for 16 h at 60 rpm.

GeneChip hybridization and raw data production

The arrays were washed and stained on a Fluidics Station 450 (Affymetrix) using the Hybridization Wash and Stain Kit (Affymetrix). To increase the signal strength, we employed the antibody amplification protocol (FS450_0003). The GeneChips were processed with a GeneChip Scanner 3000 (Affymetrix) using the default settings. Raw data CEL files were generated using GeneChip Operating Software GCOS 1.4 (Affymetrix).

Minimum information about a microarray experiment (MIAME) compliance

A complete set of raw data files is available at the European Bioinformatics Institute's ArrayExpress certified repository; the accession number is E-TABM-192 (Rustici et al. 2013). In addition, graphical displays of the normalized GeneChip signals in the context of yeast genome annotation data are available at GermOnline (www.germonline.org) (Lardenois et al. 2010).

GeneChip data processing

Yeast Genome 2.0 GeneChip data were processed and normalized using the AMEN software tool as published (Chalmel et al. 2007).

Genome-wide in vivo Ume6 binding data

We integrated the output of a Ume6 chromatin immunoprecipitation—chip (ChIP-Chip) assay done with haploid W303 yeast strain grown in rich medium (YPD) (Harbison et al. 2004).

URS1 motif predictions

The Ume6 target site URS1 was predicted at a genome-wide level in reference (Lardenois et al. 2015).

Gene filtration and cluster analysis

First, we identified 1571 probesets (corresponding to 1560 genes) defined as differentially expressed within a sample set from the diploid wild-type strain (*UME6*), the *ume6* deletion mutant (*ume6*) and the combined set using a standard deviation ≥ 1.0. Second, we filtered 3139 probesets (3095 genes) showing a fold-change ≥ 2 in paired wild-type versus mutant samples. The intersection of both lists yielded 1404 probesets (1393 genes). To determine the statistical significance of their signal variations, we used permutation tests [p value (FDR) ≤ 0.01], which yielded 1399 probesets (1390 genes). Finally, these genes were grouped according to their expression patterns into 12 clusters using the partitioning around medoids (PAM) algorithm as published (Online Resource Figure S5) (Chalmel et al. 2007).

Gene ontology term enrichment

For each cluster, a Gene Ontology (2015) term enrichment was performed via DAVID (da Huang et al. 2009). The biological process (BP) sub-ontology was used to identify the functional pathways over-represented in each group, using a hyper-geometric law with Benjamini correction

Author's personal copy

for multiple testing, and the whole yeast genome as reference dataset. The BP terms with a p value <0.01 % were then clustered with a medium stringency and each cluster received as name the BP annotation representing more than 10 % of the cluster with the strongest p value.

Protein network analysis

Protein network analysis was performed using CytoScape version 3.2.0. (Saito et al. 2012). The network was extracted from BIND (Isserlin et al. 2011) using the dedicated Cytoscape interface. The analysis was centered at genes differentially expressed and not expressed during wild-type mitosis (such genes were identified in clusters G9, G8, G1, and G10), as well as their direct interactors. We identified 14 connected components (CCs): two of them have more than 20 members; among them more than 10 are differentially expressed and not expressed during mitosis. One CC is presented in Fig. 6 to illustrate the approach.

Chromatin immunoprecipitation

In vivo Ume6-DNA binding to the *SIP4* promoter was monitored in cells cultured in rich media (YPD, YPA) or sporulation medium (SPII) at 4, 8, and 10 h using the strain background described in reference (Lardenois et al. 2015). 50 ml of a mid-log YPA culture was fixed with 1 % formaldehyde for 15 min at room temperature. Ume6/DNA complexes were quenched with 140 mM glycine (Sigma, St Louis USA) for 5 min. Anti-Ume6 immune complexes were immunoprecipitated, washed, and eluted before crosslinks were reverted. DNA was precipitated and treated with proteinase K. DNA fragments were amplified by Q-PCR as published (Mallory et al. 2012). Relative ChIP signals were calculated using the formula 2^-IP (CT target–CT control)/input (CT target–CT control) with *NUP85* enrichment used as a negative control. Binding to *SPO13* was used as a positive control as published (Law et al. 2014). The oligonucleotide primers used to amplify the *SIP4* promoter were 5′-GCCGTTCGACCGGTGTT-3′ (forward) and 5′-TTTGCCGCCGAGTTCTG-3′ (reverse). For *SPO13,* we used 5′-GCTAGTTAGT ACCTTTGCACGGAAA-3′ (forward) and 5′-TCTTATTGCGCTAATTGTCTGTTAGAC-3′ (reverse).

RT-PCR assays

Yeast Genome 2.0 GeneChip data were validated by RT-PCR assays as published (Lardenois et al. 2015). Total RNA was isolated using the hot phenol method as described (Primig et al. 2000). Briefly, cell pellets were treated with hot phenol (65 °C) and phenol/chloroform (1:1). Total RNA was precipitated overnight with two volumes of 100 % ethanol and 0.1 volume of 3 M NaOAc (pH 5) at −80 °C. The RNA was digested with 2 units of DNaseI for 30 min at 37 °C, and then 2 μg of DNaseI-treated RNA was reverse transcribed into cDNA using reverse transcriptase and random primers supplied in the High Capacity cDNA Reverse Transcription Kit (Applied Biosystems). 1 μl of cDNA was amplified at 28 cycles (denaturation at 94 °C for 1 min, annealing at 60 °C for 1 min, and elongation at 72 °C for 1 min) using Taq DNA Polymerase (Qiagen). The PCR product was run on a 2 % agarose gel in 1 × TAE buffer containing GelRed DNA dye (Biotium) and photographed using the Gel Doc XR+ imaging system (BIO-RAD). The sequences of oligonucleotide primers used for cDNA amplification were 5′-ATTGGCGACCTGGAAATGGA-3′ (*CSM4*, forward); 5′-TGAA CACACCTCATCGCTCAA-3′ (*CSM4*, reverse); 5′-GGACT TGACCTTTGG GGGAG-3′ (*FKS3*, forward); 5′-AGACG TTCCAAAACCTCGCT-3′ (*FKS3*, reverse); 5′-GGACCCTC CTCAATCAAGCC-3′ (*HFM1*, forward); and 5′-ACTTGTTCACCCGC TTCCAT-3′ (*HFM1*, reverse).

Results

Experimental design and quality control

We RNA-profiled key stages of the diploid yeast life cycle in the presence or absence of Ume6-dependent epigenetic chromatin modification using robust Yeast Genome 2.0 GeneChips that cover nearly all protein-coding genes. We note that the mRNA data generated by these microarrays are comparable to the most recent expression profiling methods based on RNA-Sequencing (Nookaew et al. 2012). We analyzed triplicate biological samples from asynchronous fermenting (YPD) or respiring (YPA) diploid SK1 *MAT***a**/α cells harvested during late-log phase and semi-synchronous sporulating cells 4, 8, and 10 h after meiotic induction. At these time points cells progress through meiosis I prophase (4 h), meiosis I (8 h), or meiosis II (10 h), respectively (supplementary Online Resource Figure S1). The output from these experiments was combined with published Yeast Genome 2.0 expression data from haploid BF264-15Dau *MAT***a** cells undergoing synchronous mitotic cell cycles in rich medium (YPD) (Orlando et al. 2008). We identified transcripts expressed during meiotic development that are undetectable in fermenting and respiring diploid *MAT***a**/α cells and during successive phases of the mitotic cell cycle in fermenting haploid *MAT***a** cells. Total RNA samples from the wild-type strain and the *ume6*/*ume6* mutant were of high quality (Online Resource Figure S2 and Online Resource Figure S3), and the microarray signal intensity distributions fell into broadly similar ranges for each sample, indicating that the GeneChip hybridization reactions yielded data that are comparable once normalized (Online Resource Figure S4A, B).

Author's personal copy

Genome-wide expression signal distributions across samples reflect the diploid *ume6*/*ume6* mutant phenotype

To determine the degree of reproducibility between biological replicates, we compared their global signal patterns to each other using a correlation distance matrix. As expected, wild-type replicates cultured in YPD, YPA, or SPII were consistently grouped together and distinct signal patterns emerged as cells exit growth and enter meiotic differentiation (Fig. 1). Conversely, samples from *ume6*/*ume6* mutant cells cultured in pre-sporulation medium (YPA) and sporulation medium (SPII) are broadly similar (note that replicates at SPII 8 h and 10 h are interspersed) and grouped with the wild-type in SPII 4 h. This sample broadly corresponds to the end of pre-meiotic DNA replication, which is the phase where mutant cells accumulate (Strich et al. 1994). The plot also highlights that *ume6*/*ume6* mutants show distinct global profiles in the presence of glucose and acetate, which indicates that the pattern of gene derepression during vegetative growth is widely influenced by the carbon source (Fig. 1).

Global RNA profiling of growth and development in the absence of Ume6 reveals known and new patterns of de-regulation

Our approach was designed to cover changes in RNA levels during growth and development related to the deletion of *UME6* as broadly as possible. As a consequence, we identified all core Ume6 target genes determined in an earlier RNA profiling study (Williams et al. 2002), apart from the dubious gene *YBR116C* not represented on the Yeast Genome 2.0 GeneChip, and *YIR016W* and *YMR101C* that are not differentially expressed in the current study. We filtered 1390 transcripts showing differential expression signals across the sample sets (Online Resource Figure S5; see "Materials and methods" for more details on the procedure) and grouped them into twelve clusters according to their peak expression in YPD, YPA, or SPII media (Fig. 2, Online Resource File S1). Clusters 1–2 contain genes actively transcribed during vegetative growth and meiotic M-phase in the wild-type but not in the *ume6*/*ume6* mutant that arrests before entering M-phase. Clusters 3–7 comprise genes that are progressively down-regulated during sporulation in the wild-type but that show altered patterns in the mutant. Clusters 8 and 9 include the well-studied early meiotic genes, which are de-repressed in the mutant cultured in YPA (but often not in YPD, see Fig. 1) and then persist in SPII. In wild-type yeast, these genes peak at 4 h during sporulation, and decline at the later time points. Cluster 10 shows a category of genes that are induced during early and middle meiosis in wild-type yeast without declining at later phases. These genes are de-repressed in respiring *ume6*/*ume6* cells. Clusters 11 and 12 contain middle meiotic genes and acetate-inducible genes, which fail to be activated to normal levels in *ume6* mutant cells that arrest prior to meiotic M-phase. We note that some of these genes may also play a role in temperature stress response because they are induced during the first hour after haploid cells were released from a commonly employed cell cycle synchronization procedure (Orlando et al. 2008).

Genome-wide in vivo Ume6-DNA binding data are important for identifying direct target genes. These data indicate that Ume6 directly binds the promoters of various loci in all clusters. We find Ume6-promoter interactions to be significantly enriched in Cluster 6 (binomial exact test, p value 2.622×10^{-5}), containing genes involved in carbon source metabolism, and Cluster 9 (binomial exact test, p value 1.27×10^{-8}), harboring early meiotic genes (Harbison et al. 2004). We sought to further confirm direct Ume6 association with a target gene in our diploid strain background, because high-throughput chromatin precipitation studies are typically carried out in haploid strains. We selected *SIP4* (encoding a transcription factor involved in gluconeogenesis), since (1) its mRNA is strongly de-repressed in *ume6* mutants cultured in YPD (cluster 8), (2) we find four URS1 motifs in its promoter, and (3) its upstream intergenic region is bound by Ume6 in haploid cells (Online Resource Figure S6A–C) (Williams et al. 2002; Harbison et al. 2004). We find that in fermenting diploid cells, Ume6 binds to the *SIP4* promoter in vivo to a level comparable with the known target *SPO13* (Online Resource Figure S6D). This indicates that individual binding assays and large-scale assays in haploid and diploid cells yield coherent results for this locus (Fig. 2).

Taken together, our findings permit two conclusions: first, our experiment produced the anticipated pattern of direct targets that increase in *ume6*/*ume6* cells and are associated with upstream URS1 motifs bound by Ume6 in vivo, and indirectly dependent transcripts that fail to accumulate or to decrease because of impaired growth and arrested meiotic development. Second, previously known Ume6-controlled early meiotic genes and metabolic loci represented only a fraction of the complete set of Ume6-dependent genes.

Functional classification of Ume6-dependent genes

To explore the functional significance of the clusters, we determined which annotation terms from the biological process Gene Ontology were enriched (Huntley et al. 2014). Cells lacking Ume6 fail to efficiently induce genes important for ribosome biogenesis, nitrogen mobilization, mitochondrial functions, and nutrient transport (C1–C5), while loci involved in DNA replication, metabolic

Author's personal copy

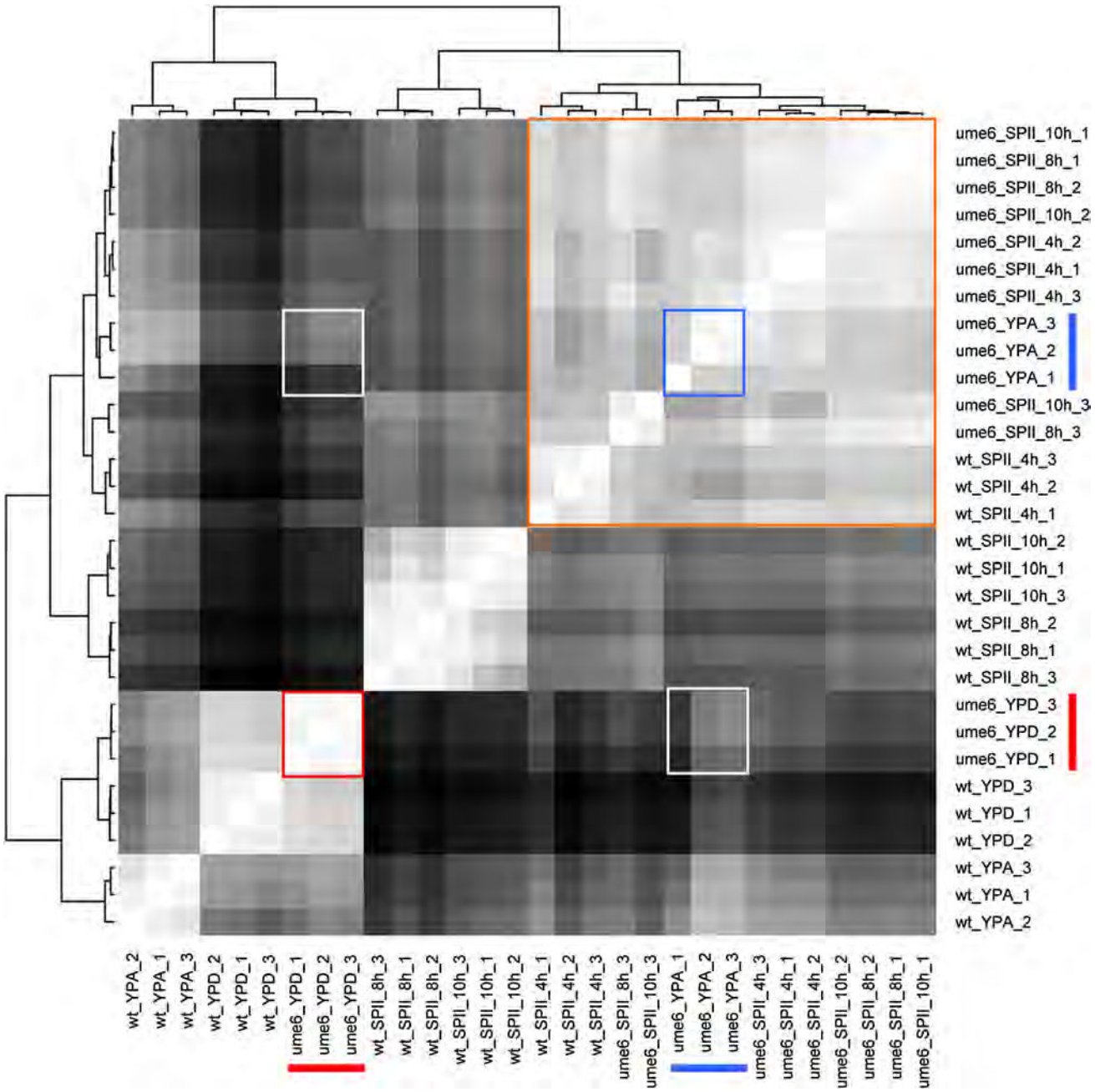

Fig. 1 Expression signal comparison across samples. A distance matrix comparing the samples from wild-type (wt) cells and a *ume6*/*ume6* mutant (ume6) in growth media (YPD, YPA) and sporulation medium (SPII 4, 6 and 8 h) is shown. *Red* and *blue bars* indicate triplicate samples from *ume6*/*ume6* cells in YPD and YPA, respectively. *Red* and *blue squares* indicate samples comparisons among replicates in YPD or YPA. *White squares* indicate sample comparisons in YPD against YPA. An *orange square* outlines similar samples across media and strains. On the color scale white represents identical samples and black identifies the most dissimilar samples.

processes, cell wall organization, and temperature stress response remain elevated in starving *ume6*/*ume6* cells cultured in SPII medium (C6–C7). Clusters 8 and 9 contain known meiotic functions; while Clusters 10 and 11 are associated with processes such as cell architecture, proteolysis, and spore formation. Cluster 12 indicates that starving mutant cells (after 8–10 h in SPII) fail to induce loci important for metabolic processes during spore formation and maturation (Fig. 3). These results reflect the broad implication of Ume6-dependent gene expression in cell growth, nutritional response, and cell differentiation (see Online Resource File S1 for details).

Author's personal copy

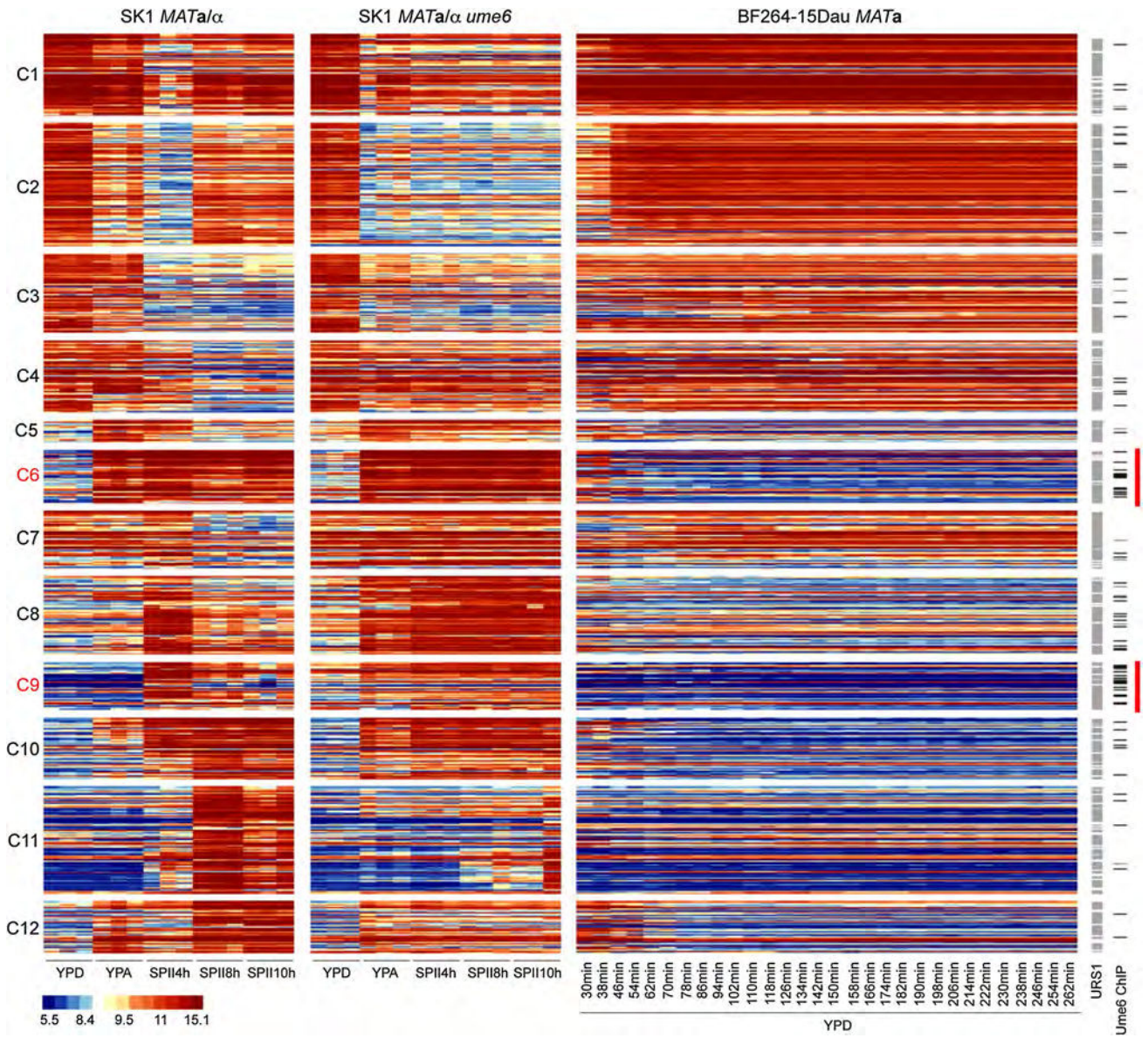

Fig. 2 RNA profiles of diploid wild-type and *ume6* strains in growth media and sporulation medium versus haploid cells in YPD growth medium. A false-color heatmap is shown for GeneChip expression signals. Every *line* corresponds to a probeset (transcript) and every *column* to a sample replicate. *Strains* are indicated at the *top*; growth media (YPD, YPA) and time points in sporulation medium (SPII 4, 8 and 10 h) are shown at the *bottom*. Cluster numbers are given to the *left*. Predicted Ume6 target motifs (URS1) and in vivo target promoters (Ume6 ChIP) are shown to the *right*. A *color scale* for log2-transformed data is given. *Red bars* mark increased occurrence of Ume6 binding in clusters C6 and C9

Genes induced in starving *ume6*/*ume6* mutant cells are involved in cell cycle progression, metabolic functions, and stress response

We next asked which genes are not expressed during sporulation in the wild-type strain but exhibit elevated transcript levels in *ume6*/*ume6* mutant cells that arrest prior to entry into meiotic M-phase when cultured in SPII. This approach identified loci falling into six categories (Fig. 4). The first two categories comprise loci that are expressed during growth but not meiotic development in the wild-type, while mutant cells contain measurable transcript levels in SPII medium. These genes are typically important for stress response (*FSH1*, *GPX2*, *SER2*) and mitochondrial functions (*MRPL19*, *FMC1*, *MSY1*, *YFH7*). Additionally, this category contains two poorly characterized genes (*YLR179C*, *YLL053C*), for which our results thus broadly suggest roles in starvation. Interestingly, the second category also includes a negative regulator of the inducer of meiosis *IME1* (*COM2*), a G1 cyclin (*CLN3*), and two genes

Author's personal copy

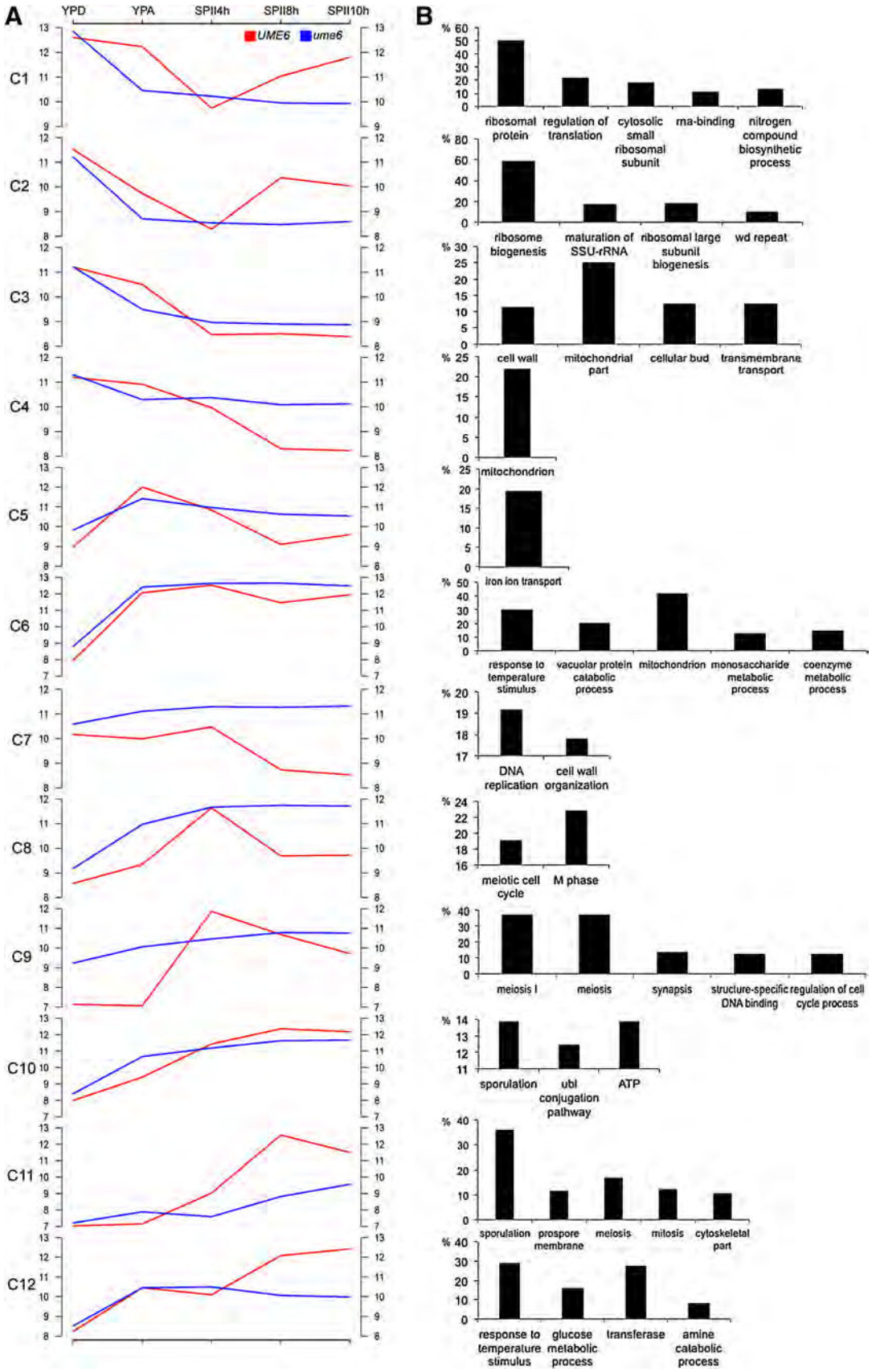

Author's personal copy

◀ **Fig. 3** Gene Ontology enrichment in expression clusters. **a** A graphical display shows the log2-transformed median expression signals in clusters C1–C12 for wild-type cells (*UME6*) in *red* and *ume6/ume6* mutant cells (*ume6*) in *blue*. Samples are indicated at the *top*. **b** *Bar diagrams* show the percentage (*y*-axis) of enriched GO terms (*x*-axis) in each cluster (hyper-geometric law, Benjamini correction for multiple testing, *p* value <0.01; annotations clustered with medium stringency by DAVID (da Huang et al. 2009)

important for polarized/pseudohyphal growth (*HMS2*, *PCL1*). The third category, which is elevated in YPA, includes only *AFT1*, an acetate-inducible transcription factor involved in iron homeostasis. The fourth category contains genes typically weakly or not expressed in growing wild-type cells but repressed during sporulation. This class includes a gene essential for DNA replication initiation (*CDC6*) and three genes of unknown function (*YBR056W-A*, *YLR462W*, *YPL067C*) that may play roles in the cellular starvation response. The genes in the fifth and sixth categories are detected only in *ume6* cells and reflect the progressive breakdown of cellular function in sporulation-deficient cells deprived of nutrients, through genes such as *AGP3* (amino acid permease), *YHL044W* (stress response membrane protein), *YLR053C* (mRNA decay), and *YNR064C* (detoxification). We note that the *ume6/ume6* deletion strain employed in this study and in earlier work (Williams et al. 2002) also lacks the repressor Gal80; we therefore used its targets *GAL2*, *GAL3,* and *GAL10* as positive controls for up-regulated genes. Functional annotation data we refer to are available at the *Saccharomyces Genome Database* (www.yeastgenome.org; (Costanzo et al. 2014)). These results reveal molecular events underlying the failure of mutant cells to enter meiotic M-phase after having completed pre-meiotic DNA replication.

Ume6-dependent genes reflect a comprehensive response of diploid cells to nutritional signals triggering gametogenesis

We next sought to explore genes induced during sporulation but undetectable in asynchronously growing diploid cells (YPD, YPA) or in synchronized haploid fermenting cells (YPD). We expected to identify genes important for Ume6-dependent functions specifically during meiosis and gametogenesis. This step yielded 183 genes falling into two groups. The first group contains 82 genes likely directly repressed by Ume6 [from C6 (3 genes), C8 (19), C9 (40), C10 (20)]. The second group contains 101 genes that appear in most cases to be indirectly dependent on Ume6 [C11 (95) and C12 (6)] as shown in Fig. 5a (for more details on these genes use the filter options in Online

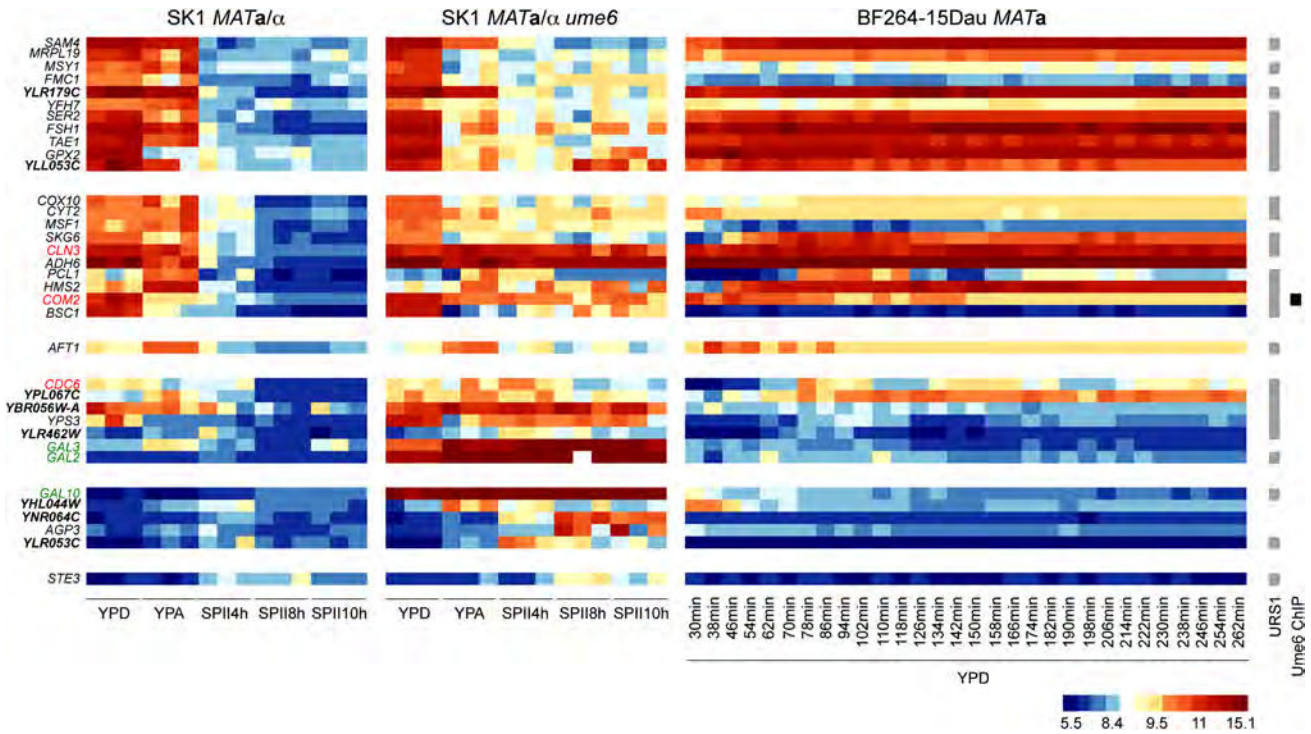

Fig. 4 Gene expression in starving *ume6* cells. A heatmap for genes up-regulated in *ume6* cells cultured SPII medium is shown like in Fig. 2 for six different classes of patterns. A *color scale* is given at the bottom. Genes relevant for meiosis and cell cycle progression are given in *red*. Reference genes are shown in *green*. Poorly characterized genes are given in *bold*. Predicted Ume6 target motifs (URS1) are shown to the *right*. *Black bars* indicate Ume6 in vivo binding (Ume6 ChIP) (Harbison et al. 2004)

Author's personal copy

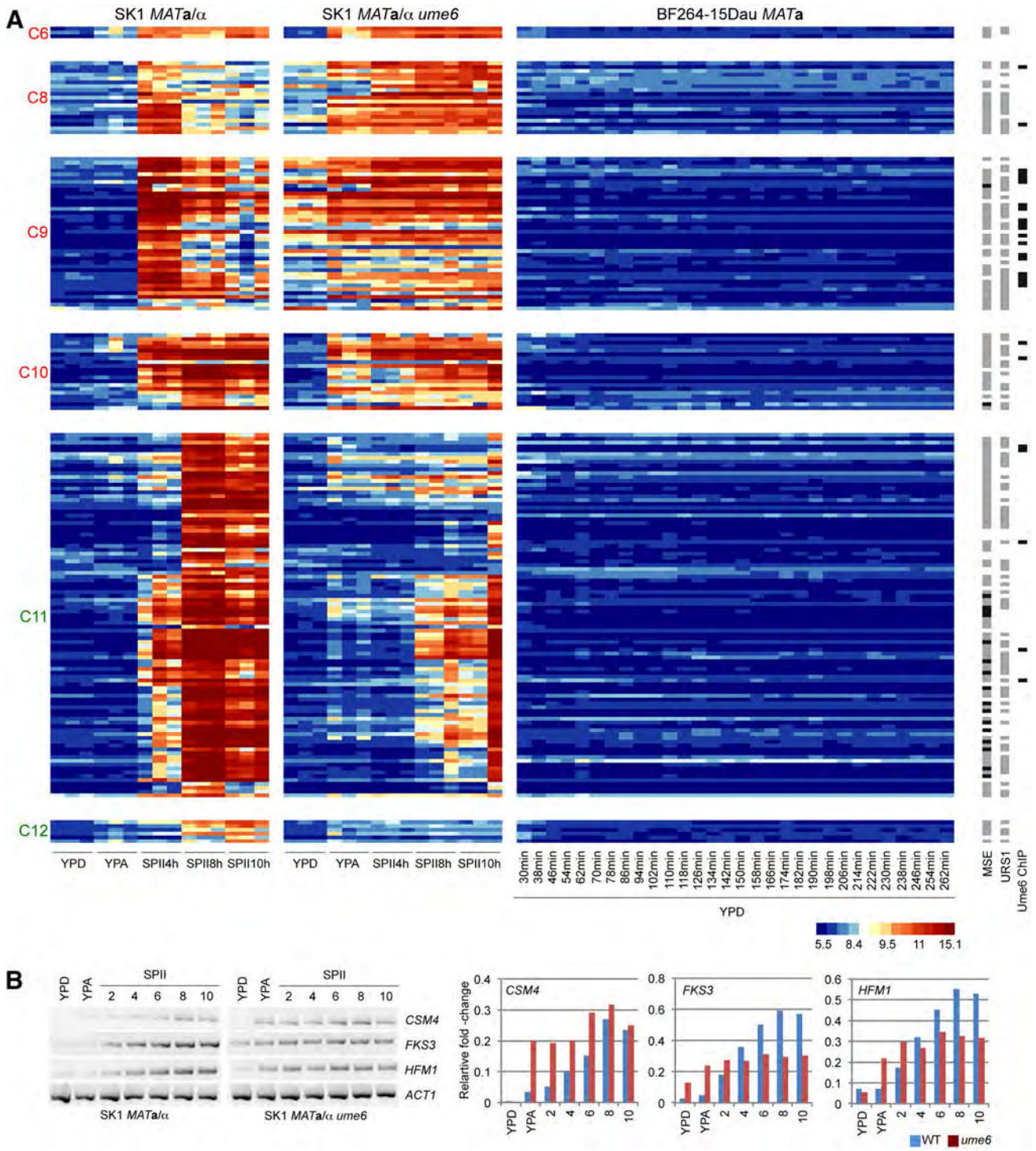

Fig. 5 Ume6-dependent genes not expressed in YPD. **a** A heatmap is shown like in Fig. 2. Clusters containing likely direct Ume6 target genes are given in *red*. Clusters containing indirectly Ume6-dependent genes are shown in *green*. *Strains* are indicated at the *top*. Predicted Ume6 (URS1) and Ndt80 (MSE) sites are shown in *gray* to the *right*, known MSEs are represented in *black*. *Black bars* indicate in vivo Ume6 binding (Ume6 ChIP) (Harbison et al. 2004). **b** The output of RT-PCR assays is shown for the target genes as indicated in samples cultured in rich medium (YPD), pre-sporulation medium (YPA), and sporulation medium (SPII) at the time points given. Wild-type (SK1 *MAT***a**/α) and mutant strains (SK1 *MAT***a**/α *ume6*) are shown at the *bottom*. The band intensities were quantified and shown in *color-coded* histograms where samples (*x*-axis) are plotted against the relative fold-change (*y*-axis). *Legends* indicate the target genes and the *color code* for the strains

Author's personal copy

Resource File S1). Members of the former group accumulate in YPD or YPA (or both) in the mutant, while those falling into the latter group typically fail to be induced in the mutant because of its meiotic arrest phenotype. Genes directly relevant for the phenotypes shown by *ume6*/*ume6* cells are therefore likely present in the first group (Davey et al. 2012; Shively et al. 2013; Costanzo et al. 2014).

C6 contains a gene important for respiration (*MOH1*), a Sin3 co-factor (*STB2*), and a gene that decreases sporulation efficiency when deleted and that promotes invasive growth when over-expressed (*LEE1*). In all three cases, the mRNA accumulates only in YPA and no Ume6 binding to their upstream region was detected in fermenting haploid cells (Harbison et al. 2004).

C8 notably contains three genes important for meiosis and spore formation (*CSM4*, *PCH2*, *RMD6*), and a gene involved in double-strand break repair (*RAD59*). The remaining genes are involved in cell division (*DOC1*, *IPL1*, *MPS2*), metabolic functions (*AHD7*, *ATG23*, *DAL1*, *GTT2*, *MCH2*, *PCD1*, *SRX1*, *SUL1*, *SUL2*), and stress response (*CIS1*). Two poorly characterized loci are implicated in vacuole morphology (*YLR173 W*) or induce invasive growth upon over-expression (*YKL071 W*).

C9 includes genes annotated as involved in metabolic functions (*DAL4*, *DAL80*, *HES1*, *MET16*, *PHO92*, *SRT1*), cell division and mating (*BNR1*, *TID3*), ribosome biogenesis (*RNP1*), and DNA repair (*BSC4*). Furthermore, it contains nearly all loci thought or known to be important for early meiotic functions such as formation of the synaptonemal complex (*ECM11*, *GMC2*, *HOP1*, *HOP2*, *ZIP1*, *ZIP2*), meiotic recombination (*DMC1*, *HFM1*, *REC8*, *REC102*, *REC114*, *SPO11*, *MEC1*, *MEI4*, *MEI5*, *MEK1*, *MND1*, *MSH4*), homolog pairing (*NDJ1*), meiosis and spore formation (*MPC54*, *SLZ1*, *SPO1*, *SPO13*, *SPO22*), meiotic splicing (*MER1*), and spore wall assembly (*FKS3*). Given their expression profiles in wild-type cells and the *ume6* mutant, three poorly characterized genes (*YKR005C*, *YBR184W*, *YOL131W*) are likely involved in stress response, metabolic functions, or developmental processes. Consistently, cells lacking *YKR005C* are sensitive to starvation and cells overexpressing the gene undergo invasive growth (Davey et al. 2012; Shively et al. 2013).

C10 comprises genes that accumulate only in *ume6* cells cultured in YPA but not YPD that are important for meiosis and spore formation (*AMA1*, *MAM1*, *CDA1*, *CDA2*, *CRR1*, *ECM8*), autophagy (*ATG4*), translation (*HEF3*), stress (*PAI3*, *SPG1*), and metabolism (*DCI1*, *DSF1*, *GIP2*, *PHM6*). Five poorly characterized genes are promising candidates for novel Ume6-dependent loci that play roles in cell growth and differentiation (*YEL057C*, *YGR153W*, *YJL045W*, *YKL107W*, *YPL119C-A*).

C11 and C12 are clusters of metabolic and sporulation genes that in nearly all cases depend upon Ume6 indirectly, since they are not (or only barely) de-repressed in dividing *ume6*/*ume6* cells and they fail to be induced in arrested mutant cells. These genes typically depend upon the transcriptional activator Ndt80 (which binds the Middle Sporulation Element, MSE). We note that C11 includes three DNA binding transcription factors, including Ndt80, known to be regulated by Ume6 (*GAT3*, *GAT4*, *NDT80*) (Pak and Segall 2002), a gene involved in spore wall assembly (*LDS1*) and a locus of unknown function (*YLR012C*), for which promoters are bound by Ume6 in vivo (Harbison et al. 2004). These results extend Ume6′s role in the comprehensive metabolic/stress/meiotic response of a diploid cell to an environmental stimulus triggering meiotic differentiation.

We next sought to validate the GeneChip expression data and selected three genes involved in chromosome segregation in meiosis (*CSM4*, Cluster 8), the control of spore wall formation via regulation of 1,3-β-glucan synthase (*FKS3*, Cluster 9), and a DNA helicase family member involved in meiotic recombination (*HFM1*, Cluster 9). In all cases, we find that RT-PCR assays of wild-type and *ume6* mutant samples cultured in growth media (YPD, YPA) and sporulation medium (SPII) reiterate the pattern obtained with GeneChips; *ACT1* was used as a loading control (Fig. 5b).

Ume6 target protein network interactions connect proteolysis, meiotic recombination, and nuclear division

We next used protein network data to explore the interactions among Ume6-dependent proteins shown in Fig. 5. The connected component (CC) shown in Fig. 6 links APC/C-dependent protein degradation (*DOC1*, cluster 8, encoding a co-factor involved in substrate recognition), meiotic recombination (*DMC1*, cluster 9, encoding a recombinase important for double-strand break repair), and the nuclear division cycle (*NDC80*, cluster 9, which codes for a component of the kinetochore-associated Ndc80 complex). This CC also highlights possible functions for two poorly characterized proteins (Ypl260w, Ylr456w) in meiotic cell division because they interact with Ndc80.

Network interactions identify hub proteins among Ume6 target genes that are relevant for the *ume6*/*ume6* mutant's growth and meiotic arrest phenotypes. These findings underline the usefulness of genomic data integration in providing leads for further experimentation exploring mechanisms of how Ume6-dependent epigenetic modifications coordinate different aspects of cell growth and development.

Discussion

We report a genome-wide mRNA-profiling study based on highly reliable Yeast Genome 2.0 GeneChip technology. Our

Author's personal copy

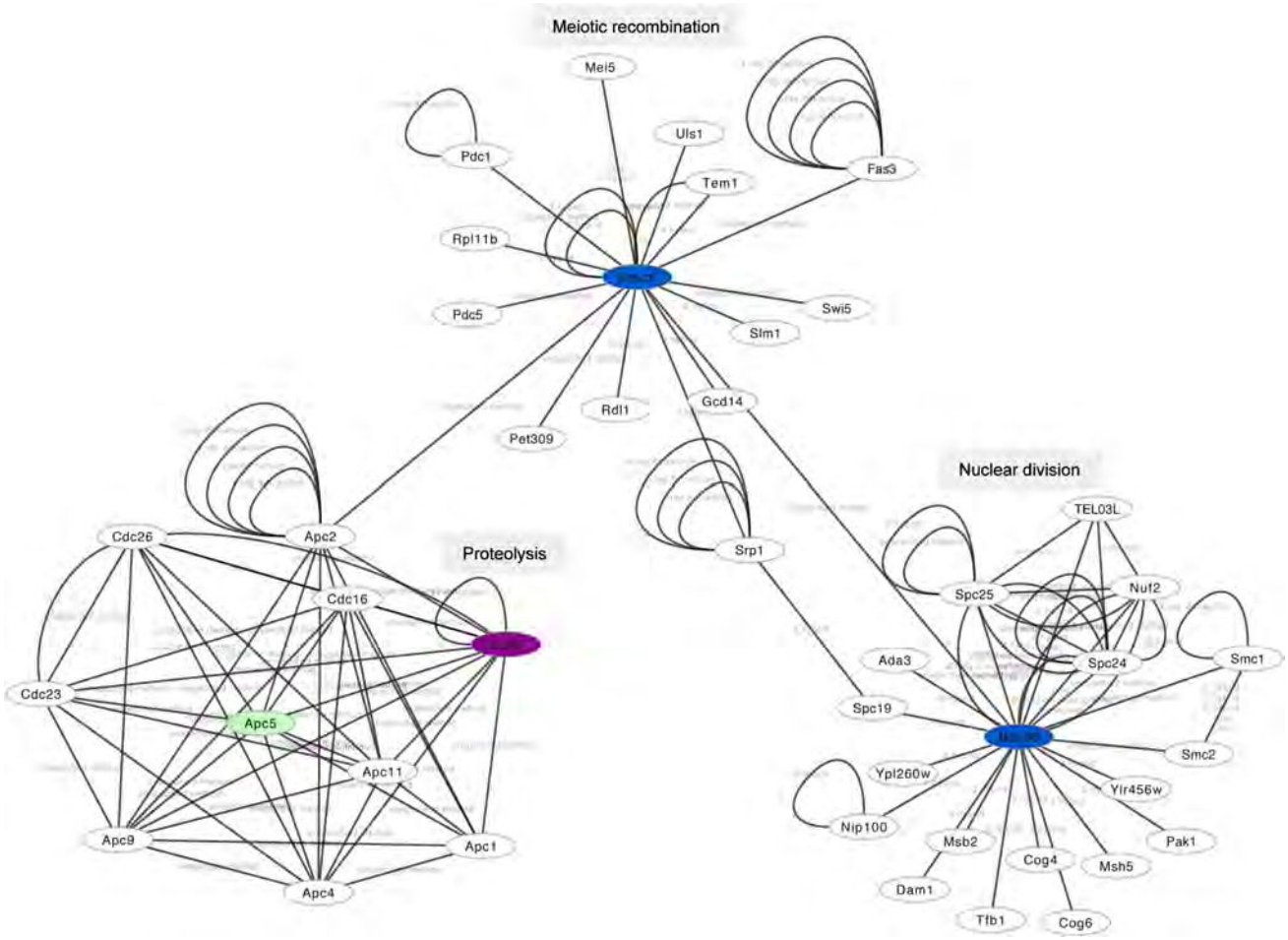

Fig. 6 Protein network interactions. A protein network view created with Cytoscape 3.2.0. is shown. Ume6 target proteins that are repressed in mitosis and that fall into cluster 8 and 9 are shown in *magenta* and *blue*, respectively. Apc5, shown in *green*, is among indirect targets. The network annotation data provided by BIND (see "Materials and methods") were manually edited for clarity. We note that some complexes refer to publications that report the interaction but do not provide information about the experimental approach used to detect it. Such cases are termed unspecified (interaction detection) method

work identified the transcriptome of mitosis and meiosis in the presence and absence of Ume6, which is the DNA binding subunit of chromatin modification enzymes important for normal cell growth and development. We identify direct Ume6 target genes by integrating GeneChip expression profiling data with predicted URS1 motifs and previously published large-scale Ume6-DNA binding data. Furthermore, we link consecutive waves of Ume6-controlled genes via protein network data. The present study therefore represents a rich source of genetic leads for further mechanistic work on elucidating the complex Ume6 gene deletion phenotype.

The usefulness of integrating expression profiling, in vivo protein/DNA binding, and motif predictions

In an earlier RNA profiling experiment using the first generation of Yeast GeneChips (Ye6100), we compared single samples of fermenting (YPD) and respiring (YPA) wild-type control strains to *ume6*/*ume6* mutants in the SK1 and W303 backgrounds; the minimal URS1 motif (5′-GGCGGC-3′ or 5′-CGGCGG-3′) was identified in the promoter regions by iterative scans of the intergenic sequences (Williams et al. 2002). The aim of this experiment was to identify a core set of strain- and carbon source-independent Ume6 target genes. While this previous study indeed identified reference genes repressed by Ume6 and a set of novel targets, it remained incomplete for several reasons. For example, single samples from each strain background rather than true replicates were analyzed, and the Ye6100 GeneChips used were based on very early (hence incomplete and partially erroneous) yeast genome annotation data (Goffeau et al. 1996). In addition, regulatory motif searches did not include information about DNA sequence conservation across related yeasts (Cliften et al.

Author's personal copy

2003; Kellis et al. 2003) and much less was known about gene function (Costanzo et al. 2014) or protein–protein interactions (Orchard et al. 2014). Finally, no data were available for synchronized mitotically diving cells (Orlando et al. 2008) and genome-wide in vivo Ume6/DNA binding patterns (Harbison et al. 2004).

The present study was designed to rectify these issues and thus identify the largest possible set of transcripts that statistically significantly depends on Ume6 (hence, its interactors such as Rpd3 and Isw2), in the strain background that is most relevant for analyses of growth and meiotic development (SK1). To distinguish direct from indirect targets, we used URS1 motif predictions and in vivo Ume6 DNA binding data. While our approach turned out to be efficient, some issues remain—such as incoherent data. For example, promoters were identified that are bound in vivo by Ume6, possess a URS1 motif, but the transcript expression level does not change in the mutant strain. We recently found an explanation for this phenomenon: many yeast loci encode multiple isoforms, only one of which is regulated by Ume6 (Lardenois et al. 2015; Liu et al. 2015; Stuparevic et al. 2015). Such cases cannot be identified with Yeast Genome 2.0 GeneChips because they cover only a small sequence within the target open reading frame's 3′-region. Other confounding factors include Ume6 binding sites other than the canonical URS1 motif (Sweet et al. 1997) or the ability of Ume6 to recruit factors onto promoters independently of its target motifs within three-dimensional chromatin structures (Yadon et al. 2010).

In general, distinct transcript levels obtained with microarrays are attributed to transcriptional effects (especially in the case of DNA binding transcription factors). However, mechanisms unrelated to mRNA synthesis can also influence signal intensities, such as changes in transcript half-life or elevated chromosomal instability resulting in multiple chromosomes in a mutant strain. In this context, we note that haploid *ume6* cells in W303 and S288C backgrounds are reported to contain two copies of chromosomes 9 and 16 (among other alterations) (Fazzio et al. 2001). We do not know if similar effects occur in diploid SK1 *ume6*/*ume6* cells but we cannot exclude the possibility. Therefore, RNA profiling data indicating 2-fold changes of transcript levels for genes located on chromosomes 9 and 16 should be interpreted with the caveat of polyploidy in mind. We note, in any case, that typical *bona fide* Ume6 target genes for which Ume6 binds a URS1 motif in vivo show higher than twofold changes and are therefore unlikely to be affected by the issue.

Why do cells lacking Ume6 fail to undergo meiosis?

It seems paradoxical that a transcriptional repressor whose destruction is required for meiotic progression should be essential for the process. A trivial explanation is that mutant cells have a growth phenotype that perturbs mitosis such that efficient entry into meiosis is not possible. Ume6 is indeed important for normal cell divisions and in the Σ1278b strain background it is even essential for growth (Strich et al. 1994, 2011; Suzuki et al. 2003). However, in our SK1 and JHY222 backgrounds and earlier work using W303, we did not observe a mitotic phenotype strong enough to explain the arrest of *ume6* mutant cells after pre-meiotic DNA replication (Williams et al. 2002). As in the case of the 3′-5′ exoribonuclease Rrp6, which is also degraded during meiotic M-phase and required for normal sporulation (Lardenois et al. 2015), it is likely the case that altered levels of proteins important for the transition between mitotic growth and meiotic development are at least partially responsible for the phenotype. For example, we observe that *COM2*, a negative regulator of *IME1* (Inducer of Meiosis 1), remains transcriptionally active in *ume6*/*ume6* cells cultured in sporulation medium (Kahana-Edwin et al. 2013). We also find that the DNA replication activator *CDC6* and the G1 cyclin *CLN3* (which promotes entry into the mitotic cell division cycle) fail to be transcriptionally down-regulated prior to entry into meiotic M-phase (Ofir et al. 2004; Shi and Tu 2013). It is, however, difficult to discern if this effect is the cause or the consequence of the *ume6*/*ume6* mutant's meiotic cell cycle arrest.

Fermenting and/or respiring cells that lack Ume6 derepress a number of genes that can interfere with normal mitotic growth when over-expressed, such as *ADY3*, *MAM1*, *NDJ1*, *RME1*, *RED1*, *SPO13,* and *SPS22* (McCarroll and Esposito 1994; Sopko et al. 2006; Varela et al. 2010). We do not know if all meiotic mRNAs are efficiently translated during mitotic growth like it is the case for *SPO13*; however, it is plausible that at least some of them are, and that the combined effects of several inhibitory proteins brings the mitosis–meiosis transition to a halt before mutant cells can enter meiotic M-phase. Another explanation might be the premature accumulation of developmental stage-specific proteins involved in meiotic recombination (e.g., *REC114*, *SPO11*, *DMC1*), formation of the synaptonemal complex (including *HOP1*, *HOP2*, *ZIP1*, *ZIP2*), and segregation of meiotic chromosomes (*CSM4*), which may trigger a checkpoint. While this remains speculative, we note that *NDC80*, encoding a protein involved in chromosome segregation and spindle checkpoint activity, and *PCH2*, encoding a component of the pachytene checkpoint, are induced in *ume6*/*ume6* cells cultured in growth media (see Saccharomyces Genome Database for gene annotation references, (Costanzo et al. 2014), GermOnline for expression data (Lardenois et al. 2010), Online Resource File S1).

Ume6 is tightly regulated at the level of protein stability by the APC/C when diploid cells switch from fermentation to respiration and then sporulation (Mallory et al. 2007, 2012; Law et al. 2014). Interestingly, we find that

Author's personal copy

DOC1, which is important for the APC/C's ability to recognize its substrates and to ubiquitinate them, is induced in cells lacking Ume6 (Online Resource File S1) (Carroll and Morgan 2002; Passmore et al. 2003). This points to a possible negative feedback loop mechanism between Ume6 and the APC/C, whereby Ume6 partially inhibits the APC/C by keeping *DOC1* expression low. As Ume6 levels diminish during the onset of meiosis, *DOC1* expression increases, which might accelerate Ume6 degradation.

Conclusion and outlook

Given that the budding yeast transcriptome comprises mRNAs, developmental stage-specific mRNA isoforms with extended 5′- and 3′-UTRs and long non-coding RNAs (lncRNAs), it seems reasonable to assume that Ume6 is not only important for the former two transcript categories, but also for RNAs with little or no coding potential (Cho et al. 1998; Chu et al. 1998; Primig et al. 2000; Wyers et al. 2005; Nagalakshmi et al. 2008; Xu et al. 2009; Lardenois et al. 2011, 2014; Kim Guisbert et al. 2012; Waern and Snyder 2013). Indeed, we have observed by RT-PCR assays that *ume6*/*ume6* and *rpd3*/*rpd3* mutant cells cultured in YPD and YPA accumulate a number of lncRNAs, such as meiotic unannotated transcripts (MUTs), cryptic unstable transcripts (CUTs), and stable unannotated transcripts (SUTs) to higher levels than the wild-type control strain (Y. Liu and B. Xie, unpublished). Genome-wide DNA strand-specific RNA profiling using RNA-Sequencing will answer the question to what extent lncRNAs are controlled by Ume6-dependent epigenetic mechanisms, and if their abnormal accumulation in mitotic cells contributes to the complex growth and developmental phenotype of *ume6*/*ume6* mutant cells.

Acknowledgments Michael Primig extends his special thanks to Rochelle Easton Esposito for her support, guidance, and mentorship during several years he spent with her as a postdoctoral researcher at the University of Chicago and as an assistant professor at the Biozentrum in Basel. We thank Olivier Collin and Olivier Sallou for GermOnline systems administration and Aaron Mitchell for the SK1 *MAT***a**/α *ume6*/*ume6* mutant strain. This work was supported by a Young Investigator fellowship from the Institut National de Santé et de Recherche Médicale (Inserm) awarded to A. Lardenois and an Inserm Avenir grant (R07216NS) awarded to M. Primig.

Conflict of interest The authors disclose no conflicts of interest.

Ethical standards The research does not involve human participants or animals.

References

Anderson SF, Steber CM et al (1995) UME6, a negative regulator of meiosis in *Saccharomyces cerevisiae*, contains a C-terminal Zn2Cys6 binuclear cluster that binds the URS1 DNA sequence in a zinc-dependent manner. Protein Sci 4(9):1832–1843. doi:10.1002/pro.5560040918

Banerjee M, Uppuluri P et al (2013) Expression of UME6, a key regulator of Candida albicans hyphal development, enhances biofilm formation via Hgc1- and Sun41-dependent mechanisms. Eukaryot Cell 12(2):224–232. doi:10.1128/EC.00163-12

Bartholomew CR, Suzuki T et al (2012) Ume6 transcription factor is part of a signaling cascade that regulates autophagy. Proc Natl Acad Sci USA 109(28):11206–11210. doi:10.1073/pnas.1200313109

Baryshnikova A, Costanzo M et al (2010) Synthetic genetic array (SGA) analysis in *Saccharomyces cerevisiae* and *Schizosaccharomyces* pombe. Methods Enzymol 470:145–179. doi:10.1016/S0076-6879(10)70007-0

Carlisle PL, Kadosh D (2010) Candida albicans Ume6, a filament-specific transcriptional regulator, directs hyphal growth via a pathway involving Hgc1 cyclin-related protein. Eukaryot Cell 9(9):1320–1328. doi:10.1128/EC.00046-10

Carlisle PL, Banerjee M et al (2009) Expression levels of a filament-specific transcriptional regulator are sufficient to determine Candida albicans morphology and virulence. Proc Natl Acad Sci USA 106(2):599–604. doi:10.1073/pnas.0804061106

Carroll CW, Morgan DO (2002) The Doc1 subunit is a processivity factor for the anaphase-promoting complex. Nat Cell Biol 4(11):880–887. doi:10.1038/ncb871

Chalmel F, Rolland AD et al (2007) The conserved transcriptome in human and rodent male gametogenesis. Proc Natl Acad Sci USA 104(20):8346–8351

Childers DS, Mundodi V et al (2014) A 5′ UTR-mediated translational efficiency mechanism inhibits the Candida albicans morphological transition. Mol Microbiol 92(3):570–585. doi:10.1111/mmi.12576

Cho RJ, Campbell MJ et al (1998) A genome-wide transcriptional analysis of the mitotic cell cycle. Mol Cell 2(1):65–73

Chu S, DeRisi J et al (1998) The transcriptional program of sporulation in budding yeast. Science 282(5389):699–705

Cliften P, Sudarsanam P et al (2003) Finding functional features in Saccharomyces genomes by phylogenetic footprinting. Science 301(5629):71–76

Costanzo MC, Engel SR et al (2014) Saccharomyces genome database provides new regulation data. Nucleic Acids Res 42(Database issue):D717–D725. doi:10.1093/nar/gkt1158

da Huang W, Sherman BT et al (2009) Systematic and integrative analysis of large gene lists using DAVID bioinformatics resources. Nat Protoc 4(1):44–57. doi:10.1038/nprot.2008.211

Davey HM, Cross EJ et al (2012) Genome-wide analysis of longevity in nutrient-deprived *Saccharomyces cerevisiae* reveals importance of recycling in maintaining cell viability. Environ Microbiol 14(5):1249–1260. doi:10.1111/j.1462-2920.2012.02705.x

de Lichtenberg U, Jensen LJ et al (2005) Dynamic complex formation during the yeast cell cycle. Science 307(5710):724–727. doi:10.1126/science.1105103

Fazzio TG, Kooperberg C et al (2001) Widespread collaboration of Isw2 and Sin3-Rpd3 chromatin remodeling complexes in transcriptional repression. Mol Cell Biol 21(19):6450–6460

Gene Ontology C (2015) Gene ontology consortium: going forward. Nucleic Acids Res 43(Database issue):D1049–D1056. doi:10.1093/nar/gku1179

Goffeau A, Barrell BG et al (1996) Life with 6000 genes. Science 274(5287):546, 563–567

Goldmark JP, Fazzio TG et al (2000) The Isw2 chromatin remodeling complex represses early meiotic genes upon recruitment by Ume6p. Cell 103(3):423–433

Harbison CT, Gordon DB et al (2004) Transcriptional regulatory code of a eukaryotic genome. Nature 431(7004):99–104

Author's personal copy

Hillenmeyer ME, Fung E et al (2008) The chemical genomic portrait of yeast: uncovering a phenotype for all genes. Science 320(5874):362–365

Huntley RP, Sawford T et al (2014) The GOA database: gene ontology annotation updates for 2015. Nucleic Acids Res. doi:10.1093/nar/gku1113

Isserlin R, El-Badrawi RA et al (2011) The biomolecular interaction network database in PSI-MI 2.5. Database (Oxford) 2011: baq037. doi:10.1093/database/baq037

Kadosh D, Struhl K (1997) Repression by Ume6 involves recruitment of a complex containing Sin3 corepressor and Rpd3 histone deacetylase to target promoters. Cell 89(3):365–371

Kahana-Edwin S, Stark M et al (2013) Multiple MAPK cascades regulate the transcription of IME1, the master transcriptional activator of meiosis in Saccharomyces cerevisiae. PLoS One 8(11):e78920. doi:10.1371/journal.pone.0078920

Kassir Y, Adir N et al (2003) Transcriptional regulation of meiosis in budding yeast. Int Rev Cytol 224:111–171

Kellis M, Patterson N et al (2003) Sequencing and comparison of yeast species to identify genes and regulatory elements. Nature 423(6937):241–254

Kim Guisbert KS, Zhang Y et al (2012) Meiosis-induced alterations in transcript architecture and noncoding RNA expression in *S. cerevisiae*. RNA 18(6):1142–1153. doi:10.1261/rna.030510.111

Kratzer S, Schuller HJ (1997) Transcriptional control of the yeast acetyl-CoA synthetase gene, ACS1, by the positive regulators CAT8 and ADR1 and the pleiotropic repressor UME6. Mol Microbiol 26(4):631–641

Kurdistani SK, Robyr D et al (2002) Genome-wide binding map of the histone deacetylase Rpd3 in yeast. Nat Genet 31(3):248–254

Lardenois A, Gattiker A et al (2010) GermOnline 4.0 is a genomics gateway for germline development, meiosis and the mitotic cell cycle. Database: the journal of biological databases and curation 2010: baq030. doi:10.1093/database/baq030

Lardenois A, Liu Y et al (2011) Execution of the meiotic noncoding RNA expression program and the onset of gametogenesis in yeast require the conserved exosome subunit Rrp6. Proc Natl Acad Sci USA 108(3):1058–1063. doi:10.1073/pnas.1016459108

Lardenois A, Stuparevic I et al (2015) The conserved histone deacetylase Rpd3 and its DNA binding subunit Ume6 control dynamic transcript architecture during mitotic growth and meiotic development. Nucleic Acids Res 43(1):115–128. doi:10.1093/nar/gku1185

Law MJ, Mallory MJ et al (2014) Acetylation of the transcriptional repressor Ume6p allows efficient promoter release and timely induction of the meiotic transient transcription program in yeast. Mol Cell Biol 34(4):631–642. doi:10.1128/MCB.00256-13

Liu Y, Stuparevic I et al (2015) The conserved histone deacetylase Rpd3 and the DNA binding regulator Ume6 repress BOI1′s meiotic transcript isoform during vegetative growth in Saccharomyces cerevisiae. Mol Microbiol. doi:10.1111/mmi.12976

Mallory MJ, Cooper KF et al (2007) Meiosis-specific destruction of the Ume6p repressor by the Cdc20-directed APC/C. Mol Cell 27(6):951–961

Mallory MJ, Law MJ et al (2012) Gcn5p-dependent acetylation induces degradation of the meiotic transcriptional repressor Ume6p. Mol Biol Cell 23(9):1609–1617. doi:10.1091/mbc.E11-06-0536

McCarroll RM, Esposito RE (1994) SPO13 negatively regulates the progression of mitotic and meiotic nuclear division in Saccharomyces cerevisiae. Genetics 138(1):47–60

Messenguy F, Vierendeels F et al (2000) In Saccharomyces cerevisiae, expression of arginine catabolic genes CAR1 and CAR2 in response to exogenous nitrogen availability is mediated by the Ume6 (CargRI)-Sin3 (CargRII)-Rpd3 (CargRIII) complex. J Bacteriol 182(11):3158–3164

Michaillat L, Mayer A (2013) Identification of genes affecting vacuole membrane fragmentation in Saccharomyces cerevisiae. PLoS One 8(2):e54160. doi:10.1371/journal.pone.0054160

Mitchell AP (1994) Control of meiotic gene expression in Saccharomyces cerevisiae. Microbiol Rev 58(1):56–70

Nagalakshmi U, Wang Z et al (2008) The transcriptional landscape of the yeast genome defined by RNA sequencing. Science 320(5881):1344–1349

Ngounou Wetie AG, Sokolowska I et al (2014) Protein-protein interactions: switch from classical methods to proteomics and bioinformatics-based approaches. Cellular and molecular life sciences : CMLS 71(2):205–228. doi:10.1007/s00018-013-1333-1

Nookaew I, Papini M et al (2012) A comprehensive comparison of RNA-Seq-based transcriptome analysis from reads to differential gene expression and cross-comparison with microarrays: a case study in Saccharomyces cerevisiae. Nucleic Acids Res 40(20):10084–10097. doi:10.1093/nar/gks804

O'Connor L, Caplice N et al (2010) Differential filamentation of Candida albicans and Candida dubliniensis Is governed by nutrient regulation of UME6 expression. Eukaryot Cell 9(9):1383–1397. doi:10.1128/EC.00042-10

Ofir Y, Sagee S et al (2004) The role and regulation of the preRC component Cdc6 in the initiation of premeiotic DNA replication. Mol Biol Cell 15(5):2230–2242. doi:10.1091/mbc.E03-08-0617

Orchard S, Ammari M et al (2014) The MIntAct project—IntAct as a common curation platform for 11 molecular interaction databases. Nucleic Acids Res 42(Database issue):D358–D363. doi:10.1093/nar/gkt1115

Orenstein Y, Linhart C et al (2012) Assessment of algorithms for inferring positional weight matrix motifs of transcription factor binding sites using protein binding microarray data. PLoS One 7(9):e46145. doi:10.1371/journal.pone.0046145

Orlando DA, Lin CY et al (2008) Global control of cell-cycle transcription by coupled CDK and network oscillators. Nature 453(7197):944–947

Pak J, Segall J (2002) Regulation of the premiddle and middle phases of expression of the NDT80 gene during sporulation of *Saccharomyces cerevisiae*. Mol Cell Biol 22(18):6417–6429

Park HD, Luche RM et al (1992) The yeast UME6 gene product is required for transcriptional repression mediated by the CAR1 URS1 repressor binding site. Nucleic Acids Res 20(8):1909–1915

Passmore LA, McCormack EA et al (2003) Doc1 mediates the activity of the anaphase-promoting complex by contributing to substrate recognition. EMBO J 22(4):786–796. doi:10.1093/emboj/cdg084

Primig M, Williams RM et al (2000) The core meiotic transcriptome in budding yeasts. Nat Genet 26(4):415–423

Prinz S, Avila-Campillo I et al (2004) Control of yeast filamentous-form growth by modules in an integrated molecular network. Genome Res 14(3):380–390. doi:10.1101/gr.2020604

Rundlett SE, Carmen AA et al (1998) Transcriptional repression by UME6 involves deacetylation of lysine 5 of histone H4 by RPD3. Nature 392(6678):831–835. doi:10.1038/33952

Rustici G, Kolesnikov N et al (2013) ArrayExpress update–trends in database growth and links to data analysis tools. Nucleic Acids Res 41(Database issue):D987–D990. doi:10.1093/nar/gks1174

Saito R, Smoot ME et al (2012) A travel guide to Cytoscape plugins. Nat Methods 9(11):1069–1076. doi:10.1038/nmeth.2212

Shi L, Tu BP (2013) Acetyl-CoA induces transcription of the key G1 cyclin CLN3 to promote entry into the cell division cycle in Saccharomyces cerevisiae. Proc Natl Acad Sci USA 110(18):7318–7323. doi:10.1073/pnas.1302490110

Shively CA, Eckwahl MJ et al (2013) Genetic networks inducing invasive growth in *Saccharomyces cerevisiae* identified through systematic genome-wide overexpression. Genetics 193(4):1297–1310. doi:10.1534/genetics.112.147876

Author's personal copy

Sopko R, Huang D et al (2006) Mapping pathways and phenotypes by systematic gene overexpression. Mol Cell 21(3):319–330. doi:10.1016/j.molcel.2005.12.011

Spivak AT, Stormo GD (2012) ScerTF: a comprehensive database of benchmarked position weight matrices for Saccharomyces species. Nucleic Acids Res 40(Database issue):D162–D168. doi:10.1093/nar/gkr1180

Strich R, Slater MR et al (1989) Identification of negative regulatory genes that govern the expression of early meiotic genes in yeast. Proc Natl Acad Sci USA 86(24):10018–10022

Strich R, Surosky RT et al (1994) UME6 is a key regulator of nitrogen repression and meiotic development. Genes Dev 8(7):796–810

Strich R, Khakhina S et al (2011) Ume6p is required for germination and early colony development of yeast ascospores. FEMS Yeast Res 11(1):104–113. doi:10.1111/j.1567-1364.2010.00696.x

Stuparevic I, Becker E et al (2015) The histone deacetylase Rpd3/Sin3/Ume6 complex represses an acetate-inducible isoform of VTH2 in fermenting budding yeast cells. FEBS Lett. doi:10.1016/j.febslet.2015.02.022

Suzuki C, Hori Y et al (2003) Screening and characterization of transposon-insertion mutants in a pseudohyphal strain of Saccharomyces cerevisiae. Yeast 20(5):407–415

Sweet DH, Jang YK et al (1997) Role of UME6 in transcriptional regulation of a DNA repair gene in Saccharomyces cerevisiae. Mol Cell Biol 17(11):6223–6235

Tsukada M, Ohsumi Y (1993) Isolation and characterization of autophagy-defective mutants of Saccharomyces cerevisiae. FEBS Lett 333(1–2):169–174

Varela E, Schlecht U et al (2010) Mitotic expression of Spo13 alters M-phase progression and nucleolar localization of Cdc14 in budding yeast. Genetics 185(3):841–854. doi:10.1534/genetics.109.113746

Waern K, Snyder M (2013) Extensive transcript diversity and novel upstream open reading frame regulation in yeast. G3 (Bethesda) 3(2):343–352. doi:10.1534/g3.112.003640

Williams RM, Primig M et al (2002) The Ume6 regulon coordinates metabolic and meiotic gene expression in yeast. Proc Natl Acad Sci USA 99(21):13431–13436

Wingender E (2008) The TRANSFAC project as an example of framework technology that supports the analysis of genomic regulation. Brief Bioinform 9(4):326–332. doi:10.1093/bib/bbn016

Wyers F, Rougemaille M et al (2005) Cryptic pol II transcripts are degraded by a nuclear quality control pathway involving a new poly(A) polymerase. Cell 121(5):725–737. doi:10.1016/j.cell.2005.04.030

Xu Z, Wei W et al (2009) Bidirectional promoters generate pervasive transcription in yeast. Nature 457(7232):1033–1037. doi:10.1038/nature07728

Yadon AN, Van de Mark D et al (2010) Chromatin remodeling around nucleosome-free regions leads to repression of noncoding RNA transcription. Mol Cell Biol 30(21):5110–5122. doi:10.1128/MCB.00602-10

Yoshikawa K, Tanaka T et al (2011) Comprehensive phenotypic analysis of single-gene deletion and overexpression strains of *Saccharomyces cerevisiae*. Yeast 28(5):349–361. doi:10.1002/yea.1843

Zeidler U, Lettner T et al (2009) UME6 is a crucial downstream target of other transcriptional regulators of true hyphal development in Candida albicans. FEMS Yeast Res 9(1):126–142. doi:10.1111/j.1567-1364.2008.00459.x

11. Regulatory mechanisms governing developmental stage specific transcript isoform expression

1) ORC1: Xie et al., RNA Biol 2016

RNA BIOLOGY
2016, VOL. 13, NO. 9, 772–782
http://dx.doi.org/10.1080/15476286.2016.1191738

Taylor & Francis
Taylor & Francis Group

RESEARCH PAPER

Ndt80 activates the meiotic *ORC1* transcript isoform and *SMA2* via a bi-directional middle sporulation element in *Saccharomyces cerevisiae*

Bingning Xie[a], Joe Horecka[b], Angela Chu[b], Ronald W. Davis[b,c], Emmanuelle Becker[a], and Michael Primig[a]

[a]Inserm U1085 IRSET, Université de Rennes 1, Rennes, France; [b]Stanford Genome Technology Center, Palo Alto, CA, USA; [c]Departments of Biochemistry and Genetics, Stanford University, Stanford, CA, USA

ABSTRACT

The origin of replication complex subunit *ORC1* is important for DNA replication. The gene is known to encode a meiotic transcript isoform (*mORC1*) with an extended 5′-untranslated region (5′-UTR), which was predicted to inhibit protein translation. However, the regulatory mechanism that controls the m*ORC1* transcript isoform is unknown and no molecular biological evidence for a role of *mORC1* in negatively regulating Orc1 protein during gametogenesis is available. By interpreting RNA profiling data obtained with growing and sporulating diploid cells, mitotic haploid cells, and a starving diploid control strain, we determined that m*ORC1* is a middle meiotic transcript isoform. Regulatory motif predictions and genetic experiments reveal that the activator Ndt80 and its middle sporulation element (MSE) target motif are required for the full induction of *mORC1* and the divergently transcribed meiotic *SMA2* locus. Furthermore, we find that the MSE-binding negative regulator Sum1 represses both *mORC1* and *SMA2* during mitotic growth. Finally, we demonstrate that an MSE deletion strain, which cannot induce *mORC1*, contains abnormally high Orc1 levels during post-meiotic stages of gametogenesis. Our results reveal the regulatory mechanism that controls *mORC1*, highlighting a novel developmental stage-specific role for the MSE element in bi-directional *mORC1*/*SMA2* gene activation, and correlating *mORC1* induction with declining Orc1 protein levels. Because eukaryotic genes frequently encode multiple transcripts possessing 5′-UTRs of variable length, our results are likely relevant for gene expression during development and disease in higher eukaryotes.

ARTICLE HISTORY
Received 8 April 2016
Revised 12 May 2016
Accepted 13 May 2016

KEYWORDS
Bi-directional promoter; MSE; meiosis; *NDT80*; *ORC1*; *SUM1*; *SMA2*; sporulation; isoform; 5′-UTR

Introduction

DNA replication in budding yeast is a multi-step process initiated by the origin of replication binding complex (ORC), which includes 6 subunits.[1] *ORC1* encodes a conserved ATPase essential for the mitotic cell cycle.[2,3] While Orc1 functions during pre-meiotic DNA replication and protects repetitive ribosomal DNA (rDNA) sequences from becoming unstable during meiotic recombination, no role is known for the protein during middle and late stages of meiosis and spore formation.[4] The mitotic isoform of *ORC1* is divergently expressed with the long non-coding RNA *XUT1538*, which belongs to a class of regulatory lncRNAs that are targeted by the cytoplasmic 5′–3′ exoribonuclease Xrn1.[5] Paradoxically, *ORC1* expression is strongly induced in diploid cells that enter meiotic M-phase,[6,7] and this induction pattern coincides with the transcriptional activation of divergently expressed meiosis-specific *SMA2*. This gene is important for the spore membrane pathway that ensures proper encapsulation of haploid nuclei into spores.[8-10] Bi-directional transcription patterns, which may involve pairs of mRNAs, long non-coding RNAs (lncRNAs) or a combination of both, have been described as an intrinsic property of yeast promoters, but the regulatory mechanisms underlying this phenomenon are often not understood. [9,11,12]

An earlier RNA- and ribosome profiling study of yeast sporulation reported that *ORC1* encodes a meiotic isoform with an extended 5′-untranslated region (UTR) that was predicted to inhibit Orc1 translation during post-meiotic stages of spore development *via* upstream open reading frames (uORFs).[13] However, Orc1 protein levels during meiosis and gametogenesis have not been determined, and the transcription factors that control the expression of m*ORC1* during growth and development are unknown.

Meiotic M-phase requires middle genes that are specific for the process and genes that function during mitosis and meiosis. The transcriptional activator Ndt80 induces both types of genes *via* direct interaction with MSEs,[14] while Sum1 represses meiosis-specific genes, including *NDT80*,[15] during vegetative growth either alone or by recruiting the histone deacetylase Hst1 to a sequence motif that overlaps certain MSEs.[16,17] *NDT80* is transcriptionally activated during meiotic prophase I in a 2-step process, whereby the gene is first de-repressed prior to meiotic M-phase I, when Ume6 and Sum1 activities are progressively down-regulated, and then strongly induced *via* an auto-activating loop when cells trigger the meiotic divisions;[18] reviewed in.[19] Ndt80 target promoters were identified in a large-scale *in vivo* protein-DNA binding assay of samples from sporulating cells.[20] This experiment, together with position weight matrices (PWMs), which represent patterns such as transcription

CONTACT Michael Primig michael.primig@inserm.fr Inserm U1085 IRSET, 9 ave du Professeur Léon Bernard, Rennes, France
Supplemental data for this article can be accessed on the publisher's website.
© 2016 Taylor & Francis Group, LLC

factor target motifs in DNA sequences, identified genes that are likely regulated by Ndt80.[21,22]

In this study we report that cells switch to a long *ORC1* transcript isoform containing an extended 5′-UTR (*mORC1*) prior to entry into meiotic M-phase, while starvation alone fails to induce this transcript. Importantly, we show that in meiosis Ndt80 directly activates *mORC1* together with the divergently expressed *SMA2* locus *via* its bi-directional MSE target motif, while Sum1 acts as a mitotic repressor for both transcripts. Finally, we demonstrate that Orc1 protein becomes undetectable when cells finish pre-meiotic DNA replication and start expressing *mORC1*, while Orc1 remains detectable in an MSE deletion mutant that fails to induce the long isoform. These findings agree with large-scale ribosome profiling data.[13] Our data suggest a novel role for the Ndt80 activator in yeast meiosis, which is to down-regulate Orc1 protein via induction of an untranslatable transcript isoform. The results therefore highlight an interesting regulatory design that enables an activator to repress a target gene product during eukaryotic cell differentiation.

Results

Datasets and experimental rationale

In earlier work, we used tiling arrays to determine the transcriptome of diploid budding yeast during fermentation, respiration and sporulation in comparison to vegetative growth of haploid cells.[9,23,24] Initially, we focused on meiotic lncRNAs and later on developmentally regulated transcript isoforms with extended 5′-UTRs. Published tiling array data are available at the ReproGenomics Viewer (RGV, rgv.genouest.org; Fig. S1[25]) and the Saccharomyces Genomics Viewer (SGV, sgv.genouest.org[26]). Furthermore, we interpreted DNA strand-specific RNA-Sequencing data from mitotically growing haploid and diploid wild type versus *xrn1* mutant cells in S288C, W303 and SK1 strain backgrounds,[5] and our unpublished RNA-Sequencing data (not DNA strand-specific) from *MAT***a**/*α* and *MATα*/*α* cells cultured in YPD, YPA and SPII media (E. Becker, M. H. Guilleux, K. Waern, M. Snyder and M. Primig et al., in preparation).

The 5′-UTR expression analysis by Lardenois, Liu *et al.* included a non-exhaustive list of early, middle and late transcript isoforms, which lacked the meiotic isoform *mORC1* because the segmentation algorithm used to analyze tiling array data failed to detect it.[9,23] The *ORC1* locus is, however, an interesting case: its mRNA is cell cycle regulated in mitotically growing cells and strongly induced during meiotic development, although the the protein it encodes is *a priori* dispensable after pre-meiotic DNA replication is finished.

Diploid yeast cells express divergent ORC1/XUT1538 transcripts in mitosis and mORC1/SMA2 only in meiosis but not starvation

Diploid cells growing asynchronously in the presence of glucose (YPD) or acetate (YPA) and synchronized haploid cells undergoing a full mitotic cell cycle express only the mitotic *ORC1* transcript isoform (to which we also refer as the short isoform; Fig. 1A), while the 5′-extended *mORC1* isoform is undetectable. We also observed a faint signal corresponding to what appeared to be an lncRNA divergently expressed from the *ORC1* promoter. In fact, this RNA turned out to be the Xrn1-sensitive unstable transcript *XUT1538*.[5] We note that the activity of Xrn1 is strong in S288C and W303 but attenuated in SK1 (Fig. 1B). This indicates that the *ORC1* promoter is bidirectional during vegetative growth.

*MAT***a**/*α* cells cultured in sporulation medium (SPII) induce *mORC1* when they exit pre-meiotic DNA replication and enter M-phase. This coincides with the transcriptional onset of divergently expressed *SMA2*, which overlaps the constitutively expressed antisense lncRNA *SUT292* (Fig. 1C). A Northern blot by Brar et al. 2012 suggests that SK1 cells exclusively express the short *ORC1* transcript isoform during vegetative growth and pre-meiotic DNA replication when Orc1 is needed. Critically, at the onset of meiotic M-phase approximately 6 hours after transfer into sporulation medium, cells completely switch to expressing the long transcript isoform. Note that the meiotic isoform has the size predicted for a full-length *ORC1* transcript with a 5′-extended UTR (see Fig. 5C in reference[13]). Genomics data thus reveal a complex regulatory pattern involving 5 transcripts: haploid and diploid cells undergoing mitotic growth express *SUT292* and divergent *ORC1*/*XUT1538* transcripts downstream of it, while middle meiotic cells continue to express *SUT292* but co-induce divergent *mORC1*/*SMA2* transcripts *via* a developmentally regulated bi-directional promoter element (Fig. 1D).

We have previously reported that early and middle meiotic isoforms are not induced by starvation alone, since they typically do not accumulate to normal (or even detectable) levels in sporulation-deficient *MATα*/*α* control cells.[23] In the case of *ORC1*, tiling array data and RNA-Sequencing data from starving SK1 *MATα*/*α* cells cultured in sporulation medium indicate that they do not induce the long isoform. We conclude that *mORC1*'s transcriptional activation or its stability (or both) depend on meiosis (Fig. 2A, B).

Divergent promoters driving isoforms pair them with ubiquitous transcripts or developmentally stage-specific mRNAs

We find that the expression of *mORC1/SMA2* during gametogenesis is likely not an isolated case. Further examples include *ORC3/SPO75* (which overlaps antisense *MMM1*), *PEX32/POP7* (which overlaps antisense CUT028), *PCM1/SOM1* (for which *mSOM1* overlaps antisense *HHY1*) and *IWR1/YDL114W*; see sgv.genouest.org, rgv.genouest.org and the Yeast Promoter Atlas at ypa.csbb.ntu.edu.tw/.[27] Meiotic *IWR1 (mIWR1)* is not detectable by tiling arrays in haploid cycling cells (Fig. S2A top and bottom panels). The tiling array data indicate the presence of an unknown weakly expressed SUT-type antisense transcript that overlaps *IWR1*; however, the function of this transcript, if it has any at all, is presently unclear. High-throughput data for *mIWR1, IWR1* and *YDL114W* obtained with SK1 are reproduced by RT-PCR assays using samples from the distantly related strain JHY222 (which is derived from the standard background S288C[9,28]), indicating that the phenomenon is not strain-specific but generally occurs in budding yeast (Fig. S2B). We note that *mIWR1* accumulates to lower levels than *YDL114W*, which may reflect distinct RNA synthesis rates or decay rates. These results concur with the finding that yeast promoters are intrinsically bi-directional.[11,12]

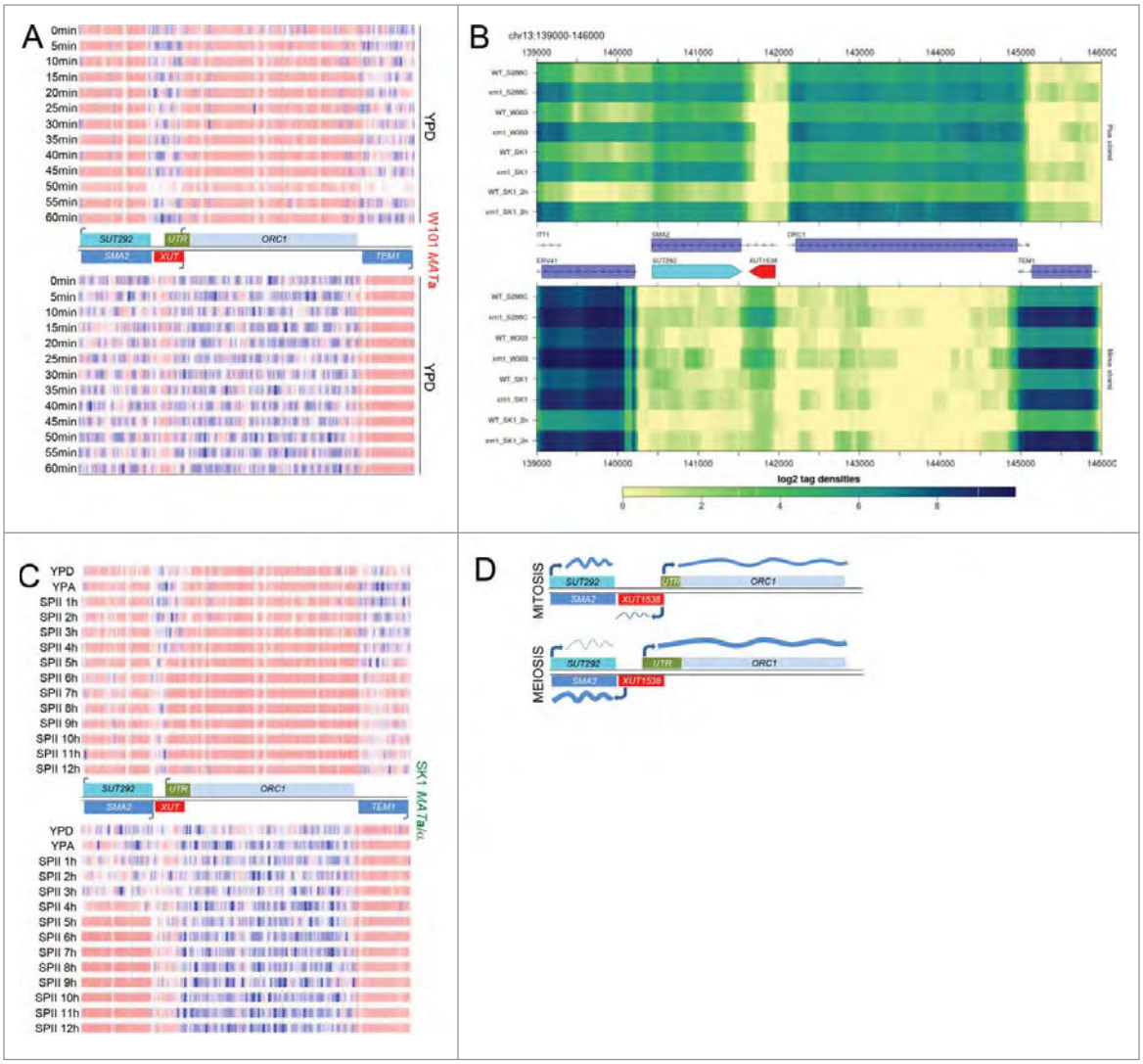

Figure 1. *ORC1* isoform expression during growth and differentiation. (A) Color-coded heatmaps generated with RGV version 1.0, show DNA strand-specific Sc_tlg tiling array expression data ordered in rows for samples and columns for each oligonucleotide probe (blue is low, red is high; bicolor pivot 3.9 on the log scale). The strain background is shown to the right in red, time points are given in minutes to the left. A schematic represents the loci (shades of blue for ORFs and SUT, green for the UTR, and red for XUT) on both DNA strands (black lines). Arrows indicate transcription start sites. Note that the data shown, which cover one mitotic cycle, are part of a larger experiment reported in reference.[24] (B) A heatmap shows RNA-Sequencing data for 3 wild type strains (WT S288C, W303 and SK1) and corresponding strains lacking Xrn1 activity (xrn1) given to the left. All strains are haploid unless their DNA content is indicated (2n). Cells were cultured in YPD. The complete dataset was reported in reference.[5] (C) A heatmap like in panel A shows samples from diploid wild type cells cultured in rich media (YPD, YPA) and sporulation medium (SPII) taken at the time points indicated in hours (h). The strain is indicated to the right in green. Genome-wide data are from reference.[9] (D) A schematic summarizes the mitotic (top) and meiotic (bottom) expression profiles of *SMA2* and *ORC1* (dark and light blue rectangles, respectively) and the lncRNAs *SUT292* and XUT1538 (blue and red rectangles). Transcripts are shown as wavy blue lines. Black lines represent the top and bottom DNA strands. Arrows indicate transcription start sites.

mORC1/SMA2 repression in mitosis requires Sum1 while their full induction in meiosis depends on Ndt80

A search for regulatory motifs in the *ORC1* promoter region identified an MSE immediately upstream of *mORC1* (Fig. 3A, B). Given the base composition of m*ORC1*s MSE it is likely bound by the meiotic activator Ndt80 and the mitotic repressor Sum1, which is consistent with *ORC1* transcript isoform's middle meiosis-specific expression pattern (Fig. 3C).[17]

We next sought to prove that the predicted promoter element is indeed biologically active. To this end, we first designed combinations of oligonucleotide primers for RT-PCR assays to validate tiling array data and RNA-Seq data in wild type cells, and to study the expression of mitotic and meiotic isoforms encoded by *ORC1* in the absence of the Ndt80 activator and *Sum1* repressor. None of the gene deletions affected the mitotic isoform in JHY222 cells cultured in rich media (YPD, YPA) and sporulation medium (SPII) at bi-hourly time points (2h-10h) (Fig. 4A). To the contrary, we found that *mORC1* was moderately de-repressed in *sum1* cells cultured in rich medium (YPD) and sporulation medium (SPII), while it was nearly undetectable in *ndt80* mutant cells cultured in rich media and sporulation medium under the conditions used (Fig. 4A). We next assayed the divergently transcribed *SMA2* gene and found a broadly similar induction pattern in JHY222 wild type cells as compared to tiling array data obtained in the SK1 background (Fig. 4B). As expected, *SMA2* mRNA did not accumulate to normal meiotic levels in the absence of *NDT80* and was elevated in *sum1* mutant cells cultured in growth, pre-sporulation, and sporulation media (Fig. 4B). These results are consistent with a role for Ndt80 and Sum1 in

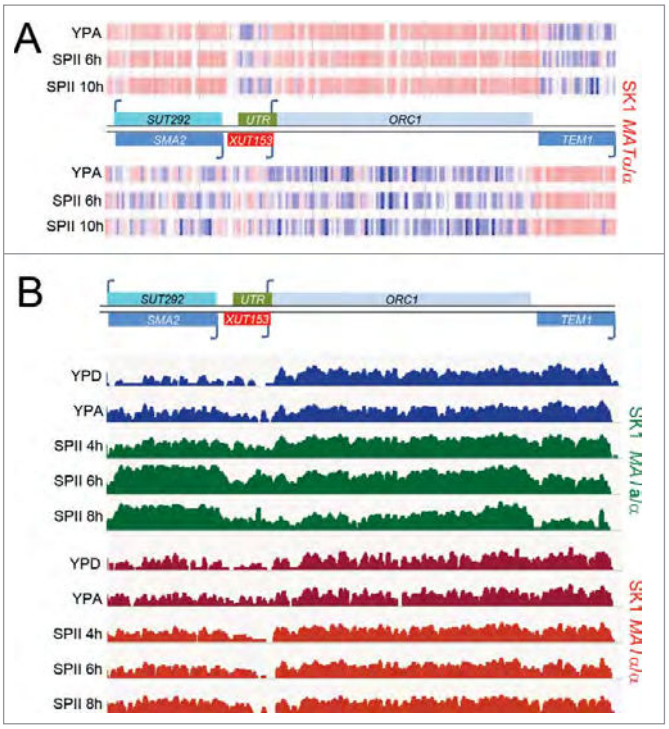

Figure 2. *mORC1* induction requires sporulation. (A) (SPII, 4h, 6h, 8h). Tiling array data for *ORC1* are shown as in Fig. 1 for sporulation deficient SK1 *MATα/α* cells cultured in pre-sporulation medium (YPA) and sporulation medium (SPII, 4, 6, 8h). (B) A schematic shows the region containing the *ORC1* locus as in Fig. 1. RNA-Sequencing data (not DNA strand-specific) are given as a color-coded histogram (IGV version 2.3.40 set at log scale data range min 0 and max 800) for cells cultured rich media in blue (YPD, YPA) and for sporulation medium in green (SPII) as shown to the left. The wild type (SK1 *MAT***a**/*α* in green) and sporulation deficient control strains (SK1 *MATα/α* in red) are indicated to the right.

the regulation of *mORC1*. The observed lack of *mORC1* induction in *ndt80* mutant cells could, however, be an indirect effect because *ndt80* cells arrest during pachytene stage of meiotic prophase I, which might impair the transcription of the long *ORC1* isoform.[14]

Ndt80 and Sum1 directly act on mORC1/SMA2 via an MSE element

The results described above complement earlier work where we predicted an MSE in the intergenic region of *ORC1* and *SMA2*, which was reported to be bound by Ndt80 *in vivo*.[9,20] The combined results are consistent with – but do not prove – a direct role for Ndt80/MSE. To provide unambiguous evidence for a novel function of Ndt80 in activating a meiotic *ORC1* transcript isoform, we deleted the MSE (in a congenic strain background for technical reasons related to selectable marker genes; Fig. 5A) and found that *mORC1* indeed failed to be induced in middle meiosis, while the mutation did not alter the mitotic isoform's expression level (Fig. 5B). Consistently, *SMA2* mRNA also failed to be meiotically induced in the absence of a functional MSE in the gene's promoter region. (Fig. 5C). We note that a low level

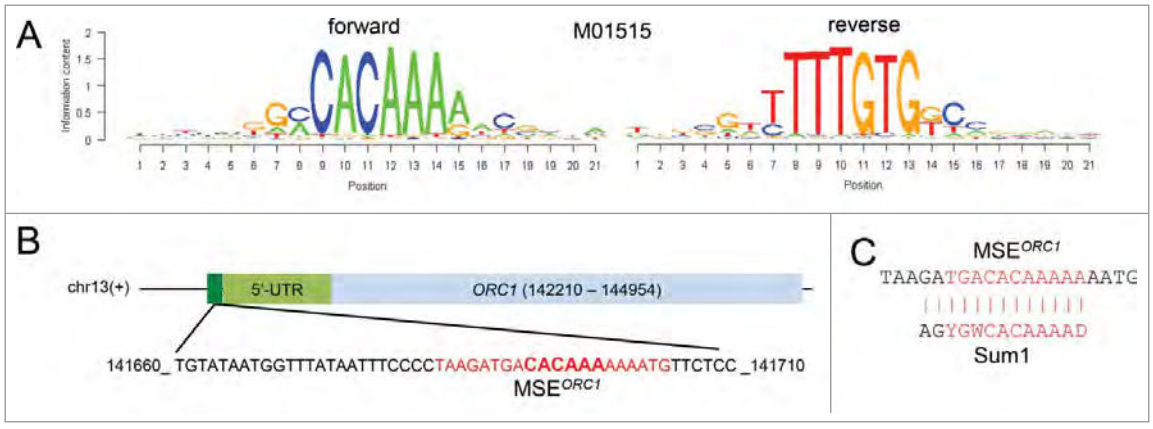

Figure 3. MSE prediction. (A) Logos of the predicted MSE (M01515) are shown as graphs plotting information content (y-axis) vs. position for each base in the sequence for forward (left) and reverse (right) DNA strands (x-axis). (B) A schematic represents the MSE in dark green, the 5′-UTR in light green and *ORC1* in light blue. A black line represents the top DNA strand (+). The chromosome number is indicated. The base coordinates and the base composition of the 5′-*mORC1* region, which contains a predicted MSE (bases are shown in red with the core bases enlarged and in bold), are shown at the bottom. (C) The predicted *ORC1* MSE is aligned with the Sum1 target motif; a vertical line indicates base matches and similarities. Bases in the core sequence are given in red.

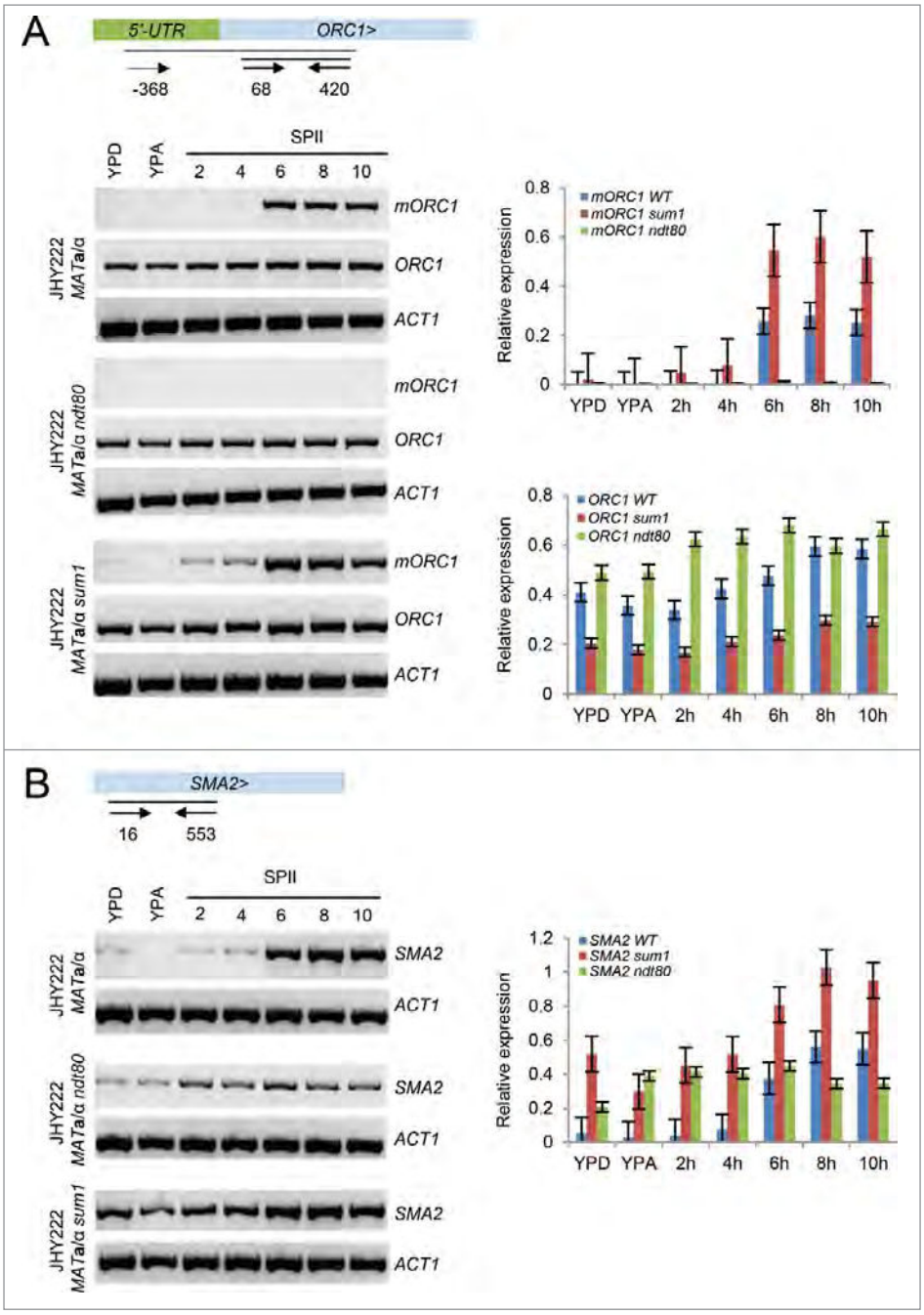

Figure 4. Ndt80-dependent *mORC1*/*SMA2* expression. (A) A schematic shows the *ORC1* 5′-UTR in green and the ORF in light blue; > indicates the transcriptional direction. Small arrows symbolize oligonucleotide primers and black lines represent PCR products. Their coordinates with respect to the first base in the ATG start codon are given. The output of RT-PCR assays is shown for *ORC1* isoforms (*mORC1*, *ORC1*) and *ACT1*. The wild type, *ndt80* and *sum1* strain backgrounds are shown to the left. Cells were harvested in rich media (YPD, YPA) and sporulation medium (SPII) at the bi-hourly time points indicated at the top. Two bar graphs show quantified signals from RT-PCR assays in panel A for *mORC1* (top) and *ORC1* (bottom) for the wild type (blue), *sum1* (red) and *ndt80* (green) strains given in the legends. Relative expression levels (y-axis) are plotted against samples (x-axis) as shown. Bars indicate the values obtained in duplicate experiments. (B) A schematic on top shows the *SMA2* locus and the position of oligonucleotide primers (arrows) beneath a black line indicating the PCR fragment. The output of RT-PCR assays for *SMA2* in wild type, *ndt80* and *sum1* strains is shown and bar diagrams are given as in panel A.

of MSE-independent *SMA2* expression appear to be mediated by at least one other promoter element. This is, however, likely insufficient for Sma2 function since the *ORC1* MSE deletion strain displays a sporulation phenotype similar to the one previously reported for the *sma2* mutant: cells progress through the meiotic divisions but mostly fail to form asci because the nuclei are not properly packaged (Fig. 6A, B).[8,10] The simplest explanation is that Sum1 contributes to the repression of *mORC1* and *SMA2* during mitotic growth, while Ndt80 activates the transcripts from middle meiosis onwards by directly interacting with a bi-directional MSE present in the *ORC1* promoter.

mORC1 expression and Orc1 protein levels are negatively correlated

Our findings, together with the prediction by Brar et al., that the long isoform of *ORC1* may inhibit protein translation,

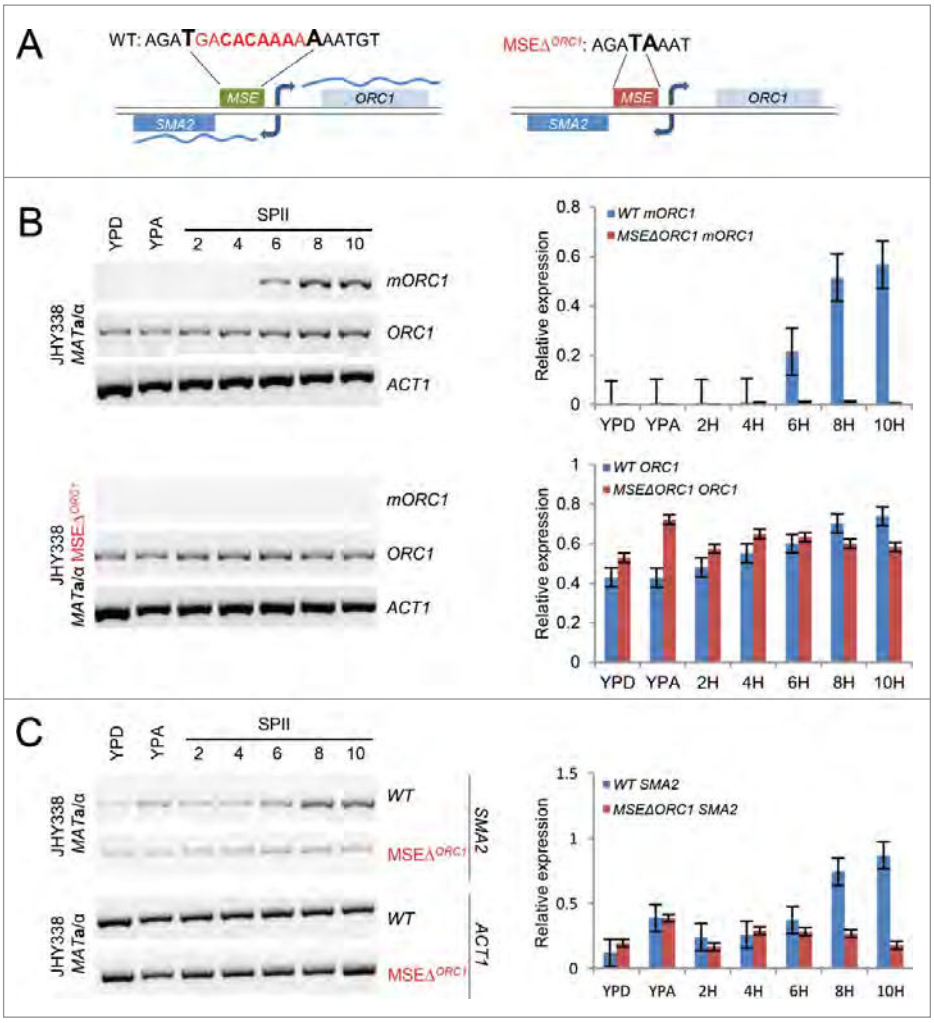

Figure 5. Bi-directional MSE-dependent *mORC1/SMA2* expression. (A) A schematic shows the wild type and MSE mutant sequences upstream of *ORC1*. The deleted sequence is given in red, flanking bases are enlarged and given in bold. (B) The output of RT-PCR assays with samples from wild type cells versus cells lacking the MSE upstream of *mORC1* (MSEΔ^{ORC1}) is shown for the *ORC1* isoforms and for *ACT1*. RT-PCR signals are given as bar diagrams. (C) RT-PCR data are given for *SMA2* and *ACT1* in wild type (WT) and motif deletion strains (MSEΔ^{ORC1}) as in panel B.

raises the interesting possibility that Ndt80 represses Orc1 after pre-meiotic DNA replication by activating a transcript isoform that sequesters ribosomes at its 5′ end *via* uORFs; (reference[13]; Fig. S3). The extended *ORC1* 5′-UTR contains 2 such uORFs encoding proteins of 113 and 64 amino acids, respectively, that are in frame with the main ORF (Fig. 7A). We reasoned that the induction of *mORC1* should correlate with declining Orc1 protein levels as cells enter meiotic M-phase and found this indeed to be the case. Importantly, we detected the Orc1 protein during and after M-phase in the *ORC1*$^{MSE\Delta}$ deletion strain that cannot induce *mORC1* (Fig. 7B, C; Fig. S4). These findings are consistent with the regulatory design proposed in Fig. 8: *mORC1* and *SMA2* are repressed in mitosis by the Sum1 complex and activated in meiosis by Ndt80, which enables Sma2 but not Orc1 protein to accumulate when cells exit meiosis and enter gamete formation.

Discussion

The yeast meiotic transcriptome comprises classical early, middle and late mRNAs, meiotic transcript isoforms that possess either 5′- or 3′-extended UTRs, and lncRNAs.[6,7,9,23,29,30] These findings raise the question if the transcriptional regulatory network, which controls developmental stage-specific mRNAs, also contributes to the regulation of meiotically induced mRNA isoforms and lncRNAs. In this report, we begin to unravel the regulatory mechanism controlling the meiotic isoform of *ORC1*, which is co-induced with divergent *SMA2* when diploid cells undergo meiosis and gametogenesis. We also present evidence supporting the conceptually new model that the activator Ndt80 negatively regulates post-meiotic Orc1 protein levels by inducing the long isoform of *ORC1*, which inhibits translation via an extended 5′UTR.

The ORC1 promoter drives divergent mRNA/lncRNA expression in mitotically growing cells

It is unclear what role, if any, the divergent lncRNA in the *ORC1* locus might play during growth and development. It is perhaps noteworthy that the transcript, although annotated as *XUT1538*,[5] also shows features typical for two other types of lncRNAs, since it is detectable in wild type cells (SUTs[12]) and it accumulates in the absence of Rrp6 (CUTs[31]). Given the considerable overlap between these transcript classes, especially in the cases of SUTs and XUTs,

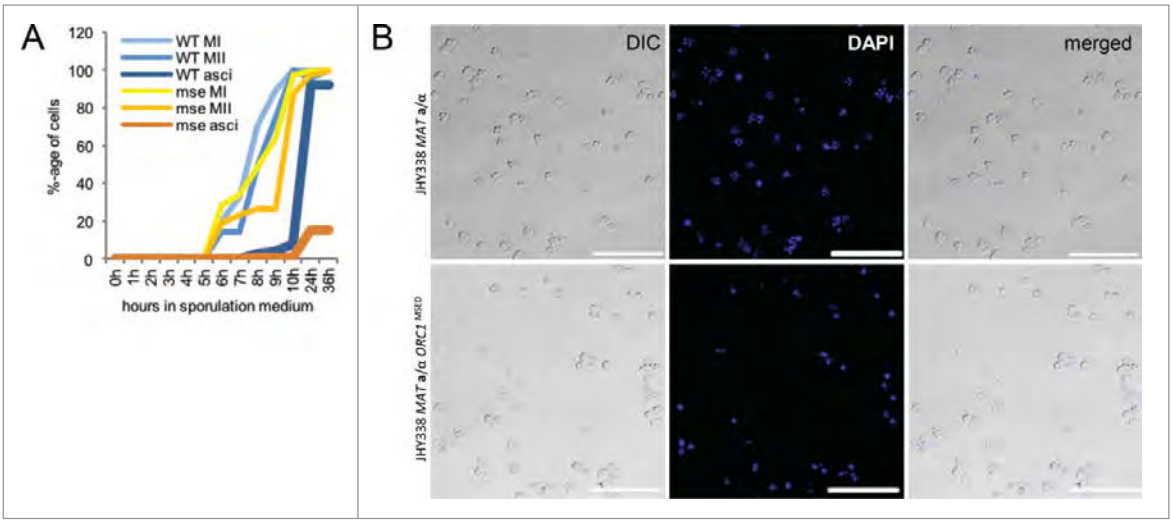

Figure 6. Phenotypic analysis of the MSE deletion mutant. (A) A graph shows the percentage of wild type and MSE mutant cells cells (y-axis) at the bi-nuclear (MI), tetra-nuclear (MII) and ascus stage over time in sporulation medium shown in hours (x-axis). (B) Representative images of wild type (top) and MSE deletion (bottom) strains are shown using differential interference contrast (DIC, left), fluorescent staining of DNA (DAPI, middle) or both (merged, right). The strains are given to the left. A bar indicates 50μm.

more work is needed to understand the molecular mechanisms governing their variable synthesis and decay rates.

Establishing developmental stage-specific middle meiotic isoform expression

Contrary to early meiotic transcript isoforms present in mitotic *ume6* cells,[23] one would not expect middle meiotic transcript isoforms such as *mORC1* to strongly accumulate in a fermenting *sum1* mutant because their activator Ndt80 is undetectable in cells cultured in rich medium. Indeed, we find that *mORC1* is weakly de-repressed in fermenting JHY222 *sum1* cells and during incubation in sporulation medium. For *SMA2* the level of mitotic accumulation in *sum1* cells is elevated as compared to *mORC1*, which might be due to distinct RNA half-lives. Taken together, our results are consistent with a role for Sum1 in repressing *mORC1* and *SMA2* during mitotic growth *via* the putative target sequence within the $ORC1^{MSE}$ (see Fig. 3C and Fig. 8). In addition, it is conceivable that *SMA2* expression is partially inhibited during mitosis by *SUT292* and *XUT1538 via* well-established antisense- and promoter interference mechanisms[32,33]; for review see reference.[34]

A new role for Ndt80 in the activation of a meiotic transcript isoform that inhibits translation

One might expect *ORC1* to be transcriptionally repressed when cells exit pre-meiotic DNA replication, because there is no further need for assembling an origin recognition complex at autonomously replicating sequence (ARS) elements. Yet, earlier work with microarrays containing probes for the 3′-regions of ORFs shows that *ORC1* gene expression strongly increases as cells progress through meiotic development.[6,7] Recent studies using tiling arrays and RNA-Sequencing helped explain this puzzling fact: cells induce a long transcript isoform with an extended 5′-UTR proposed to inhibit Orc1 translation.[13,29] However, neither microarrays nor RNA-Seq experiments unambiguously show that the 5′-extended isoform is synthesized through to the same transcription termination site (TTS) as the short isoform. We propose that data in previously published work and this study are consistent with the notion that both isoforms use a common TTS as the model in Fig. 8 implies.[13,23]

A key question that we sought to answer is which regulator activates *mORC1* and *SMA2* at the onset of meiotic M-phase. The presence of an MSE prompted us to assay *mORC1* induction in an *ndt80* mutant strain and we found that the long transcript isoform does not accumulate to normal levels in the absence of Ndt80. In spite of the predicted MSE′s presence in the promoter, this effect could still be indirect because *ndt80* mutant cells arrest at the pachytene checkpoint prior to entry into M-phase and therefore simply might be unable to induce *mORC1*. Two lines of evidence argue against this interpretation and in favor of our model (Fig. 8). First, a high-throughput protein-DNA binding assay based on chromatin immunoprecipitation and microarrays (ChIP-Chip) showed that Ndt80 binds the *ORC1* upstream region *in vivo*.[20] Second, deleting the MSE in the *ORC1* promoter prevents normal induction of the meiotic *ORC1* isoform and strongly reduces *SMA2* expression during sporulation. We currently do not know why we detect low levels of *SMA2* in the MSE mutant strain. Another weak promoter element might mediate basal expression or the mRNA might be unusually stable in meiotic cells.

An intriguing aspect of the model in Fig. 8 is that Ndt80 could potentially drive bi-directional transcription of mRNA/isoform pairs *via* MSEs that both have a biological function. Such a novel role for Ndt80 is consistent with earlier reports suggesting that yeast promoters typically mediate bi-directional transcription.[11,12] Our findings raise the possibility that promoters driving the expression of divergent transcript may have brought about an evolutionary advantage: cells need to induce *SMA2* given its important role in sporulation,[8,10] while *ORC1* is not involved in late meiotic processes. Therefore, the induction

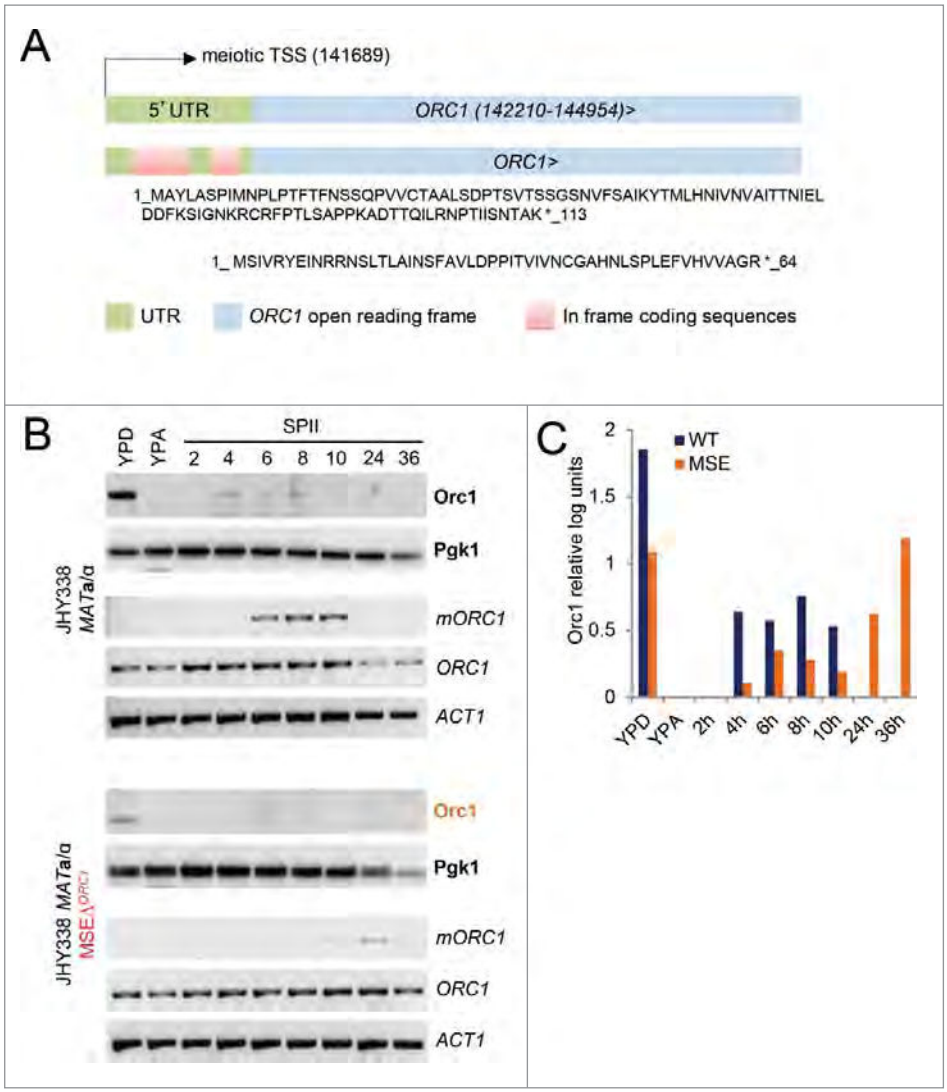

Figure 7. *ORC1* RNA vs. Orc1 protein levels. (A) A schematic shows the *ORC1* locus in blue and the extended 5′UTR in gray at the top. Genome coordinates for the *ORC1* ORF and the meiotic transcription start site (TSS) are given. Two in frame upstream ORFs located in the 5′-UTR are shown in red at the bottom. The amino acid sequences are indicated and an asterisk represents the stop codon. (B) Cells from wild type (JHY388 *MAT***a**/*α*) and MSE mutant (JHY338 *MAT***a**/*α* MSEΔ^{ORC1}) strains were cultured in growth media (YPD, YPA) an sporulation medium (SPII) at the time points indicated in hours. As shown to the right, protein samples were analyzed for Orc1, using Pgk1 as a loading control. RNA samples were assayed for the long isoform (*mORC1*), and the short isoform (*ORC1*), using *ACT1* as a loading control. (C) A color-coded graph shows quantified log-transformed units (y-axis) representing Orc1 protein levels in panel B for samples from growing and sporulating cells (x-axis). Samples from wild type (WT) cells are shown in black, those from mutant (MSEΔ^{ORC1}) cells are shown in orange.

of an extended isoform, which inhibits Orc1 translation *via* uORFs, represents an elegant solution for down-regulating a protein without the need for repressing the promoter. In addition, we speculate that this mechanism, which keeps the *ORC1* promoter chromatin in an open configuration during the entire process of gametogenesis, may also allow for rapid induction of *ORC1* during spore germination and initiation of the first round of mitosis.

ORC1 is a model locus suitable to study the regulation of 5′-extended developmental stage specific transcripts and their role in controlling protein levels when cells switch from growth to development. Our findings extend the known roles of Ndt80/Sum1 to the transcriptional control of middle meiotic transcript isoforms. Bearing in mind that the DNA binding fold of Ndt80 was suggested to be evolutionarily linked to the major tumor suppressor TP53,[35] our results are potentially relevant for transcriptional mechanisms implicated in development and disease in humans.

Experimental procedures

Yeast strains

The tiling array data were produced with wild type SK1 *MAT***a**/*α* and sporulation deficient *MATα*/*α* control strains. RT-PCR assays were done with samples from SK1 *MAT***a**/*α* and JHY222 *MAT***a**/*α* as published.[23] The expression of the long *ORC1* isoform was analyzed in JHY222 *MAT***a**/*α* *ndt80* and *sum1* homozygous deletion strains and JHY338 *MAT***a**/*α* *ORC1*Δ^{MSE} (Table 1). Yeast strains were cultured at 30°C in standard rich medium with glucose (YPD) or acetate (YPA) and sporulation medium (SPII).

Yeast Sc_tlg tiling array data and RNA-Sequencing data

In this study, we employed unpublished non-DNA strand-specific RNA-Sequencing data that were produced using the Illumina GAII system. Duplicate samples from wild type SK1 *MAT***a**/*α* and meiosis-deficient *MATα*/*α* control cells were

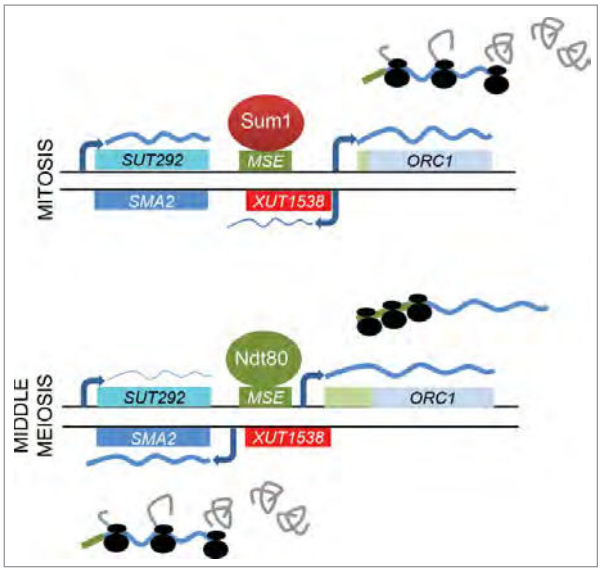

Figure 8. A model for m*ORC1*/*SMA2* induction in meiosis. A schematic depicts the mitotic (top) and meiotic (bottom) regulation of *ORC1* and *SMA2* shown as light and dark blue rectangles, respectively, by Sum1 (dark red) and Ndt80 (green). Mitotic and meiotic *ORC1* 5′-UTRs are shown in green. *SUT292* and XUT1538 are given in blue and red, respectively. The MSE is given as a light green rectangle. Transcripts are shown as wavy lines for which the thickness represents the expression level. Black lines represent the top and bottom DNA strands.

cultured in rich medium (YPD), pre-sporulation medium (YPA), and sporulation medium (SPII, 4h, 6h, 8h; Becker et al., in preparation). Furthermore, we interpreted published Yeast Sc_tlg GeneChip expression data from duplicate samples of asynchronously growing SK1 *MAT***a**/*α* cells cultured in rich medium (YPD) or pre-sporulation medium (YPA), and differentiating cells cultured in sporulation medium (SPII). In addition, dividing and starving meiosis-deficient *MATα*/*α* cells were used as a control.[9] SK1 is a strain background commonly employed in genetic and genomic analyses of meiosis because of its efficient sporulation properties.[7] Published Sc_tlg GeneChip data from single samples of synchronized cells undergoing mitotic growth and division were obtained with the W101 *MAT***a** strain.[24] Mitotic gene expression is typically studied in haploid cells because of well-established cell synchronization protocols.[36,37] Graphical displays of tiling array data are available online at SGV (Saccharomyces Genome Viewer, sgv.genouest.org[26]) and RGV (ReproGenomics Viewer, rgv.genouest.org[25]). A DNA strand-specific RNA-Seq data set was used to interpret the transcriptomes of asynchronously growing haploid wild type and *xrn1* temperature sensitive mutants in the S288C, W303, and SK1 backgrounds, and diploid SK1 wild type and *xrn1* mutant cells.[5]

RT-PCR assays

Total RNA was isolated using the hot phenol method as described.[7] Briefly, cell pellets were treated with hot phenol (65°C) and phenol/chloroform (1:1). Total RNA was precipitated overnight with 2 volumes of 100 % ethanol and 0.1 volume of 3 M NaOAc (pH 5) at −80°C. The RNA was digested with 2 units of DNaseI for 30 min at 37°C, and then 2 μg of RNA was reverse transcribed into cDNA using reverse transcriptase and random primers supplied in the

Table 1. Yeast strains.

Strain ID	Background and genotype	Reference
MPY1	JHY222 *MAT***a**/*MATα HAP1*/*HAP1 MKT1* (D30G)/*MKT1*(D30G) *RME1*(INS 308A)/*RME1*(INS 308A) *TAO3*(E1493Q)/*TAO3* (E1493Q)	9
MPY392	JHY222 *MAT***a**/*MATα HAP1*/*HAP1 MKT1* (D30G)/*MKT1*(D30G) *RME1*(INS 308A)/*RME1*(INS 308A) *TAO3*(E1493Q)/*TAO3* (E1493Q) *rrp6*::kanMX4/*rrp6*::kanMX4	
NKY1551	SK1 *MAT***a**/*MATα ho*::*LYS2*/*ho*::*LYS2 ura3*/*ura3 lys2*/*lys2 leu2*::*hisG*/*leu2*::*hisG arg4-Nsp*/*arg4-Bgl his4x*::*LEU2-URA3*/*his4B*::*LEU2*	7
NKY471	SK1 *MATα*/*MATα ho*::*LYS2*/*ho*::*LYS2 ura3*/*ura3 lys2*/*lys2*	
MPY454	W101 *MAT***a** *ho*::*lys5 gal2*	24
MPY631	JHY222 *MAT***a**/*MATα HAP1*/*HAP1 MKT1* (D30G)/*MKT1*(D30G) *RME1*(INS 308A)/*RME1*(INS 308A) *TAO3*(E1493Q)/*TAO3* (E1493Q) *sum1*::kanMX4/*sum1*::kanMX4	This study
MPY553	JHY222 *MAT***a**/*MATα HAP1*/*HAP1 MKT1* (D30G)/*MKT1*(D30G) *RME1*(INS 308A)/*RME1*(INS 308A) *TAO3*(E1493Q)/*TAO3* (E1493Q) *ndt80*::kanMX4/*ndt80*::kanMX4	This study
MPY742	JHY338 *MAT***a**/*MATα ura3*/*ura3 leu2*/*leu2 lys2*/ + *his3*/+	This study
MPY794	JHY338 *MAT***a**/*MATα ura3*/*ura3 leu2*/*leu2 lys2*/ + *his3*/+ mseΔ^{ORC1}/mseΔ^{ORC1}	This study

High Capacity cDNA Reverse Transcription Kit (Applied Biosystems). 1 μl of cDNA was amplified for 28 cycles (denaturation at 94°C for 1 min, annealing at 60°C for 1 min, and extension at 72°C for 1 min) using Taq DNA Polymerase (Qiagen). PCR products were run on a 2% agarose gel in 1×TAE buffer containing GelRed DNA dye (Biotium) and photographed using the Gel Doc XR+ imaging system (Bio-Rad). Primer sequences are given in Table 2.

Prediction of MSEs

We screened a 2 kb region upstream of the annotated *ORC1* locus (Chr13:14210-142210) using the *Match* tool of the TRANSFAC professional database.[38] We employed the MSE motif M01515 with cut-off scores minimizing false positives. The logo was produced with the R package *seqLogo*.[39,40] A single MSE motif was predicted with a core score of 1.00 and a matrix score of 0.949.

MSE deletion

The predicted Ndt80 target site MSE in the *ORC1* promoter region was deleted using the 50:50 genome editing method as recently described.[41,42] Genomic PCR was used to screen deletion strains for successful integration/excision events. For this study we analyzed two independent isolates that were verified by DNA sequencing. We note that the construction of this

Table 2. Oligonucleotides for RT-PCR assay.

Target genes	Forward primer	Reverse primer	Size (bp)
ORC1	5′-TCGATGGAGGTCAGAAGAGA-3	5′-TTCGGCTAATTCTGCAGTGA-3′	353
mORC1	5′-AGGACTGCTATGGGGCATGT-3′	5′-TTCGGCTAATTCTGCAGTGA-3′	789
SMA2	5′- CGTCTGATTGTGTGGGGTGT-3′	5′-GGGCATTTCCTGTGTGCTTG-3′	538

Table 3. Oligonucleotides to construct and validate MSE deletion.

Purpose	*ORC1* 50:50-U2	*ORC1* D2-50
MSE deletion	5′-TAAGTGCATGGTA TGGAGTGTATAATGGT TTATAATTTCCCCTAAGAT AAATGTTCTCCCAA AAATTTACCAAGAA AAAAAATTAAGAAT ACTACACACGTACGC TGCAGGTCGAC-3′	5′-TGTGTAGTA TTCTTAATTTTTTTT CTTGGTAAATTTTTG GGAGAACATTTATCG ATGAATTCGAGCTCG-3′
	Forward primer	Reverse primer
Validation of MSEΔ^{ORC1}	5′-TGGTATGGAG TGTATAATGG-3′	5′-CCCAAGCATC AATTGTGTAG-3′

strain required the *ura3Δ0* auxotrophic marker present only in the JHY338 background, which is derived from prototrophic JHY222. Oligonucleotide sequences are given in Table 3.

Sporulation landmarks

Diploid cells were cultured in growth medium, presporulation medium and sporulation medium, harvested, and fixed in ethanol as described.[7] The percentage of bi-, and tetranuclear cells and asci was determined using a standard manual cell counter.

Light- and fluorescence microscopy

Yeast cells were stained with DAPI (Interchim) at 5 μg/ml and inspected using a Zeiss AxioImager fluorescence microscope (Zeiss). Pictures were taken with an AxioCam camera using default settings of AxioVision software (Zeiss).

Protein analysis

Protein extracts were prepared and analyzed by Western blotting as published.[9] Briefly, 35 μg of a total protein extract was loaded on a 4-20% SDS-PAGE gradient gel, and run first at 60V for 30 minutes and then at 120 V for one hour. Proteins were transferred onto a PVDF membrane (Millipore) at 60mA for 2.5 hours using a semi-dry electroblotter (Hoefer). The membrane was blocked in 5% milk (Regilait) for one hour at room temperature, and incubated over night at 4°C on a shaker with the primary polyclonal anti-Orc1 antibody (Santa Cruz) at a dilution of 1:200. A monoclonal antibody against Pgk1 (Invitrogen) was used at 1:15′000. Secondary anti-goat and anti-mouse antibodies (ThermoScientific) diluted at 1:30'000 or 1:5000, respectively, were incubated at room temperature for one hour, before the signal was revealed using an ECL kit (General Electric) and the ChemiDoc XRS imaging system (Bio-Rad). Band intensities were quantified using Quantity One 1-D analysis software (Bio-Rad).

Disclosure of Potential Conflicts of Interest

No potential conflicts of interest were disclosed.

Acknowledgments

We thank Olivier Collin and Olivier Sallou for the GenOuest bioinformatics infrastructure, Thomas Darde for extensive help with RGV, and Marc Descrimes for generating heatmaps representing RNA-Seq data.

Funding

This work was supported by a National Institute of Health grant (5P01HG000205) to R.W. Davis, a Ligue Contre le Cancer PhD fellowship to B. Xie and funding provided by the University of Rennes 1 and Institut National de Sante et de Recherche Medicale to M. Primig.

References

1. Li H, Stillman B. The origin recognition complex: a biochemical and structural view. Sub-cell Biochem 2012; 62:37-58; PMID:22918579; http://dx.doi.org/10.1007/978-94-007-4572-8_3
2. Bell SP, Mitchell J, Leber J, Kobayashi R, Stillman B. The multidomain structure of Orc1p reveals similarity to regulators of DNA replication and transcriptional silencing. Cell 1995; 83:563-8; PMID:7585959; http://dx.doi.org/10.1016/0092-8674(95)90096-9
3. Klemm RD, Austin RJ, Bell SP. Coordinate binding of ATP and origin DNA regulates the ATPase activity of the origin recognition complex. Cell 1997; 88:493-502; PMID:9038340; http://dx.doi.org/10.1016/S0092-8674(00)81889-9
4. Vader G, Blitzblau HG, Tame MA, Falk JE, Curtin L, Hochwagen A. Protection of repetitive DNA borders from self-induced meiotic instability. Nature 2011; 477:115-9; PMID:21822291; http://dx.doi.org/10.1038/nature10331
5. Wery M, Descrimes M, Vogt N, Dallongeville AS, Gautheret D, Morillon A. Nonsense-Mediated Decay Restricts LncRNA Levels in Yeast Unless Blocked by Double-Stranded RNA Structure. Mol Cell 2016; 61(3):379-92; PMID:26805575
6. Chu S, DeRisi J, Eisen M, Mulholland J, Botstein D, Brown PO, Herskowitz I. The transcriptional program of sporulation in budding yeast. Science 1998; 282:699-705; PMID:9784122; http://dx.doi.org/10.1126/science.282.5389.699
7. Primig M, Williams RM, Winzeler EA, Tevzadze GG, Conway AR, Hwang SY, Davis RW, Esposito RE. The core meiotic transcriptome in budding yeasts. Nat Genet 2000; 26:415-23; PMID:11101837; http://dx.doi.org/10.1038/82539
8. Rabitsch KP, Toth A, Galova M, Schleiffer A, Schaffner G, Aigner E, Rupp C, Penkner AM, Moreno-Borchart AC, Primig M, et al. A screen for genes required for meiosis and spore formation based on whole-genome expression. Curr Biol 2001; 11:1001-9; PMID:11470404; http://dx.doi.org/10.1016/S0960-9822(01)00274-3
9. Lardenois A, Liu Y, Walther T, Chalmel F, Evrard B, Granovskaia M, Chu A, Davis RW, Steinmetz LM, Primig M, et al. Execution of the meiotic noncoding RNA expression program and the onset of gametogenesis in yeast require the conserved exosome subunit Rrp6. Proc Natl Acad Sci U S A 2011; 108:1058-63; PMID:21149693; http://dx.doi.org/10.1073/pnas.1016459108
10. Maier P, Rathfelder N, Maeder CI, Colombelli J, Stelzer EH, Knop M. The SpoMBe pathway drives membrane bending necessary for cytokinesis and spore formation in yeast meiosis. EMBO J 2008; 27:2363-74; PMID:18756268; http://dx.doi.org/10.1038/emboj.2008.168
11. Neil H, Malabat C, d'Aubenton-Carafa Y, Xu Z, Steinmetz LM, Jacquier A. Widespread bidirectional promoters are the major source of cryptic transcripts in yeast. Nature 2009; 457:1038-42; PMID:19169244; http://dx.doi.org/10.1038/nature07747
12. Xu Z, Wei W, Gagneur J, Perocchi F, Clauder-Munster S, Camblong J, Guffanti E, Stutz F, Huber W, Steinmetz LM. Bidirectional promoters generate pervasive transcription in yeast. Nature 2009; 457:1033-7; PMID:19169243; http://dx.doi.org/10.1038/nature07728
13. Brar GA, Yassour M, Friedman N, Regev A, Ingolia NT, Weissman JS. High-resolution view of the yeast meiotic program revealed by ribosome profiling. Science 2012; 335:552-7; PMID:22194413; http://dx.doi.org/10.1126/science.1215110
14. Xu L, Ajimura M, Padmore R, Klein C, Kleckner N. NDT80, a meiosis-specific gene required for exit from pachytene in Saccharomyces cerevisiae. Mol Cell Biol 1995; 15:6572-81; PMID:8524222; http://dx.doi.org/10.1128/MCB.15.12.6572
15. Corbi D, Sunder S, Weinreich M, Skokotas A, Johnson ES, Winter E. Multisite phosphorylation of the Sum1 transcriptional repressor by S-phase kinases controls exit from meiotic prophase in yeast. Mol Cell

Biol 2014; 34:2249-63; PMID:24710277; http://dx.doi.org/10.1128/MCB.01413-13
16. Xie J, Pierce M, Gailus-Durner V, Wagner M, Winter E, Vershon AK. Sum1 and Hst1 repress middle sporulation-specific gene expression during mitosis in Saccharomyces cerevisiae. Embo J 1999; 18:6448-54; PMID:10562556; http://dx.doi.org/; http://dx.doi.org/10.1093/emboj/18.22.6448
17. Pierce M, Benjamin KR, Montano SP, Georgiadis MM, Winter E, Vershon AK. Sum1 and Ndt80 proteins compete for binding to middle sporulation element sequences that control meiotic gene expression. Mol Cell Biol 2003; 23:4814-25; PMID:12832469; http://dx.doi.org/10.1128/MCB.23.14.4814-4825.2003
18. Tsuchiya D, Yang Y, Lacefield S. Positive feedback of NDT80 expression ensures irreversible meiotic commitment in budding yeast. PLoS Genet 2014; 10:e1004398; PMID:24901499; http://dx.doi.org/10.1371/journal.pgen.1004398
19. Winter E. The Sum1/Ndt80 transcriptional switch and commitment to meiosis in Saccharomyces cerevisiae. Microbiol Mol Biol Rev 2012; 76:1-15; PMID:22390969; http://dx.doi.org/10.1128/MMBR.05010-11
20. Klutstein M, Siegfried Z, Gispan A, Farkash-Amar S, Zinman G, Bar-Joseph Z, Simchen G, Simon I. Combination of genomic approaches with functional genetic experiments reveals two modes of repression of yeast middle-phase meiosis genes. BMC Genomics 2010; 11:478; PMID:20716365; http://dx.doi.org/10.1186/1471-2164-11-478
21. Spivak AT, Stormo GD. ScerTF: a comprehensive database of benchmarked position weight matrices for Saccharomyces species. Nucleic Acids Res 2012; 40:D162-8; PMID:22140105; http://dx.doi.org/10.1093/nar/gkr1180
22. Van Loo P, Marynen P. Computational methods for the detection of cis-regulatory modules. Brief Bioinform 2009; 10:509-24; PMID:19498042; http://dx.doi.org/10.1093/bib/bbp025
23. Lardenois A, Stuparevic I, Liu Y, Law MJ, Becker E, Smagulova F, Waern K, Guilleux MH, Horecka J, Chu A, et al. The conserved histone deacetylase Rpd3 and its DNA binding subunit Ume6 control dynamic transcript architecture during mitotic growth and meiotic development. Nucleic Acids Res 2015; 43:115-28; PMID:25477386; http://dx.doi.org/10.1093/nar/gku1185
24. Granovskaia MV, Jensen LJ, Ritchie ME, Toedling J, Ning Y, Bork P, Huber W, Steinmetz LM. High-resolution transcription atlas of the mitotic cell cycle in budding yeast. Genome Biol 2010; 11:R24; PMID:20193063; http://dx.doi.org/10.1186/gb-2010-11-3-r24
25. Darde TA, Sallou O, Becker E, Evrard B, Monjeaud C, Le Bras Y, Jégou B, Collin O, Rolland AD, Chalmel F. The ReproGenomics Viewer: an integrative cross-species toolbox for the reproductive science community. Nucleic Acids Res 2015; 43:W109-16; PMID:25883147; http://dx.doi.org/10.1093/nar/gkv345
26. Lardenois A, Gattiker A, Collin O, Chalmel F, Primig M. GermOnline 4.0 is a genomics gateway for germline development, meiosis and the mitotic cell cycle. Database 2010; 2010:baq030; PMID:21149299; http://dx.doi.org/10.1093/database/baq030
27. Chang DT, Huang CY, Wu CY, Wu WS. YPA: an integrated repository of promoter features in Saccharomyces cerevisiae. Nucleic Acids Res 2011; 39:D647-52; PMID:21045055; http://dx.doi.org/10.1093/nar/gkq1086
28. Liti G, Carter DM, Moses AM, Warringer J, Parts L, James SA, Davey RP, Roberts IN, Burt A, Koufopanou V, et al. Population genomics of domestic and wild yeasts. Nature 2009; 458:337-41; PMID:19212322; http://dx.doi.org/10.1038/nature07743
29. Kim Guisbert KS, Zhang Y, Flatow J, Hurtado S, Staley JP, Lin S, Sontheimer EJ. Meiosis-induced alterations in transcript architecture and noncoding RNA expression in S. cerevisiae. RNA 2012; 18:1142-53; PMID:22539527; http://dx.doi.org/10.1261/rna.030510.111
30. Wilhelm BT, Marguerat S, Watt S, Schubert F, Wood V, Goodhead I, Penkett CJ, Rogers J, Bähler J. Dynamic repertoire of a eukaryotic transcriptome surveyed at single-nucleotide resolution. Nature 2008; 453:1239-43; PMID:18488015; http://dx.doi.org/10.1038/nature07002
31. Wyers F, Rougemaille M, Badis G, Rousselle JC, Dufour ME, Boulay J, Régnault B, Devaux F, Namane A, Séraphin B, et al. Cryptic pol II transcripts are degraded by a nuclear quality control pathway involving a new poly(A) polymerase. Cell 2005; 121:725-37; PMID:15935759; http://dx.doi.org/10.1016/j.cell.2005.04.030
32. Hongay CF, Grisafi PL, Galitski T, Fink GR. Antisense transcription controls cell fate in Saccharomyces cerevisiae. Cell 2006; 127:735-45; PMID:17110333; http://dx.doi.org/10.1016/j.cell.2006.09.038
33. van Werven FJ, Neuert G, Hendrick N, Lardenois A, Buratowski S, van Oudenaarden A, Primig M, Amon A. Transcription of two long noncoding RNAs mediates mating-type control of gametogenesis in budding yeast. Cell 2012; 150:1170-81; PMID:22959267; http://dx.doi.org/10.1016/j.cell.2012.06.049
34. Pelechano V, Steinmetz LM. Gene regulation by antisense transcription. Nat Rev Genet 2013; 14:880-93; PMID:24217315; http://dx.doi.org/10.1038/nrg3594
35. Lamoureux JS, Stuart D, Tsang R, Wu C, Glover JN. Structure of the sporulation-specific transcription factor Ndt80 bound to DNA. EMBO J 2002; 21:5721-32; PMID:12411490; http://dx.doi.org/10.1093/emboj/cdf572
36. Cho RJ, Campbell MJ, Winzeler EA, Steinmetz L, Conway A, Wodicka L, Wolfsberg TG, Gabrielian AE, Landsman D, Lockhart DJ, et al. A genome-wide transcriptional analysis of the mitotic cell cycle. Mol Cell 1998; 2:65-73; PMID:9702192; http://dx.doi.org/10.1016/S1097-2765(00)80114-8
37. Spellman PT, Sherlock G, Zhang MQ, Iyer VR, Anders K, Eisen MB, Brown PO, Botstein D, Futcher B. Comprehensive identification of cell cycle-regulated genes of the yeast Saccharomyces cerevisiae by microarray hybridization. Mol Biol Cell 1998; 9:3273-97; PMID:9843569; http://dx.doi.org/10.1091/mbc.9.12.3273
38. Matys V, Kel-Margoulis OV, Fricke E, Liebich I, Land S, Barre-Dirrie A, Reuter I, Chekmenev D, Krull M, Hornischer K, et al. TRANSFAC and its module TRANSCompel: transcriptional gene regulation in eukaryotes. Nucleic Acids Res 2006; 34:D108-10; PMID:16381825; http://dx.doi.org/10.1093/nar/gkj143
39. 3-900051-07-0 RDCTI. R: A language and environment for statistical computing. R Foundation for Statistical Computing, Vienna, Austria, 2012.
40. Bembom O. seqLogo: Sequence logos for DNA sequence alignments.R package
41. Lardenois A, Stuparevic I, Liu Y, Law MJ, Becker E, Smagulova F, Waern K, Guilleux MH, Horecka J, Chu A, et al. The conserved histone deacetylase Rpd3 and its DNA binding subunit Ume6 control dynamic transcript architecture during mitotic growth and meiotic development. Nucleic Acids Res 2015; 43:115-28; PMID:25477386; http://dx.doi.org/10.1093/nar/gku1185
42. Horecka J, Davis RW. The 50:50 method for PCR-based seamless genome editing in yeast. Yeast 2014; 31:103-12; PMID:24639370; http://dx.doi.org/10.1002/yea.2992

2) BOI1: Liu, Stuparevic et al., Mol Microbiol 2015

Molecular Microbiology (2015) 96(4), 861–874 ■
doi:10.1111/mmi.12976
First published online 21 March 2015

The conserved histone deacetylase Rpd3 and the DNA binding regulator Ume6 repress *BOI1*'s meiotic transcript isoform during vegetative growth in *Saccharomyces cerevisiae*

Yuchen Liu,[1†§] Igor Stuparevic,[1‡§] Bingning Xie,[1] Emmanuelle Becker,[1,2] Michael J. Law[3] and Michael Primig[1*]

[1]*Inserm U1085 IRSET, Inserm, 35042 Rennes, France.*
[2]*Departement des sciences de la vie et de l'environnement, Université de Rennes 1, 35042 Rennes, France.*
[3]*School of Osteopathic Medicine, Rowan University, Stratford, NJ 08084, USA.*

Summary

***BOI1* and *BOI2* are paralogs important for the actin cytoskeleton and polar growth. *BOI1* encodes a meiotic transcript isoform with an extended 5′-untranslated region predicted to impair protein translation. It is, however, unknown how the isoform is repressed during mitosis, and if Boi1 is present during sporulation. By interpreting microarray data from *MAT*a cells, *MAT*a/α cells, a starving *MAT*α/α control, and a meiosis-impaired *rrp6* mutant, we classified *BOI1*'s extended isoform as early meiosis-specific. These results were confirmed by RNA-Sequencing, and extended by a 5′-RACE assay and Northern blotting, showing that meiotic cells induce the long isoform while the mitotic isoform remains detectable during meiosis. We provide evidence via motif predictions, an *in vivo* binding assay and genetic experiments that the Rpd3/Sin3/Ume6 histone deacetylase complex, which represses meiotic genes during mitosis, also prevents the induction of *BOI1*'s 5′-extended isoform in mitosis by direct binding of Ume6 to its URS1 target. Finally, we find that Boi1 protein levels decline when cells switch from fermentation to respiration and sporulation. The histone deacetylase Rpd3 is conserved, and eukaryotic genes frequently encode transcripts with variable 5′-UTRs. Our findings are therefore relevant for regulatory mechanisms involved in the control of transcript isoforms in multi-cellular organisms.**

Accepted 17 February, 2015. *For correspondence. E-mail michael.primig@inserm.fr; Tel. +33223236178; Fax +33223235500. Present addresses: †School of Medicine, Jianghan University, 430056 Wuhan, China; ‡Faculty of Food Technology and Biotechnology, University of Zagreb, 10000 Zagreb, Croatia. §These authors made an equal contribution.

© 2015 John Wiley & Sons Ltd

Introduction

BOI1 and *BOI2* are partially functionally redundant paralogs, which encode proteins important for establishing cell polarity and bud formation; cells lacking both genes cannot grow at 30°C, show an aberrant morphology and grow very poorly at 20°C (Bender *et al.*, 1996; Matsui *et al.*, 1996; Cole *et al.*, 2009; Liao *et al.*, 2013). A detailed cytological analysis in budding yeast revealed a role for Boi1 and Boi2 in a pathway preventing chromosomes from being broken apart during late stages of mitosis in anaphase and telophase, when sister chromatids are separated and pulled to opposite poles before cells split during cytokinesis (Norden *et al.*, 2006). Recent work suggests only Boi2, but not Boi1, to be important for spindle disassembly (Pigula *et al.*, 2014). Direct evidence for a role in polar growth was also reported for the fission yeast Boi1/2 homolog Pob1p (Toya *et al.*, 1999). For single mutants, no meiotic defect has been reported in genome-wide functional genomics studies (Deutschbauer *et al.*, 2002; Enyenihi and Saunders, 2003).

BOI1 and *BOI2* transcripts are ubiquitously expressed during growth and starvation in all haploid and diploid cell types, while the proteins are controlled at the level of cell cycle stage-specific localisation (Primig *et al.*, 2000; Norden *et al.*, 2006; Granovskaia *et al.*, 2010). Earlier microarray profiling analyses revealed that both genes continue to be transcribed when diploid cells undergo meiotic development (Chu *et al.*, 1998; Primig *et al.*, 2000). More recently, *BOI1* was found to encode a meiotic transcript isoform with an extended 5′-untranslated region (UTR) in a recent high-throughput experiment, which combined transcript profiling by RNA-Sequencing (RNA-Seq) and ribosome profiling. The meiotic 5′-untranslated region (5′-UTR) contains a so-called AUG upstream open reading frame (uORF), which is predicted to exert a negative effect on the translation of the protein encoded by the down-

Fig. 1. *BOI1* early meiosis-specific isoform expression.
A. False-color heatmaps representing tiling array data are shown for the 5′-region of *BOI1*. Samples are from cells cultured in rich media (YPD, YPA) and hourly time points in sporulation medium (SPII 1 h–12 h). Haploid cells were grown in YPD and harvested every five minutes (0–135 min). The strains are given to the right; media are given to the left. The output of the segmentation algorithm is shown as grey rectangles. Red rectangles correspond to differentially expressed patterns indicating a complex 5′-leader sequence for *BOI1*. The ORF is shown as a blue rectangle. An ARS element is shown in grey. The log2 scale is shown at the bottom.
B. The output of a 5′-RACE experiment is given for the mitotic isoform (*BOI1*) and the meiotic isoform (*mBOI1*) from cells grown in rich media with glucose (YPD) or acetate (YPA) or in sporulation medium (SPII 4, 6, 8 h). The black arrow marks the correct band for *BOI1*, the red arrow marks a parasitic band not related to the gene. The molecular weight markers (MW) are given in base pairs (bp) to the left. The strain background is indicated at the bottom.
C. RT-PCR assays using primer pairs located in the extended 5′-UTR (mUTR) and the ORF (*BOI1*) are shown for samples cultured in growth media (YPD, YPA) and sporulation medium (SPII) at the given time points. *ACT1* was used as a loading control. The strain is indicated to the left.
D. A Northern blot is shown for long and short isoforms. *ACT1* is used as a loading control; we note that this gene's mRNA, although widely employed to monitor RNA quantities in various types of experiments, can fluctuate during sporulation in some strain backgrounds (see, for example, (Lin *et al*., 2011).

stream ORF (Brar *et al*., 2012). uORFs located within 5′-UTRs are involved in a well studied mechanism controlling mRNA translation, for example in the case of *GCN4*, which is a major regulator of genes involved in amino acid biosynthesis (for review, see (Hinnebusch, 2005)). No direct evidence for declining Boi1 levels during meiosis is available, however, and nothing is known about the transcriptional mechanism controlling the gene's meiotic isoform.

A group of meiosis-specific genes is repressed during vegetative growth by a tripartite complex comprising the histone deacetylase Rpd3 and the co-repressor Sin3 that are recruited to DNA by Ume6, which binds the upstream regulatory site 1 (URS1) (Strich *et al*., 1994; Rundlett *et al*., 1998). Target gene repression is progressively relieved during respiration and sporulation when Ume6 is degraded via a multi-step mechanism involving the Spt-Ada-Gcn5 Acetyltransferase (SAGA) complex, the anaphase promoting complex/cyclosome (APC/C) and the inducer of meiosis 1 (Ime1) (Mallory *et al*., 2007; Law *et al*., 2014). Ume6 was shown to bind the upstream region of *BOI1 in vivo* in a large-scale chromatin immunoprecipitation assay analysing mitotic cells, but since *BOI1* is expressed in vegetatively growing cells the functional significance of this finding remained unclear (Harbison *et al*., 2004). Predicting biologically active regulatory motifs has become more reliable due to large-scale *in vivo* binding data, which are now available for nearly all known yeast transcription factors (TFs) (Harbison *et al*., 2004; Xie *et al*., 2011). The TRANSFAC database provides position weight matrices (PWMs) for TFs. A PWM is generated by aligning the DNA sequences the target TF binds to, and log transforming the number of observations of each base at each position in the matrix (Wingender, 2008; Spivak and Stormo, 2012).

In this study we report a detailed analysis of *BOI1* isoform expression in fermenting, respiring, starving and sporulating cells using tiling array data obtained with wild-type strains and an *rrp6* mutant (Lardenois *et al*., 2011; Stuparevic and Liu *et al*., in preparation) and RNA-Sequencing data (Becker *et al*., in preparation). We validate and extend the high-throughput data by RT-PCR, 5′-RACE assays and Northern blotting. We combine published Ume6 *in vivo* binding data with predicted URS1 motifs, a chromatin immunoprecipitation (ChIP) assay and genetic experiments, to demonstrate that Rpd3 and Ume6 are needed to repress *BOI1*'s meiotic isoform in cells undergoing rapid mitotic growth. Finally, we report that increasing levels of the 5′-extended *BOI1* transcript correlate with declining levels of Boi1 protein as cells transit from fermentation to respiration and sporulation. These results provide insight how Boi1's mitotic mechanism of regulation is altered during meiotic development, and they provide initial evidence that the HDAC Rpd3/Ume6 complex negatively regulates Boi1.

Results

BOI1 encodes a transcript isoform with an extended 5′-UTR expressed in early meiosis but not vegetative growth and starvation

We used tiling array data to determine the transcript architecture of *BOI1* and *BOI2* in fermenting, respiring, and sporulating diploid *MAT***a**/α cells as compared to a sporulation-deficient starving *MAT*α/α control strain and vegetatively growing haploid *MAT***a** cells (Lardenois *et al*., 2011). For *BOI1* we find that wild-type *MAT***a**/α cells express a transcript isoform with an extended 5′-UTR from meiotic pro-phase onwards, while starving control cells and synchronously growing haploid cells do not express this long transcript at any point during prolonged nutrient deprivation or the mitotic cell cycle. The extended isoform entirely covers the ARS202 origin of replication (Fig. 1A). We were unable to investigate *BOI2* because the gene is juxtaposed to *SPR6*, which is highly expressed during growth and starvation, and encodes a transcript strongly

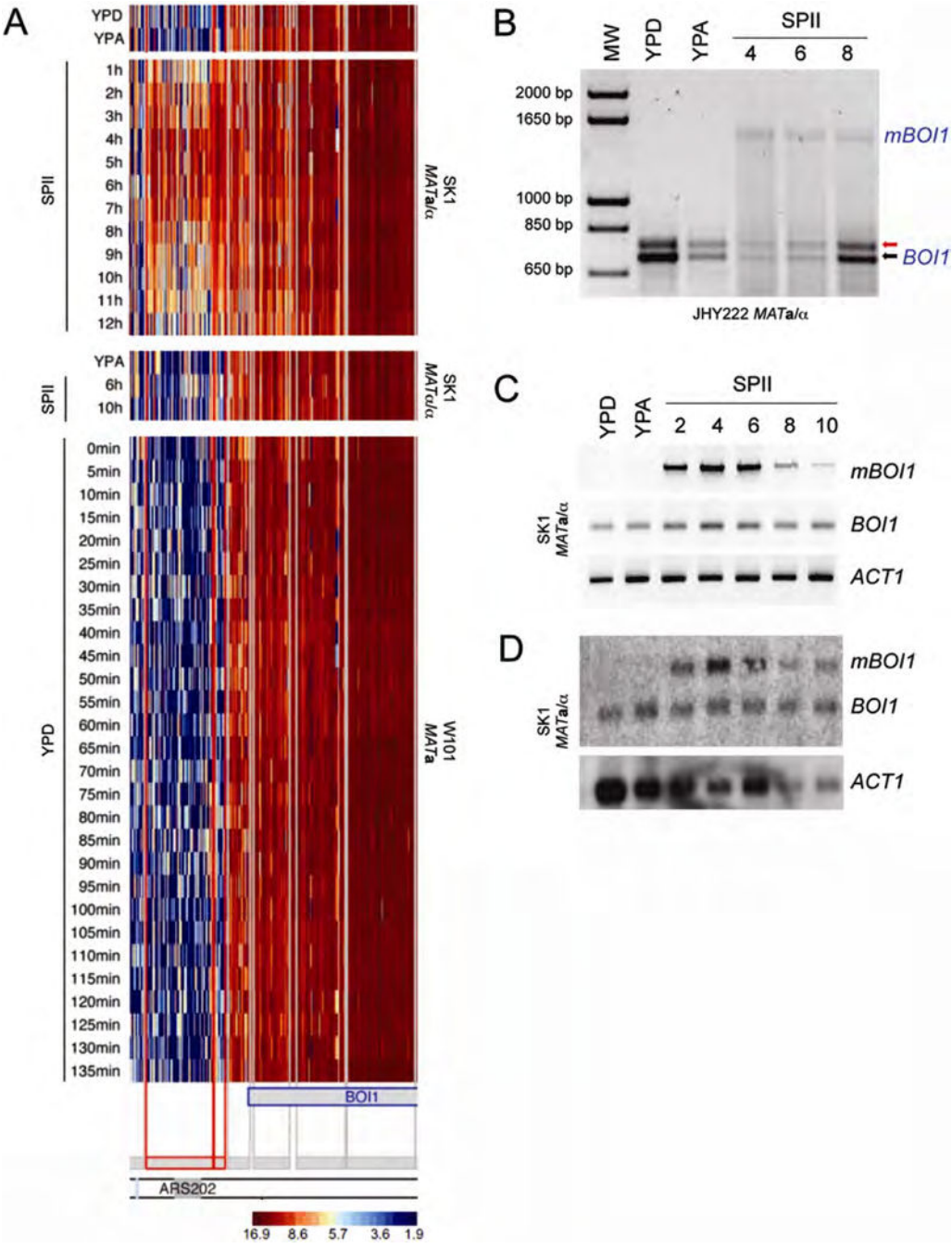

induced during sporulation that covers the *BOI2* upstream region (Fig. S1).

Cells express two BOI1 isoforms when progressing from mitotic growth to meiotic differentiation

Neither tiling array data nor RNA-Seq data reveal if cells co-express the short mitotic isoform and the long meiotic isoform during sporulation, or if the 5′-extended transcript becomes the dominant mRNA. This is, however, an interesting question from a functional perspective since the long isoform was predicted to inhibit protein translation (Brar *et al.*, 2012). If that mechanism was solely responsible for the protein pattern observed, one might expect cells to predominantly express the extended transcript. We therefore used 5′-rapid amplification of cDNA ends (5′-RACE) assays to study isoform levels and found that fermenting and respiring cells

express the short mitotic isoform, while cells during early meiosis (SPII 4–6 hours) express both the 5′-extended and the short mitotic isoform; post-meiotic cells (SPII 8 hours) slowly start reverting back to the mitotic pattern (Fig. 1B). Unexpectedly, we observed two bands for *BOI1*. We therefore determined by DNA sequencing that the faster migrating band indeed corresponded to *BOI1* (272/273 bases identical, Fig. S2A and B), while the slower band was amplification artefact unrelated to the target gene, perhaps stemming from GC-rich sequences in the yeast genome (Fig. S2C). Next, we confirmed the 5′-RACE data by Northern blotting using probes that monitor isoforms in combination with RT-PCR assays that validate array data (Fig. 1C–D). We conclude that vegetatively growing cells express only the short mitotic isoform, while in early meiotic cells the 5′-extended isoform is transiently induced reaching peak levels at 4–6 hours.

Meiosis-deficient mutants fail to normally induce the long isoform of BOI1

We then sought to complement tiling array data by RNA-Seq and confirmed that diploid *MAT***a**/α cells express a 5′-extended *BOI1* isoform from early meiosis onwards. Consistently, the transcript levels decrease as cells exit M-phase and enter spore formation. As expected, starving *MAT*α/α cells do not express the meiotic isoform, and do not downregulate *BOI1* eight hours after having been transferred into sporulation medium (Fig. 2A; the complete dataset will be published elsewhere; Becker *et al*., in preparation). We next asked if a strain lacking the 3′–5′ exoribonuclease Rrp6, which fails to undergo efficient meiosis and spore formation, expresses the *BOI1* isoform when cultured in sporulation medium (Lardenois *et al*., 2011). Tiling array data indicate that the meiotic isoform of *BOI1* is expressed at lower levels in cells lacking Rrp6 (Fig. 2B; the complete dataset will be published elsewhere; Stuparevic and Liu *et al*., in preparation). We confirmed this finding by RT-PCR assays carried out with samples from wild-type cells and an *rrp6* mutant strain cultured in rich media and sporulation medium (Fig. 2C). Taken together, the results show that the 5′-extended isoform of *BOI1* is only induced to normal levels when cells undergo efficient meiotic development, and that nutrient deprivation alone is not sufficient to fully de-repress the extended isoform.

The BOI1 upstream region contains a predicted URS1 motif

BOI1's isoform shows an expression pattern reminiscent of early meiotic genes and Ume6, a mitotic repressor of meiotic genes, was found to bind to the *BOI1* promoter *in vivo* in a high-throughput chromatin immunoprecipitation assay (Fig. S3; Harbison *et al*., 2004); see also www.germonline.org (Lardenois *et al*., 2010)). Consequently, we examined the locus using PWMs (Fig. 3A) and found a predicted URS1 element just upstream of the putative meiotic transcription start site (meiTSS) for *BOI1*'s developmental-stage specific isoform (Fig. 3B). This target motif is strongly bound by Ume6 *in vivo* as shown by a chromatin immunoprecipitation (ChIP) assay; the *NUP85* locus was used as a negative control (Fig. 3C) (Lardenois *et al*., 2014). Our data are consistent with the notion that Ume6 and, by inference, its interactors Rpd3 and Sin3 are recruited to the *BOI1* promoter region during vegetative growth.

Rpd3 and Ume6 repress the 5′-extended meiotic isoform of BOI1 in mitosis

The long *BOI1* isoform showed the pattern of a typical Rpd3/Sin3/Ume6-dependent early meiotic gene, and Ume6 binds *in vivo* to the *BOI1* upstream region, which contains a predicted URS1 motif. We therefore hypothesized that Ume6 and Rpd3 repress the meiotic isoform during mitotic growth. First, we sought to further validate the tiling array data and RNA-Seq data using RT-PCR and different combinations of oligonucleotide primer pairs to analyse RNA samples from diploid wild-type SK1 and JHY222 strains (Fig. 3D). Primers located in the 5′-UTR (*mBOI1*) revealed no signal in an SK1 sample from fermenting cells (YPD), a weak signal in a sample from respiring cells (YPA), strong signals during early meiosis (SPII 2–4 h), and decreasing signals during post-meiotic spore formation (SPII 8–12 h; Fig. 3E). We then repeated the experiment using wild-type JHY222 cells, which sporulate well but not quite as fast and as efficient as SK1 cells, to assess the degree of reproducibility of our results between distinct genetic backgrounds (Lardenois *et al*., 2011). We find a similar pattern except for a stronger signal in respiring cells and a broader peak of induction (Fig. 3F). Then, we confirmed that *BOI1* encodes an extended isoform rather than two overlapping transcripts being transcribed on the same strand in the same direction. To this end, we carried out an RT-PCR assay with a primer pair located at the 5′ and 3′ ends of the locus, which generate a long DNA fragment (*lmBOI1*). This experiment nearly perfectly reproduced the pattern observed in SK1 (compare panels E and F). Primers located within the coding region (*BOI1*) yielded the expected homogenous pattern in all samples. We employed *ACT1* as a loading control.

Importantly, we found that SK1 mutant *ume6* and *rpd3* cells and JHY2223 mutant *ume6* cells express the extended transcript during vegetative growth in the presence of glucose or acetate. Moreover, the mutant cells

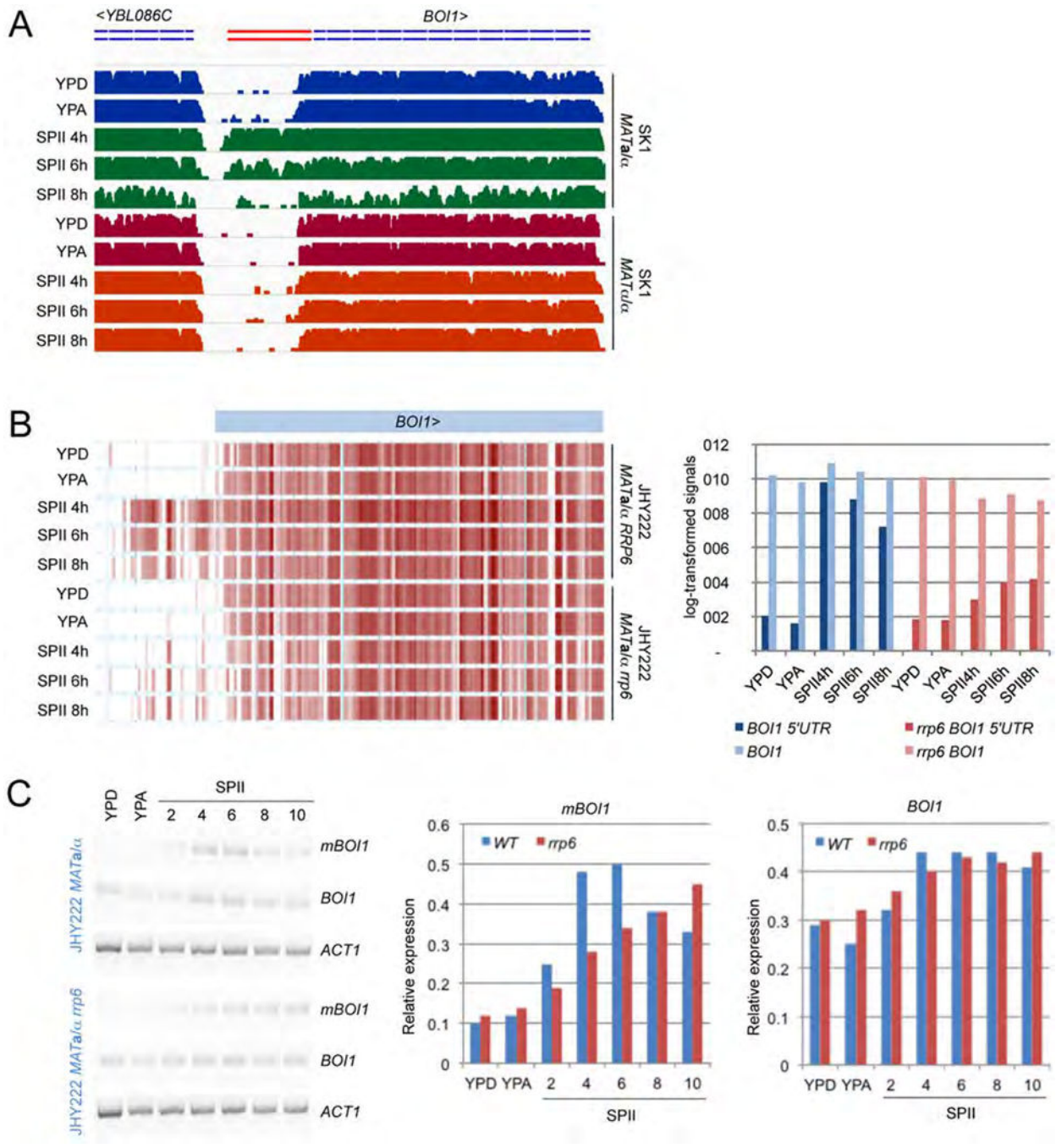

Fig. 2. Lack of normal *mBOI1* induction in sporulation-impaired cells.
A. Histograms depicting RNA-Seq data (not DNA strand specific) obtained with SK1 strains are shown. RNA was analysed from fermenting (YPD), respiring (YPA) and sporulating (SPII 4, 6, 8 hours) cells as indicated. Mitotic and meiotic samples from the wild-type strain are given in blue and green, respectively. Corresponding samples from the control strain are shown in red and orange. Thin dotted blue lines represent the ORFs, and a red dotted line represents the extended 5′-UTR as determined by DNA strand specific tiling arrays.
B. A heatmap (left panel) is shown for tiling array data obtained with wild-type and *rrp6* mutant cells cultured in growth media and sporulation medium as indicated. The strains are indicated to the right. A color-coded bar diagram (right panel) quantifies log-transformed tiling array signals for the segments that correspond to the ORF (*BOI1*) or the extended UTR (*BOI1* 5′UTR; y-axis) in wild-type cells (blue) versus *rrp6* mutant cells (red) that were cultured in growth media (YPD, YPA) and sporulation medium (SPII) at three time points as indicated.
C. To the left, the output of RT-PCR assays is shown for samples indicated at the top from wild-type versus *rrp6* mutant strains indicated to the left. Data are given for the mitotic isoform (*BOI1*), and the meiotic isoform (*mBOI1*). *ACT1* was used as a loading control. To the right, two bar diagrams summarize the RT-PCR band's relative signal intensities (y-axis) for each sample from wild-type cells (WT in blue) and mutant cells (*rrp6* in red; x-axis). Signals corresponding to the extended 5′-UTR (*mBOI1*) and the ORF (*BOI1*) are shown. The samples were harvested after incubation in rich media (YPD, YPA) and sporulation medium (SPII) at the time points given in hours (x-axis).

© 2015 John Wiley & Sons Ltd,

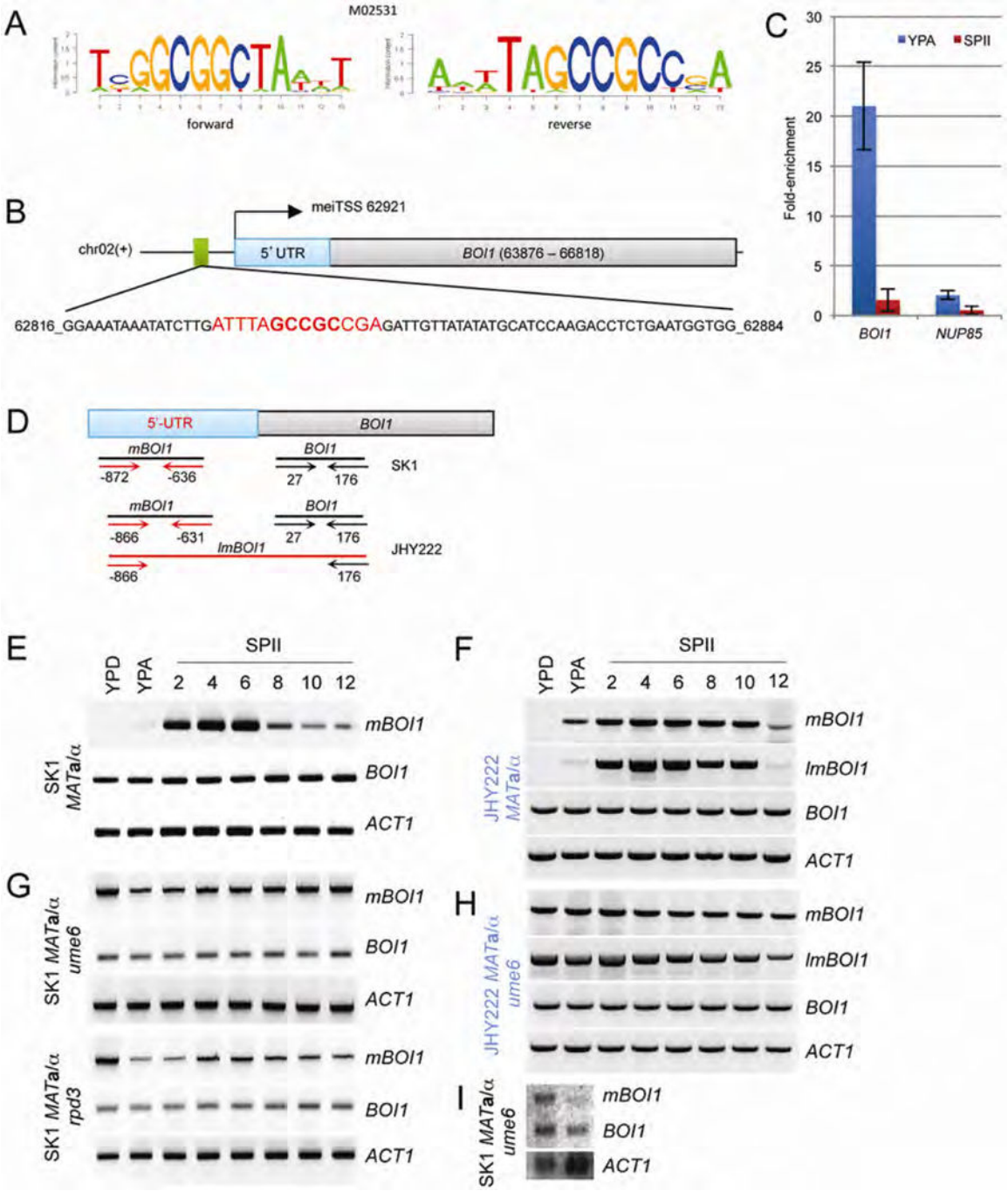

also failed to induce the isoform when cultured in sporulation medium (Fig. 3G and H). Finally, we complemented the RT-PCR data by a Northern blot showing that both short and long isoforms are present in *ume6* mutant cells cultured in YPD and YPA; we note that the long isoform is weaker in respiring SK1 *ume6* cells (compare panels G and I). Taken together, the data imply that the HDAC repressor complex Rpd3/Sin3/Ume6 represses the meiotic *BOI1* isoform during mitotic growth.

The Boi1 protein rapidly declines when cells switch from fermentation to respiration and sporulation

The 5′-extension of *BOI1*'s isoform harbours a uORF, which was predicted to downregulate Boi1 protein translation during meiosis and spore formation (Brar *et al.*, 2012). To further study this question, we tagged Boi1 with a C-terminal myc epitope. The diploid Boi1^{myc} strain showed no discernible growth phenotype, we therefore conclude

Fig. 3. URS1 motif prediction and Rpd3/Ume6 function in *mBOI1* control.
A. Logos show the forward and reverse DNA sequences of a PWM (M02531) for the JASPAR URS1 motif provided by TRANSFAC.
B. A schematic shows the predicted URS1 site (green rectangle), the 5′-UTR (light blue) and the ORF (light grey). A black line represents DNA. The chromosome number, the DNA strand (+), and the genome coordinates of the meiotic transcription start site (TSSmei) and *BOI1* in the reference strain S288C are shown. The match to the PWM is given in red, the core URS1 motif is shown in bold.
C. A bar diagram shows the fold enrichment (y-axis) in a ChIP assay of Ume6 *in vivo* binding to *BOI1* and the *NUP85* control observed in cells cultured in YPA (blue) and SPII at 3 hours (red). An error bar is given.
D. A schematic shows the 5′-UTR and ORF as blue and grey rectangles, respectively. Diagnostic PCR fragments are indicated as red and black lines covering different isoforms. Arrows represent forward and reverse PCR primers for which the coordinates are given in bp in each strain background.
E, F. The results of RT-PCR assays for SK1 and JHY222 wild-type strains are given for mitotic transcripts and meiotic isoforms. To reveal the meiotic isoform we employed two primer combinations that reveal the extended 5′-mUTR (*mBOI1*) or the long isoform (*lmBOI1*) as indicated. *ACT1* was used as a loading control.
G, H. Data are shown for *rpd3* and *ume6* mutants in SK1 and a *ume6* mutant in JHY222. All strains are diploid (*MAT***a**/α).
I. A Northern blot is shown for the meiotic (*mBOI1*) and mitotic (*BOI1*) isoforms in *ume6* mutant cells grown in YPD (lane 1) and YPA (lane 2). *ACT1* was used as a loading control.

that the protein is functional within the limits of our assay. An RT-PCR assay of samples from this strain revealed constitutive expression of *BOI1* during growth and development, moderate expression of *mBOI1* in respiring cells (YPA), and the expected induction pattern during sporulation (SPII; Fig. 4A, top panel). The corresponding time-course experiment revealed an approximately 3.5-fold decrease of Boi1 when cells change from glucose metabolism to using acetate as the sole non-fermentable carbon source. Furthermore, the protein is undetectable by Western blot in protein extracts from cells cultured in sporulation medium for two hours, and it remains absent until spore formation is initiated at 10 hours (in the W303 background; Fig. 4A, bottom panel). We then compared this pattern of protein levels to the one reported for Ume6, by including a late time point at 24 hours covering spore maturation and found that Boi1 did not re-accumulate at late stages of yeast gametogenesis like Ume6 (Fig. 4B; Mallory *et al*., 2007). Pgk1 was used as a loading control. Our results show that the Boi1 protein is indeed downregulated at the post-transcriptional level in respiring cells and differentiating cells until late stages of spore maturation, which is consistent with the prediction by Brar *et al*. that a uORF present in the long isoform inhibits protein translation.

The Boi1 level decreases and the protein is altered in fermenting ume6 mutant cells

Our RT-PCR data and protein data in JHY222 negatively correlate the induction of *BOI1*'s meiotic isoform with Boi1 protein levels in a dose dependent manner (in YPD, YPA and SPII 2 h). If the long isoform indeed inhibited protein translation, mutant cells that de-repress the meiotic isoform in mitosis should contain little or no Boi1 protein. To test this idea, we myc-tagged Boi1 in a *ume6* deletion strain, and monitored *BOI1* transcript isoforms and Boi1 protein levels in rich medium with glucose (YPD). The meiotic isoform is de-repressed in *ume6* cells cultured in YPD also in the W303 background (Fig. 4C left panel). Furthermore, we observe in three independent experiments that the concentration of Boi1 protein is indeed reduced approximately 10-fold in fermenting cells that lack Ume6 (Fig. 4C right panel). In addition, we find that Boi1 appears to be physically altered such that it migrates slower in the gel; no such change in migration was observed in the case of Pgk1 (Fig. 4C, right panel). Our finding that fermenting *ume6* mutant cells contain very little Boi1 provides further evidence that the long isoform is negatively correlated with protein levels.

We then asked if the extended 5′-UTR contained an in-frame ATG start codon indicating that the long isoform might be translated into a larger protein with an N-terminal extension, but found several stop codons in frame with *BOI1* (Fig. S4). Furthermore, we predict one uORF encoding a peptide of 45 amino acids 5 bases downstream of the mTSS (Fig. 4D), which is in keeping with previous observations (Brar *et al*., 2012). We conclude that an increased level of *mBOI1* in vegetatively growing mutant *ume6* cells correlates with a very low level of Boi1, and that the altered migration properties of Boi1 in fermenting cells lacking Ume6 are not due to an extended N-terminus.

Discussion

In this study we classify *BOI1*'s extended transcript as early meiosis-specific in the context of a broader expression program we have recently discovered using DNA strand specific tiling arrays (Lardenois *et al*., 2011; 2014). *BOI1* was initially not identified as a candidate for the expression of 5′-extended isoforms by the segmentation algorithm we employed, because of the convoluted expression signals associated with its 5′-leader sequence. However, additional information from RNA-Sequencing data (Becker *et al*., in preparation), RT-PCR and 5′-RACE assays and a Northern blot experiment enabled us to clarify the issue. We note that in the course of this work Brar *et al*. reported that *BOI1* (but not *BOI2*) encodes a transcript containing a

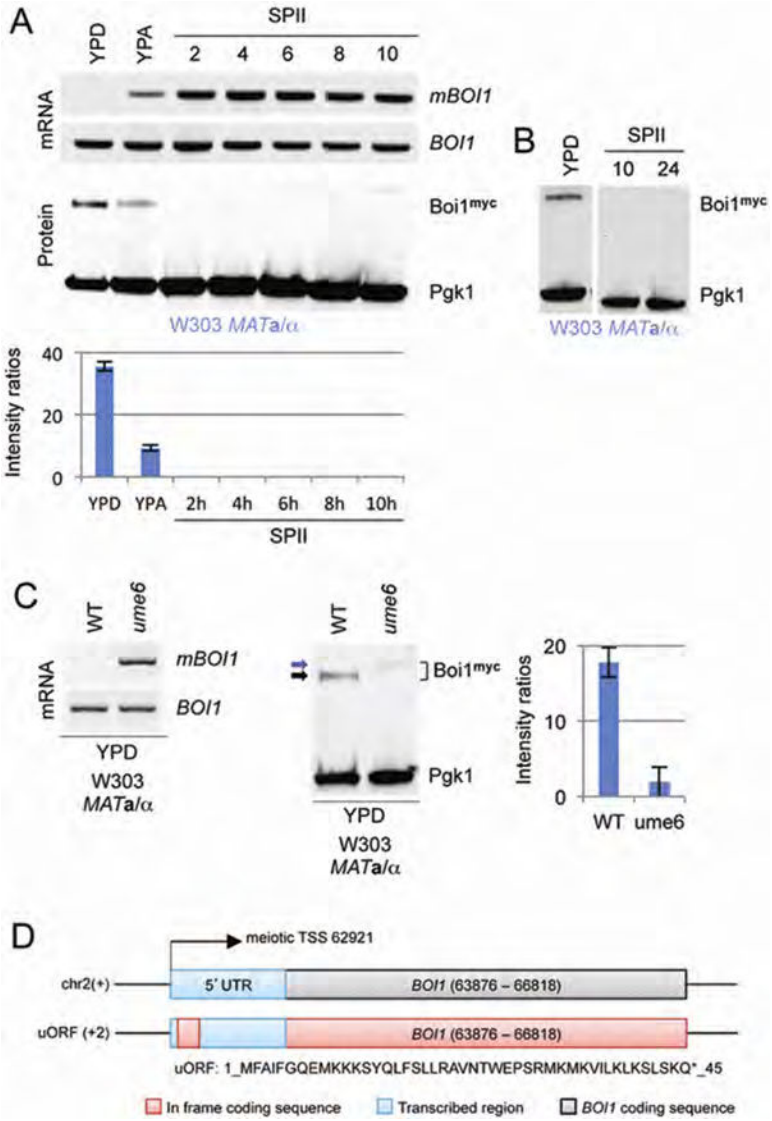

Fig. 4. Analysis of Boi1 protein levels.
A. In the top panel, the output of an RT-PCR assay of the meiotic isoform (*mBOI1*) and the mitotic isoform in wild-type cells cultured in rich media with glucose or acetate (YPD, YPA), or sporulation medium (SPII) at bi-hourly time points from 2–10 hours is shown. The bottom panel shows a Western blot for C-terminally myc-tagged Boi1 (Boi1^{myc}). Pgk1 was used as a loading control. The strain background is given and mRNA or protein data are indicated to the left. A histogram with error bars showing the standard deviation (SD) depicts samples (x-axis) versus Boi1^{myc}/Pgk1 intensity ratios (y-axis).
B. A Western blot analysis of tagged Boi1 (Boi1^{myc}) in wild-type (WT) cells versus mutant (*ume6*) cells cultured in rich media with glucose (YPD) is shown. The strain backgrounds are indicated. Black and blue arrows mark the fast and slow migrating forms of Boi1, respectively. Band intensities are shown as bar diagrams. An SD error bar is given.
C. A schematic shows the *BOI1* locus with its UTR (blue) and ORF (grey) at the top and a 45 amino acid uORF in frame with the main ORF in red at the bottom. Black lines represent the DNA strands. An arrow indicates the meiotic transcription start site (TSS). The chromosome number and genome coordinates are given.

meiotic 5′-extension, which was predicted to negatively regulate protein translation in sporulating cells via a uORF (Brar *et al*., 2012).

BOI1 is a prototype locus for studying the regulation and function of developmental stage specific transcript isoforms

Following a yeast genome duplication event, identical gene pairs – called paralogs – evolved in different ways. Either one of the loci was lost, or each paralog acquired different roles for example in mitosis or meiosis, or both genes fulfil partially redundant functions, which is the case for *BOI1* and *BOI2* (Dahmann and Futcher, 1995; Dietrich *et al*., 2004; Kellis *et al*., 2004). The genes share no synteny, as opposed to other genome regions such as those containing for example *VTH1* and *VTH2*, for which the orientation of neighbouring genes located up-stream and down-stream is conserved (see the Saccharomyces Genome Database (SGD) at www.yeastgenome.org and the Saccharomyces Genomics Viewer (SGV) at www.germonline.org; Lardenois *et al*., 2010)). The intergenic region between *BOI1* and the upstream ORF *YBL086C* is relatively large (1274 bp in S288C), while *BOI2*'s upstream region comprises 580 bp and appears to be mostly covered by the mRNA encoded by *SPR6* (see Fig. S1). The distinct pattern of synteny is not relevant for Boi1/Boi2 protein function during mitosis, since they are regulated at the post-translational level, and no role has been found in meiosis (Bender *et al*., 1996; Matsui *et al*., 1996; Norden *et al*., 2006). However, our results mark out *BOI1* as a useful model locus to study the regulation and, ultimately,

the possible function of 5′-extended isoforms in the control of protein translation during growth and development.

How is Boi1 downregulated at the post-transcriptional level during meiosis and spore formation?

Based on a recent ribosome profiling study and our Western blot data in wild-type cells and a *ume6* mutant strain, we speculate that *BOI1* may at least in part be negatively controlled at the level of translation when cells induce the developmentally regulated isoform harbouring an upstream open reading frame (uORF; Brar *et al.*, 2012). Such uORFs are present in UTRs throughout the yeast genome (Zhang and Dietrich, 2005). For the well-studied *GCN4* locus, it was shown that uORFs act as competitive inhibitors preventing the translation of the down-stream ORF via a mechanism called reinitiation (Hinnebusch, 2005; Gunisova and Valasek, 2014). Such a mode of regulation is consistent with the presence of uORFs in the extended *BOI1* 5′-UTR, and our finding that *ume6* cells grown in YPD, which de-repress the meiotic isoform, contain very little Boi1.

We noticed that the protein migrates slower in the absence of Ume6 than in wild-type cells. This might be a consequence of protein modification rendering it unstable or somehow unable to fold correctly, which would make it a target for the unfolded protein response pathway (Schroder *et al.*, 2000). An alternative – or rather additional – explanation to isoform-mediated translational control is that Boi1 becomes unstable in cells growing in the presence of acetate and gets rapidly degraded by a target-specific protease in cells as they initiate meiosis; this would also explain why the cells do not appear to completely switch from the short to the long isoform during meiosis. Such a two-step mechanism was found to downregulate Ume6 levels during respiration and early/middle meiosis (Mallory *et al.*, 2007; Law *et al.*, 2014). Interestingly, while Ume6 in *S. cerevisiae* appears to be regulated via protein stability during growth and development (Mallory *et al.*, 2007; 2012; Law *et al.*, 2014), the orthologous protein in the human pathogen *C. albicans* is negatively controlled via its 5′-UTR when cells switch to filamentous growth (Childers *et al.*, 2014).

A complex mechanism involving the conserved HDAC complex Rpd3/Sin3/Ume6 regulates Boi1 during growth and development

A large-scale *in vivo* binding assay revealed that Ume6 binds to the *BOI1* upstream region but this interaction did not have the same effect as in the cases of early meiotic genes that are, contrary to *BOI1*, repressed during mitotic growth (Harbison *et al.*, 2004). An obvious explanation for this result – given that we identified a URS1 motif bound by Ume6 *in vivo* at the 5′-end of the isoform, and that growing *rpd3* and *ume6* mutant cells de-repress the isoform – is that the Rpd3/Sin3/Ume6 HDAC complex shuts down the transcription of *BOI1*'s meiotic isoform in mitosis. In the presence of acetate, cells partially degrade Ume6, which enables the long isoform to accumulate. Once cells have initiated meiosis, Ume6 is destroyed and the extended isoform is fully induced during early and middle meiosis, while the mitotic isoform continues to be detectable. A similar regulatory mechanism controls meiotic isoforms encoded by *CFT2* and *RTT10*; however, in these cases proteins levels do not decline, but rather increase when cells progress from respiration to sporulation (Fig. 5); (Lardenois *et al.*, 2014). This underlines how important it is to experimentally validate predicted 5′-UTR functions at the molecular level in follow-up studies. As

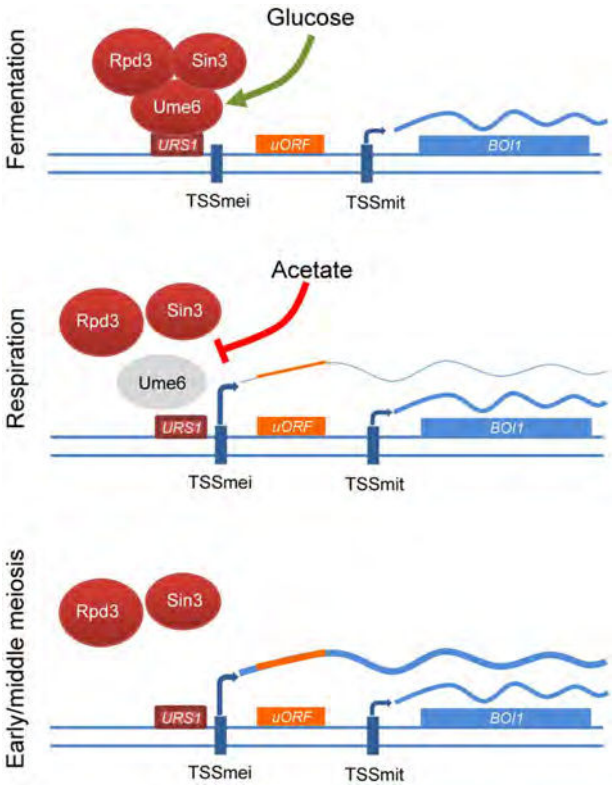

Fig. 5. A model for the regulation of *BOI1*. The model is based on large-scale *in vivo* Ume6 DNA-binding data from reference (Harbison *et al.*, 2004) and our own results. The Rpd3/Sin3/Ume6 repressor complex is shown during fermentation (top) and respiration/sporulation (bottom) where the DNA binding subunit Ume6 is temporarily degraded in the presence of acetate (Mallory *et al.*, 2007). Blue arrows symbolize transcription start sites active during mitosis (TSSmit) or meiosis (TSSmei). A red rectangle represents the URS1 motif. A black line is DNA. ORF and uORFs are represented by blue and orange rectangles, respectively. mRNAs are shown as blue lines of varying thickness depending on the expression level.

Table 1. Yeast strains.

Strain ID	Genotype	Reference
MPY1	JHY222 *MAT***a**/*MATα HAP1*/*HAP1 MKT1*(D30G)/*MKT1*(D30G) *RME1*(INS 308A)/*RME1*(INS 308A) *TAO3*(E1493Q)/*TAO3*(E1493Q)	(Lardenois *et al.*, 2011)
MPY392	JHY222 *MAT***a**/*MATα HAP1*/*HAP1 MKT1*(D30G)/*MKT1*(D30G) *RME1*(INS 308A)/*RME1*(INS 308A) *TAO3*(E1493Q)/*TAO3*(E1493Q) *rrp6*::*kanMX4*/*rrp6*::*kanMX4*	(Lardenois *et al.*, 2011)
MPY70	SK1 *MAT***a**/*MATα ho*::*LYS2*/*ho*::*LYS2 ura3*/*ura3 lys2*/*lys2 leu2*::*hisG*/*leu2*::*hisG arg4-Nsp*/*arg4-Bgl his4x*::*LEU2-URA3*/*his4B*::*LEU2*	(Primig *et al.*, 2000)
MPY309	SK1 *MATα*/ *MATα ho*::*LYS2*/*ho*::*LYS2 ura3*/*ura3 lys2*/*lys2*	(Lardenois *et al.*, 2011)
MPY454	W101 *MAT***a** *ho*::*lys5 gal2*	(Granovskaia *et al.*, 2010)
MPY441	SK1 *MAT***a**/*MATα ho*::*hisG*/*ho*::*hisG lys2*/*lys2 ura3*/*ura3 leu2*::*hisG*/*leu2*::*hisG arg4-Nsp*/*arg4-Bgl his4x*::*LEU2-URA3*/*his4B*::*LEU2 trp1*::*hisG*/*trp1*::*hisG rpd3*::*KanMX4*/*rpd3*::*KanMX4*	(Burgess *et al.*, 1999)
MPY542	JHY222 *MAT***a**/*MATα HAP1*/*HAP1 MKT1*(D30G)/*MKT1*(D30G) *RME1*(INS 308A)/*RME1*(INS 308A) *TAO3*(E1493Q)/*TAO3*(E1493Q) *ume6*::*KanMX4*/*ume6*::*KanMX4*	(Lardenois and Stuparevic *et al.*, 2014)
MPY702	SK1 *MAT***a**/*MATα ura3*/*ura3 leu2*/*leu2 trp1*/*trp1 lys2*/*lys2 ho*::*LYS2*/*ho*::*LYS2 gal80*::*LEU2*/*gal80*::*LEU2 ume6*::*TRP1*/*ume6*::*TRP1*	(Shimizu *et al.*, 2003)
MPY766	JHY222 *MAT***a**/*MATα HAP1*/*HAP1 MKT1*(D30G)/*MKT1*(D30G) *RME1*(INS 308A)/*RME1*(INS 308A) *TAO3*(E1493Q)/*TAO3*(E1493Q) *BOI1*/*BOI1*-Myc::*KanMX4*	This study
MPY769	W303 *MAT***a**/*MATα ade2*/*ADE2 can1-100*/*CAN1 CYH2*/*cyh2 his3-11,15*/*his3-11,15 LEU1*/*leu1-c LEU2*/*leu2-3,112 trp1-1*::*URA3*::*trp1-3′D*/*trp1-1 ura3-1*/*ura3-1 BOI1*/*BOI1*-Myc::*KanMX4*	This study
MPY770	W303 *MAT***a**/*MATα ade2*/*ade2 ade6*/*ADE6 can1-100*/*can1ADE2:CAN1 his3-11,15*/*his3-11,15 leu2-3,112*/*leu2-3,112 trp1-1*/*trp1-1 ume6D1*/*ume6D1 ura3-1*/*ura3-1 BOI1*/*BOI1*-Myc::*KanMX4*	This study

far as *BOI1* is concerned, it is unclear what happens during late stages of spore formation but from tiling array data, RNA-Seq, Northern blotting, and 5′-RACE assays we conclude that after exiting meiotic M-phase cells progressively switch back to expressing only the short mitotic isoform. We speculate that the short isoform persists until late stages of sporulation because Boi1 – perhaps together with Boi2 – is important for the first round of mitosis immediately after germination (Joseph-Strauss *et al.*, 2007; Geijer *et al.*, 2012).

Our results provide initial insight into how *BOI1* expression is altered by a conserved HDAC complex when cells respond to nutritional cues. This is also the first case of an early meiotic isoform that negatively correlates with protein levels during initial stages of gametogenesis (Lardenois *et al.*, 2014). The HDAC Rpd3 is conserved during evolution, and a growing body of evidence shows that eukaryotic genes encode multiple isoforms (Nagalakshmi *et al.*, 2008; Yang and Seto, 2008; Waern and Snyder, 2013; Andersson *et al.*, 2014; Brown *et al.*, 2014; Haberle *et al.*, 2014). Therefore, our results likely have broad implications for flexible 5′-UTRs that influence protein levels during cell growth and cell differentiation in eukaryotes.

Experimental procedures

Yeast strains and media

The tiling array data were generated with sporulation competent SK1 *MAT***a**/α and sporulation deficient *MAT*α/α strains. RT-PCR validation experiments were carried out in SK1 *MAT***a**/α and JHY222 *MAT***a**/α strains as previously reported (Lardenois *et al.*, 2011). The induction of extended 5′-mUTR expression was analyzed in SK1 *MAT***a**/α *ume6* and *rpd3*, and JHY222 *MAT***a**/α *ume6* deletion strains (Table 1). Sporulation experiments were carried out using standard rich medium with glucose (YPD) or acetate (YPA) and sporulation medium (SPII).

Tiling array data

The molecular methods and bioinformatics approaches used for raw data processing and normalization and transcript identification were published in reference (Lardenois *et al.*, 2011).

RT-PCR

RT-PCR oligonucleotide primers were designed with Primer3 (simgene.com/Primer3). To take strain-specific mutations into account, we downloaded the *BOI1* open reading frame's DNA sequence from the Saccharomyces Genome Database (SGD; yeastgenome.org), and aligned it with the SK1 genome using the Saccharomyces Genome Resequencing Project (SGRP) browser (sanger.ac.uk/research/projects/genomeinformatics/sgrp.html). RT-PCR reactions were carried out using 2 µg of RNA reverse transcribed with Reverse Transcriptase (High Capacity cDNA Reverse Transcription kit; Life Technologies, USA) and amplified using Taq Polymerase (Qiagen, France) at 60°C for 26 cycles. DNA samples were separated on 2% agarose gels and photographed using an ImageQuant 350 digital Imaging System at the default settings (General Electric, USA). Primer sequences are given in Table 2.

5′-Rapid Amplification of cDNA Ends (5′-RACE) analysis

We used the 5′-RACE version 2.0 kit (Invitrogen). RNA integrity was verified by gel electrophoresis and the concentration was determined using a Nanodrop spectrophotometer

Table 2. RT-PCR primers.

Genes	Forward primers	Reverse primers	Size (bp)
BOI1	5′-CAAAGGGGCCAAATCTTTTC-3′	5′-AAATTGCGCCCATAATACCA-3′	150
mBOI1	5′-AGCCGCATGAAGATGAAAGT-3′	5′-CCGGAGAACACTCAAATTCC-3′	236 (SK1 237)
lmBOI1	5′-AGCCGCATGAAGATGAAAGT-3′	5′-AAATTGCGCCCATAATACCA-3′	1042 (SK1 1048)

(Thermo Scientific). First strand cDNA was synthesized using a gene-specific primer (GSP1) and SuperScript II reverse transcriptase, and the mRNA template was removed by treatment with RNase H and RNase T1. Unincorporated dNTPs, GSP1, and proteins were separated from cDNA using a S.N.A.P. Column. A homopolymeric tail was added to the 3′-end of the cDNA using Terminal deoxynucleotidyl Transferase and dCTP. DNA amplification was carried out with GSP2 and UAP (Universal Amplification Primer). The PCR products of the expected size were purified from the agarose gel and sequenced. The primer sequences are shown in Table 3.

Northern blotting

Total RNA samples were prepared from fermenting (YPD), respiring (YPA) and sporulating (SPII) diploid cells and further processed as published (Lardenois *et al*., 2014). Oligonucleotide sequences are shown in Table 4.

URS1 motif prediction

We searched for predicted URS1 sites in a 2 kb region ranging from 61876 to 63876 immediately upstream of *BOI1*. We used several PWMs (M01503, M01898 and M02531) provided by the TRANSFAC Professional database (Matys *et al*., 2006) and Jaspar (Mathelier *et al*., 2014). The *Match* tool was employed with minFP cut-offs scores. Among 10 sites predicted, we selected the one that was detected with the high quality matrix M02531. The motif logo was generated with R *seqLogo* package (Bembom).

Table 3. 5′-RACE primers.

Gene	Reverse primer
BOI1 GSP1	5′-TGGTCTTTGCAATTCTGTGG-3′
BOI1 GSP2	5′-TCGTGTTTTCCTCATTTCTGG-3′
BOI1 sequencing	5′-AAATTGCGCCCATAATACCA-3′

Chromatin immunoprecipitation (ChIP) assay

In vivo Ume6 binding to the URS1 motif present in the *BOI1* up-stream region was assayed as published (Lardenois *et al*., 2014). Oligonucleotides used are shown in Table 5. Oligonucleotides used for the *NUP85* control are published in (Lardenois *et al*., 2014).

Analysis of the BOI1 5′-UTR

We extracted the DNA sequence corresponding to the 5′-UTR according to the boundaries of the segmentation algorithm in S288C on chromosome2 (chr02+: 62921–63876). The Expasy tools (Artimo *et al*., 2012) and ORF Finder (Rombel *et al*., 2002) were used to identify ORFs with the classical genetic code, start and stop codons being required and the DNA length set at > 100 bp. An ORF at 62926–63063 was identified corresponding to a 45 amino acid peptide in frame with the annotated *BOI1* ORF.

Protein tagging

A one-step tagging method based on PCR was employed to construct a strain expressing Boi1 with a C-terminal myc tag using cassette plasmids and oligonucleotides as published (Wach *et al*., 1994; Janke *et al*., 2004). Colonies were first examined by diagnostic PCR for correct integration and then validated by Western blotting. Oligonucleotides used are shown in Table 6.

Table 4. Northern blot primers.

Genes	Forward primers	Reverse primers	Size (bp)
BOI1	5′-CGCATCAACAGGAGAACAGA-3′	5′-TCCGGAGACTTGATGCTCTT-3′	434
ACT1	5′-CTCGTGCTGTCTTCCCATCT-3′	5′-AGATGGACCACTTTCTGCGT-3′	1025

Table 5. ChIP primers.

Genes	Forward primers	Reverse primers	Size (bp)
BOI1	5′-GACCTCTGAATGGTGGCTAATTAAG-3′	5′-TTGCGAACATGATAGCAGTTA-3′	434

Table 6. Primers for C-terminal myc tagging.

Gene	Plasmid	Forward primer	Reverse primer	References
BOI1	pYM18	5′-GATTACCTGGAAAGTTCAGCAT TTGAATACCCTGGTGGCAGACT TCGTACGCTGCAGGTCGAC-3′	5′-AGGTGTTTAAGTTGGTCAAGA AGTAACTAATGATTGCAGTTCT CAATCGATGAATTCGAGCTCG-3′	(Wach *et al.*, 1994; Janke *et al.*, 2004)

Western blotting

Samples were prepared from fermenting (YPD), respiring (YPA) and sporulating (SPII) cells as previously described. 25 µg of total protein extract was run on a 4–20% gradient gel (BioRad, USA) for one hour. Proteins were transferred onto ImmobilonPSQ membranes (Millipore, France) using an electro-blotter (TE77X; Hoefer, USA) in modified Towbin buffer (48 mM Tris base, 40 mM glycine and 0.1% SDS) and methanol (20% vol/vol anode; 5% vol/vol cathode) for two hours. Tagged Boi1 was detected with a monoclonal anti-myc-HRP antibody (Life Technologies, USA) at 1:1000. The antibody was incubated in hybridization buffer overnight at 4°C. The signals were revealed using the ECL-Plus Chemiluminescence kit (GE Healthcare, USA) and the ImageQuant 350 system (GE Healthcare, USA). Band intensities determined using the ImageQuant TL 7.0 software set at default parameters. A rabbit polyclonal anti-Pgk1 antibody (Invitrogen, USA) was used as a loading control.

Acknowledgements

We thank Olivier Collin for providing us with access to the GenOuest bioinformatics infrastructure, and Olivier Sallou for system administration. Yuchen Liu received a 4th-year fellowship from FRM (FDT20100920148). This work was supported by the Région Bretagne CREATE grant (R11016NN), and SAD grant (R13124NN) awarded to M. Primig.

References

Andersson, R., Gebhard, C., Miguel-Escalada, I., Hoof, I., Bornholdt, J., Boyd, M., *et al.* (2014) An atlas of active enhancers across human cell types and tissues. *Nature* **507:** 455–461.

Artimo, P., Jonnalagedda, M., Arnold, K., Baratin, D., Csardi, G., de Castro, E., *et al.* (2012) ExPASy: SIB bioinformatics resource portal. *Nucleic Acids Res* **40:** W597–W603.

Bembom, O. (2014) seqLogo: Sequence logos for DNA sequence alignments. In.: Bioconductor, pp.

Bender, L., Lo, H.S., Lee, H., Kokojan, V., Peterson, V., and Bender, A. (1996) Associations among PH and SH3 domain-containing proteins and Rho-type GTPases in yeast. *J Cell Biol* **133:** 879–894.

Brar, G.A., Yassour, M., Friedman, N., Regev, A., Ingolia, N.T., and Weissman, J.S. (2012) High-resolution view of the yeast meiotic program revealed by ribosome profiling. *Science* **335:** 552–557.

Brown, J.B., Boley, N., Eisman, R., May, G.E., Stoiber, M.H., Duff, M.O., *et al.* (2014) Diversity and dynamics of the Drosophila transcriptome. *Nature* **512:** 393–399.

Burgess, S.M., Ajimura, M., and Kleckner, N. (1999) GCN5-dependent histone H3 acetylation and RPD3-dependent histone H4 deacetylation have distinct, opposing effects on IME2 transcription, during meiosis and during vegetative growth, in budding yeast. *Proc Natl Acad Sci USA* **96:** 6835–6840.

Childers, D.S., Mundodi, V., Banerjee, M., and Kadosh, D. (2014) A 5′ UTR-mediated translational efficiency mechanism inhibits the Candida albicans morphological transition. *Mol Microbiol* **92:** 570–585.

Chu, S., DeRisi, J., Eisen, M., Mulholland, J., Botstein, D., Brown, P.O., and Herskowitz, I. (1998) The transcriptional program of sporulation in budding yeast. *Science* **282:** 699–705.

Cole, K.C., Barbour, J.E., Midkiff, J.F., Marble, B.M., and Johnson, D.I. (2009) Multiple proteins and phosphorylations regulate Saccharomyces cerevisiae Cdc24p localization. *FEBS Lett* **583:** 3339–3343.

Dahmann, C., and Futcher, B. (1995) Specialization of B-type cyclins for mitosis or meiosis in S. cerevisiae. *Genetics* **140:** 957–963.

Deutschbauer, A.M., Williams, R.M., Chu, A.M., and Davis, R.W. (2002) Parallel phenotypic analysis of sporulation and postgermination growth in Saccharomyces cerevisiae. *Proc Natl Acad Sci USA* **99:** 15530–15535.

Dietrich, F.S., Voegeli, S., Brachat, S., Lerch, A., Gates, K., Steiner, S., *et al.* (2004) The Ashbya gossypii genome as a tool for mapping the ancient Saccharomyces cerevisiae genome. *Science* **304:** 304–307.

Enyenihi, A.H., and Saunders, W.S. (2003) Large-scale functional genomic analysis of sporulation and meiosis in Saccharomyces cerevisiae. *Genetics* **163:** 47–54.

Geijer, C., Pirkov, I., Vongsangnak, W., Ericsson, A., Nielsen, J., Krantz, M., and Hohmann, S. (2012) Time course gene expression profiling of yeast spore germination reveals a network of transcription factors orchestrating the global response. *BMC Genomics* **13:** 554.

Granovskaia, M.V., Jensen, L.J., Ritchie, M.E., Toedling, J., Ning, Y., Bork, P., *et al.* (2010) High-resolution transcription atlas of the mitotic cell cycle in budding yeast. *Genome Biol* **11:** R24.

Gunisova, S., and Valasek, L.S. (2014) Fail-safe mechanism of GCN4 translational control – uORF2 promotes reinitiation by analogous mechanism to uORF1 and thus secures its key role in GCN4 expression. *Nucleic Acids Res* **42:** 5880–5893.

Haberle, V., Li, N., Hadzhiev, Y., Plessy, C., Previti, C., Nepal, C., *et al.* (2014) Two independent transcription initiation codes overlap on vertebrate core promoters. *Nature* **507:** 381–385.

Harbison, C.T., Gordon, D.B., Lee, T.I., Rinaldi, N.J., Macisaac, K.D., Danford, T.W., *et al.* (2004) Transcriptional

regulatory code of a eukaryotic genome. *Nature* **431:** 99–104.
Hinnebusch, A.G. (2005) Translational regulation of GCN4 and the general amino acid control of yeast. *Annu Rev Microbiol* **59:** 407–450.
Janke, C., Magiera, M.M., Rathfelder, N., Taxis, C., Reber, S., Maekawa, H., *et al*. (2004) A versatile toolbox for PCR-based tagging of yeast genes: new fluorescent proteins, more markers and promoter substitution cassettes. *Yeast* **21:** 947–962.
Joseph-Strauss, D., Zenvirth, D., Simchen, G., and Barkai, N. (2007) Spore germination in Saccharomyces cerevisiae: global gene expression patterns and cell cycle landmarks. *Genome Biol* **8:** R241.
Kellis, M., Birren, B.W., and Lander, E.S. (2004) Proof and evolutionary analysis of ancient genome duplication in the yeast Saccharomyces cerevisiae. *Nature* **428:** 617–624.
Lardenois, A., Gattiker, A., Collin, O., Chalmel, F., and Primig, M. (2010) GermOnline 4.0 is a genomics gateway for germline development, meiosis and the mitotic cell cycle. *Database* **2010:** baq030.
Lardenois, A., Liu, Y., Walther, T., Chalmel, F., Evrard, B., Granovskaia, M., *et al*. (2011) Execution of the meiotic noncoding RNA expression program and the onset of gametogenesis in yeast require the conserved exosome subunit Rrp6. *Proc Natl Acad Sci USA* **108:** 1058–1063.
Lardenois, A., Stuparevic, I., Liu, Y., Law, M.J., Becker, E., Smagulova, F., *et al*. (2014) The conserved histone deacetylase Rpd3 and its DNA binding subunit Ume6 control dynamic transcript architecture during mitotic growth and meiotic development. *Nucleic Acids Res* **43:** 115–128.
Law, M.J., Mallory, M.J., Dunbrack, R.L., Jr, and Strich, R. (2014) Acetylation of the transcriptional repressor Ume6p allows efficient promoter release and timely induction of the meiotic transient transcription program in yeast. *Mol Cell Biol* **34:** 631–642.
Liao, Y., He, F., Gong, T., Bi, E., and Gao, X.D. (2013) Msb1 interacts with Cdc42, Boi1, and Boi2 and may coordinate Cdc42 and Rho1 functions during early stage of bud development in budding yeast. *PLoS ONE* **8:** e66321.
Lin, W., Wang, M., Jin, H., and Yu, H.G. (2011) Cohesin plays a dual role in gene regulation and sister-chromatid cohesion during meiosis in Saccharomyces cerevisiae. *Genetics* **187:** 1041–1051.
Mallory, M.J., Cooper, K.F., and Strich, R. (2007) Meiosis-Specific Destruction of the Ume6p Repressor by the Cdc20-Directed APC/C. *Mol Cell* **27:** 951–961.
Mallory, M.J., Law, M.J., Sterner, D.E., Berger, S.L., and Strich, R. (2012) Gcn5p-dependent acetylation induces degradation of the meiotic transcriptional repressor Ume6p. *Mol Biol Cell* **23:** 1609–1617.
Mathelier, A., Zhao, X., Zhang, A.W., Parcy, F., Worsley-Hunt, R., Arenillas, D.J., *et al*. (2014) JASPAR 2014: an extensively expanded and updated open-access database of transcription factor binding profiles. *Nucleic Acids Res* **42:** D142–D147.
Matsui, Y., Matsui, R., Akada, R., and Toh-e, A. (1996) Yeast src homology region 3 domain-binding proteins involved in bud formation. *J Cell Biol* **133:** 865–878.
Matys, V., Kel-Margoulis, O.V., Fricke, E., Liebich, I., Land, S., Barre-Dirrie, A., *et al*. (2006) TRANSFAC and its module TRANSCompel: transcriptional gene regulation in eukaryotes. *Nucleic Acids Res* **34:** D108–D110.
Nagalakshmi, U., Wang, Z., Waern, K., Shou, C., Raha, D., Gerstein, M., and Snyder, M. (2008) The transcriptional landscape of the yeast genome defined by RNA sequencing. *Science* **320:** 1344–1349.
Norden, C., Mendoza, M., Dobbelaere, J., Kotwaliwale, C.V., Biggins, S., and Barral, Y. (2006) The NoCut pathway links completion of cytokinesis to spindle midzone function to prevent chromosome breakage. *Cell* **125:** 85–98.
Pigula, A., Drubin, D.G., and Barnes, G. (2014) Regulation of Mitotic Spindle Disassembly by an Environmental Stress-Sensing Pathway in Budding Yeast. *Genetics* **198:** 1043–1057.
Primig, M., Williams, R.M., Winzeler, E.A., Tevzadze, G.G., Conway, A.R., Hwang, S.Y., *et al*. (2000) The core meiotic transcriptome in budding yeasts. *Nat Genet* **26:** 415–423.
Rombel, I.T., Sykes, K.F., Rayner, S., and Johnston, S.A. (2002) ORF-FINDER: a vector for high-throughput gene identification. *Gene* **282:** 33–41.
Rundlett, S.E., Carmen, A.A., Suka, N., Turner, B.M., and Grunstein, M. (1998) Transcriptional repression by UME6 involves deacetylation of lysine 5 of histone H4 by RPD3. *Nature* **392:** 831–835.
Schroder, M., Chang, J.S., and Kaufman, R.J. (2000) The unfolded protein response represses nitrogen-starvation induced developmental differentiation in yeast. *Genes Dev* **14:** 2962–2975.
Shimizu, M., Takahashi, K., Lamb, T.M., Shindo, H., and Mitchell, A.P. (2003) Yeast Ume6p repressor permits activator binding but restricts TBP binding at the HOP1 promoter. *Nucleic Acids Res* **31:** 3033–3037.
Spivak, A.T., and Stormo, G.D. (2012) ScerTF: a comprehensive database of benchmarked position weight matrices for Saccharomyces species. *Nucleic Acids Res* **40:** D162–D168.
Strich, R., Surosky, R.T., Steber, C., Dubois, E., Messenguy, F., and Esposito, R.E. (1994) UME6 is a key regulator of nitrogen repression and meiotic development. *Genes Dev* **8:** 796–810.
Toya, M., Iino, Y., and Yamamoto, M. (1999) Fission yeast Pob1p, which is homologous to budding yeast Boi proteins and exhibits subcellular localization close to actin patches, is essential for cell elongation and separation. *Mol Biol Cell* **10:** 2745–2757.
Wach, A., Brachat, A., Pohlmann, R., and Philippsen, P. (1994) New heterologous modules for classical or PCR-based gene disruptions in Saccharomyces cerevisiae. *Yeast* **10:** 1793–1808.
Waern, K., and Snyder, M. (2013) Extensive transcript diversity and novel upstream open reading frame regulation in yeast. *G3 (Bethesda)* **3:** 343–352.
Wingender, E. (2008) The TRANSFAC project as an example of framework technology that supports the analysis of genomic regulation. *Brief Bioinform* **9:** 326–332.
Xie, Z., Hu, S., Qian, J., Blackshaw, S., and Zhu, H. (2011) Systematic characterization of protein-DNA interactions. *Cell Mol Life Sci* **68:** 1657–1668.
Yang, X.J., and Seto, E. (2008) The Rpd3/Hda1 family of lysine deacetylases: from bacteria and yeast to mice and men. *Nat Rev Mol Cell Biol* **9:** 206–218.

Zhang, Z., and Dietrich, F.S. (2005) Identification and characterization of upstream open reading frames (uORF) in the 5′ untranslated regions (UTR) of genes in Saccharomyces cerevisiae. *Curr Genet* **48:** 77–87.

Supporting information

Additional supporting information may be found in the online version of this article at the publisher's web-site.

Molecular Microbiology (2016) 99(1), 217 ■ doi:10.1111/mmi.13297

Corrigendum

The conserved histone deacetylase Rpd3 and the DNA binding regulator Ume6 repress *BOI1*'s meiotic transcript isoform during vegetative growth in *Saccharomyces cerevisiae*

Yuchen Liu,[1,4] Igor Stuparevic,[1,5] Bingning Xie,[1] Emmanuelle Becker,[1,2] Michael J. Law[3] and Michael Primig[1]

[1] *Inserm U1085 IRSET, 35042 Rennes, France*
[2] *Université de Rennes 1, 35042 Rennes, France*
[3] *Rowan University, School of Osteopathic Medicine, Stratford, NJ 08084, USA*

Present address:
[4] *School of Medicine, Jianghan University, Wuhan, 430056, China*
[5] *University of Zagreb, Faculty of Food Technology and Biotechnology, 10000 Zagreb, Croatia*

Due to erroneous file processing Fig. 3E included a duplicated image for *mBOI1*, the Northern blot in Fig. 3I was inverted and the Western blot in Fig. 4B showed the wrong strain. We corrected the panels and revised the legend of Fig. 4. We note that *mBOI1* is expressed weaker in fermenting, rather than in respiring *ume6* cells by Northern blot (Fig. 3I). We sincerely apologize for the errors and emphasize that they do not affect the conclusions reported in the paper.

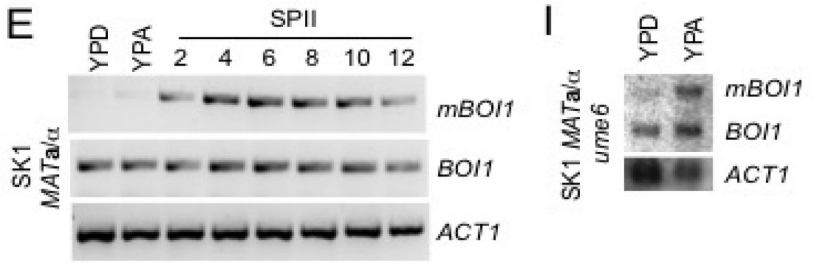

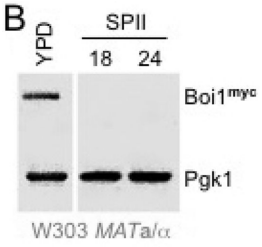

Fig. 4. (A) is unchanged. (B) A Western blot is shown for Boi1^{myc} in a wild type strain cultured in rich medium (YPD) and sporulation medium (SPII 18h, 24h). (C) The left panel shows an RT-PCR assay of *BOI1* isoforms in wild type and mutant strains as indicated. The right panel shows a Western blot of Boi1^{myc} in wild-type (WT) cells versus mutant cells cultured in rich medium (YPD). The strain backgrounds are indicated. Black and blue arrows mark the fast and slow migrating forms of Boi1^{myc}, respectively. Band intensities are shown as bar diagrams. An SD error bar is given. The original panel (C) is renamed into (D).

Reference

Liu, Y., Stuparevic, I., Xie, B., Becker, E., Law, M.J. and Primig, M. (2015) The conserved histone deacetylase Rpd3 and the DNA binding regulator Ume6 repress *BOI1*'s meiotic transcript isoform during vegetative growth in *Saccharomyces cerevisiae*. *Mol Microbiol* **96:** 861–874. doi: 10.1111/mmi.12976

© 2016 John Wiley & Sons Ltd

3) *CDC14* meiotic isoform regulation by Ume6

Introduction

Cdc14 is a protein phosphatase bound by Cdc55. It localizes to the nucleolus in early meiosis, and is liberated in anaphase by FEAR and Mitotic Exit Network, which enables Cdc14 to inactivate mitotic CDKs (Clb-CDKs) and to promote exit from mitosis (Marston A., et al. Developmental Cell.2003). Cdc14 promotes mitotic exit by dephosphorylating Cdk1, which is a component of the anaphase promoting complex/cyclosome (APC/C) (Stegmeier F, et al., Annu. Rev. Genet.2004), and also by targeting Swi5, which is a key transcription factor that activates the Antagonist of Mitotic Exit Network (AMEN) pathway. It has dual roles to activate *AMN1* to inhibit mitotic exit, and to inactivate Sic1 to allow S phase initiation. Sic1 is also an inhibitor of Cdk1. Thus, dephosphorylation of Swi5 by Cdc14 can ultimately activate Sic1 to suppress the activity of Cdk1 (McCollum D, et al., Trends Cell Biol. 2011). In addition to regulating mitotic exit, Cdc14 was also found to play complex roles in various cellular processes in mitosis, such as cytokinesis, DNA replication, and spindle stability (Breitkreutz A, et al., Science. 2010; Ho Y, et al., Nature. 2002; Visintin R, et al., Nature 1999).

Cdc14 has an important function in meiosis as well. Meiosis is specified by one round of DNA replication follow up with two rounds of cell division. In the absence of *CDC14* function, chromosome segregation is impaired and the cell undergoes only one meiotic division. This is due to the delayed disassembly of the meiotic I spindle in the *cdc14* mutant cell (Breitkreutz A, et al., Science. 2010; Ho Y, et al., Nature. 2002; Visintin R, et al., Nature 1999).

A previous study about mRNA isoform changes during meiosis has found 5' UTR extensions of mRNA to be induced during early, middle, and late meiosis. *CDC14* also has such a 5'UTR extension during meiosis. However, it is not known how transcript isoforms of CDC14 are regulated in meiosis. Here we carried out study to explore the mechanism that controls the transcript isoform changes of *CDC14*.

Materials and methods

Yeast strains and growth media. Strain used in this study are MPY70 (SK1 WT) and MYP702 (SK1 *ume6*). Media were prepared according to standard protocols for growth (YPD, YPA) and sporulation (SPII).

RT-PCR assay. RNA was extracted by Hot phenol method, followed by DNase I treatment with

TURBO DNA-free Kit (Ambion, USA). RT-PCR reactions were carried out using 2 μg of RNA reverse transcribed with Reverse Transcriptase (High Capacity cDNA Reverse Transcription kit; Life Technologies, USA) and amplified using Taq Polymerase (Qiagen, France) at 60ºC for 26 cycles. RT-PCR products were separated on 2% agarose gels and photographed using an ImageQuant 350 digital Imaging 381 System at the default settings (General Electric, USA). Primers used for RT-PCR were designed with Primer3 (simgene.com/Primer3; Table 1).

Table 1. Primers for RT-PCR assay

Gene	Forward Primer	Reverse Primer
CDC14	5'-CCAACCTTCTACGGCGAATA-3'	5'-GCTGGGTTCGTTATCTTCCA-3'
mCDC14	5'-GCATTTGAAGGCCATTGCTA-3'	5'-GGCATGAAGGGAGGGTCTAC-3'
ACT1	5'-CTCGTGCTGTCTTCCCATCT-3'	5'-AGATGGACCACTTTCGTCGT-3'

Results and discussion

CDC14 is a gene function in late meiosis, however it has a long isoform induced specifically in middle meiosis according to the tilling array result from Lardenois et al. This is consistent with the idea that the long isoform of *CDC14* has role in regulating Cdc14 translation. *CDC14* has an URS1 element in is promoter. The URS1 element is bound by Ume6-Rpd3 histone deacetylase complex which inactivates its target promoters. If the Ume6-Rpd3 histone deacetylase complex is responsible for the suppression of the meiotic long isoform of *CDC14* (*mCDC14*) in mitosis, then *mCDC14* should be de-repressed in a vegetatively growing *ume*6 mutant. To test this idea, we assayed the expression of *mCDC14* in *ume6* cells.

As shown by the RT-PCR result in Figure 1, *mCDC14* is indeed de-repressed in growing mitotic *ume6* cells, while *CDC14* expression stays constant from mitosis to meiosis. Since *ume6* cell is deficient in meiosis, the signals for *mCDC14* are very weak during meiotic time course. The result also shows that *mCDC14* is somehow becoming unstable in presporulation medium since the expression signals become weak in acetate medium already. Probably there is another mechanism, which inhibits transcription of *mCDC14*, or acetate enhances the degradation of *mCDC14*. This result shows that Ume6-Rpd3 histone deacetylase complex is responsible for the suppression of the meiotic long isoform of *CDC14* (*mCDC14*) in mitosis.

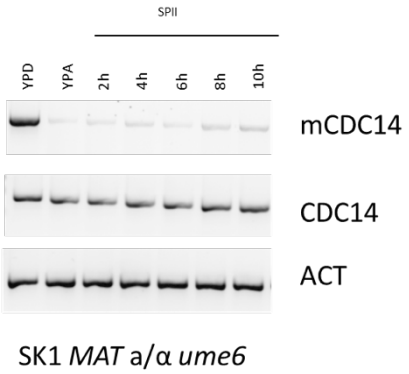

Figure 1. Expression pattern of *mCDC14*, *CDC14* in SK1 *ume6* mutant. RT-PCR was performed with mitotic samples (YPD and YPA) and meiotic time course (SPII2h to 10h). *ACT1* was used as a loading control.

4) RNA-mediated mechanisms controlling mRNA translation in meiosis

Introduction

In previous work it was shown that Rim4 is a protein involved in meiotic protein translation control via its interaction with 5'-UTRs in mRNAs (Berchowitz et al., Cell 2015). Earlier and ongoing protein profiling work in our laboratory using quantitative mass spectrometry, has identified Rim4 as a protein, which first appears in in pre-sporulation medium and later accumulates to very high levels in meiotic and post-meiotic cells (Becker et al., J Proteomics 2015; Becker et al., in preparation). Many other proteins were found to show fluctuations in mitosis and meiosis, including some for which we find overlapping antisense lncRNAs of the SUT and MUT type that can form dsRNAs *in vivo* some of which are able to influence protein expression (Becker et al., in preparation; Wery et al., Mol Cell 2016).

Materials and Methods

Rim4 Western Blot

Yeast cells expressing a tagged form of Rim4 (gift from A. Amon; Berchowitz et al., Genes Dev 2013) were harvested at log phase in YPA and during meiosis in SPII 6h and 8h and frozen in liquid nitrogen. To prepare a total protein extract, cells were treated with 0.2M NaOH and suspended in 50µl SDS sample buffer as described (V.V. Kushnirov. Yeast. 2000). 20µg protein extract per sample was loaded on a gradient 4%-20% SDS-PAGE gel (BIORAD, France) and run at 60V for 30 minutes and at 120V for 90 minutes. Proteins were transferred to a PVDF membrane at 50mA for 3 hours (Millipore, France). The membrane was blocked with 5% milk at room temperature for 2 hours, and incubated over night at 4ºC with the monoclonal anti-V5 antibody (ThermoScientific, France) at a dilution of 1:5000. After stripping and blocking, the membrane was incubated at room temperature for 2 hours with a monoclonal antibody against Pgk1 (Invitrogen, France) at 1:15000. An anti-mouse secondary antibody (GE Healthcare, France) was incubated at room temperature for 1 hour at 1:5000 to reveal Rim4 and Pgk1. Images were generated using the ChemiDoc XRS+

System; band intensities were quantified using ImageLab software (BIORAD).

J2 dsRNA detection

Yeast samples in presporulation medium (YPA) and sporulation medium (SPII) were cultured using a standard protocol (Lardenois A., et al., PNAS.2011). 35 µg RNA was incubated with J2 anti-dsRNA antibody (Scions, France) and 1 µl RNasin (Promega, France). Magnetic beads (Life Technology) were added The RNA was extracted with phenol/chloroform (25:24:1) and treated with DNaseI (Ambion) for 30 minutes at 37ºC. 180 ng RNA was used for reverse transcription using the High-capacity cDNA kit (ThermoFisher). cDNA was amplified by PCR for 30 cycles at an annealing temperature of 60ºC and an elongation time of 1 minute using a standard PCR machine (Biometra, France).

Table: oligonucleotide sequences

	Forward primer	Reverse Primer
PRY1	CCGATGTGGTCTTGTCTGCT	TTGAGCGTAGGAGGCCAAAG
SWI6	TGAGACCCGTGGATTTTGGG	GCTCTTTCGACTCCGCTTCT
GAP1	TTGTTGCCGCCTCCAAAAAG	CCCCAGTAGGAACCCCAAAC

Results and discussion

To confirm previous results from our and other laboratories I performed a Western blot analysis using a strain harboring tagged Rim4 that was harvested during fermentation (YPA medium), and meiotic M-phase (6h and 8h in SPII sporulation medium). My result showed a pattern of strong up-regulation for Rim4 in meiosis as compared to mitosis (respiration) and thus confirmed quantitative mass spectrometry data (Figure 1).

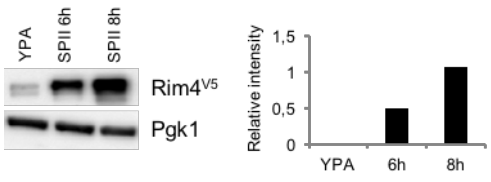

Figure 1. Rim4 Western blot. Samples and target proteins are given at the top and left. A bar diagram quantifies bands.

Further work validated and extended dsRNA profiling data for Pry1 that shows a variable pattern of protein detection in mitosis (detected in YPA) and meiosis (detected at 6h but not at 8h) Becker et al., in preparation) and for which mRNA and antisense SUT209 were shown to form dsRNAs *in vivo* in vegetatively growing cells (Wery et al., Mol Cell 2016). I used the J2 antibody to precipitate dsRNAs in respiring and sporulating

Figure 2. dsRNA assay. Samples are given at the bottom, target genes to the right, and antibody presence at the top.

diploid cells and confirmed their presence in all samples (Figure 2). This associates dsRNA formation with variable protein concentrations during cell growth and differentiation but it is currently unclear if dsRNA interferes with Pry1 translation.

Yeast strains

ID	Genotype	Reference
MPY716	MATa/MATa ARG4/arg4-bglII HIS4/his4-xhoI ura3Δ/ura3Δ leu2::hisG/leu2::hisG ho::LYS2/ho::LYS2 lys2/lys2	Joe Horecka
MPY721	MATa/MATa ARG4/arg4-bglII HIS4/his4-xhoI ura3Δ0/ura3Δ0 leu2::hisG/leu2::hisG ho::LYS2/ho::LYS2 lys2/lys2 pTEF1-RRP6 at ho/pTEF1-RRP6 at ho	Joe Horecka
MPY576	MATa/MATa HAP1/HAP1 MKT1 (D30G)/MKT1(D30G) RME1(INS 308A)/ RME1(INS 308A) TAO3(E1493Q)/TAO3 (E1493Q) GAL1-RRP6	Joe Horecka
MPY665	ARG4/arg4-bglII HIS4/his4-xhoI ura3 Δ /ura3 Δ leu2::hisG/leu2::hisG ho::LYS2/ho::LYS2 lys2/lys2 pTEF1-MUT1312/pTEF1-MUT1312	Joe Horecka
MPY646/648	MAT**a**/MATα lys 2 trp1::hisG ura3 LYS2::ho rrp6db con-served	Mike Law
MPY702	SK1 MATa/MATα gal80::LEU2/gal80::LEU2 ho::LYS2/ho::LYS2 leu2/leu2 lys2/lys2 trp1/trp1 ume6D::TRP1/ume6D::TRP1 ura3yura3	Aaron Mitchell
MPY542	JHY222 MAT**a**/MATα ume6::KanMX4/ume6::KanMX4	Joe Horecka
MPY815/816	JHY222: MATa/MATα SWI4-myc	Bingning Xie
MPY689	SK1 MAT**a**/MATα ARG4/arg4-bglII HIS4/his4-xhoI ura3 Δ /ura3 Δ leu2::hisG/leu2::hisG ho::LYS2/ho::LYS2 lys2/lys2 CYC1t-SUT200/CYC1t-SUT200	Joe Horecka
MPY687	SK1 MAT**a**/MATα ARG4/arg4-bglII HIS4/his4-xhoI ura3 Δ /ura3 Δ leu2::hisG/leu2::hisG ho::LYS2/ho::LYS2 lys2/lys2 pTEF1-SUT200/pTEF1-SUT200	Joe Horecka
MPY685	SK1 MAT**a**/MATα ARG4/arg4-bglII HIS4/his4-xhoI ura3 Δ /ura3 Δ leu2::hisG/leu2::hisG ho::LYS2/ho::LYS2 lys2/lys2 ho::pTEF1-SUT200	Joe Horecka
MPY553	JHY222 MATa/MATα HAP1/HAP1 MKT1(D30G)/MKT1(D30G) RME1(INS 308A)/RME1(INS 308A) TAO3(E1493Q)/TAO3(E1493Q) ndt80::kanMX4/ndt80::kanMX4	Joe Horecka
MPY672	SK1 MAT**a**/MATα ARG4/arg4-bglII HIS4/his4-xhoI ura3 Δ /ura3 Δ leu2::hisG/leu2::hisG ho::LYS2/ho::LYS2 lys2/lys2 pTEF1-MUT1465/pTEF1-MUT1465	Joe Horecka
MPY674	SK1 MAT**a**/MATα ARG4/arg4-bglII HIS4/his4-xhoI ura3 Δ /ura3 Δ leu2::hisG/leu2::hisG ho::LYS2/ho::LYS2 lys2/lys2 CYC1t-MUT1465/CYC1t-MUT1465	Joe Horecka
MPY542	JHY222: MATa/MATα HAP1/HAP1 MKT1 (D30G)/MKT1(D30G) RME1(INS 308A)/ RME1(INS 308A) TAO3(E1493Q)/TAO3 (E1493Q) ume6::KanMX4/ume6::KanMX4	Joe Horecka
MPY70	MAT**a**/MATα ho:LYS2/ho:LYS2, ura3/ura3, lys2/lys2,leu2:hisG/leu2:hisG, arg4-Nsp/arg4-Bgl, his4x:LEU2-URA3/his4B:LEU2	NKY1551: Nancy Kleckner
MPY1	αHAP1/HAP1 MKT1 (D30G)/MKT1(D30G) RME1(INS 308A)/ RME1(INS 308A) TAO3(E1493Q)/TAO3 (E1493Q)	Lardenois et al., PNAS 2011

Conclusion

In the 5-FU study, I found that lncRNAs respond to 5-FU by accumulating in treated cells, and that the elevated expression of antisense lncRNAs, which can form dsRNA with their sense mRNAs, is in some cases negatively associated with protein levels. As a consequence, the mRNA/lncRNA involved in cell cycle regulation may result in impeding cell cycle progression upon drug treatment like in the case of *ACE2*. mRNA responds to 5-FU not only by forming dsRNA with its antisense noncoding RNA, but also by altering transcript architecture, since 5'-extended meiotic isoforms also accumulate in starvation-synchronized cells treated with 5-FU. 5-FU exerts its RNA based cytotoxicity by targeting Rrp6, and loss of Rrp6 makes cells more sensitive to 5-FU treatment. Therefore, we explored if Rrp6 overexpression makes cells more resistant to 5-FU treatment. We tested the idea in both Rrp6 overexpression-strains and a strain with a stable Rrp6 allele and found that cells are indeed more resistant to 5-FU treatment in the presence of elevated Rrp6 levels. Thus, my research suggests that lncRNAs could be targets for improved 5-FU based chemotherapy, and Rrp6 could be target to alleviate tumor resistance to 5-FU treatment.

For the study about the mechanism that regulates Rrp6 during meiosis, I confirmed that sense/antisense pairs can form dsRNA during meiosis and the pair formed by *RRP6* and *MUT1312* negatively correlates with Rrp6 protein levels. Overexpression of *MUT1312* also decreases Rrp6 protein level in mitosis, which both are regulated during mitosis cell cycle. *MUT477* and the *SWI4* 5'-UTR also seems to form dsRNA, which may regulate Swi4 post-transcriptionally during meiosis.

For the study about the role of Rrp6 in meiosis, I found that Rrp6 have negative role in repressing the meiotic isoform of mRNA and meiotic induced lncRNAs MUTs, as both are accumulated in the strain lack of *RRP6*, and I found that MUTs are polyadenylated.

For the study about the regulation of MUTs, I did a genome wide transcription factor motif screen and found that the activation of MUTs for which I detected MSE elements in their upstream regions, depends on Ndt80, a middle meiotic activator. Ndt80 controls bidirectional transcripts by binding to MSE elements in their promoter region. *MUT1465* and *BBP1* is a prototype lncRNA/mRNA pair induced by Ndt80 during middle meiosis. I found induction of this pair is "one stone hit two birds" at the same time to activate the meiosis needed *BBP1* gene and inactivate the *CLN2* which is not needed in meiosis. The inhibition of *CLN2* appears to occur via induction of *MUT1465* which result in transcription read-through to the *CLN2* locus. Finally, *SUT200/CDC6*

also appears to be controlled by a read through mechanism that inhibits *CDC6* expression during stages after pre-meiotic DNA replication.

For the study of lncRNA expression in different yeast strains, I found that repression of certain MUTs is different in JHY222 and SK1 backgrounds since in *ume6* mutants in these strains I observe different de-repression patterns of MUT in mitosis. This may be due to the extensive differences in JHY222 and SK1 genome sequences.

For the meiotic isoform regulation study, I found Ndt80 to be responsible for the bidirectional induction of meiotic *ORC1* and *SMA2* and Ume6/Rdp3 to be responsible for the inhibition of certain meiotic transcript isoform in mitosis.

Discussion

lncRNA based 5-FU cytotoxicity

For the study of lncRNA based mechanism of 5-FU cytotoxicity, we found lncRNAs weakly induced in the treated cells as compared with the *rrp6* mutant we used as a positive control. This is to be expect because the drug inhibits Rrp6 to a certain extent but the deletion strain lost 100% of Rrp6 activity. We found a negative correlation between mRNA/lncRNA formed dsRNA and protein levels. This may indicate that dsRNA formation can inhibit translation. Sinturel F, et al., reported that overlapping sense/antisense mRNA pairs can form dsRNA that influence the translation of mRNA and its stability: the mRNA with a stop codon in the overlapping region will result in NO-GO decay, since translating ribosomes cannot move forward because they are blocked by dsRNA. Thus, it is possible that lncRNA accumulated in 5-FU treated cells inhibits mRNA translation post-transcriptionally by forming dsRNA with its overlapping sense mRNA. More work should be done to check this possibility directly by preventing expression of the lncRNA or overexpressing the lncRNA in wild type cells under normal condition. Another interesting point is that certain meiotically induced ncRNAs (MUTs) were found to be cell cycle regulated in mitosis like it was reported before in the case of SUTs.

Rrp6 overexpression mediated 5-FU resistance

For the resistance to 5-FU by elevated Rrp6 expression: this was not reported before but it is not surprising since an *rrp6* mutant is more sensitive to 5-FU treatment, therefore *RRP6* is a 5-FU resistance gene. It is therefore to be expected that elevating the expression level of a resistance gene

will lead to impaired drug treatment. However, this finding is particularly interesting and important since *RRP6* has a human homologue, which is called EXOSC10. Data in the human protein atlas indicate that some certain cancer samples, such as colon cancer, show variable EXOSC10 levels. Therefore, Rrp6/EXOSC10 could be a good target for the improvement of 5-FU based cancer therapy.

5-FU induced meiotic mRNA isoforms

For the isoform changes in 5-FU treated cells: this is not surprising since 5'UTR alteration is one mechanism of generating transcript isoforms, with splicing being another one. Alternative splicing has been reported to respond to drug treatment in higher eukaryotes as well as in budding yeast treated with 5-FU. However, it is interesting to see that certain 5'-extended meiotic isoforms actually are not meiosis specific, but cell cycle regulated. Due to their fluctuation therefore they cannot be detected in unsynchronized mitosis control sample in the previous studies where the signal was diluted. The isoform changes seem to be coherent with mRNA and lncRNA changes. For example, in the case of *CDC14*, which is needed for mitotic exit, the upregulation is consistent with the down regulation of the AMEN pathway, thus allowing mitotic exit to remain active and leading to an abnormal cell cycle. Therefore, isoform changes may also have significant meaning as they control key pathways, and they could also be important targets for the improvement of 5-FU based chemotherapy.

Rrp6 controls meiotic lncRNA

For the function of *RRP6* in meiosis, I found that it is important to control the meiotic isoform and MUTs to restrict MUT expression to meiosis. *rrp6* mutants show elevated expression of both meiotic isoforms and MUTs, and they have weak induction during mitosis. This is consistent with the already known function of Rrp6 to degrade unstable nascent transcripts. In addition, I also found that certain MUTs are polyadenylated and deletion of *RRP6* will result in elevated polyadenylation of these MUTs. This is coherent with earlier reports that Rrp6 controls polyadenylation of rRNA and mRNA.

Regulation of *Rrp6 during meiosis*

For the regulation of Rrp6 during meiosis, I confirmed high-throughput data showing that *MUT1312* forms dsRNA with *RRP6* mRNA, and that this phenomenon is negatively correlated with Rrp6 protein levels during meiosis. Furthermore, I found that overexpression of *MUT1312* in mitosis results in down-regulation of Rrp6 protein. *RRP6* mRNA levels do not change during

meiosis except during mid-late meiosis at 8h where it decreases during a brief period. However, mRNA increases again later, while the protein does not re-accumulate. This may indicate that *MUT1312* inhibits the translation of Rrp6 during meiosis. Alternatively, since *RRP6* mRNA increases at later stages, it may be that *MUT1312* stabilizes *RRP6* mRNA during late meiosis via dsRNA formation, since Rrp6 is important for the germinating cell. EXOSC10 is also associated with an antisense ncRNA that overlaps with its 3' part, and human EXOSC10 is essential for the cell cycle. dsRNA formation might be a new mechanism for cells to restore maternal RNAs during development of the zygote before zygote genome activation. Although no literature reported this mechanism, I think it is plausible and worth to be further investigated.

lncRNA mediating inhibition of translation

Another interesting dsRNA is *MUT477* and the meiotic extended 5'UTR of *SWI4*. I found the formation of dsRNA to be negatively correlated with protein levels in this case as well. However, as opposed to *RRP6/MUT1312*, *MUT477* overlaps only with the meiotic extended 5'UTR of *SWI4* rather than the 3'end. The 5'UTR is important for translation of mRNA, since it allows ribosome to search and bind to the mRNA. A dsRNA formed in the 5'UTR region could block the entry of ribosomes into mRNA, and thus inhibit translation. However, more experiments should be done to provide direct evidence for this hypothesis.

Regulation role of MUTs during meiosis

SUT200 is located upstream of *CDC6*, which originally led us to think that it inhibits *CDC6* by promoter interference. However, my experimental results show that it might rather be read-through from *SUT200* into *CDC6* lead to inhibition of *CDC6*. More work should be down to further prove this idea, for example by using an antibody against the RNA PolII initiation complex to see if the promoter accessibility is affected.

For the mechanism that induce MUTs expression in meiosis, I found that Ndt80 is the major transcription factor, which induces MUT expression during middle meiosis in those cases that possess an MSE element in their promoter region. An interesting example is *MUT1465/BBP1*, for which I found that the bidirectional induction by Ndt80 not only activate a gene important for meiosis (*BBP1*), but also indirectly shut down a gene not needed for it (*CLN2)* by transcriptional read-through from *MUT1465*. The *MUT1465* locus seems to interact with the *CLN2* 3'end in mitosis, which enables the fast re-cycling and re-use of the RNA Polymerase II and cofactors to allow normal expression of *CLN2* during mitosis. This kind of looping is common in budding yeast

to facilitate gene expression.

For the ncRNA induction difference in two strains, I think this may due to the sequence difference of the two strains and also the different phenotypes of *RRP6* deletion, which is not strictly essential in JHY222 but it is in SK1.

Regulation of meiotic isoforms

For the isoform changes, we further provide the mechanism of how the middle meiosis isoform is regulated by Ndt80, which is a middle meiosis activator that induces the meiotic isoform during middle meiosis.

Taken together, my studies during the PhD project provide a new perspective about 5-FU cytotoxicity by showing that abnormally accumulated lncRNAs may mediated inhibition of protein translation by dsRNA formation. This reveals new targets for improvement of 5-FU chemotherapy. I also provide evidence for the role of long non-coding RNA in meiosis via (1) formation of dsRNA with overlapping antisense mRNA to potentially inhibit the translation of sense mRNAs; and (2) inhibition of downstream mRNA by transcriptional read-through of lncRNAs. Furthermore, my work revealed an Ndt80-dependent mechanism that induces MUTs during meiosis. In addition, the regulatory mechanisms controlling mRNA isoform changes during meiosis were also explored, showing that Ume6/Rpd3 represses meiotic isoforms in mitosis and that Ndt80 activates a meiotic mRNA isoform encoded by *ORC1* via a bi-directional promoter.

References

Lind M.J., M.J. (2008). "Principles of cytotoxic chemotherapy". Medicine. 36 (1): 19–23.doi:10.1016/j.mpmed.2007.10.003.

Parker WB (Jul 2009). "Enzymology of purine and pyrimidine antimetabolites used in the treatment of cancer". Chemical Reviews. 109 (7): 2880–93. doi:10.1021/cr900028p. PMC 2827868free to read. PMID 19476376.

Rowinsky EK, Donehower RC (Oct 1991). "The clinical pharmacology and use of antimicrotubule agents in cancer chemotherapeutics". Pharmacology & Therapeutics. 52 (1): 35–84. doi:10.1016/0163-7258(91)90086-2. PMID 1687171.

Yue QX, Liu X, Guo DA (Aug 2010). "Microtubule-binding natural products for cancer therapy". Planta Medica. 76 (11): 1037–43. doi:10.1055/s-0030-1250073. PMID 20577942.

Damayanthi Y, Lown JW (Jun 1998). "Podophyllotoxins: current status and recent developments". Current Medicinal Chemistry. 5 (3): 205–52. PMID 9562603.

Lind M.J., M.J. (2008). "Principles of cytotoxic chemotherapy". Medicine. 36 (1): 19–23. doi:10.1016/j.mpmed.2007.10.003.

Parker WB (Jul 2009). "Enzymology of purine and pyrimidine antimetabolites used in the treatment of cancer". Chemical Reviews. 109 (7): 2880–93. doi:10.1021/cr900028p. PMC 2827868free to read. PMID 19476376.

Lodish H, Berk A, Zipursky SL, et al. (2000). Molecular Cell Biology. 4th edition. The Role of Topoisomerases in DNA Replication. New York: W. H. Freeman.

Goodsell DS (2002). "The molecular perspective: DNA topoisomerases". Stem Cells. 20 (5): 470–1. doi:10.1634/stemcells.20-5-470. PMID 12351817.

Nitiss JL (May 2009). "Targeting DNA topoisomerase II in cancer chemotherapy". Nature Reviews. Cancer. 9 (5): 338–50. doi:10.1038/nrc2607. PMC 2748742free to read. PMID 19377506.

Antineoplastic Agents in Encyclopedia of Molecular Pharmacology, 2nd Edition, Volume 1. Eds. Offermanns S and Rosenthal W. Springer, 2008. ISBN 9783540389163 P 155
Sneader W. (2005). Drug Discovery, p. 255.

Chu E (September 2007). "Ode to 5-Fluorouracil". Clinical Colorectal Cancer. 6 (9): 609. doi:10.3816/CCC.2007.n.029.

Heidelberger C.; Chaudhuri N. K.; Danneberg P.; et al. (March 1957). "Fluorinated pyrimidines, a new class of tumour-inhibitory compounds". Nature. 179 (4561): 663–6. doi:10.1038/179663a0. PMID 13418758.

Longley D. B.; Harkin D. P.; Johnston P. G. (May 2003). "5-fluorouracil: mechanisms of action and clinical strategies". Nat. Rev. Cancer. 3 (5): 330–8. doi:10.1038/nrc1074. PMID 12724731

Makino, D. L., M. Baumgartner and E. Conti (2013). "Crystal structure of an RNA-bound 11-subunit eukaryotic exosome complex." Nature 495(7439): 70-75.

Januszyk, K. and C. D. Lima (2014). "The eukaryotic RNA exosome." Curr Opin Struct Biol 24: 132-140.

Butler JS1, Mitchell P.Rrp6, Rrp47 and cofactors of the nuclear exosome. Adv Exp Med Biol. 2010;702:91-104.

Kurt Januszyk, Christopher D Lima. The eukaryotic RNA exosome, Current Opinion in Structural Biology.2014.24: 132-140.

Midtgaard SF1, Assenholt J, Jonstrup AT, Van LB, Jensen TH, Brodersen DE.Structure of the nuclear exosome component Rrp6p reveals an interplay between the active site and the HRDC domain. Proc Natl Acad Sci U S A. 2006 Aug 8;103(32):11898-903. Epub 2006 Aug 1.
Michael W. Briggs, Karina T.D. Burkard and J.Scott Butler. Rrp6p, the yeast homologue of the human PM-Scl 100-kDa autoantigen, is essential for efficient 5.8S rRNA 3'end formation.J. Biol. Chem. 1998, 273:13255-13263.

Schneider, C., G. Kudla, W. Wlotzka, A. Tuck and D. Tollervey (2012). "Transcriptome-wide analysis of exosome targets." Mol Cell 48(3): 422-433.

Grem JL, Fischer PH (1989) Enhancement of 5-fluorouracil's anticancer activity by dipyridamole. Pharmacol Ther 40:349–371.

Bergers G1, Benjamin LE.Tumorigenesis and the angiogenic switch. Nat Rev Cancer. 2003 Jun;3(6):401-10.

Salonga D1, Danenberg KD, Johnson M, Metzger R, Groshen S, Tsao-Wei DD, Lenz HJ, Leichman CG, Leichman L, Diasio RB, Danenberg PV.Colorectal tumors responding to 5-fluorouracil have low gene expression levels of dihydropyrimidine dehydrogenase, thymidylate synthase, and thymidine phosphorylase. Clin Cancer Res. 2000 Apr;6(4):1322-7.

Dan S1, Tsunoda T, Kitahara O, Yanagawa R, Zembutsu H, Katagiri T, Yamazaki K, Nakamura Y, Yamori T. An integrated database of chemosensitivity to 55 anticancer drugs and gene expression profiles of 39 human cancer cell lines. Cancer Res. 2002 Feb 15;62(4):1139-47.

Lee, H., C. Kim, J. L. Ku, W. Kim, S. K. Yoon, H. J. Kuh, J. H. Lee, S. W. Nam and E. K. Lee (2014). "A long non-coding RNA snaR contributes to 5-fluorouracil resistance in human colon cancer cells." Mol Cells 37(7): 540-546.

Wang, X. S. et al. Rapid identification of UCA1 as a very sensitive and specific unique marker for human bladder carcinoma. Clin. Cancer. Res. 12, 4851–4858 (2006).

Bian Z, Jin L, Zhang J, Yin Y, Quan C, Hu Y, Feng Y, Liu H, Fei B, Mao Y, Zhou L, Qi X, Huang S, Hua D, Xing C, Huang Z. LncRNA-UCA1 enhances cell proliferation and 5-fluorouracil resistance in colorectal cancer by inhibiting miR-204-5p. Sci Rep. 2016 Apr 5;6:23892. doi: 10.1038/srep23892.

Crick F. Central dogma of molecular biology. Nature. 1970 Aug 8;227(5258):561-3.

He J, Chen Q, Wei Y, Jiang F, Yang M, Hao S, Guo X, Chen D, Kang L. MicroRNA-276 promotes egg-hatching synchrony by up-regulating brm in locusts. Proc Natl Acad Sci U S A. 2016 Jan 19;113(3):584-9. doi: 10.1073/pnas.1521098113. Epub 2016 Jan 4.

Saraiya AA1, Li W, Wang CC. Transition of a microRNA from repressing to activating translation depending on the extent of base pairing with the target. PLoS One. 2013;8(2):e55672. doi: 10.1371/journal.pone.0055672. Epub 2013 Feb 6.

Guttman M1, Amit I, Garber M, French C, Lin MF, Feldser D, Huarte M, Zuk O, Carey BW, Cassady JP, Cabili MN, Jaenisch R, Mikkelsen TS, Jacks T, Hacohen N, Bernstein BE, Kellis M, Regev A, Rinn JL, Lander ES. Chromatin signature reveals over a thousand highly conserved large non-coding RNAs in mammals. Nature. 2009 Mar 12;458(7235):223-7. doi: 10.1038/nature07672. Epub 2009 Feb 1.

Batista PJ, Chang HY. Long noncoding RNAs: cellular address codes in development and disease. Cell. 2013 Mar 14;152(6):1298-307. doi: 10.1016/j.cell.2013.02.012.

Ingolia NT1, Ghaemmaghami S, Newman JR, Weissman JS. Genome-wide analysis in vivo of translation with nucleotide resolution using ribosome profiling. Science. 2009 Apr 10;324(5924):218-23. doi: 10.1126/science.1168978. Epub 2009 Feb 12.

Brar GA1, Yassour M, Friedman N, Regev A, Ingolia NT, Weissman JS. High-resolution view of the yeast meiotic program revealed by ribosome profiling. Science. 2012 Feb 3;335(6068):552-7. doi: 10.1126/science.1215110. Epub 2011 Dec 22.

Peters, N. T., Rohrbach, J. A., Zalewski, B. A., Byrkett, C. M. & Vaughn, J. C. RNA editing and regulation of Drosophila 4f-rnp expression by sas-10 antisense readthrough mRNA transcripts. RNA 9, 698–710 (2003).

Nishizawa, M. et al. Nutrient-regulated antisense and intragenic RNAs modulate a signal transduction pathway in yeast. PLoS Biol. 6, 2817–2830 (2008).

Carrieri, C. et al. Long non-coding antisense RNA controls Uchl1 translation through an embedded SINEB2 repeat.

Nature 491, 454–457 (2012).

Cesana, M. et al. A long noncoding RNA controls muscle differentiation by functioning as a competing endogenous RNA. Cell 147, 358–369 (2011).

Hansen, T. B. et al. Natural RNA circles function as efficient microRNA sponges. Nature 495, 384–388 (2013).

Memczak, S. et al. Circular RNAs are a large class of animal RNAs with regulatory potency. Nature 495, 333–338 (2013).

Hellwig, S. & Bass, B. L. A starvation-induced noncoding RNA modulates expression of Dicer-regulated genes. Proc. Natl Acad. Sci. USA 105, 12897–12902 (2008).

Yassour M, Pfiffner J, Levin JZ, Adiconis X, Gnirke A, Nusbaum C, Thompson DA, Friedman N, Regev A: Strand-specific RNA sequencing reveals extensive regulated long antisense transcripts that are conserved across yeast species. Genome Biol 2010, 11:R87.

Zhang L, Ma H, Pugh BF: Stable and dynamic nucleosome states during a meiotic developmental process. Genome Res 2011, 21:875-884

Xiang, J.F. et al. Human colorectal cancer-specific CCAT1-L lncRNA regulates long-range chromatin interactions at the MYC locus. Cell Res. 24, 513–531 (2014).

Calin, G.A. et al. Ultraconserved regions encoding ncRNAs are altered in human leukemias and carcinomas. Cancer Cell 12, 215–229 (2007).

Huarte, M. et al. A large intergenic noncoding RNA induced by p53 mediates global gene repression in the p53 response. Cell 142, 409–419 (2010).

Arun, G., Diermeier, S., Akerman, M., Chang, K.C., Wilkinson, J.E., Hearn, S., Kim, Y., MacLeod, A.R., Krainer, A.R., Norton, L., et al. (2016). Differentiation of mammary tumors and reduction in metastasis upon Malat1 lncRNA loss. Genes Dev. 30, 34–51.

Peters, J.M. (2006) The anaphase promoting complex/cyclosome: a machine designed to destroy. Nat. Rev. Mol. Cell Biol. 7, 644–656

Thornton, B.R. and Toczyski, D.P. (2006) Precise destruction: an emerging picture of the APC. Genes Dev. 20, 3069–3078

Cooper KF, Egeland DE, Mallory MJ, Jarnik M, Strich R: Ama1p is a Meiosis-Specific Regulator of the Anaphase Promoting Complex/Cyclosome in yeast. Proc Natl Acad Sci USA 2000, 97:14548-14553.

McDonald CM, Cooper KF, Winter E: The Ama1-Directed Anaphase-Promoting Complex Regulates the Smk1 Mitogen-Activated Protein Kinase During Meiosis in Yeast. Genetics 2005, 171:901-911.

Diamond AE, Park JS, Inoue I, Tachikawa H, Neiman AM: The anaphase promoting complex targeting subunit Ama1 links meiotic exit to cytokinesis during sporulation in Saccharomyces cerevisiae. Mol Biol Cell 2009, 20:134-145.

Tan GS, Magurno J, Cooper KF: Ama1p-activated anaphase-promoting complex regulates the destruction of Cdc20p during meiosis II. Mol Biol Cell 2011, 22:315-326.

Salah SM, Nasmyth K: Destruction of the securin Pds1p occurs at the onset of anaphase during both meiotic divisions in yeast. Chromosoma 2000, 109:27-34.

Shonn MA, McCarroll R, Murray AW: Requirement of the spindle checkpoint for proper chromosome segregation in budding yeast meiosis. Science 2000, 289:300-303.

Oelschlaegel T, Schwickart M, Matos J, Bogdanova A, Camasses A, Havlis J,Shevchenko A, Zachariae W: The yeast APC/C subunit Mnd2 prevents premature sister chromatid separation triggered by the meiosis-specific APC/C-Ama1. Cell 2005, 120:773-788.

Cooper KF, Mallory MJ, Guacci V, Lowe K, Strich R: Pds1p is required for meiotic recombination and prophase I progression in Saccharomyces cerevisiae. Genetics 2009, 181:65-79.

Breitkreutz A, Choi H, Sharom JR, Boucher L, Neduva V, Larsen B, Lin ZY, Breitkreutz BJ, Stark C, Liu G, Ahn J, Dewar-Darch D, Reguly T, Tang X, Almeida R, Qin ZS, Pawson T, Gingras AC, Nesvizhskii AI, Tyers M (2010) A global protein kinase and phosphatase interaction network in yeast. Science 328:1043-1046.

Ho Y, Gruhler A, Heilbut A, Bader GD, Moore L, Adams S-L, Millar A, Taylor P, Bennett K, Boutilier K, Yang L, Wolting C, Donaldson I, Schandorff S, Shewnarane J, Vo M, Taggart J, Goudreault M, Muskat B, Alfarano C, Dewar D, Lin Z, Michalickova K, Willems AR, Sassi H, Nielsen PA, Rasmussen KJ, Andersen JR, Johansen LE, Hansen LH, Jespersen H, Podtelejnikov A, Nielsen E, Crawford J, Poulsen V, Sorensen BD, Matthiesen J, Hendrickson RC, Gleeson F, Pawson T, Moran MF, Durocher D, Mann M, Hogue CWV, Figeys D, Tyers M (2002) Systematic identification of protein complexes in Saccharomyces cerevisiae by mass spectrometry. Nature (London) 415:180-183.

Visintin R, Hwang ES, Amon A (1999) Cfi1 prevents premature exit from mitosis by anchoring Cdc14 phosphatase in the nucleolus. Nature 398:818-823.

Stegmeier F, Amon A (2004). "Closing mitosis: the functions of the Cdc14 phosphatase and its regulation". Annu. Rev. Genet. 38: 203–32. doi:10.1146/annurev.genet.38.072902.093051. PMID 15568976.
McCollum D, Gould KL (2001) Timing is everything: Regulation of mitotic exit and cytokinesis by the MEN and SIN. Trends Cell Biol 11:89-95.

Mele Marta and Rinn John. Cat's cradling the 3D genome by the act of lncRNA transcription. Mol Cell. 2016. 62:657-664.

Wyers, F., Rougemaille, M., Badis, G., Rousselle, J.C., Dufour, M.E., Boulay, J., Regnault, B., Devaux, F., Namane, A., Seraphin, B. et al. (2005) Cryptic pol II transcripts are degraded by a nuclear quality control pathway involving a new poly(A) polymerase. Cell 121, 725–737

Kim KD, Tanizawa H, Iwasaki O, Noma KI. Transcription factors mediate condensin recruitment and global chromosomal organization in fission yeast. Nat Genet. 2016 Aug 22. doi: 10.1038/ng.3647

Sharp P.A., and Burge C.B. Classification of introns: U2-type or U12-type[J]. Cell. 1997, 91(7): 875-879.
Patel A., and Steitz J., Splicing double: insights from the second spliceosome[J]. Nature Reviews Molecular Cell Biology. 2003, 4: 960-970.

Blencowe B.J. Alternative splicing: new insights from global analyses[J]. Cell. 2006, 126: 37-47.

Wang B.B., and Brendel V. Genome-wide comparative analysis of alternative splicing in plants[J]. Proc. Natl. Acad. Sci. USA. 2006, 103(18): 7175-7180.

Clancy MJ. 1998. Meiosis: step-by-step through sporulation. Curr Biol 8: R461–R463.
Vershon AK, Pierce M. 2000. Transcriptional regulation of meiosis in yeast. Curr Opin Cell Biol 12: 334–339.
Wolgemuth DJ, Laurion E, Lele KM: Regulation of the mitotic and meiotic cell cycles in the male germ line. Recent Prog Horm Res2002, 57:75-101.
Habu T, Taki T, West A, Nishimune Y, Morita T: The mouse and human homologs of DMC1, the yeast meiosis-specific homologous recombination gene, have a common unique form of exon-skipped transcript in meiosis. Nucleic Acids Res 1996,24:470-477.
Sato S, Seki N, Hotta Y, Tabata S: Expression profiles of a human gene identified as a structural homologue of meiosis-specific recA-like genes. DNA Res 1995, 2:183-186.

Julian P Venables. Alternative splicing in the testes. Current Opinion in Genetics & Development 2002, 12:615–619.

De Angioletti M, Lacerra G, Sabato V, Carestia C (2004). "Beta+45 G --> C: a novel silent beta-thalassaemia mutation, the first in the Kozak sequence". Br J Haematol 124 (2): 224–31. doi:10.1046/j.1365-2141.2003.04754.x. PMID 14687034.

Grem, J. L. & Fischer, P. H. Enhancement of 5-fluorouracil's anticancer activity by dipyridamole. Pharmacol. Ther. 40, 349–371 (1989).

Salonga, D. et al. Colorectal tumors responding to 5-fluorouracil have low gene expression levels of

dihydropyrimidine dehydrogenase, thymidylate synthase, and thymidine phosphorylase. Clin. Cancer Res. 6, 1322–1327 (2000).

Zembutsu, H. et al. Genome-wide cDNA microarray screening to correlate gene expression profiles with sensitivity of 85 human cancer xenografts to anticancer drugs. Cancer Res. 62, 518–527 (2002).

Lardenois A1, Liu Y, Walther T, Chalmel F, Evrard B, Granovskaia M, Chu A, Davis RW, Steinmetz LM, Primig M. Execution of the meiotic noncoding RNA expression program and the onset of gametogenesis in yeast require the conserved exosome subunit Rrp6. Proc Natl Acad Sci U S A. 2011 Jan 18;108(3):1058-63. doi: 10.1073/pnas.1016459108. Epub 2010 Dec 13.

Lee H, Kim C, Ku JL, et al (2014). A long non-coding RNA snaR contributes to 5-fluorouracil resistance in human colon cancer cells. Mol Cells, 37, 540-6.

Wang, X. S. et al. Rapid identification of UCA1 as a very sensitive and specific unique marker for human bladder carcinoma. Clin. Cancer. Res. 12, 4851–4858 (2006).

Mullen, T. E.; Marzluff, W. F. (1 January 2008). "Degradation of histone mRNA requires oligouridylation followed by decapping and simultaneous degradation of the mRNA both 5' to 3' and 3' to 5'". Genes & Development. 22 (1): 50–65. doi:10.1101/gad.1622708.

Thompson, D.M. and Parker, R. (2007) Cytoplasmic decay of intergenic transcripts in Saccharomyces cerevisiae. Mol. Cell. Biol. 27, 92–101

van Dijk, E.L., Chen, C.L., d'Aubenton-Carafa, Y., Gourvennec, S., Kwapisz, M., Roche, V., Bertrand, C., Silvain, M., Legoix-Ne, P., Loeillet, S. et al. (2011) XUTs are a class of Xrn1-sensitive antisense regulatory non-coding RNA in yeast. Nature 475, 114–117

David, L., Huber, W., Granovskaia, M., Toedling, J., Palm, C.J., Bofkin, L., Jones, T., Davis, R.W. and Steinmetz, L.M. (2006) A high-resolution map of transcription in the yeast genome. Proc. Natl. Acad. Sci. U.S.A. 103, 5320–5325

Neil, H., Malabat, C., d'Aubenton-Carafa, Y., Xu, Z., Steinmetz, L.M. and Jacquier, A. (2009) Widespread bidirectional promoters are the major source of cryptic transcripts in yeast. Nature 457, 1038–1042

Xu, Z., Wei, W., Gagneur, J., Perocchi, F., Clauder-Munster, S., Camblong, J., Guffanti, E., Stutz, F., Huber, W. and Steinmetz, L.M. (2009) Bidirectional promoters generate pervasive transcription in yeast. Nature 457, 1033–1037

Wu Y, Huang C, Meng X, Li J (2015). "Long Noncoding RNA MALAT1: Insights into its Biogenesis and Implications in Human Disease". Current Pharmaceutical Design. 21 (34): 5017–28. doi:10.2174/1381612821666150724115625. PMID 26205289.

Yoshimoto R, Mayeda A, Yoshida M, Nakagawa S (January 2016). "MALAT1 long non-coding RNA in cancer". Biochimica et Biophysica Acta. 1859 (1): 192–9. doi:10.1016/j.bbagrm.2015.09.012. PMID 26434412.

Scartozzi M1, Maccaroni E, Giampieri R, Pistelli M, Bittoni A, Del Prete M, Berardi R, Cascinu S. 5-Fluorouracil pharmacogenomics: still rocking after all these years? Pharmacogenomics. 2011 Feb;12(2):251-65. doi: 10.2217/pgs.10.167.

Fang F1, Hoskins J, Butler JS. 5-fluorouracil enhances exosome-dependent accumulation of polyadenylated rRNAs. Mol Cell Biol. 2004 Dec;24(24):10766-76.

Kammler S1, Lykke-Andersen S, Jensen TH. The RNA exosome component hRrp6 is a target for 5-fluorouracil in human cells. Mol Cancer Res. 2008 Jun;6(6):990-5. doi: 10.1158/1541-7786.MCR-07-2217.

Silverstein RA1, González de Valdivia E, Visa N. The incorporation of 5-fluorouracil into RNA affects the ribonucleolytic activity of the exosome subunit Rrp6. Mol Cancer Res. 2011 Mar;9(3):332-40. doi: 10.1158/1541-7786.MCR-10-0084. Epub 2011 Feb 2.

Xu Z, Wei W, Gagneur J, Perocchi F, Clauder-Münster S, Camblong J, Guffanti E, Stutz F, Huber W, Steinmetz LM. Bidirectional promoters generate pervasive transcription in yeast. Nature. 2009 Feb 19;457(7232):1033-7. doi:

10.1038/nature07728. Epub 2009 Jan 25.

Schneider C, Kudla G, Wlotzka W, Tuck A, Tollervey D. Transcriptome-wide analysis of exosome targets. Mol Cell. 2012 Nov 9;48(3):422-33. doi: 10.1016/j.molcel.2012.08.013. Epub 2012 Sep 20

Gudipati RK1, Xu Z, Lebreton A, Séraphin B, Steinmetz LM, Jacquier A, Libri D. Extensive degradation of RNA precursors by the exosome in wild-type cells. Mol Cell. 2012 Nov 9;48(3):409-21. doi: 10.1016/j.molcel.2012.08.018. Epub 2012 Sep 20.

Geisler S1, Coller J. RNA in unexpected places: long non-coding RNA functions in diverse cellular contexts. Nat Rev Mol Cell Biol. 2013 Nov;14(11):699-712. doi: 10.1038/nrm3679. Epub 2013 Oct 9.

Melé M, Rinn JL. "Cat's Cradling" the 3D Genome by the Act of LncRNA Transcription. Mol Cell. 2016 Jun 2;62(5):657-64. doi: 10.1016/j.molcel.2016.05.011.

Wapinski O1, Chang HY. Long noncoding RNAs and human disease. Trends Cell Biol. 2011 Jun;21(6):354-61. doi: 10.1016/j.tcb.2011.04.001. Epub 2011 May 6.

Xiang JF, Yin QF, Chen T, Zhang Y, Zhang XO, Wu Z, Zhang S, Wang HB, Ge J, Lu X, Yang L, Chen LL. Human colorectal cancer-specific CCAT1-L lncRNA regulates long-range chromatin interactions at the MYC locus. Cell Res. 2014 May;24(5):513-31. doi: 10.1038/cr.2014.35. Epub 2014 Mar 25.

Huarte M., Guttman M., Feldser D., Garber M., Koziol M.J., Kenzelmann-Broz D., Khalil A.M., Zuk O., Amit I., Rabani M., et al. A large intergenic noncoding RNA induced by p53 mediates global gene repression in the p53 response. Cell. 2010;142:409–419. doi: 10.1016/j.cell.2010.06.040.

Calin GA1, Liu CG, Ferracin M, Hyslop T, Spizzo R, Sevignani C, Fabbri M, Cimmino A, Lee EJ, Wojcik SE, Shimizu M, Tili E, Rossi S, Taccioli C, Pichiorri F, Liu X, Zupo S, Herlea V, Gramantieri L, Lanza G, Alder H, Rassenti L, Volinia S, Schmittgen TD, Kipps TJ, Negrini M, Croce CM. Ultraconserved regions encoding ncRNAs are altered in human leukemias and carcinomas. Cancer Cell. 2007 Sep;12(3):215-29.

Daniel, B.L., Paul, D.H., Patrick, G.J. 5-Fluorouracil: mechanisms of action and clinical strategies. Nat. Rev. Cancer. 2003;3:330–338.

Sinturel F., Navickas A., Wery M., Descrimes M., Morillon A., Torchet C., Benard L. Cytoplasmic control of sense-antisense mRNA pairs. Cell Rep. 2015;12:1853–1864.

Wery M, Descrimes M, Vogt N, Dallongeville AS, Gautheret D, Morillon A. Nonsense-Mediated Decay Restricts LncRNA Levels in Yeast Unless Blocked by Double-Stranded RNA Structure. Mol Cell. 2016 Feb 4;61(3):379-92. doi: 10.1016/j.molcel.2015.12.020. Epub 2016 Jan 21.

Kim KD, Tanizawa H, Iwasaki O, Noma KI. Transcription factors mediate condensin recruitment and global chromosomal organization in fission yeast. Nat Genet. 2016 Aug 22. doi: 10.1038/ng.3647

Stern M, Jensen R, Herskowitz I. Five SWI genes are required for expression of the HO gene in yeast. J Mol Biol. 1984 Oct 5;178(4):853-68.

Harris MR1, Lee D, Farmer S, Lowndes NF, de Bruin RA. Binding specificity of the G1/S transcriptional regulators in budding yeast. PLoS One. 2013 Apr 4;8(4):e61059. doi: 10.1371/journal.pone.0061059. Print 2013.

Leem SH, Chung CN, Sunwoo Y, Araki H. Meiotic role of SWI6 in Saccharomyces cerevisiae. Nucleic Acids Res. 1998 Jul 1;26(13):3154-8.

Pelechano V, García-Martínez J, Pérez-Ortín JE. A genomic study of the inter-ORF distances in Saccharomyces cerevisiae. Yeast. 2006 Jul 15;23(9):689-99.

Alam T, Medvedeva YA, Jia H, Brown JB, Lipovich L, Bajic VB. Promoter analysis reveals globally differential regulation of human long non-coding RNA and protein-coding genes. PLoS One. 2014 Oct 2;9(10):e109443. doi: 10.1371/journal.pone.0109443. eCollection 2014.

Cross FR, Hoek M, McKinney JD, Tinkelenberg AH. Role of Swi4 in cell cycle regulation of CLN2 expression. Mol

Cell Biol. 1994 Jul;14(7):4779-87.

Primig M, Williams RM, Winzeler EA, Tevzadze GG, Conway AR, Hwang SY, Davis RW, Esposito RE. The core meiotic transcriptome in budding yeasts. Nat Genet. 2000 Dec;26(4):415-23.

Liti G, Carter DM, Moses AM, Warringer J, Parts L, James SA, Davey RP, Roberts IN, Burt A, Koufopanou V, Tsai IJ, Bergman CM, Bensasson D, O'Kelly MJ, van Oudenaarden A, Barton DB, Bailes E, Nguyen AN, Jones M, Quail MA, Goodhead I, Sims S, Smith F, Blomberg A, Durbin R, Louis EJ. Population genomics of domestic and wild yeasts. Nature. 2009 Mar 19;458(7236):337-41. doi: 10.1038/nature07743. Epub 2009 Feb 11.
Valeriote F, Santelli G: 5-Fluorouracil (FUra). Pharmacol Ther 24:107-132, 1984.
Siomi MC, Sato K, Pezic D, Aravin AA: PIWI-interacting small RNAs: the vanguard of genome defence. Nat Rev Mol Cell Biol 2011, 12:246-258.

Rajan KS, Ramasamy S. Retrotransposons and piRNA: the missing link in central nervous system. Neurochem Int. 2014 Nov;77:94-102. doi: 10.1016/j.neuint.2014.05.017. Epub 2014 Jun 9.

Franck Morceau, Sébastien Chateauvieux, Anthoula Gaigneaux, Mario Dicato and Marc Diederich. Long and Short Non-Coding RNAs as Regulators of Hematopoietic Differentiation. Int. J. Mol. Sci. 2013, 14(7), 14744-14770; doi:10.3390/ijms140714744

Pedro J. Batista and Howard Y. Chang. Long noncoding RNAs: Cellular address codes in development and disease. Cell. Author manuscript; available in PMC 2014 Mar 14.

Guttman M, Russell P, Ingolia NT, Weissman JS, Lander ES. (2013). Ribosome Profiling Provides Evidence that Large Noncoding RNAs Do Not Encode Proteins. Cell. 154, 1, p240–251

Brar GA, Yassour M, Friedman N, Regev A, Ingolia NT, Weissman JS. High-resolution view of the yeast meiotic program revealed by ribosome profiling. Science. 2012 Feb 3;335(6068):552-7. doi: 10.1126/science.1215110. Epub 2011 Dec 22.

Ingolia NT, Ghaemmaghami S, Newman JR, Weissman JS. Genome-wide analysis in vivo of translation with nucleotide resolution using ribosome profiling. Science. 2009 Apr 10;324(5924):218-23. doi: 10.1126/science.1168978. Epub 2009 Feb 12.

Banfai, B. et al. Long noncoding RNAs are rarely translated in two human cell lines. Genome Res. 22, 1646–1657 (2012)

Gascoigne, D. K. et al. Pinstripe: a suite of programs for integrating transcriptomic and proteomic datasets identifies novel proteins and improves differentiation of protein-coding and non-coding genes. Bioinformatics 28, 3042–3050 (2012).

Beltran, M. et al. A natural antisense transcript regulates Zeb2/Sip1 gene expression during Snail1‐induced epithelial–mesenchymal transition. Genes Dev. 22, 756–769 (2008).

Hastings, M. L., Milcarek, C., Martincic, K., Peterson, M. L. & Munroe, S. H. Expression of the thyroid hormone receptor gene, erbAα, in B lymphocytes: alternative mRNA processing is independent of differentiation but correlates with antisense RNA levels. Nucleic Acids Res. 25, 4296–4300 (1997).

Krystal, G. W., Armstrong, B. C. & Battey, J. F. N‐myc mRNA forms an RNA–RNA duplex with endogenous antisense transcripts. Mol. Cell. Biol. 10, 4180–4191 (1990).

Munroe, S. H. & Lazar, M. A. Inhibition of c‐erbA mRNA splicing by a naturally occurring antisense RNA. J. Biol. Chem. 266, 22083–22086 (1991).

Huarte M. The emerging role of lncRNAs in cancer. Nature Medicine 21, 1253–1261 (2015) doi:10.1038/nm.3981

Schmitt AM, Chang HY. Long Noncoding RNAs in Cancer Pathways. Cancer Cell. 2016 Apr 11;29(4):452-63. doi: 10.1016/j.ccell.2016.03.010.

https://youngbloodbiology.wikispaces.com/Components+of+the+Genome+and+Interphase
Balasubramanian MK, Bi E, Glotzer M. Comparative analysis of cytokinesis in budding yeast, fission yeast and animal

cells. Curr Biol. 2004 Sep 21;14(18):R806-18.

Clancy MJ 1998. Meiosis: step-by-step through sporulation. Curr Biol 8: R461–R463
Vershon AK, Pierce M 2000. Transcriptional regulation of meiosis in yeast. Curr Opin Cell Biol 12: 334–339

SIMCHEN, G., PINON, R. & SALTS, Y. (1972). Sporulation in Saccharomyces cereuisiae. Premeiotic DNA synthesis, readiness and commitment. Experimental Cell Research 15, 207-218.

Wyers, F., Rougemaille, M., Badis, G., Rousselle, J.C., Dufour, M.E., Boulay, J., Regnault, B., Devaux, F., Namane, A., Seraphin, B. et al. (2005) Cryptic pol II transcripts are degraded by a nuclear quality control pathway involving a new poly(A) polymerase. Cell 121, 725–737

David, L., Huber, W., Granovskaia, M., Toedling, J., Palm, C.J., Bofkin, L., Jones, T., Davis, R.W. and Steinmetz, L.M. (2006) A high-resolution map of transcription in the yeast genome. Proc. Natl. Acad. Sci. U.S.A. 103, 5320–5325

Neil, H., Malabat, C., d'Aubenton-Carafa, Y., Xu, Z., Steinmetz, L.M. and Jacquier, A. (2009) Widespread bidirectional promoters are the major source of cryptic transcripts in yeast. Nature 457, 1038–1042

Xu, Z., Wei, W., Gagneur, J., Perocchi, F., Clauder-Munster, S., Camblong, J., Guffanti, E., Stutz, F., Huber, W. and Steinmetz, L.M. (2009) Bidirectional promoters generate pervasive transcription in yeast. Nature 457, 1033–1037

van Dijk, E.L., Chen, C.L., d'Aubenton-Carafa, Y., Gourvennec, S., Kwapisz, M., Roche, V., Bertrand, C., Silvain, M., Legoix-Ne, P., Loeillet, S. et al. (2011) XUTs are a class of Xrn1-sensitive antisense regulatory non-coding RNA in yeast. Nature 475, 114–117

Houseley, J., Rubbi, L., Grunstein, M., Tollervey, D. and Vogelauer, M.(2008) A ncRNA modulates histone modification and mRNA induction in the yeast GAL gene cluster. Mol. Cell 32, 685–695
Camblong, J., Beyrouthy, N., Guffanti, E., Schlaepfer, G., Steinmetz, L.M.and Stutz, F. (2009) Trans-acting antisense RNAs mediate transcriptional gene cosuppression in S. cerevisiae. Genes Dev. 23,1534–1545

Camblong, J., Iglesias, N., Fickentscher, C., Dieppois, G. and Stutz, F.(2007) Antisense RNA stabilization induces transcriptional gene silencing via histone deacetylation in S. cerevisiae. Cell 131, 706–717

Castelnuovo, M. et al. Bimodal expression of PHO84 is modulated by early termination of antisense transcription. Nat. Struct. Mol. Biol. 20, 851–858 (2013).

Nadal-Ribelles M, Solé C, Xu Z, Steinmetz LM, de Nadal E, Posas F. Control of Cdc28 CDK1 by a stress-induced lncRNA. Mol Cell. 2014 Feb 20;53(4):549-61. doi: 10.1016/j.molcel.2014.01.006. Epub 2014 Feb 6.

Nishizawa M, Komai T, Katou Y, Shirahige K, Ito T, Toh-E A. Nutrient-regulated antisense and intragenic RNAs modulate a signal transduction pathway in yeast. PLoS Biol. 2008 Dec 23;6(12):2817-30. doi: 10.1371/journal.pbio.0060326.

Eric A Alcid, and Toshio Tsukiyama. Expansion of antisense lncRNA transcriptomes in budding yeast species since the loss of RNAi. Nat Struct Mol Biol. 2016 May;23(5):450-5. doi: 10.1038/nsmb.3192. Epub 2016 Mar 28.

Yassour M, Pfiffner J, Levin JZ, Adiconis X, Gnirke A, Nusbaum C, Thompson DA, Friedman N, Regev A. Strand-specific RNA sequencing reveals extensive regulated long antisense transcripts that are conserved across yeast species. Genome Biol. 2010;11(8):R87. doi: 10.1186/gb-2010-11-8-r87. Epub 2010 Aug 26.

Chen HM, Neiman AM. A conserved regulatory role for antisense RNA in meiotic gene expression in yeast. Curr Opin Microbiol. 2011 Dec;14(6):655-9. doi: 10.1016/j.mib.2011.09.010. Epub 2011 Sep 29.

Zhang L, Ma H, Pugh BF. Stable and dynamic nucleosome states during a meiotic developmental process. Genome Res. 2011 Jun;21(6):875-84. doi: 10.1101/gr.117465.110. Epub 2011 Apr 22.

Decker CJ, Parker R. Analysis of double-stranded RNA from microbial communities identifies double-stranded RNA virus-like elements. Cell Rep. 2014 May 8;7(3):898-906. doi: 10.1016/j.celrep.2014.03.049. Epub 2014 Apr 24.

Lybecker M, Zimmermann B, Bilusic I, Tukhtubaeva N, Schroeder R. The double-stranded transcriptome of Escherichia coli. Proc Natl Acad Sci U S A. 2014 Feb 25;111(8):3134-9. doi: 10.1073/pnas.1315974111. Epub 2014 Jan

22.

Whipple JM, Youssef OA, Aruscavage PJ, Nix DA, Hong C, Johnson WE, Bass BL. Genome-wide profiling of the C. elegans dsRNAome. RNA. 2015 May;21(5):786-800.doi:10.1261/rna.048801.114. Epub 2015 Mar 24.

Portal MM, Pavet V, Erb C, Gronemeyer H. Human cells contain natural double-stranded RNAs with potential regulatory functions. Nat Struct Mol Biol. 2015 Jan;22(1):89-97. doi: 10.1038/nsmb.2934. Epub 2014 Dec 15.

Lu Z, Zhang QC, Lee B, Flynn RA, Smith MA, Robinson JT, Davidovich C, Gooding AR, Goodrich KJ, Mattick JS, Mesirov JP, Cech TR, Chang HY. RNA Duplex Map in Living Cells Reveals Higher-Order Transcriptome Structure. Cell. 2016 May 19;165(5):1267-79. doi: 10.1016/j.cell.2016.04.028. Epub 2016 May 12.

Zhu G, Spellman PT, Volpe T, Brown PO, Botstein D, Davis TN, Futcher B. Two yeast forkhead genes regulate the cell cycle and pseudohyphal growth. Nature. 2000 Jul 6;406(6791):90-4.
Wang Y, et al. (2003) Exit from exit: resetting the cell cycle through Amn1 inhibition of G protein signaling. Cell 112(5):697-709 PMID: 12628189

Wery M, Descrimes M, Vogt N, Dallongeville AS, Gautheret D, Morillon A. Nonsense-Mediated Decay Restricts LncRNA Levels in Yeast Unless Blocked by Double-Stranded RNA Structure. Mol Cell. 2016 Feb 4;61(3):379-92. doi: 10.1016/j.molcel.2015.12.020. Epub 2016 Jan 21.

Feng Fang, Jason Hoskins, and J. Scott Butler. 5-Fluorouracil Enhances Exosome-Dependent Accumulation of Polyadenylated rRNAs. Mol Cell Biol. 2004 Dec; 24(24): 10766–10776.

Rehman SU, Husain MA, Sarwar T, Ishqi HM, Tabish M. Modulation of alternative splicing by anticancer drugs. Wiley Interdiscip Rev RNA. 2015 Jul-Aug;6(4):369-79. doi: 10.1002/wrna.1283. Epub 2015 Apr 24.

Mariano A Garcia-Blanco, Andrew P Baraniak & Erika L Lasda. Alternative splicing in disease and therapy. Nature Biotechnology 22, 535 - 546 (2004) doi:10.1038/nbt964

Yukawa M, et al. (2009) The Rpd3/HDAC complex is present at the URS1 cis-element with hyperacetylated histone H3. Biosci Biotechnol Biochem 73(2):378-84

Gailus-Durner V, et al. (1997) Analysis of a meiosis-specific URS1 site: sequence requirements and involvement of replication protein A. Mol Cell Biol 17(7):3536-46

Fox MJ, Gao H, Smith-Kinnaman WR, Liu Y, Mosley AL. The exosome component Rrp6 is required for RNA polymerase II termination at specific targets of the Nrd1-Nab3 pathway. PLoS Genet. 2015 Feb 13;11(2):e1004999. doi: 10.1371/journal.pgen.1004999. eCollection 2015.

Barrett, Lucy W.; Fletcher, Sue; Wilton, Steve D. (27 April 2012). "Regulation of eukaryotic gene expression by the untranslated gene regions and other non-coding elements". Cellular and Molecular Life Sciences. 69 (21): 3613–3634. doi:10.1007/s00018-012-0990-9.

ANNEXE 2

VU :

Le Directeur de Thèse
(PRIMIG Michael)

VU :

Le Responsable de l'École Doctorale

VU pour autorisation de soutenance

Rennes, le

Le Président de l'Université de Rennes 1

Davis ALIS

VU après soutenance pour autorisation de publication :

Le Président de Jury,
(JÉGOU Bernard)

Abstract

The drug 5-fluorouracil (5-FU) was introduced as an effective agent in chemotherapy several decades ago. Although much work has focused on understanding its mechanism of action and the events that mediate resistance, some key issues remain unresolved. In my work I addressed the question if the deregulation of recently discovered long non-coding RNAs that depend upon the exoribonuclease Rrp6 (EXOSC10 in mammals) – an enzyme which is directly inhibited by 5-FU – may be involved in the drug's cytotoxicity. To this end, I studied the genome-wide effect of 5-FU treatment using RNA profiling in budding yeast, a major model organism for studying eukaryotic cell cycle progression. My major findings are that (i) some lncRNAs accumulate upon treatment including certain transcripts that can form double stranded RNAs with their overlapping sense mRNAs (and lncRNAs) and (ii) mRNAs and protein levels of the important Swi5 and Ace2 cell cycle regulators are decreased and their target gene mRNAs are down-regulated. In related work, I showed that (i) *RRP6* over-expression mediates elevated 5-FU resistance, which marks the protein out as a potential target for strategies to counter this critical phenomenon in cancer. Furthermore, I studied the transcriptional regulation of meiotic developmental stage specific lncRNAs, some of which are accumulating in cycling cells upon 5-FU treatment. Finally, I participated in work on the epigenetic control of mRNA isoforms that are repressed in mitosis, that can accumulate in 5-FU treated cells, and that are normally activated during various stages of meiotic cell differentiation. My work paves the way for further studies in mammalian cancer cells aiming at lncRNA accumulation upon 5-FU treatment and a possible correlation between EXOSC10 protein levels and 5-FU resistance in malignancies such as colon, breast and skin cancer.